NMI-5025 (Pt. I)

Technical Papers of the

Eighteenth Metallographic Group Meeting

held June 22-24, 1964
Atomics International
Canoga Park, California

United States
Atomic Energy Commission
Division of Technical Information

LEGAL NOTICE

Printed in USA. Price $2.25. Available from the Clearinghouse for Federal Scientific and Technical Information, National Bureau of Standards, U. S. Department of Commerce, Springfield, Va.

USAEC Division of Technical Information Extension, Oak Ridge, Tennessee

NMI - 5025 (Part I)
METALS, CERAMICS, AND MATERIALS
(TID - 4500, 43rd. Ed.)

TECHNICAL PAPERS OF THE EIGHTEENTH METALLOGRAPHIC GROUP MEETING

Held June 22 - 24, 1964

at Atomics International

Canoga Park, California

Compiled by

H. Roth Roman

Issued: August 1965

Nuclear Metals
Division of Textron Inc.
West Concord, Massachusetts

Steering Committee

A. E. Guay	Past Chairman
C. L. Angerman	Chairman
R. J. Van Thyne	Sr. Member
H. C. Kloepper	Jr. Member
H. Roth Roman	Secretary

CONTENTS

ATTENDANCE LIST

R. Carlander	Argonne National Laboratory
S. Matras	Argonne National Laboratory
R. J. Van Thyne	IIT Research Institute
S. C. Carniglia	Atomics International
R. E. Conner	Atomics International
J. J. Flaherty	Atomics International
O. O. Gamba	Atomics International
R. A. Harlow	Atomics International
H. Pearlman	Atomics International
E. E. Ritchie	Atomics International
M. E. Rosenblum	Atomics International
J. E. Shaffer	Atomics International
E. G. Szymborski	Atomics International
H. Taketani	Atomics International
J. L. Tibbetts	Atomics International
J. B. Vetrano	Atomics International
W. A. Wahl	Atomics International
C. C. Woolsey	Atomics International
A. J. Yeast	Atomics International
C. Laakso	Autonetics
L. Moudy	Autonetics
C. Nealy	Autonetics
M. S. Farkas	Battelle Memorial Institute
F. E. McGrath	Battelle Memorial Institute
M. F. Garufi	Bridgeport Brass Company
L. Robins	Bridgeport Brass Company
O. F. Kammerer	Brookhaven National Laboratory
A. E. Calabra	Dow Chemical Company, Rocky Flats
R. L. Greeson	Dow Chemical Company, Rocky Flats
F. L. Cochran	General Atomic
H. E. Shoemaker	General Atomic
L. A. Hartcorn	General Electric, HAPO
D. D. Hays	General Electric, HAPO
R. K. Koler	General Electric, HAPO
R. D. Leggett	General Electric, HAPO
F. M. Smith	General Electric, HAPO
A. F. Steeves	General Electric, KAPL
E. W. Filer	General Electric, NMPO
K. Lacefield	General Electric, NMPO
E. N. Hopkins	Iowa State University
J. Clark	Lawrence Radiation Laboratory
N. Houlding	Lawrence Radiation Laboratory
R. Nickerson	Lawrence Radiation Laboratory
E. Snell	Lawrence Radiation Laboratory
H. C. Kloepper	Mallinckrodt Chemical Works
W. Brammer	NAA Science Center
J. W. Colby	National Lead Company of Ohio
M. Cornett	National Lead Company of Ohio
W. Wise	National Lead Company of Ohio

H. R. Roman	Nuclear Metals
G. L. Dadisman	Oak Ridge National Laboratory
A. G. Dobbins	Oak Ridge National Laboratory
C. K. H. DuBose	Oak Ridge National Laboratory
R. J. Gray	Oak Ridge National Laboratory
T. M. Kegley, Jr.	Oak Ridge National Laboratory
C. L. Angerman	Savannah River Laboratory
C. G. Hoffman	Los Alamos Scientific Laboratory
F. W. Cotter	Army Materials Research Agency
D. J. Rahn	Westinghouse Electric, Atomic Products Division

METALLOGRAPHIC AND CERAMOGRAPHIC PREPARATION OF NUCLEAR MATERIALS*

by

E. W. Filer, C. A. Asaud,
K. Lacefield, and R. B. Kull

General Electric Company
Nuclear Materials and Propulsion Operation
Cincinnati, Ohio

ABSTRACT

The polishing and etching procedures for preparing metallic, ceramic and cermet specimens of nuclear materials using the Automet polisher are discussed with some typical examples of the excellent results obtained. The attack-polishing method reported by Ambler and Slattery was successfully adapted to automatic polishing allowing more pressure to be applied to the specimen. This modification has eliminated the difficulties normally encountered in the preparation of specimens containing materials of extreme variations in hardness. The advantages of this technique are discussed.

*This paper originated from work sponsored by the Fuels and Materials Development Branch, Atomic Energy Commission, under Contract AT(40-1)-2847.

INTRODUCTION

Various methods have been tried for preparing nuclear materials for metallographic and ceramographic evaluation. Out of these various methods, two standard procedures using the Automet polishers have evolved. One method is used for preparing most of the ceramics and ceramic powders, and the other, using hydrogen peroxide, has been developed for the preparation of metals, cermets and certain ceramics. It is the purpose of this paper to give the polishing procedure, methods of sectioning and mounting specimens, and a discussion of the representative results obtained.

SAMPLE PREPARATION

Sectioning

Currently most metallic, cermet, or ceramic materials for metallographic or ceramographic evaluation are sectioned using the Micromech Precision Wafering Machine,* Figure 1. The instrument resembles a modified cutter-grinder machine and was designed for precision cutting of single crystals of silicon and germanium in the electronics field. It is fully dry-boxed and has its own simple coolant recirculating system. These two features are necessary when dealing with toxic or radioactive materials such as beryllia, or urania and/or thoria. This versatile semi-automatic model enables the operator to rapidly make precision cuts and obtain crack-free sections of ceramic materials. The diamond wheel used for ceramics can be easily exchanged for a silicon carbide wheel for sectioning metallic samples. In addition, both silicon carbide and diamond wheels are available for light grinding tasks. Specimens are cemented to a graphite

*Micromech Mfg. Corp., 120 Commerce Ave., Union, N. J.

block using Lakeside cement,* Figure 2. This graphite block is then placed in a steel clamp and held in the desired position on the magnetic chuck of the Micromech, Figure 3. Some examples of the cuts showing the versatility of the machine are shown in Figure 4. The cuts are always complete, square, and of a fine surface finish. These three factors help to reduce sample grinding time considerably.

Mounting

The specimens are then mounted in an epoxy resin.† Our mounting procedure is to place the specimen in a prepared aluminum mold 1-1/4 inches in diameter by 1 inch deep, Figure 5, and cover with epoxy resin. The minimum curing time at 175° to 180°F is four (4) hours, but our general procedure is to leave the mounts cure overnight. These molds were made from aluminum bar stock with the bottom plate easily removable. The most important consideration is to put as smooth a finish as possible on the mold walls. This finish and an occasional application of mold release allow the sample to be removed with very little effort.

Metallographic Preparation

The stepwise procedure for preparing specimens, except the extremely hard ceramics, such as BeO, Al_2O_3, using the Automet Polisher is given in Table 1. Water is the lubricant when using the various grades of silicon carbide abrasive paper. It should be stressed that the times given in Table 1 for the rough grinding on the silicon carbide papers are the maximum times per step. If additional grinding is required during any stage

*Lakeside No. 70 Thermoplastic Cement C-40006, Ward's Natural Science Establishment, Inc., Rochester, New York.
†Maraglas No. 655, Hardener No. 555, manufacturer Marblette Co., 37-31 Thirtieth Street, Long Island City 1, New York.

of the preparation, then a new paper must be used. A slurry of 30 grams of Linde-B (0.05 micron γ-Al_2O_3) in 140 ml of 30 percent hydrogen peroxide* is used on the cloths for final polishing (Step 6 and 7). All cloths should be wet with water before adding the abrasive slurry, otherwise the slurry will gel. Step 7 is used only when necessary as the edges of the specimen will tend to round and relief polishing will develop with additional polishing on this type of cloth. The specimens must be washed with water immediately after removal from the hydrogen peroxide to prevent staining or etching.

Ceramographic Preparation

The procedure for preparing the hard ceramic specimens using the Automet Polisher is shown in Table 2. The lubricant is also a means of preventing airborne contamination. Normally, Step 1 is all that is required to make sure the surface is flat and all mounting material is removed from the surface. Each grinding and polishing step should be watched closely, and more or less operation time employed where deemed necessary. Final polishing with Linde-A (0.3 micron α Al_2O_3) should particularly be watched as this is usually where rounding of edges and relief polishing occurs. After each step of polishing, the samples are scrubbed with water and detergent or, if very porous, cleaned ultrasonically to remove entrapped polishing debris.

Ceramic powders for evaluation are normally mixed with the Maraglas and run through the standard procedure, except the 240 grit silicon carbide papers are omitted. On material that has been spheroidized, the mounting procedure is altered. A small amount is added to the Mara-

*Protective gloves should be worn when using hydrogen peroxide.

glas and then vibrated until the material is all in one layer. The specimens are then processed as shown in Table 2 except for Steps 1 and 2.

DISCUSSION

Sectioning

The use of the Micromech Precision Wafering Machine has greatly simplified the problem of sectioning the ceramic and toxic materials. Also, there has been a significant improvement in the quality of the specimens prepared for ceramographic evaluation. This equipment has eliminated the shattering of the grain boundaries that is normally encountered in sectioning these hard brittle materials. It has been our experience that it was extremely difficult, if not impossible, to grind below the damaged area when shattering of the grain boundaries had occurred during sectioning. It is felt that these cracked or separated grain boundaries were the nuclei for the propagation of these cracks into grain boundaries away from the surface causing cracks and loss of individual grains. The use of this equipment has eliminated most of the problem.

Mounting

The advantages of mounting specimens in epoxy resins have been enumerated many times, and we are in full agreement with most of them. Our selection of Maraglas was prompted by its hardness, acid resistance and transparency after curing. In the past the question has been raised that since the epoxy resin is cured by heating to 175°F whether excess heat was generated in the mount in curing and what the temperature overrun would be? A recording thermocouple was placed inside the liquid epoxy resin to monitor the temperature through the normal curing cycle. The furnace was controlling at 175°F and the maximum temperature measured was 185°F which occurred about 4 hours after the run started. A typical curve is shown in Figure 6.

Metallographic Polishing

Difficulties were encountered in using the standard mechanical method of preparing uranium dioxide specimens containing free uranium for metallographic evaluation. An attack-polishing reagent reported by Ambler and Slattery[1] was effective in ameliorating these difficulties. The reagent consists of a slurry of hydrogen peroxide (30%) and 5% γ-alumina. This hand polishing method has been adapted to automatic polishing which allows more pressure to be applied to the specimen during preparation. Using additional pressure reduces the preparation time, improves edge retention and less relief polishing. This technique has also been extended to other materials with good results. Using the described procedure, excellent results were obtained in preparing a specimen of uranium dioxide that had been heated for 10 hours at 2200°C in a uranium saturated hydrogen atmosphere, as shown in Figure 7. Note the good edge retention of both the uranium and the uranium dioxide, especially at the void areas.

The method has also been used successfully on graphite samples having a carbide coating. A comparison of the results obtained between our former metallographic procedure and the new method is shown in Figure 8 and 9. The former method consisted of using the Automet polishers with 240, 400 and 600 grit silicon carbide papers, water lubricant. The specimens were then hand polished using 3 micron diamond on a Microcloth followed by γ-alumina on gamal cloth. As can be seen in the old method (Figure 8), there is rounding of the edge of the carbide and there is loss of material at the interface. Using the hydrogen peroxide (Figure 9), there is good edge retention, the interface is sharp and the overall appearance of the

specimen is considerably improved. Another example of the excellent results obtained using this technique in preparing materials of extreme variation in hardness is shown in Figure 10. This photomicrograph is of carbide particles in a graphite body. Here, there is good edge retention of the carbide in contact with the graphite.

The reported results using different techniques in preparing pyrolytic graphite for metallographic examination by Brassard and Holik,[2] Coons,[3,4,5] and Stover[6] have been studied. The feasibility of using our method was tried by placing three separately mounted specimens of pyrolytic graphite in the Automet holder with two mounted specimens of a tungsten-uranium dioxide cermet. The results of using hydrogen peroxide in preparing the pyrolytic graphite specimens with the previously described technique are shown in Figures 11 and 12. As pointed out in Table 1, heavy pressures are used in the preparation of these specimens, while the methods reported in the open literature indicate very light pressures must be used. The polish obtained on the tungsten-uranium dioxide cermet prepared at the same time as the graphite was excellent, Figure 13.

This method has been used in polishing all the pure refractory metals with excellent results. A typical example of how well this technique works is shown in the photomicrograph of tungsten metal, Figure 14.

Ceramographic Polishing

As indicated in the preparation schedule of Table 2, 600 grit silicon carbide abrasive paper is not used in preparing the hard ceramic materials. Surprisingly, additional grinding on 600 grit silicon carbide paper actually reduces the surface quality attained with the last 400 grit

paper. This is shown quite effectively in a series of photomicrographs of BeO, Figure 15, which also gives the results after polishing, using 3 μ diamond and Linde A.

The procedure, Table 2, although originally developed to polish BeO, has proven to be successful on a wide variety of ceramic materials, i.e., ZrO_2, Y_2O_3, Al_2O_3, Eu_2O_3, and ThO_2 and combinations of these materials. The only modification necessary has been to vary the pressure. Powders, relatively soft compositions, and very porous bodies are prepared using slightly reduced pressures. Additionally, the basic procedure can be used to polish composites of very hard and soft materials with little or no relief at the interface and good edge retention, Figures 16 and 17. Within reason, it has been possible to place in the Automet holder mounts of many of these materials and polish them simultaneously regardless of difference in hardness. A few typical examples of the many materials that have been polished using this procedure are shown in Figure 18.

Prior examination of the ceramic spheres before mounting showed them to be very uniform in size. When these spheres were mounted and polished in the normal manner for powders, the results indicated the spheres were of different size because of sectioning. Using the vibratory mounting procedure discussed earlier, it was possible to obtain all of the spheres on one plane, then careful polishing gave the results shown in Figure 19.

A list of the various etchants that have been used on ceramic materials is given in Table 3.

SUMMARY

The procedure for preparing ceramics and ceramic powders using the Automet polisher has been outlined and typical examples of the results obtained were shown and discussed. The technique used has proven to be a widely applicable method for rapid ceramographic preparation.

The procedure using hydrogen peroxide for the metallographic preparation has been tried on various metals, ceramics, and cermets with excellent results. The main advantages of using this method are:

1. It is a very fast method for preparing specimens.
2. There is very little, if any, disturbed or flowed metal remaining on the surface.
3. Due to the elimination of the disturbed metal, the specimens will etch readily.
4. Edge retention is very good.

ACKNOWLEDGEMENT

The authors wish to thank S. A. Leighton, I. D. Miller, F. T. Williams and W. C. Young who assisted in this work, and to G. R. Anderson who developed the ceramic sphere technique.

REFERENCES

1. J. F. R. Ambler and G. F. Slattery, "New Metallographic Techniques for the Examination of Uranium, Uranium Alloys and Uranium Dioxide," Journal of Nuclear Materials, Vol. 4, 1961, p. 90.

2. Theresa V. Brassard and Andrew S. Holik, "Preparing Various Graphites for Metallographic Examination," Metal Progress, May 1962, p. 109.

3. William C. Coons, "A Rapid Method for Polishing Pyrolytic Graphite," Metal Progress, June 1962, p. 83.

4. William C. Coons, "More on Polishing Pyrolytic Graphite," Metal Progress, January 1963, p. 120.

5. William C. Coons, "More on Polishing Pyrolytic Graphite," Metal Progress, March 1963, p. 114.

6. Edward R. Stover, "Flame Polishing Pyrolytic Graphite," Metal Progress, May 1963, p. 112.

TABLE 1

PROCEDURE FOLLOWED IN PREPARING SPECIMENS FOR METALLOGRAPHIC EVALUATION USING THE AUTOMET POLISHER

Step	Polishing Media Backing Material	Abrasive Size	Time, min.	Weight Per 1-1/4" Mount, lbs.
1*	SiC paper	240 grit	1 -1/2	6
2	SiC paper	400 grit	1	6
3	SiC paper	400 grit	1	6
4	SiC paper	600 grit	1/2	4
5	SiC paper	600 grit	1/4	4-5
6	γ -alumina-Pellon	0.05 microns	4-5	5-6
7	γ -alumina-micro-cloth	0.05 microns	1/2	5-6

Water is used as the lubricant, except in Steps 6 and 7 where a slurry of 140 ml H_2O_2 (30%) and 30 g γ -alumina is used.

*This step is repeated using new paper until all specimens are flat.

TABLE 2

PROCEDURE FOLLOWED IN PREPARING CERAMIC MATERIALS FOR CERAMOGRAPHIC EVALUATION USING THE AUTOMET POLISHERS

Step	Polishing Media Backing Material	Abrasive Size	Time, min.	Weight Per 1-1/4" Mount, lbs.
1	SiC paper	240 grit	2	6
2	SiC paper	240 grit	3-5	4
3	SiC paper	400 grit	20	4
4	Diamond-nylon	3 μ	15-20	4
5	α-alumina-nylon	0.3 μ	15-20	4

Water is used as the lubricant except for Step 4 where kerosene is used.

TABLE 3

ETCHANTS USED ON VARIOUS CERAMIC MATERIALS

Ceramic	Etchant	Comments
Al_2O_3	Fused KHF_2	Immerse for several minutes at a time until suitably etched. Rinse very carefully!
	20 v/o aqueous solution of (47%) HF	Swab etch for 10-20 minutes.
BeO BeO + UO_2 BeO + UO_2 - Y_2O_3	50 v/o aqueous solution of (47%) HF	Swab for 5-10 minutes general structure. Immerse for 10-20 minutes for grain size determination.
Eu_2O_3	4 gm $CuSO_4$ 20 ml HCl 20 ml H_2O (Marble's Reagent)	Swab etch for just a few seconds.
UO_2	H_2O_2	Mix with alumina abrasive during final polish, then stain in H_2O_2 for 5 or 6 minutes.
	7 parts H_2O 2 parts H_2O_2 1 part HNO_3	Swab or immersion etch for 15 seconds. Must be made up fresh just before using.
ZrO_2 ZrO_2 + Y_2O_3 ZrO_2 + Y_2O_3 + UO_2	2 parts H_2SO_4 1 part HF or HNO_3	Immerse into boiling etchant for several minutes at a time until suitably etched.

In general, concentrated strong acids, particularly hydrofluoric and sulfuric, are the most effective. Quite often heating the acids increases their effectiveness. Occasionally, samples of BeO and Al_2O_3 are thermally etched by heating for varying times at 2500° - 2750°F in air or hydrogen. Attempts to cathodically vacuum etch Al_2O_3 and BeO have been unsatisfactory.

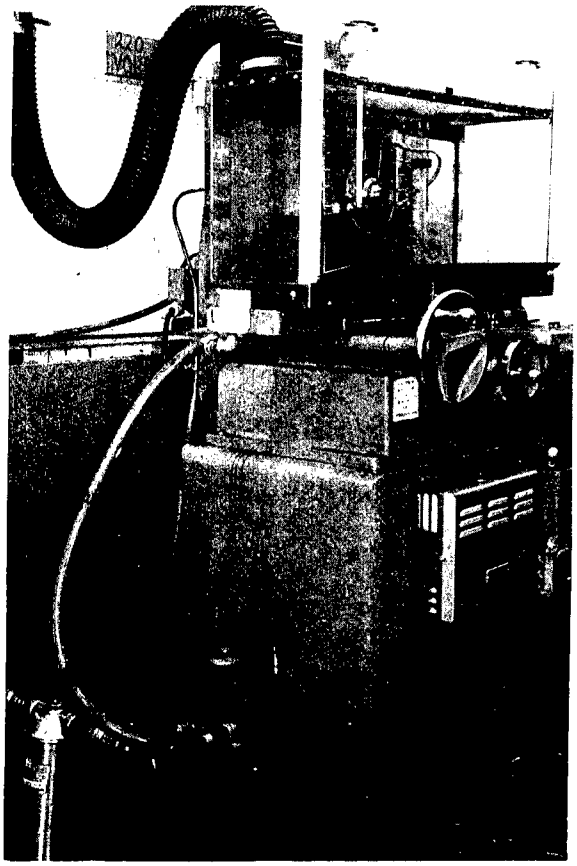

Fig. 1 - Micromech Precision Wafering Machine used for sectioning metals, ceramics and cermets. The cut-off wheel is enclosed in a dry box with an exhaust system for maintaining a negative pressure. There is also an attached recirculating system for the coolant.

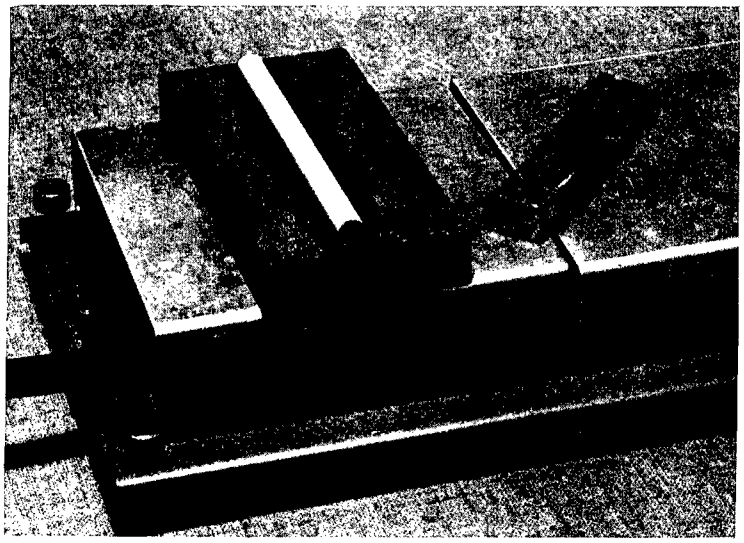

Fig. 2 - Typical method of mounting a ceramic specimen to a graphite block with Lakeside cement prior to sectioning.

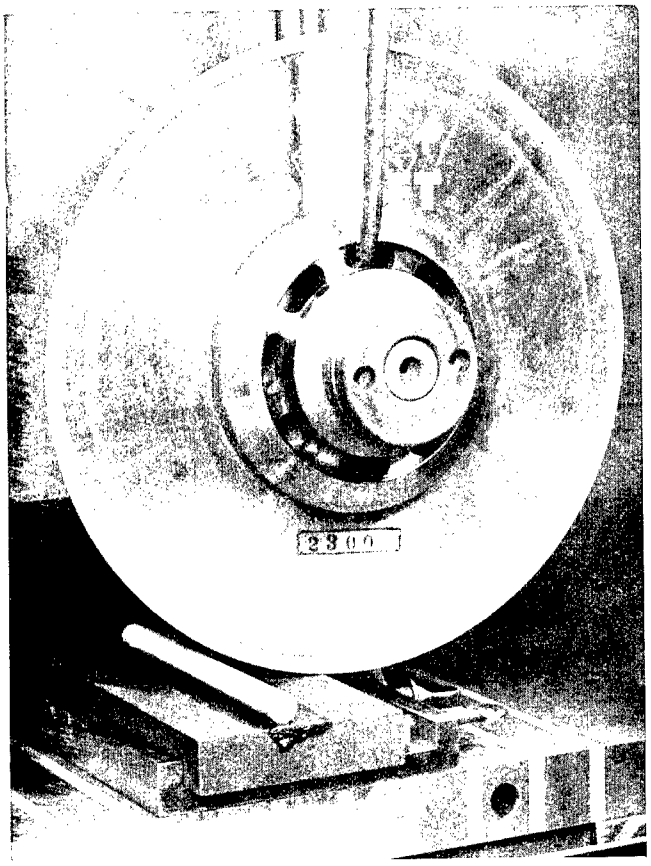

Fig. 3 - Method of holding graphite block to magnetic chuck.

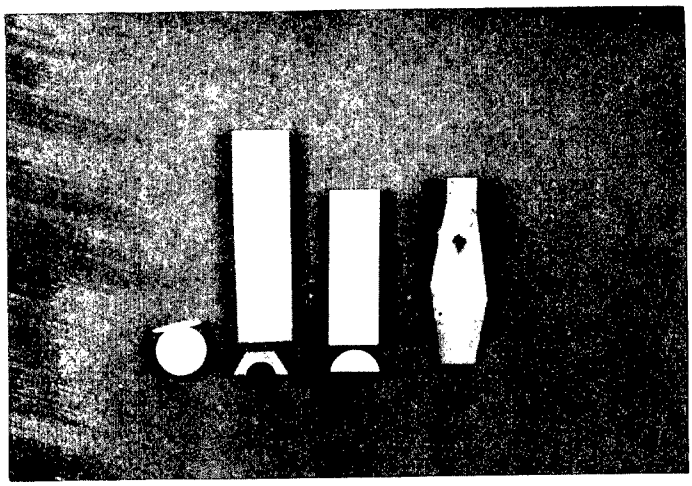

Fig. 4 - Typical sections of ceramic materials showing the versatility of the Micromech. The thin disc is about 0.007 inches thick.

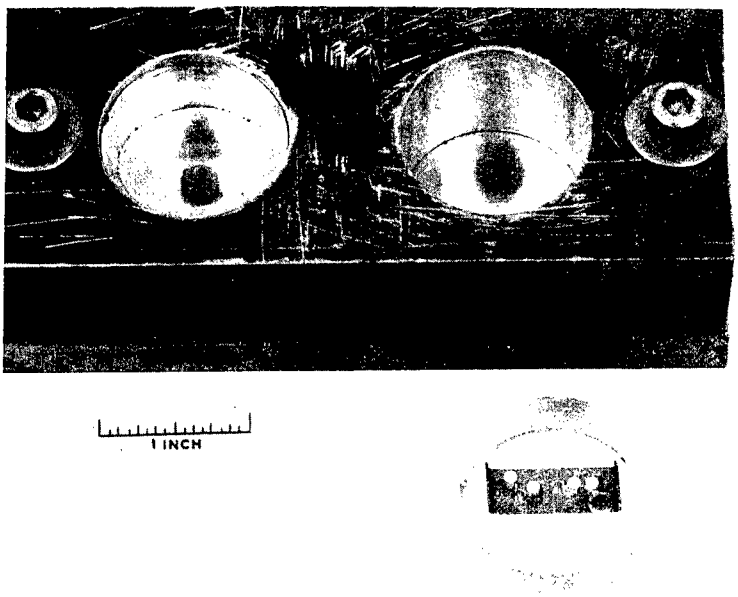

Fig. 5 - Aluminum mold used for mounting in Maraglas with one specimen in place and the other removed.

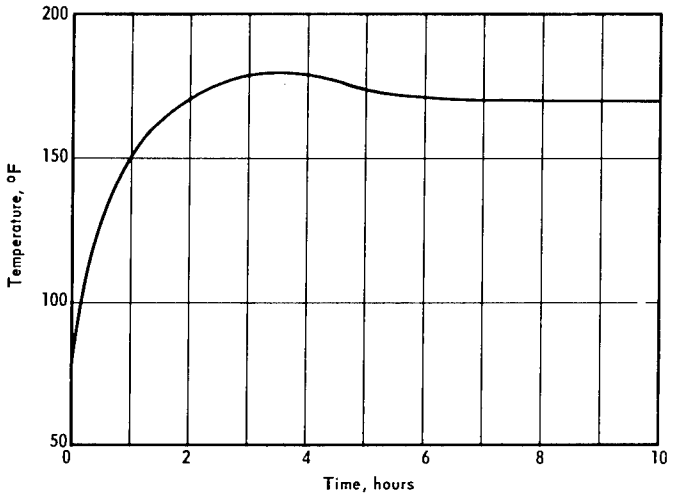

Fig. 6 - Typical heating and curing curve for Maraglas mounting material showing the maximum rise above furnace controlling temperature of 10°F.

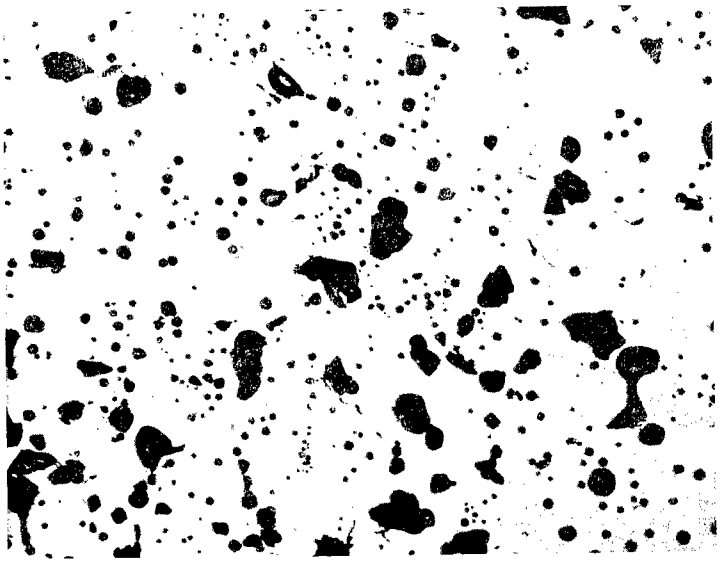

Fig. 7 - Uranium dioxide containing free uranium. The black areas are voids which are inherent in the sintered compact. As-polished, 250X.

Fig. 8 - Photomicrographs of carbide coating on a graphite body. Prepared using standard metallographic procedures. As-polished, 250X.

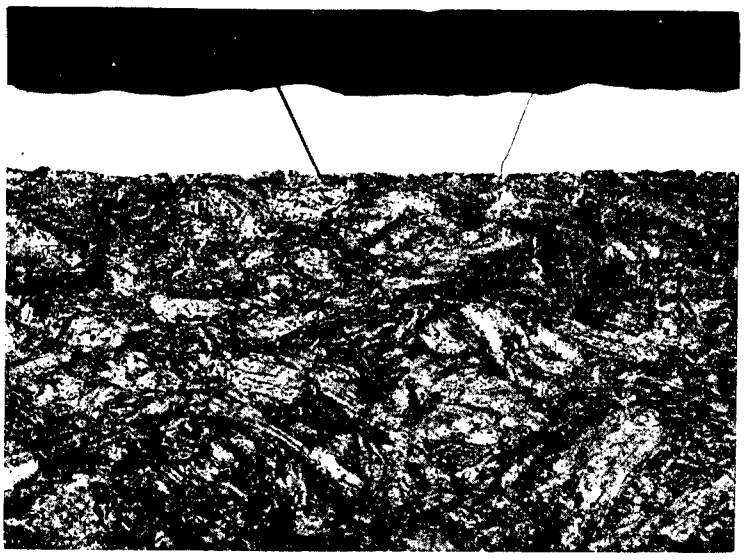

Fig. 9 - Photomicrograph of the same specimen as Fig. 8 prepared using hydrogen peroxide. As-polished, 250X.

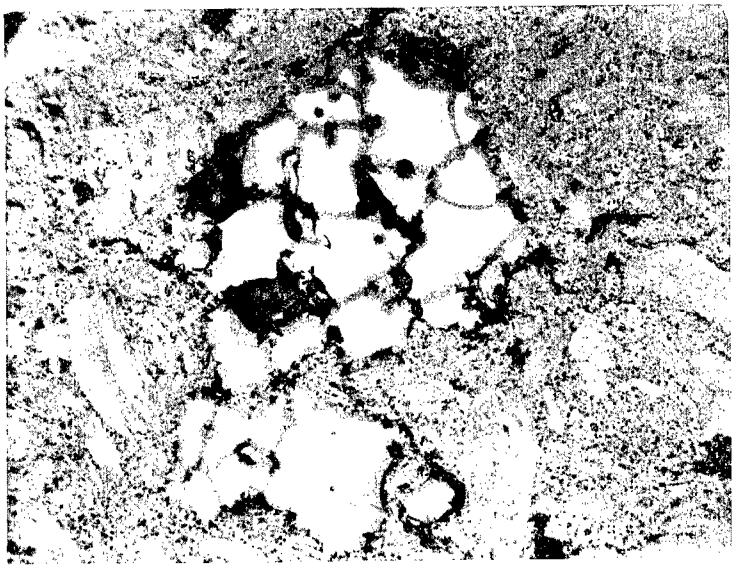

Fig. 10 - Photomicrograph of carbide particles in a graphite matrix. As-polished, 500X.

Fig. 11 - Pyrolytic graphite prepared using hydrogen peroxide. As-polished, polarized light, 100X.

Fig. 12 - Photomicrograph of pyrolytic graphite coating on a graphite matrix prepared using hydrogen peroxide. As-polished, polarized light, 100X.

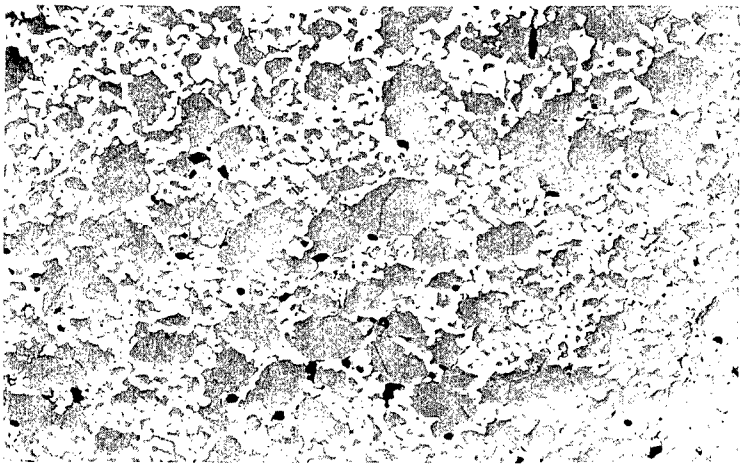

Fig. 13 - Photomicrograph of a tungsten-uranium dioxide cermet prepared using hydrogen peroxide. As polished, 100X

Fig. 14 - Photomicrograph of commercial tungsten.
Etched 20% Murakamis, 250X.

After 400 grit silicon carbide paper

After 3 μ diamond on nylon

After 600 grit silicon carbide paper

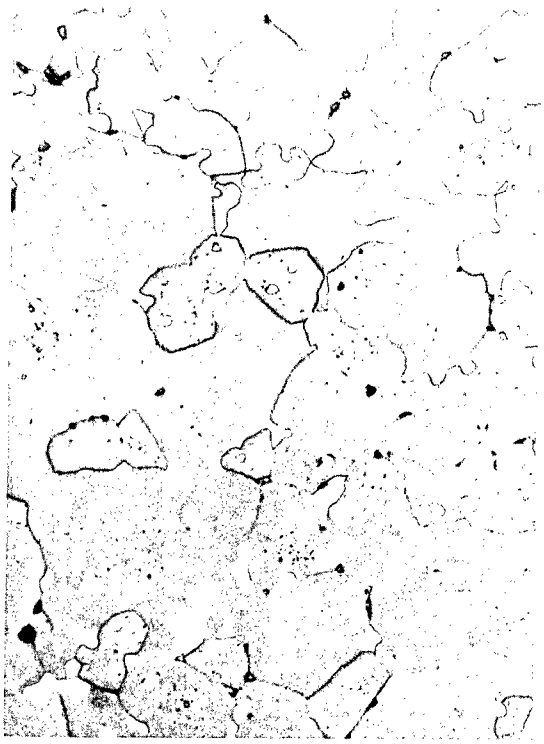

After α-alumina on nylon

Fig. 15 - A series of photomicrographs taken during the preparation of a BeO specimen. All specimens unetched and taken at 250X.

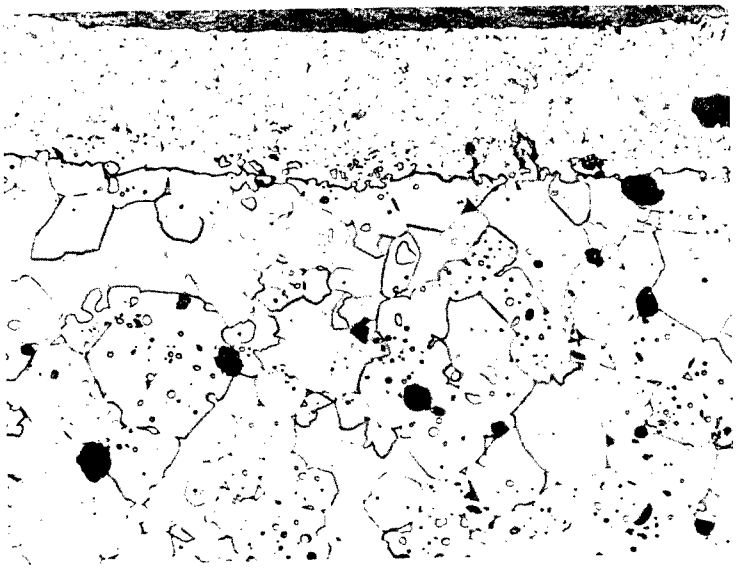

Fig. 16 - Photomicrograph of ceramic clad on fueled BeO. Etched 20% HF, 250X.

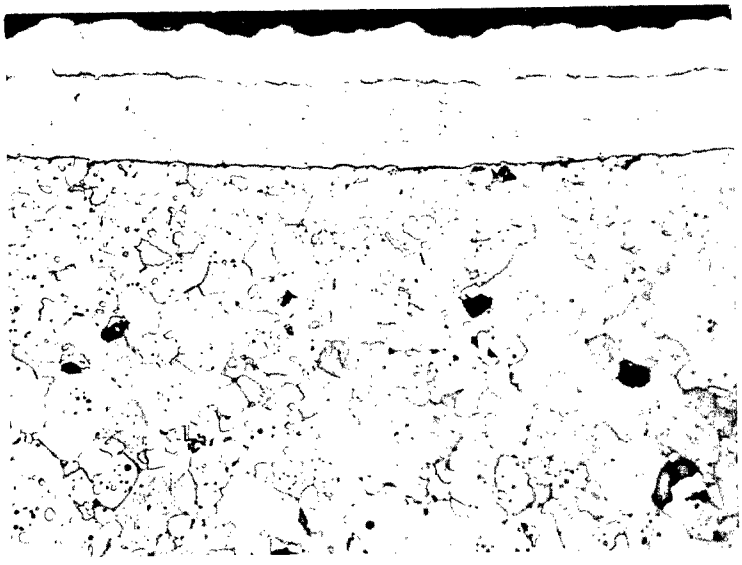

Fig. 17 - Photomicrograph of double ceramic clad on fueled BeO. Etched 20% HF, 250X.

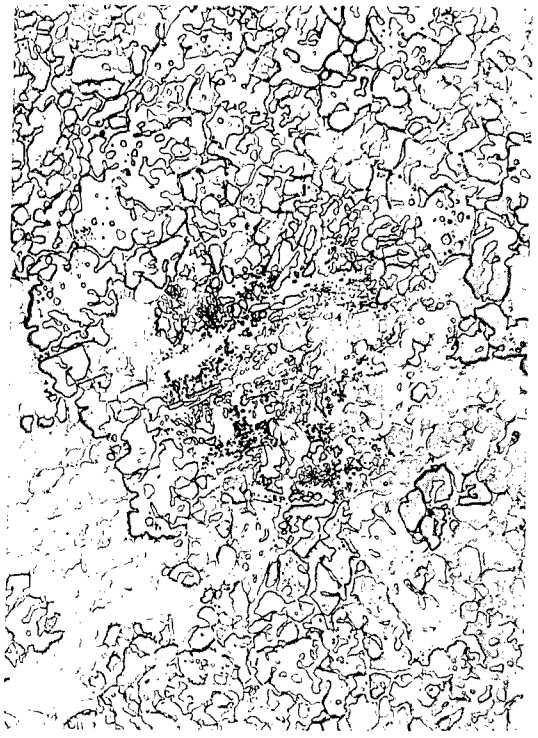

BeO-ThO_2 - As-polished, 100X

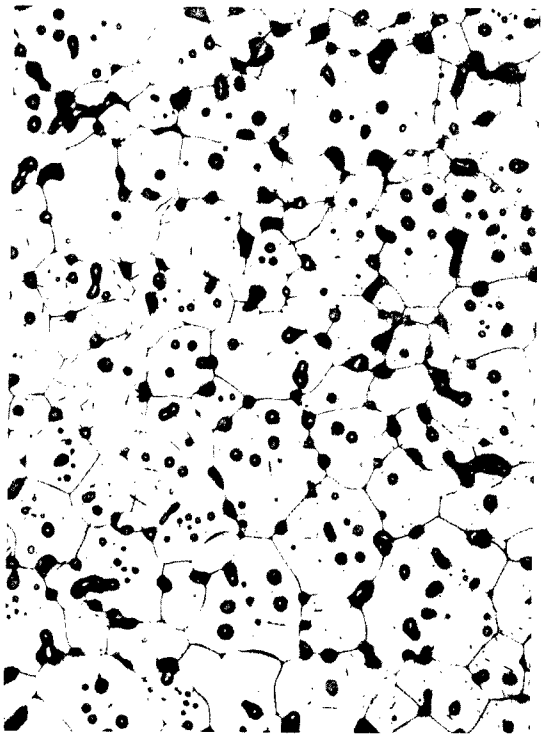

ZrO_2 - Etched, 250X

Al_2O_3 - As-polished, 250X

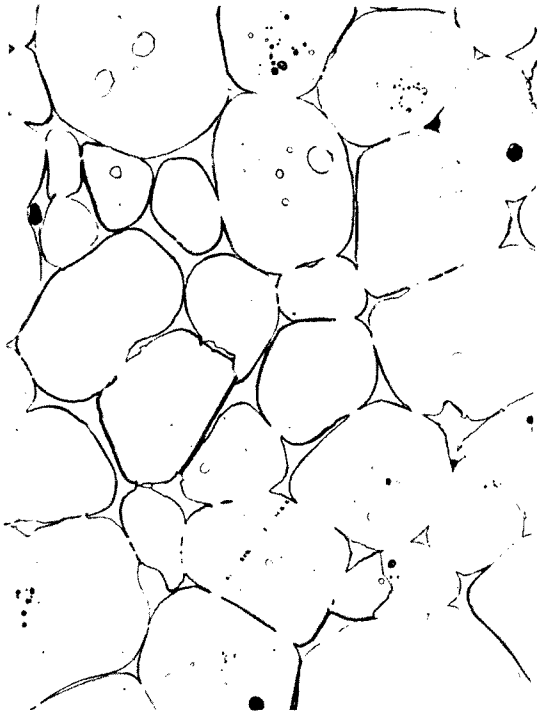

Fueled BeO - Etched, 250X

Fig. 18 - Photomicrographs of various ceramic materials.

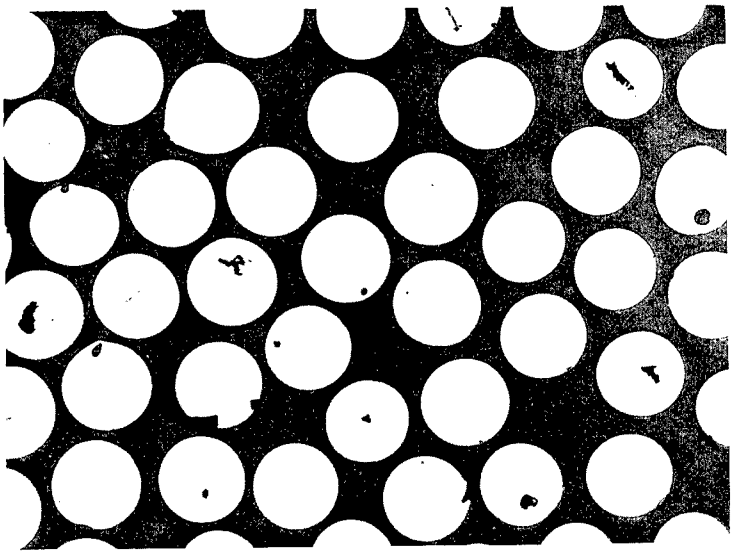

Fig. 19 - Photomicrograph of Y_2O_3-UO_2 ceramic spheres. As-polished, 250X.

dup. of 6111?

Electropolishing the Rare Earth Metals*

by

D. T. Peterson and E. N. Hopkins

Institute for Atomic Research and Department of Metallurgy
Iowa State University, Ames, Iowa

Abstract

This paper describes a method whereby the rare earth metals can be consistently electropolished and chemically etched. The method involves cooling an alcohol-perchloric electrolyte to -76 °C before electropolishing. The metals are chemically polished in the same solution.

Introduction

The rare earth metals have gained increasing prominence in the last decade as basic research materials. In many metallurgical investigations, it is desirable to have methods of polishing the metal surfaces free of contamination. This is necessary for metallographic examination as well as x-ray examination. The two more successful methods for producing metal surfaces free from contamination are chemical and electrolytic polishing. The advantages of electropolishing versus other methods of surface preparation and specifically mechanical abrasion is principally in obtaining an unworked, strain free surface.

*Contribution No. 1624. Work was performed in the Ames Laboratory of the U. S. Atomic Energy Commission.

The increasing use of the transmission electron microscope for the study of metals has also encouraged the study of electrolytic polishing.

Electrolytic polishing has been known[1] since 1925 with its metallographic aspects realized[2] in 1936 by Jacquet. Since 1936 there have been numerous investigations of polishing characteristics of electrolytes and their application to different metals.

The rare earth metals are difficult to polish either chemically, mechanically, or electrolytically due to their tendency to oxidize, particularly in an aqueous solution. A method of electrolytic polishing would have to overcome this problem before any measure of success could be obtained. All of the rare earth metals with the exception of promethium and europium have been successfully electropolished by the method described in this work. A specimen of europium was not available to try. Yttrium was included because of its similarities to the rare earth metals.

Experimental Procedure

The metals used in this investigation were samples received in the service laboratory and were not usually the purest metal obtainable. A direct current source capable of supplying up to 120 volts and 3 amps was used for electropolishing. The specimen surfaces to be electropolished were 1/4" x 1/4" . The cathode was stainless steel.

All electropolishing was done in a 250 ml open beaker on unmounted specimens. A magnetic stirrer was used to keep the solution at the desired temperature.

The electrolytes investigated were the following: phosphoric acid, nitric acid, chromic acid, sulfuric acid, perchloric acid, sodium hydroxide, hydrochloric acid, oxalic acid and potassium hydroxide. Water, alcohol, ether and glycerine were used as solvents. The samples to be electropolished were ground through successively finer grit silicon carbide abrasive paper finishing with 600 grit paper. After cleaning in absolute ethanol, the samples were electropolished at various times, temperatures and voltages. The current density could not be measured accurately because the current was always less than 0.02 milliamperes and could not be read on the meter. The beaker containing the electrolyte was placed in a bath containing dry ice and acetone and the temperature of the solution was maintained at -76 °C. The electrolyte was stirred at a moderate rate to insure an uniform and constant solution temperature.

Discussion

The successful electropolishing solutions were the perchloric acid-alcohol types recommended[3] by De Sy and Haemers. The nitric acid-alcohol mixtures showed some anodic brightening but were never as promising as the perchloric acid-alcohol mixtures. The most

successful mixture was 1% perchloric acid in methanol. It should be observed that the perchloric acid-acetic anhydride solutions proposed by Jacquet would probably also be successful but are more expensive and more dangerous and therefore were not used in these experiments.

A solution of 1% perchloric acid in methanol was found to be successful on all of the metals. The time for complete polishing varied between 5 and 10 minutes at an open circuit voltage of 50 volts with the longer polishing cycles not deteriorating the surface. The optimum temperature was found to be -76°C. At this temperature, the solution was not as chemically active as at room temperature thus allowing the metals to be electrolytically polished instead of chemically oxidized. Chemical oxidation appears to be an important factor in the electropolishing of metals. If the oxidation is very rapid, the electropolishing of the metal is retarded. The rare earth metals are good examples of this behavior because of their rapid oxidation rate.

The mechanism of the rare earth electropolishing is thought to be one of surface oxidation. A thick film is observed to be formed on some of the rare earths and can be collected on a copper grid and examined by electron microscopy selected area diffraction. A film formed on ytterbium was examined with the electron microscope and the diffraction pattern measured. This pattern corresponded to the structure of Yb_2O_3 as observed in X-ray diffraction analysis. The ytterbium sample was also observed during polishing using an optical microscope at 40 magnification. At the onset of polishing, a film is

formed within a few seconds. The film adheres for a time and after one or more minutes begins to fall away from the surface of the metal. The metal appears to be bright and scratch free at this time. The stripping of the film is not consistent over the entire area of the metal surface. In some areas the film takes much longer to fall away than in other areas. This may be due to impurities such as oxides particles on the metal surface which tend to bind the film. Also the grinding scratches are somewhat nonuniform and some areas probably require longer polishing times to become flat and smooth.

Chemical oxidation is the principle method of etching a metal surface for microscopic examination and the rare earths were etched in this manner. At room temperature, the nitric acid-alcohol mixtures (2% to 5% HNO_3) were found to be very rapid and difficult to control. By cooling the nitric-alcohol solution to low temperatures, etching could be accomplished. However, it frequently left the surface of the metal uneven and spotty. The cause of the unevenness could have been the oxidation of the sample by air during the cleaning and drying operation after electropolishing. Therefore, the specimen was etched directly in the cold perchloric-alcohol electrolyte. Since perchloric acid is a strong oxidant, the etching characteristics should be essentially the same as with nitric acid. The perchloric-alcohol etching was accomplished simply by turning off the current and allowing

the specimen to chemically oxidize for a sufficiently long time to reveal the structure. The time required for etching varied from 5 to 10 minutes. In order to re-etch a specimen that was insufficiently etched, it was necessary to electropolish for one minute prior to again chemically etching. All of the rare earth metals available were satisfactorily polished and etched by this procedure. The results of polishing the rare earths are seen in Figures 1 through 14. All specimens were etched before photographing in the -76 °C electrolyte.

Conclusions

The rare earth metals with the exception of promethium and europium have been successfully electropolished in a 1% perchloric acid - methanol mixture at very low temperatures. The mechanism by which polishing occurs appears to be a preferred oxidation reaction with peaks of the scratches oxidizing more readily than the troughs. This oxidation eventually results in a smooth surface. The rare earth metals can be consistently chemically etched in the same electrolyte as used for electropolishing.

Acknowledgments

The authors would like to acknowledge Messrs H. Baker and T. Roth and Miss Sandra Echols who helped with the experimental work in this paper.

References

1. C. P. Madsen: United States Patent 1,562,710 November, 1925.
2. P. A. Jacquet: Nature, Vol. 135, p. 1076, 1935.
3. De Sy and Haemers: Stahl und Eisen, Vol. 61, No. 1, pp. 185-187, 1941.

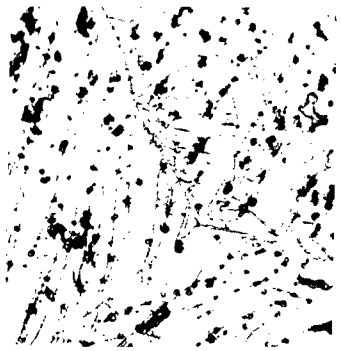

Fig. 1. Yttrium
x 250

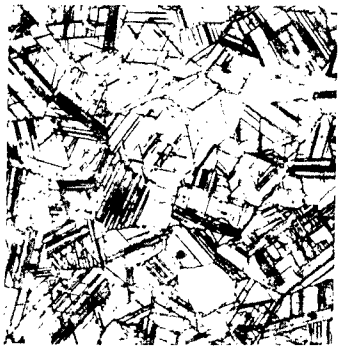

Fig. 2. Lanthanum
x 250

Fig. 3. Praseodymium
x 250

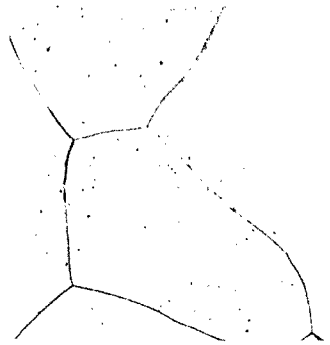

Fig. 4. Neodymium
x 250

Fig. 5. Smarium
x 250

Fig. 6. Gadolinium
x 250

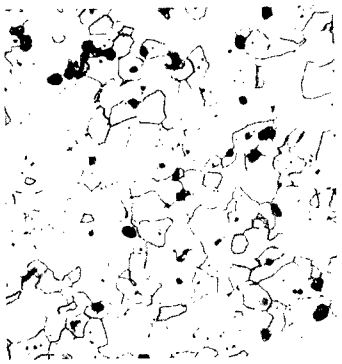

Fig. 7. Terbium
x 250

Fig. 8. Dysprosium
x 250

Fig. 9. Holmium
x 250

Fig. 10. Erbium
x 250

Fig. 11. Thulium
x 250

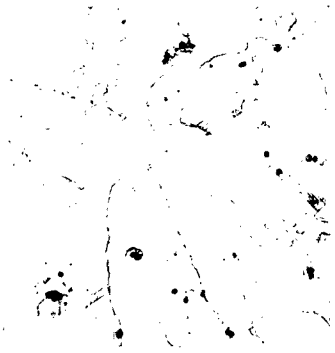

Fig. 12. Ytterbium
x 250

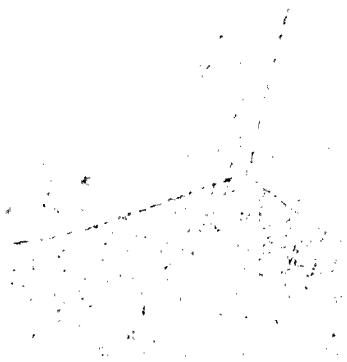

Fig. 13. Lutecium
x 250

Fig. 14. Cerium
x 250

METALLOGRAPHY OF CERAMIC FUEL AND REFRACTORY METAL COMPATIBILITY COUPLES

by

F. E. McGrath, J. A. De Mastry, and M. S. Farkas*

ABSTRACT

The simultaneous compatibility of refractory claddings with UC, UN or UO_2 and liquid lithium or cesium vapor has been determined by metallographic examination of heated compatibility assemblies.

INTRODUCTION

Nuclear thermionic-energy conversion is probably necessary for production of large quantities of electricity in space. Two conversion systems being considered are the in-pile system in which the fuel cladding is the cathode, and the out-of-pile system in which the fuel cladding is utilized for heat transfer to a thermionic systems outside of the reactor.

For the in-pile system, a fuel cladding material must have adequate strength at 2500 to 3400 F, be compatible with the nuclear fuel, be resistant to attack by cesium, and possess reasonable thermionic properties. In the out-of-pile system the fuel cladding will operate with a lithium coolant maintaining the cladding at temperatures up to 2500 F. For this system the fuel cladding must have adequate strength and be compatible with lithium.

* Authors are affiliated with Battelle Memorial Institute, 505 King Avenue, Columbus, Ohio.

The present program[1,2,3]* is aimed at assessing the compatibility of commercial, high-strength, refractory metals with UC, UN and UO_2 at temperatures up to 3400 F. In simultaneous tests the compatibility of these cladding materials with liquid lithium up to 2500 F and with cesium vapor from 2500 to 3400 F is being determined.

This paper is a review of the metallographic techniques utilized in preparing compatibility samples and the results obtained by metallographic examination.

BACKGROUND

Eight cladding materials were initially selected for testing: tungsten, W-0.9Cb, W-15Mo, W-25Re, Ta-12W, TZM (Mo-0.5Ti-0.08Zr), T-111 (Ta-8W-2Hf), and B-66 (Cb-5Mo-5V-1Zr). These are high-strength materials chosen from those refractory metals and alloys now in an advanced state of development. This selection being based on available high-temperature strength data. UC, UN and UO_2 were selected for study because they are the only high temperature compounds currently in use or in development.

In order to conduct simultaneous compatibility tests the test capsule design shown in Figure 1 was used.

Small fuel cans were prepared from 3/8-inch diameter rod, either 3/4 or 1/2 inch long. Holes 1/4 inch in diameter and either 3/8 or 5/8 inch deep were machined in the rods. A great deal of difficulty was encountered in machining some alloys. These were prepared by electric discharge machining. Typical microstructures before testing are shown in Figure 2.

The UC was prepared by arc melting and casting, while both the UN and UO_2 were prepared by powder metallurgy. The pretest microstructures are shown in Figures 3 and 4. Fuel slugs were machined into cylinders 1/4 inch long by 0.249 inch in diameter. The fuel slugs were then inserted into the cans and end caps were secured by heliarc welding. Contact between the fuel and the can is assured by leaving a 0.001 inch clearance. The nuclear fuels expand more than the refractory metal cans at temperature, thereby producing contact between the fuel and the cladding.

The completed, miniature fuel element is then weighed, its dimensions are recorded, it is examined visually, and a photomacrograph is taken prior to loading in a corrosion capsule fabricated from TZM. Figure 5 shows a view of the compatibility assembly prior to loading. The testing schedule for a typical fuel element is outlined as follows.

---

* References are listed at the end of this paper.

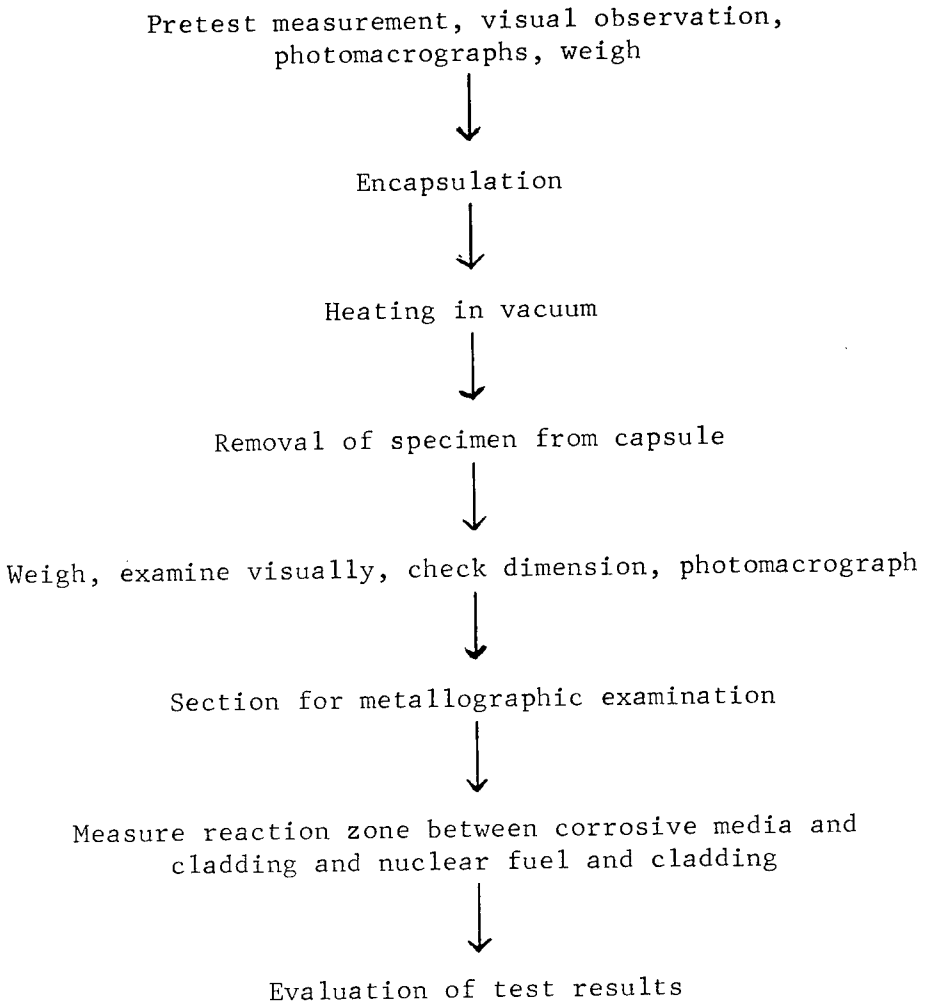

METALLOGRAPHIC SAMPLE PREPARATION

After vacuum heating 100 hours at the desired temperature the corrosion capsules are removed from the furnace and placed in a dry box. The dry box is evacuated and filled with high purity helium through a liquid nitrogen cold trap. The corrosion capsules containing cesium or lithium are cut open with a saw or a SiC cutoff wheel, and the miniature fuel elements are removed.

Mounting and Polishing

The miniature fuel elements are mounted without sectioning. Sectioning with a cutoff wheel breaks up the fuel material and also might fracture brittle interfaces. A negator spring is placed around

the outside of the fuel element to protect the edges and keep them from rounding during the grinding and polishing operation. The fuel element is then mounted in 815 Epon resin. A belt grinder is used to grind almost half way through the mount. The mounts are then vacuum impregnated with Epon. This fills the pores and cracks in the structure with hard plastic permitting retention of material during grinding and polishing.

Mechanical polishing is performed as follows:

(1) Specimens are rough polished to remove grinding scratches on a nylon or silk cloth and a slurry of 400 cc water, 5 grams chromium trioxide, and 50 grams of Linde A polishing abrasive.

(2) The final polish is performed on a wheel covered with Gamal cloth operated at slow speed. A slurry of ferric oxide with 1/2 per cent chromium trioxide in water was applied to the cloth.

(3) The niobium and tantalum alloys need additional polishing on a vibrator using a slurry of 200 cc water, 4 grams chromium trioxide, and 20 grams of Linde B polishing abrasive.

(4) Alloys containing UC were final polished with Linde B in slurry with water on microcloth. In this case chromium trioxide is not used, as it forms a film on UC which inhibits etching.

Etching

Standard etchants are used in most instances. Through experimentation it was found that a solution of 30 lactic, 10 HNO_3, and 10 HF will etch all of the alloys to some degree. Following is a list of etchants that have been used on the different alloys and fuels the proportions listed are by volume.

Tungsten	30 lactic, 10 HNO_3, 10 HF or modified Murakamis reagent
W-Cb	30 lactic, 10 HNO_3, 10 HF or modified Murakamis reagent
W-15Mo	30 lactic, 10 HNO_3, 10 HF or modified Murakamis reagent
W-25Re	30 lactic, 10 HNO_3, 10 HF

Ta-12W	30 lactic, 10 HNO_3, 10 HF for phase identificatipn; 30 H_2O, 30 HNO_3, 30 HF for general structure
T-111	Same as Ta-12W
B-66	50 lactic, 40 HNO_3, 2 HF and 45 H_2O, 30 HCL, 20 HNO_3, 5 HF
TZM	10 per cent H_2SO_4 or 30 lactic, 10 HNO_3, 10 HF
Uranium Carbide	1 HNO_3, 1 acetic acid, 1 H_2O
Uranium Nitride	2 step etch - 50 lactic, 50 HNO_3, then 50 lactic, 50 HNO_3, 10 drops HF
Uranium Oxide	1 H_2SO_4, 10 H_2O_2

Etching of compatibility specimens is usually a problem because of differences in the rate of attack of an etchant on dissimilar materials. In some cases an interface may be properly revealed by very light etching, with additional etching being required to reveal the microstructure of the cladding and fuel. In other cases, to properly reveal the structure of the fuel and cladding, the cladding is etched and examined; and after repolishing the fuel is etched and examined.

RESULTS AND CONCLUSIONS

Results of the metallographic evaluation portion of the compatibility tests are reported herein. Although in some cases unidentified reaction zones were formed, an assessment of the amount of interdiffusion was possible.

Exposure to Cesium

The tungsten, tungsten-base alloys, and the TZM alloy were found to be resistant to attack by cesium up to 3400 F for 100 hours.

A second phase was formed in the Ta-12W alloy at the cesium interface at temperatures as low as 2800 F. Electron probe techniques indicate that either carbides and/or nitrides are present. Figure 6 shows the microstructure exhibited after exposure at 3100 F. The T-111, tantalum-base alloy, exhibited similar effects. It is believed that corrosion by cesium vapor is not occurring; instead impurities in the system are being absorbed by the tantalum alloys.

At 3400 F a large degree of grain growth was exhibited by the W-15Mo and TZM alloys. This grain growth seems to be in excess of that which would be expected from recrystallization and grain growth. This grain growth may be due partly to removal, by the cesium vapor, of impurity atoms which were blocking grain growth. Cesium exposures at 3400 F for 100 hours are shown in Figure 7.

Exposure to Lithium

Exposures of 100 hours at 2800 F in lithium indicate that no reaction zone or grain boundary penetration occurred with tungsten, tungsten-base alloys or TZM (see Figure 8). The Ta-12W and the B-66 alloys exhibit definite attack when exposed under the above conditions. It is believed that the attack is due to pickup of impurities from the lithium.

Compatibility of Tungsten and Tungsten-Base Alloys with UC, UN and UO_2

Tungsten and tungsten-base alloys are generally compatible with hyperstoichiometric UC for 100 hours at 2800 F. At 3100 F slight reaction zones are formed with all of the tungsten claddings. An example is shown in Figure 9. The reaction zone appears to grow by depletion of the excess carbon in the UC. When the stoichiometric UC composition is reached, the reaction zone ceases to grow. Limited study was performed at 3400 F. At this temperature it was found that the W-15Mo alloy reacted with the UC. Figure 10 shows this reaction and indicates that liquid uranium was formed.

The tungsten and tungsten-base alloys exhibited no reaction with UN, after 100 hours at 3100 F. Figure 11 shows the W-0.9Cb alloy with a UN core after heating at 3100 F for 100 hours. No reaction zone is evident.

Compatibility of UO_2 with tungsten and tungsten-base alloys was assessed to temperatures up to 3400 F. No reaction zones were formed, as illustrated by Figure 12, showing W-0.9Cb in UO_2 after heating for 100 hours at 3400 F.

Compatibility of the Tantalum-Base Alloys with UC, UN and UO_2

At 2500 F reaction was noted between hyperstoichiometric UC and Ta-12W and T-111 after 100 hours. The reaction with T-111 being more severe. The reaction zone between Ta-12W and UC at 2800 F is →

shown in Figure 13. The reaction zone has been identified as TaC and Ta_2C. The depletion of carbon from the UC gives rise to the formation of free uranium.

The compatibility of UN with tantalum-base alloys was studied. The Ta-12W alloy did not show reaction with UN until after 100 hours at 2800 F. However, the same time at 3100 F was severe enough to cause a large reaction zone as shown in Figure 14. The clad contains a heavy intergranular precipitate believed to be nitride, and liquid uranium formation is evident near the original core-cladding interface. The T-111 alloy has yet to be studied at 2800 and 3100 F. The Ta-12W alloy did not react with UO_2 at 3100 F.

Compatibility of the Molybdenum-Base Alloys with UC, UN and UO_2

No reaction zones were formed between TZM and UC after 100 hours at 3100 F. This is shown in Figure 15.

TZM and UN exhibit good compatibility up to and possibly above 3100 F, where faint and questionable reaction zone is formed. After 100 hours at 3400 F a faint zone appears and is shown in Figure 16. Also noteworthy is the massive grain size exhibited by the TZM.

UO_2 did not react with TZM after 100 hours at 3400 F.

Compatibility of the Niobium-Base Alloys with UN, UC and UO_2

A severe reaction occurred between UC and B-66 at 2500 F, the lowest test temperature. Figure 17 exhibits this. Note the free uranium present in the interstices of the UC grains and compounds in the reaction zone.

B-66 and UN react at 2500 F as shown in Figure 18. A heavy precipitate of nitride is seen in the cladding, except for the grains immediately adjacent to the cladding. Grain boundary penetration into the B-66 is also evident.

No reaction zone was formed between B-66 and UO_2 at 2500 F.

SUMMARY

Tentative conclusions may be drawn on the basis of metallographic examination of compatibility couples heated for 100 hours. They are:

(1) In cesium vapor tungsten, tungsten-base alloys and TZM perform well at 3400 F.

(2) In lithium at temperatures up to 2500 F tungsten, tungsten-base alloys and TZM are compatible.

(3) Tungsten and tungsten-base alloys exhibit limited compatibility with hyperstoichiometric UC. Excess carbon migrates to the core cladding interface to form a reaction zone. However, when this excess carbon is depleted the reaction appears to stop. Tungsten and tungsten-base alloys appear to be compatible with UN at 3100 F and UO_2 at 3400 F.

(4) The tantalum-base alloys react with UC at 2500 F to form a zone containing Ta_2C and TaC, the depletion of carbon from the UC giving rise to free uranium. At 2800 F UN and Ta-12W react to form liquid uranium, but this alloy does not react with UO_2 at 3100 F.

(5) The molybdenum-base alloy, TZM, does not react with UC and UN at 3100 F or UO_2 at 3400 F.

(6) The niobium-base alloy, B-66, reacts with UC and UN at 2500 F, but does not react with UO_2 at the same temperature.

REFERENCES

(1) "Investigation on High-Temperature Refractory Metals and Alloys for Thermionic Converters:, First Quarterly Progress Report by J. A. De Mastry. Contract No. AF 33(657)-10404, Task Number 817305-22, April 3, 1963.

(2) "Investigation on High-Temperature Refractory Metals and Alloys for Thermionic Converters", Second Quarterly Progress Report by J. A. De Mastry. Contract No. AF 33(657)-10404, Task Number 817305-22, July 5, 1963.

(3) "Investigation on High-Temperature Refractory Metals and Alloys for Thermionic Converters", Third Quarterly Progress Report by J. A. De Mastry. Contract No. AF 33(657)-10404, Task Number 817305-22, October 5, 1963.

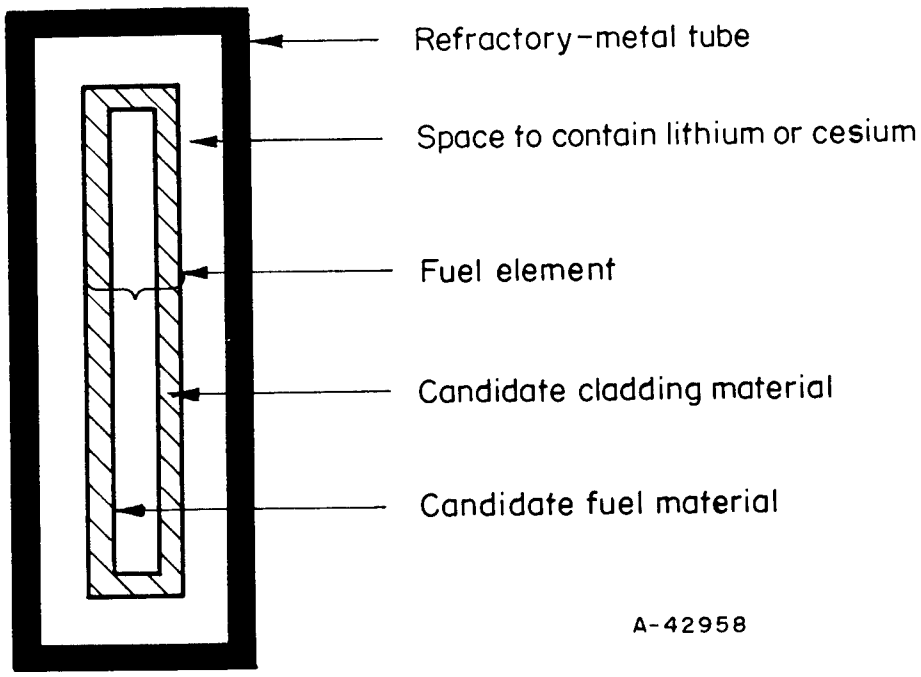

FIGURE 1. CAPSULE FOR CORROSION AND COMPATIBILITY STUDIES.

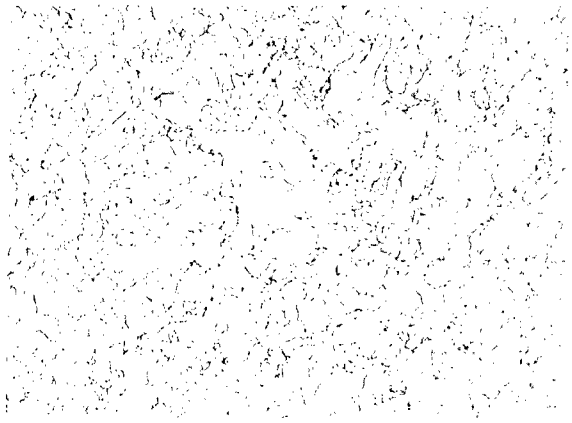

250X

a. Mo-0.5Ti-0.08Zr Alloys Stress Relieved 1/2 hr. at 2250 F

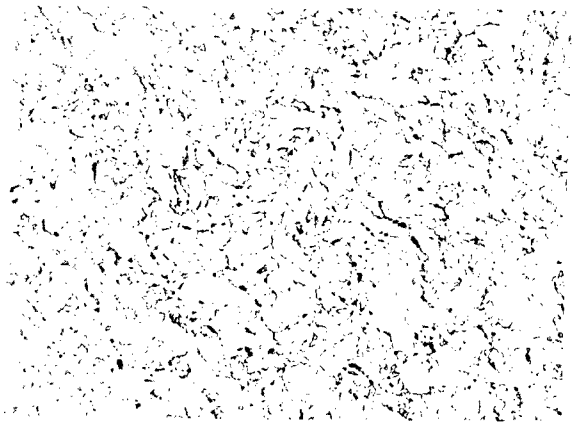

250X

b. Tungsten - Worked Structure

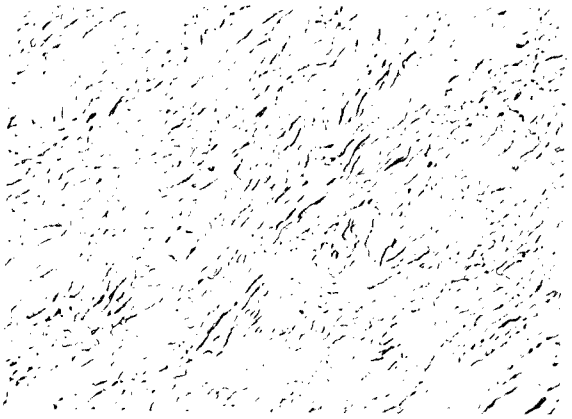

250X

c. Ta-10W - Clean, Heavily Worked Structure

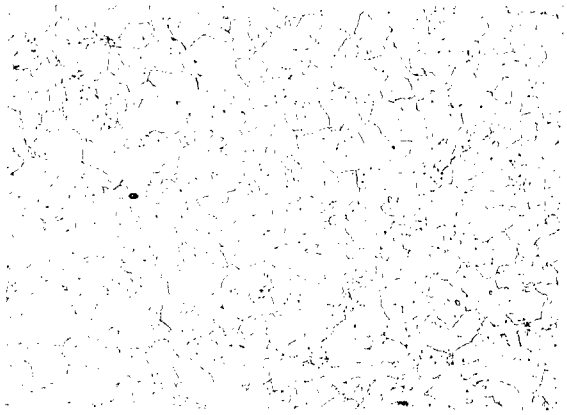

250X

d. W-25Re Alloy - Clean Structure

FIGURE 2. MICROSTRUCTURES OF AS RECEIVED CLADDING MATERIALS.

250X $UC_{4.75}$

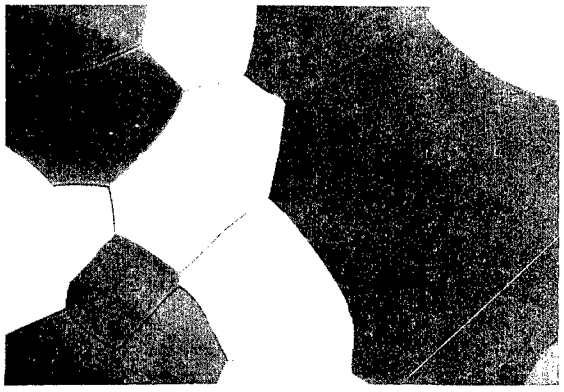

250X $UC_{4.8}$

250X $UC_{4.85}$

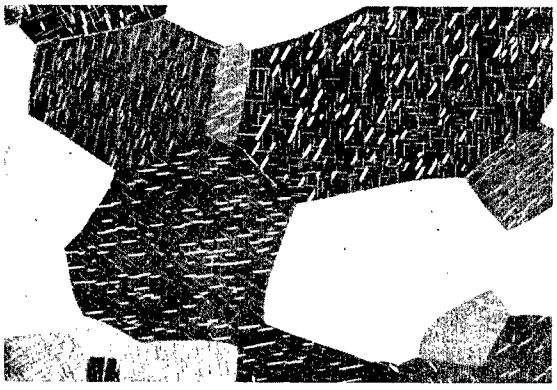

250X $UC_{4.9}$

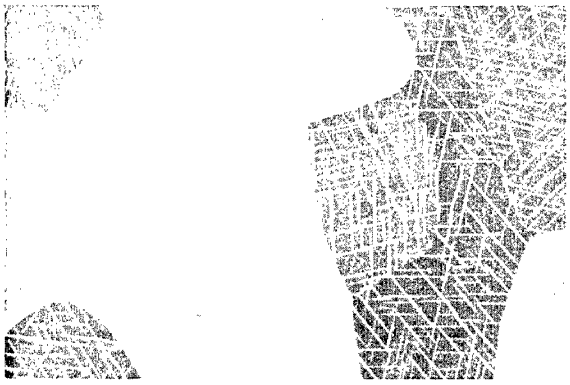

250X $UC_{5.0}$

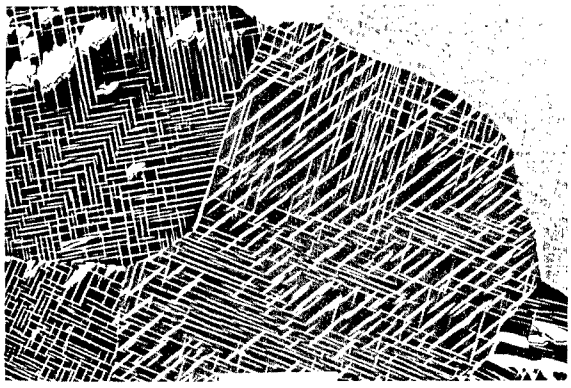

250X $UC_{5.2}$

FIGURE 3. TYPICAL MICROSTRUCTURE OF URANIUM CARBIDE SHOWING DIFFERENCES IN STRUCTURE DUE TO CARBON CONTENT.

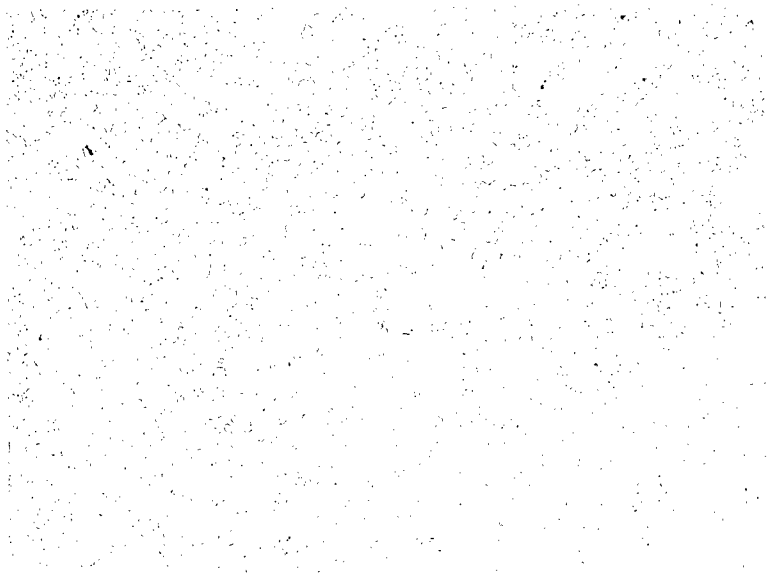

100X

a. Etched (90 per cent H_2O_2, 10 per cent H_2SO_4) microstructure of UO_2.

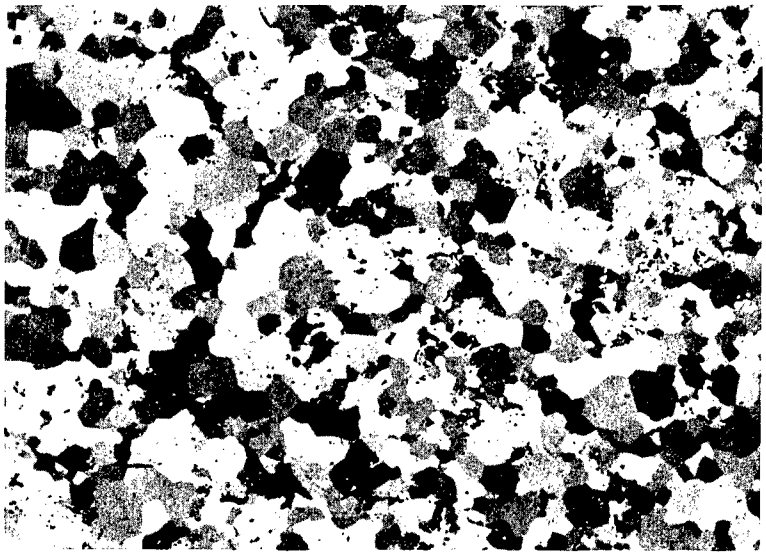

250X

b. Microstructure of UN with UO_2 and U_2N_3 impurities present.

FIGURE 4. AS FABRICATED FUELS.

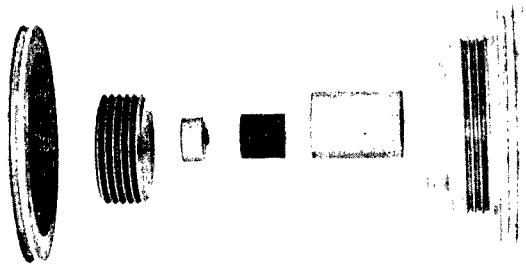

1X

FIGURE 5. EXPLODED VIFW OF CORROSION AND COMPATIBILITY ASSEMBLY. Components, from left to right, are TZM lid, fuel-element lid, fuel slug, fuel-element can, and outer can of TZM.

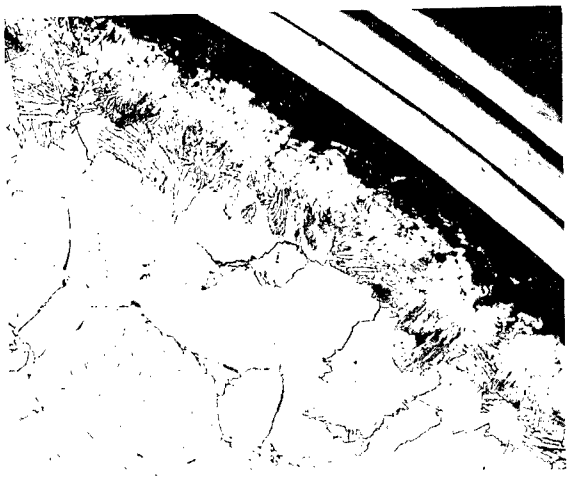

50X

a. View of surface in contact with cesium showing reaction zone; specimen had UC core.

100X

b. Surface reaction in contact with cesium; specimen had UN core.

FIGURE 6. Ta-12W ALLOY AFTER EXPOSURE TO CESIUM AT 3100 F.

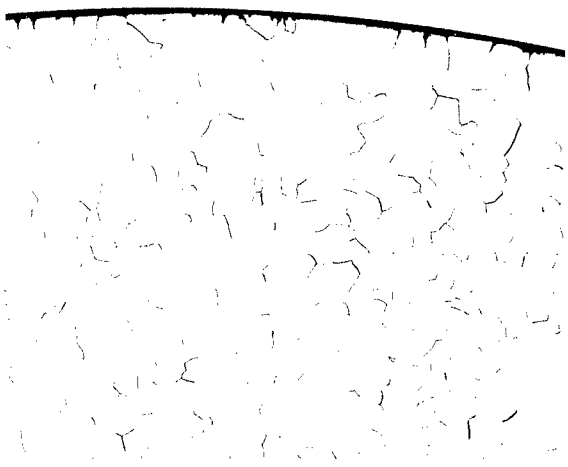

50X Tungsten

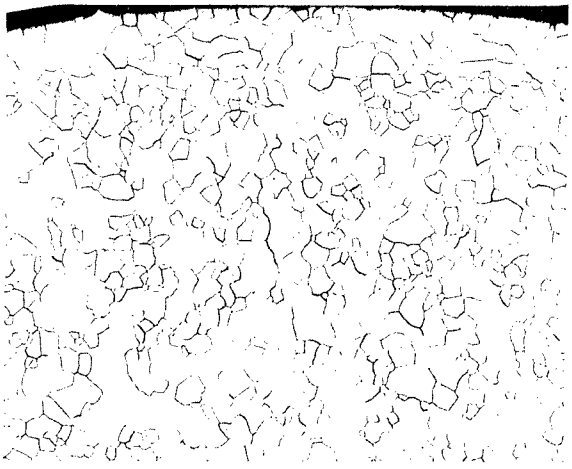

50X W-0.9Cb

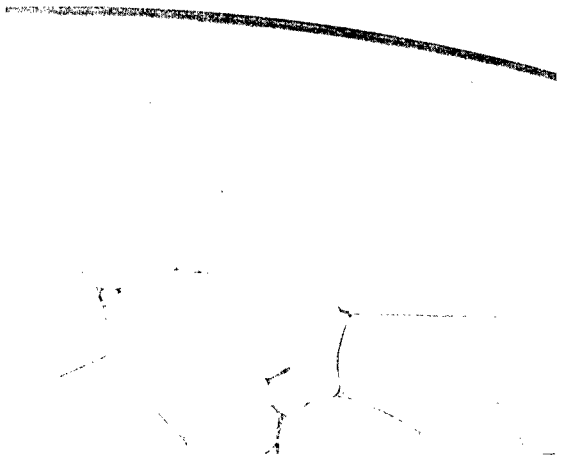

50X W-15Mo

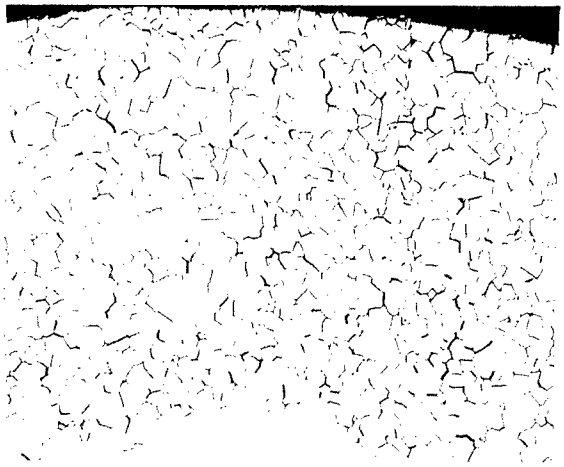

50X W-25Re

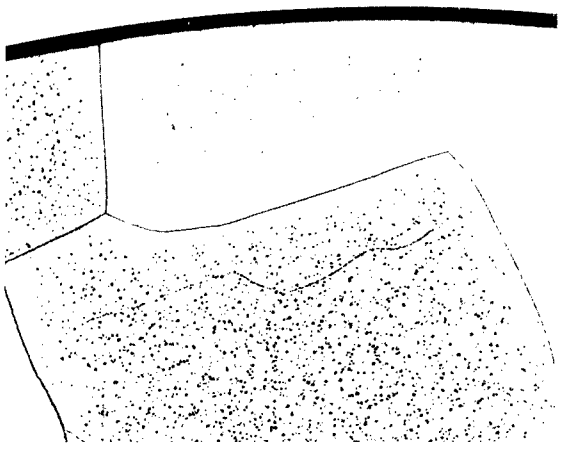

50X TZM

FIGURE 7. CLADDING AFTER EXPOSURE TO CESIUM VAPORS FOR 100 HOURS AT 3400 F.

150X Tungsten

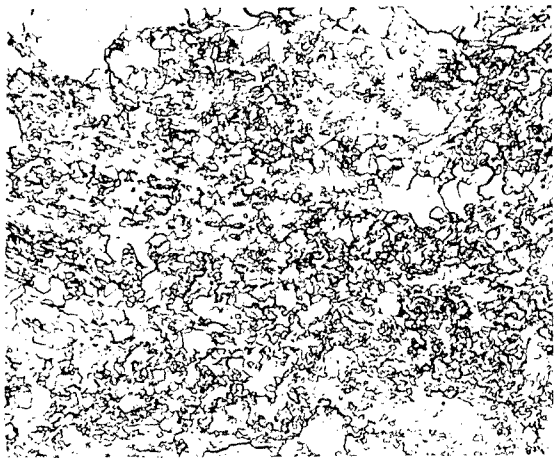

150X W-0.9Cb

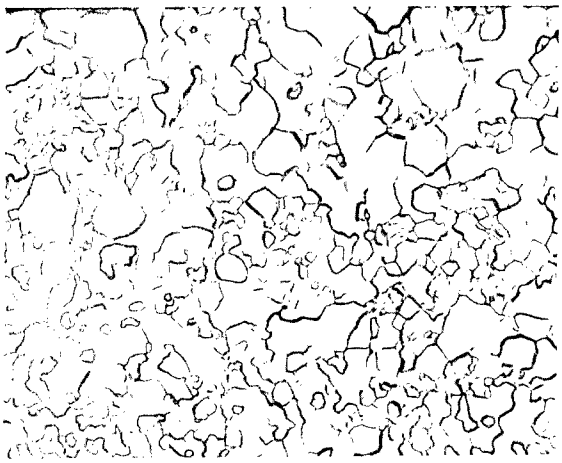

150X W-15Mo

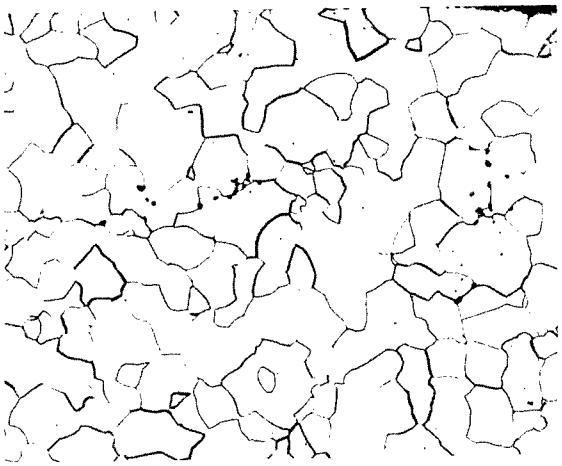

150X W-25Re

150X Ta-12W

150X B-66 (Nb-Mo-V-Zr)

FIGURE 8. AFTER EXPOSURE TO LITHIUM FOR 100 HOURS AT 2800 F.

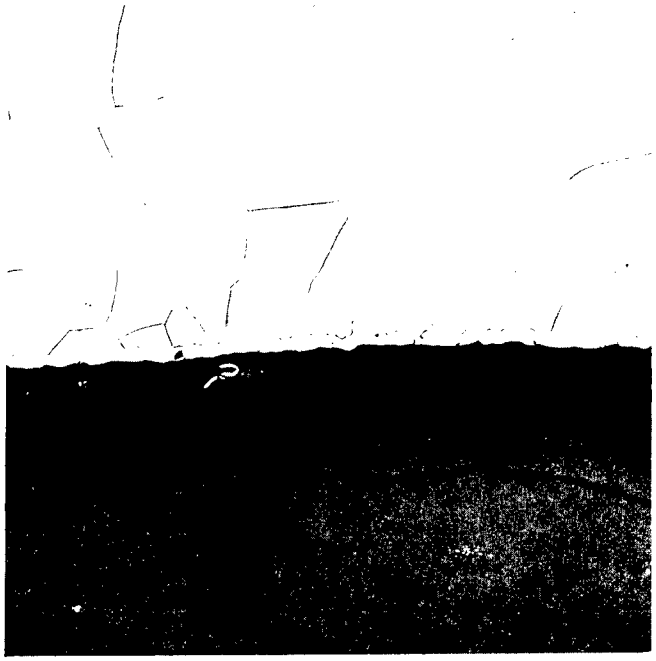

250X

FIGURE 9. TUNGSTEN IN CONTACT WITH UC AFTER 100 HOURS AT 3100 F.

250X

FIGURE 10. W-15Mo IN CONTACT WITH UC AFTER 100 HOURS AT 3400 F.

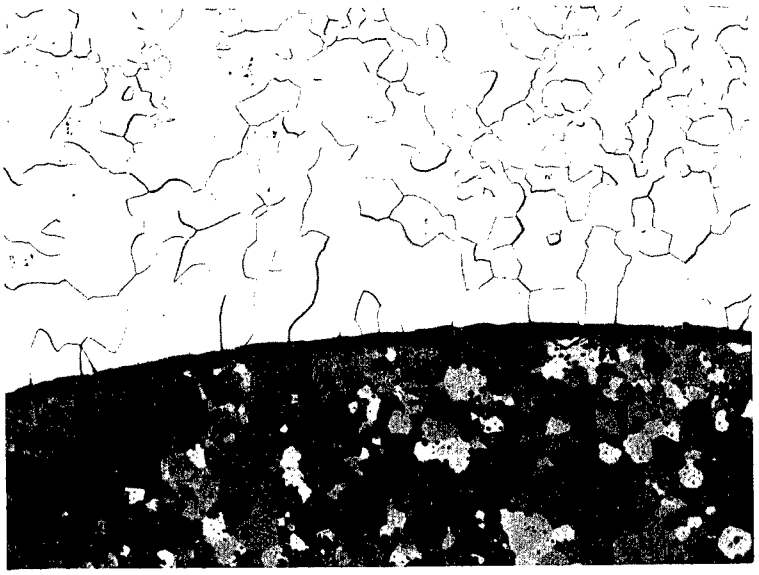

100X

FIGURE 11. W-0.9Cb ALLOY IN CONTACT WITH UN AFTER 100 HOURS AT 3100 F.

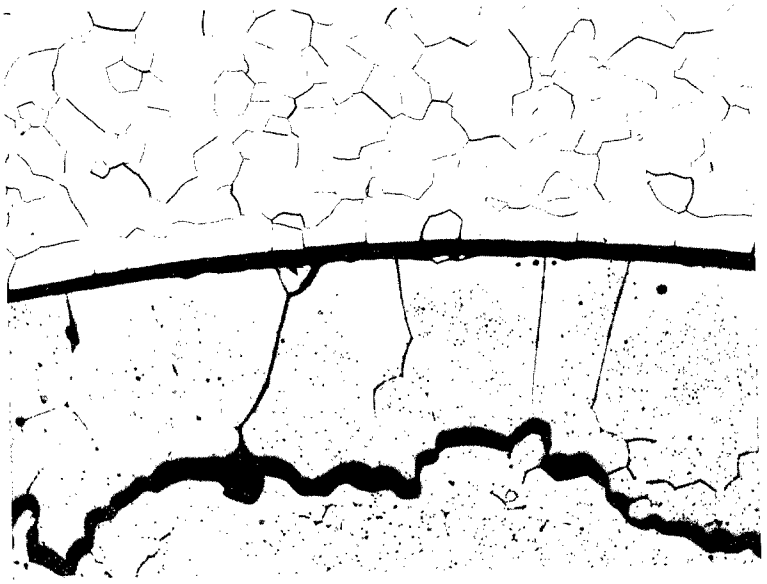

100X

FIGURE 12. W-0.9Cb ALLOY IN CONTACT WITH UO_2 AFTER 100 HOURS AT 3400 F.

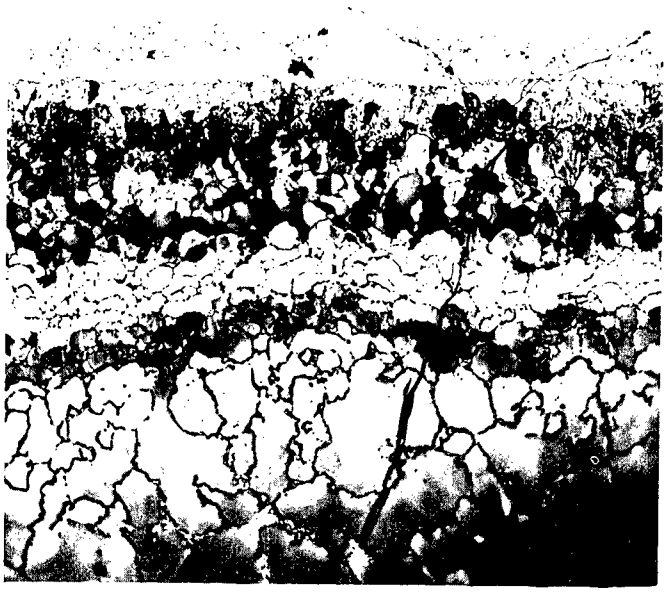

250X

FIGURE 13. Ta-12W ALLOY IN CONTACT WITH UC AFTER 100 HOURS AT 2800 F.

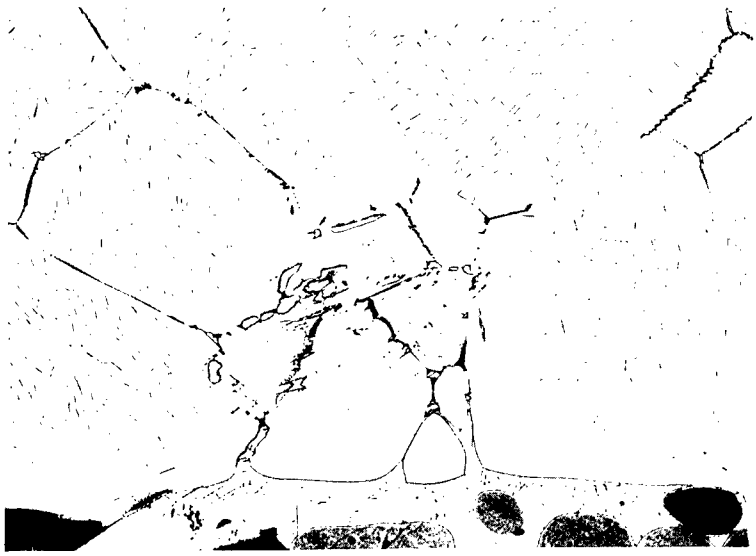

100X

FIGURE 14. Ta-12W ALLOY IN CONTACT WITH UN AFTER 100 HOURS AT 3100 F.

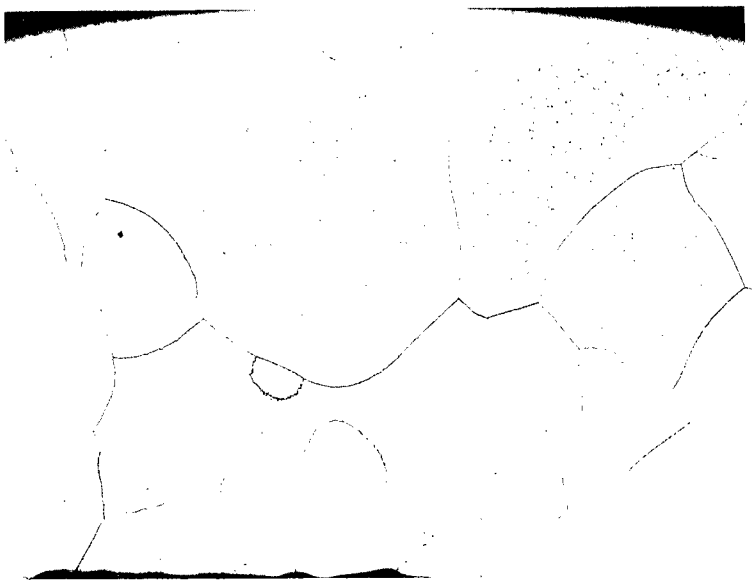

50X

FIGURE 15. TZM ALLOY IN CONTACT WITH UC AFTER 100 HOURS AT 3100 F.

100X

FIGURE 16. TZM ALLOY IN CONTACT WITH UN AFTER 100 HOURS AT 3400 F.

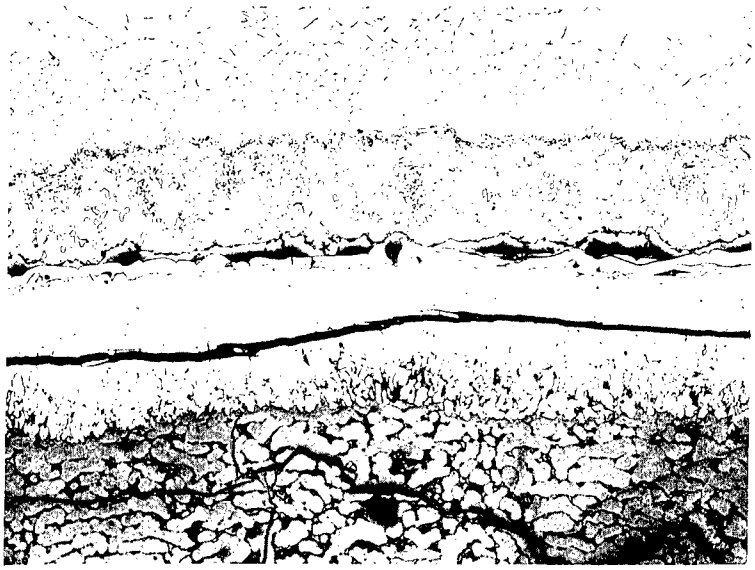

100X

FIGURE 17. B-66 IN CONTACT WITH UC AFTER 100 HOURS AT 2500 F.

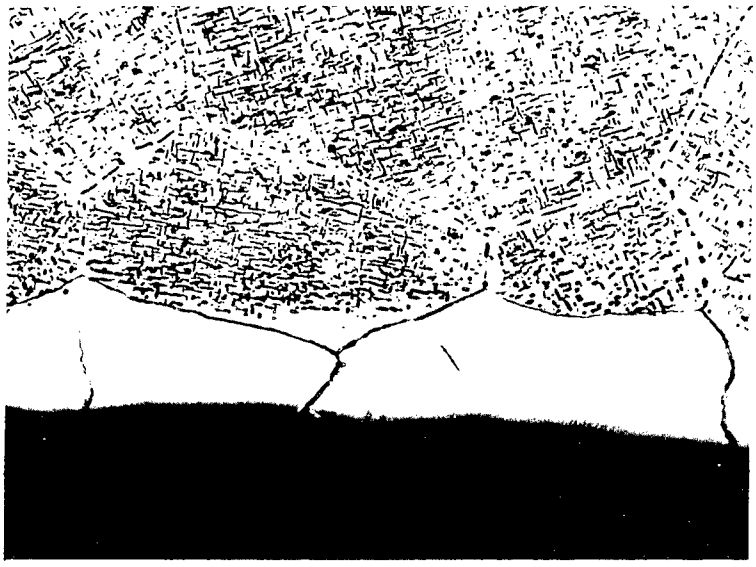

250X

FIGURE 18. B-66 IN CONTACT WITH UN AFTER 100 HOURS AT 2500 F.

METALLOGRAPHIC PREPARATION OF DICARBIDES OF THORIUM AND THORIUM-URANIUM*

T. M. Kegley, Jr. and B. C. Leslie
Metals and Ceramics Division
Oak Ridge National Laboratory

ABSTRACT

Because of the strong tendency of ThC_2 and $(Th,U)C_2$ to hydrolyze, special techniques were required to metallographically prepare these carbides. Procedures developed included vibratory polishing inside a dry box and mechanical polishing outside a dry box. Pyrolytic carbon-coated particles and arc cast specimens were prepared using these procedures.

Instead of the customary air etching, specimens were etched by immersing 1-5 min in 1:1 HNO_3-H_2O. The 1:1 HNO_3-H_2O solution passivates the polished surface presumably by forming a protective film which prevents reaction with moisture during the period required for microscopic observation and photomicrography. Short periods ($\frac{1}{2}$ to 1 min) of immersion in the 1:1 HNO_3-H_2O solution produced a passivated surface, while longer periods (5 to 45 min) etched the dicarbide specimens. Polarized light was particularly effective for observing the twinned structures of the dicarbides.

*Research sponsored by the U.S. Atomic Energy Commission under contract with the Union Carbide Corporation.

INTRODUCTION

At Oak Ridge National Laboratory, metallography has played an important role in the investigation of coated fuel particles for use in graphite fuel elements for gas-cooled reactors.[1,2,3,4] This investigation included thorium-uranium carbides in view of their possible application as breeder materials. This paper describes the methods developed at ORNL for preparing these carbides metallographically.

Since carbides which contain thorium react readily with moisture, special techniques are necessary in the metallographic preparation of these carbides. Techniques reported by others[5,6,7] employ cloth covered polishing wheels with the polishing abrasive suspended in a non-aqueous medium. In one instance, carbide specimens were prepared in an inert gas atmosphere maintained in a glove box.[7]

In recent years vibratory polishing has been established as an excellent method for preparing samples metallographically.[8] Vibratory polishing is particularly effective for preparing specimens containing hard and soft constituents such as carbides and graphite. At ORNL vibratory polishing is used extensively; consequently, a natural development was its extension to the polishing of carbides of uranium and thorium. Indeed, pyrolytic carbon-coated uranium carbide particles have been vibratorily polished quite successfully using alumina abrasive and silicone oil.[9] However, techniques used for uranium carbide specimens were not successful with thorium-containing carbide specimens because these specimens reacted with moisture from the room air surrounding the vibratory polisher.

The procedures developed for preparing these thorium-containing carbide specimens included vibratory polishing within a dry box and mechanical polishing oustide a dry box. Specimens were etched and/or passivated by immersion in a nitric acid-water solution. Specimens prepared included unsupported pyrolytic-carbon-coated carbide particles, graphite spheres containing pyrolytic-carbon-coated carbide particles, and arc cast carbide specimens. The compositions of the specimens included ThC_2, and $(Th,U)C_2$ with the composition varying from a Th/U ratio of 7 to a U/Th ratio of 9.

INITIAL EXPERIENCE

At first we believed that the procedures for vibratorily polishing pyrolytic carbon-caoted UC_2 particles were adequate for handling $(Th,U)C_2$ particles of 0.6 Th/U ratio since the first few of these particles had been prepared successfully using these procedures. Later it became apparent that these procedures were not adequate since the specimens sometimes reacted during the vibratory polishing step. We found

that by placing the vibratory polisher in a dry box these $(Th,U)C_2$ particles could be polished consistently without reaction occurring. Figure 1 shows two coated $(Th,U)C_2$ particles from the same batch; one particle was prepared with the vibratory polisher in the room atmosphere, the other particle was prepared with the vibratory polisher in a dry box. In spite of the relatively low thorium content of the $(Th,U)C_2$ and even though silicone oil was employed as the abrasive vehicle, the $(Th,U)C_2$ particle vibratorily polished in the room atmosphere has reacted. The other $(Th,U)C_2$ particle which was vibratorily polished in a dry box has not reacted.

POLISHING PROCEDURES

Two different procedures were developed for polishing the specimens; one employing vibratory polishing inside a dry box and the other mechanical polishing outside outside a dry box. Vibratory polishing has the advantage that a greater number of specimens can be processed with less attention than can be processed by mechanical polishing. Also vibratory polishing generally produces a better quality polish than mechanical polishing; that is, there are fewer scratches and a flatter surface is produced on a vibratorily polished specimen. Mechanical polishing has the advantage that a single specimen can be prepared much faster than by vibratory polishing. Also the mechanical polishing procedure does not require a dry box.

The preliminary mounting and grinding steps for both procedures were performed outside the dry box.

Mounting and Grinding

The specimens, which were mounted in epoxy resin,* were ground on 320, 400, and 600 grit silicon carbide papers using either silicone oil or absolute ethyl alcohol as lubricants. Silicone oil** and ethyl alcohol were found to be equally satisfactory as lubricants.

Vibratory Polishing Procedure

Since vibratory polishing of ThC_2 and $(Th,U)C_2$ requires a dry box, perhaps a description of the dry box employed would be useful.

---

*"Araldite" epoxy resin manufactured by Ciba Products Corporation, Fairlawn, New Jersey.

**Dow-Corning 702 Diffusion Pump Fluid.

Dry Box

The most desirable box would be a vacuum box which could be evacuated and filled with an inert gas. Since such a box was not immediately available, a containment box 6 ft long, 3 ft deep and approximately 23 ft^3 in volume was used. Figure 2 shows the particular dry box employed in preparing the specimens. The air within the box was dried with a commercially available silica gel desiccant.* About 1 lb of silica gel was placed in the box and after the initial drying, replaced at about one to two week intervals. The silica gel was regenerated for reuse by heating at 150°C. The relative humidity of the air inside the dry box measured about 15% as compared to a relative humidity of 55-65% for air outside the dry box.

Although we would have preferred an air lock arrangement for transferring specimens to and from the dry box, we were forced to transfer the specimens through one of the glove ports. During a transfer the rubber gloves covering a port were removed for a period as brief as possible so as to minimize contamination of the dry air in the box from moisture in the room air.

Vibratory Polishing

The specimens were prepared in the dry box by means of a 12-in. diameter vibratory polisher. Before being placed in the bowl of the polisher, specimens were capped with stainless steel holders to provide the necessary weight (~ 370 g) for polishing. Specimens were polished 6-18 hr using a slurry of 10 g of 0.3 μ alumina and 100 ml of silicone oil on a nylon cloth which was secured at the bottom of the polishing bowl. Further preparation was performed outside the dry box, but to retard reaction with moisture, a film of silicone oil was allowed to remain on the polished surface.

Mechanical Polishing Procedure

The specimens were first rough polished using a suspension of 0.3 μ alumina and absolute ethyl alcohol on a variable speed wheel covered with nylon cloth. The polishing wheel was operated at low speeds (100-200 rpm) to retain abrasive on the wheel as much as possible. About 3 min were required for rough polishing.

Final polishing was done using $\frac{1}{2}$ μ diamond paste on a variable speed wheel again operated at low speed. The wheel used in this step was covered with

*"Tel-Tale" silica gel manufactured by Davison Chemical Division, W. R. Grace & Company., Baltimore, Maryland.

Metcloth,* which seemed to leave fewer scratches than nylon cloth. The diamond paste was used without thinner. The final polishing step of about 3 min was necessary in order that graphite contained in some of the carbide specimens would be retained and polished.

ETCHING

Before the microstructure can be studied, a means must be available for revealing the microstructure in the polished specimens. Investigators[5,6,7] have frequently resorted to air etching as a means for revealing the microstructure of ThC_2 and $(Th,U)C_2$ of greater than 30 wt % ThC_2 (0.43 Th/U ratio). Air etching results from the exposure of polished surfaces of the carbides to moisture contained in the ambient air. These carbides may also be etched by the small amount of residual moisture contained in a glove box or even by moisture contained in optical immersion oil. Since moisture from the air reacts continuously with the carbide specimens, the specimens must be observed at an early stage before the polished surface has deteriorated. An example of an air etched specimen is given in Fig. 3, which is a photomicrograph of a pyrolytic carbon-coated $(Th,U)C_2$ particle with a Th/U ratio of 2.2.

Rather than air etching, we immersed freshly polished specimens in a 1:1 HNO_3-H_2O solution. A short period of immersion in this solution places a passive film on the specimen which prevents reaction with moisture, at least during the period required for visual observation and photomicrography. The HNO_3-H_2O solution may also be used to etch the carbide specimens by lengthening the period of immersion.

To illustrate the passivating and etching techniques, a pyrolytic carbon-coated $(Th,U)C_2$ particle of 2.2 Th/U ratio composition was selected from the same batch as the air etched particle shown in Fig. 3. This carbide particle was first passivated by immersing 30 sec in 1:1 HNO_3-H_2O. Figure 4a illustrates the bright metallic appearance of the passivated surface. The particle was then immersed again for $4\frac{1}{2}$ min in the same solution, after which the particle had the etched appearance as shown with bright field illumination in Fig. 5a. The longer immersion apparently thickened the film sufficiently that interference colors were found which varied with the orientation of the substrate. Figure 5b shows the same etched particle with polarized light illumination. Polarized light illumination particularly accents the twinning which occurs in the ThC_2 and $(Th,U)C_2$ specimens. It should be pointed out, however, that polarized light illumination would have shown the twinned structure equally as well had the particle been in the passivated condition shown in Fig. 4a. Finally, the specimen was vibratory polished 30 min in the room atmosphere, after which the particle appeared air etched as in Fig. 4b.

---

*Napless cotton cloth from Buehler, Ltd., Chicago, Illinois.

An important point should be noted. In order for the passivating and etching treatments to be effective, the active polished surface should not be exposed directly to room air. Hence, immediately after polishing the specimens were washed in absolute ethyl alcohol to remove any oil and immersed in the nitric acid solution before the alcohol evaporated completely from the polished surface. In other words, the polished specimen should not be allowed to dry in air before a passive film has been placed on it. After immersion in the nitric acid solution the specimens may be washed with absolute ethyl alcohol and dried with an air drier.

Passivating with HNO_3-H_2O

At first, ThC_2 specimens were passivated by either swabbing with or immersing in concentrated HNO_3. Later because the concentrated HNO_3 reacted with the epoxy mounting material, a 1:1 HNO_3-H_2O solution was chosen for passivating. A 1 min immersion period was chosen for passivating the ThC_2 although a shorter period might have been sufficient. A 1:1 HNO_3-H_2O solution and a 1 min immersion period were also used with $(Th,U)C_2$ specimens, except that with specimens of 2.2 Th/U ratio or less it was necessary to use a shorter period in order not to etch the specimen.

The passivating treatment presumably forms a protective film on the surface which prevents or retards reaction with moisture. It should be emphasized that this treatment gives only limited protection, although the film gives sufficient protection from moisture for the period of an hour or so required for microscopic observation. Passivated ThC_2 specimens containing graphite flakes appeared to be much more reactive with moisture than passivated specimens containing no graphite. Apparently the graphite flakes disturb the continuity of the film so that it is less protective.

Etching with nitric acid solutions, which will be mentioned subsequently, also passivates since the film formed during etching gives the same limited protection noted for passivated specimens.

Since the passivating and etching treatments gave only limited protection, specimens after examination were stored in desiccators. Desiccator storage appeared to be adequate except for graphite-containing specimens of ThC_2 and $(Th,U)C_2$ of 7 Th/U ratio. These graphite-containing specimens required a layer of petroleum jelly or silicone grease to prevent reaction during storage. It might be pointed out that grease seemed to offer better protection than liquids such as silicone oil, kerosene, ethylene glycol, and ethyl alcohol.

Etching with HNO_3-H_2O

Etching of thorium and uranium carbides by immersion in nitric acid solutions depends not so much upon the preferential removal of material, such as from grain

boundaries or from grains of particular orientations, but rather it depends upon the color contrast developed on the polished surface through the formation of an oxide film. Interference colors produced in the oxide film vary directly with the structure of the substrate.

With the exception of ThC_2 and $(Th,U)C_2$ of 7 Th/U composition, the specimens were etched by immersing 5 min in freshly prepared 1:1 HNO_3-H_2O. A freshly prepared solution was used each time since much brighter colors were obtained with a freshly mixed solution. By lengthening the immersion period to 45 min, ThC_2 and $(Th,U)C_2$ of 7 Th/U composition were etched, although the colors developed were much less brilliant than those developed in specimens containing more uranium. As Fig. 6 illustrates, the microstructure of etched ThC_2 is revealed much better with polarized light illumination than with bright field illumination. Polarized light is particularly effective for revealing the twinned structure of ThC_2 and $(Th,U)C_2$. Generally, the brilliance of the colors developed by the HNO_3-H_2O etchant increases as the uranium content of the $(Th,U)C_2$ increases.

Etching with HNO_3-CH_3COOH-H_2O

Uranium carbides are usually etched by immersing in a solution of equal parts HNO_3(70%), CH_3COOH (glacial), and H_2O. Pyrolytic carbon-caoted $(Th,U)C_2$ particles of 0.6 Th/U composition, when etched with this solution, require 5 min immersion as compared with 20-30 sec for UC_2. A passivated surface can be produced with this solution for all compositions of $(Th,U)C_2$, but only specimens with Th/U ratios below 1 develop sufficient color contrast for observation with bright field illumination. For the same period of immersion, specimens immersed in 1:1:1 HNO_3-CH_3COOH-H_2O are less brilliantly colored than those immersed in 1:1 HNO_3-H_2O.

RESULTS

Specimens which were prepared included unsupported pyrolytic carbon-coated particles, fueled graphite bodies and arc cast material. To illustrate the results obtained, microstructures of some of these specimens are presented in Figs. 7 to 15.

Examples of pyrolytic carbon-coated particles are presented in Figs. 7 to 9. Figure 9 shows two coated particles which were embedded in a fueled graphite sphere.

Arc cast specimens of both ThC_2 and $(Th,U)C_2$ were metallographically prepared. Microstructures of arc cast ThC_2 and arc cast $(Th,U)C_2$ with Th:U ratios of 7:1, 3:1, 1:1, 1:3, and 1:9 are presented in Figs. 10 to 15. The characteristic twinned

structure was observed in both the ThC_2 and $(Th,U)C_2$ structures. All the arc cast $(Th,U)C_2$ structures contained excess graphite.

Except for the presence of excess graphite and small amounts of impurities, all the $(Th,U)C_2$ compositions exhibited a single phase.

As Figs. 6 and 10 show, a complex pattern of twins and cross twins was observed in the ThC_2 microstructure. Such a complex pattern is difficult to explain; it was suggested that at least part of the twinning observed might be due to the metallographic procedure. To eliminate grinding and mechanical polishing effects, the ThC_2 was electrolytically polished with a solution of 1:1 glacial acetic acid-ortho phosphoric acid (70 %) by applying a direct current at 35 v for 1 min. After the ThC_2 was electrolytically polished, the same complex pattern of twins was observed. Thus the complex pattern observed in the arc cast ThC_2 specimen appears to be a true one.

The twinning observed in ThC_2 may be related to the transition (occurring at 1415 ± 10°C) from the high temperature face-centered cubic form to the low temperature monoclinic form which Cavin and Hill[10] reported.

CONCLUSIONS

1. Satisfactory methods were developed for vibratorily and mechanically polishing dicarbides of thorium and thorium-uranium despite a strong tendency of these carbides to hydrolyze. Specimens were vibratorily polished within a dry box using 0.3 μ alumina abrasive, silicone oil, and nylon cloth. Specimens were mechanically polished by rough polishing with a suspension of 0.3 μ alumina in ethyl alcohol on nylon cloth and final polishing with $\frac{1}{2}$ μ diamond compound on Metcloth.

2. Instead of the customary air etching, specimens of ThC_2 and $(Th,U)C_2$ were passivated and etched by immersion in 1:1 HNO_3-H_2O. Advantages of this technique over air etching were:

   a. The microstructures developed by the nitric acid etchant are considerably clearer and more definitive than those developed by air etching.

   b. The ThC_2 and $(Th,U)C_2$ specimens can be observed in open air without the necessity of immersing the specimens under oil to prevent reaction with moisture.

   c. Specimens etched or passivated with nitric acid solutions can be examined more deliberately than air etched specimens which must be examined hurriedly because of continued reaction with moisture.

ACKNOWLEDGEMENTS

The authors wish to thank J. L. Cook, N. A. Hill, and E. S. Bomar of the Ceramics Group, and Mildred Bradley of the Chemical Technology Division for supplying the specimens as well as for their encouragement of this work.

We especially wish to thank R. J. Gray, F. L. Carlsen, Jr., and C. J. McHargue for their constructive appraisal and review of this report.

REFERENCES

1. W. O. Harms, "Coated-Particle Fuel Development at the Oak Ridge National Laboratory," Proceedings of a Symposium Held at Batelle Memorial Institute, November 5,6, 1962, USAEC Report TID-7654 (1963), pp 72-79.

2. F. L. Carlsen, Jr., E. S. Bomar, and W. O. Harms, "Development of Fueled Graphite Containing Pyrolytic-Carbon Coated Particles for Nonpurged, Gas-Cooled Reactor Systems," presented at American Nuclear Society Meeting in New York, November, 1963, to be published in Nuclear Science and Engineering.

3. P. E. Reagan, F. L. Carlsen, Jr., and R. M. Carroll, "Fission-Gas Release from Pyrolytic-Carbon-Coated Fuel Particles During Irradiation," Nuclear Science and Engineering, 18, 301-318 (1964).

4. E. S. Bomar and R. J. Gray, "Thorium-Uranium Carbides for Coated Particle Graphite Fuels," in Nuclear Metallurgy, vol X, American Institute Mining, Metallurgical, and Petroleum Engineers, New York, 1964.

5. H. A. Wilhelm and P. Chiotti, "Thorium-Carbon System," Trans. Am. Soc. Metals, 42, 1295-1310 (1950).

6. N. Brett, D. Law, and D. T. Livey, "Some Investigations on the Uranium-Thorium-Carbon System," J. Inorg. Nucl. Chem., 13, 44-53 (1960).

7. G. B. Engle, Metallography of Carbide Fuel Compounds, GA-2067 (March 1961).

8. E. L. Long, Jr. and R. J. Gray, "Better Metallographic Techniques... Polishing by Vibration," Metal Progress, 74 (4), 145-48 (1958).

9. C.K.H. DuBose and R. J. Gray, Metallography of Pyrolytic Carbon Coated and Uncoated Uranium Carbide Spheres, ORNL-TM-91 (March, 1962).

10. N. A. Hill and O. B. Cavin, Monoclinic-Cubic Transformation in Thorium Dicarbide, ORNL-3588 (April 1964).

Y-50949 (a)

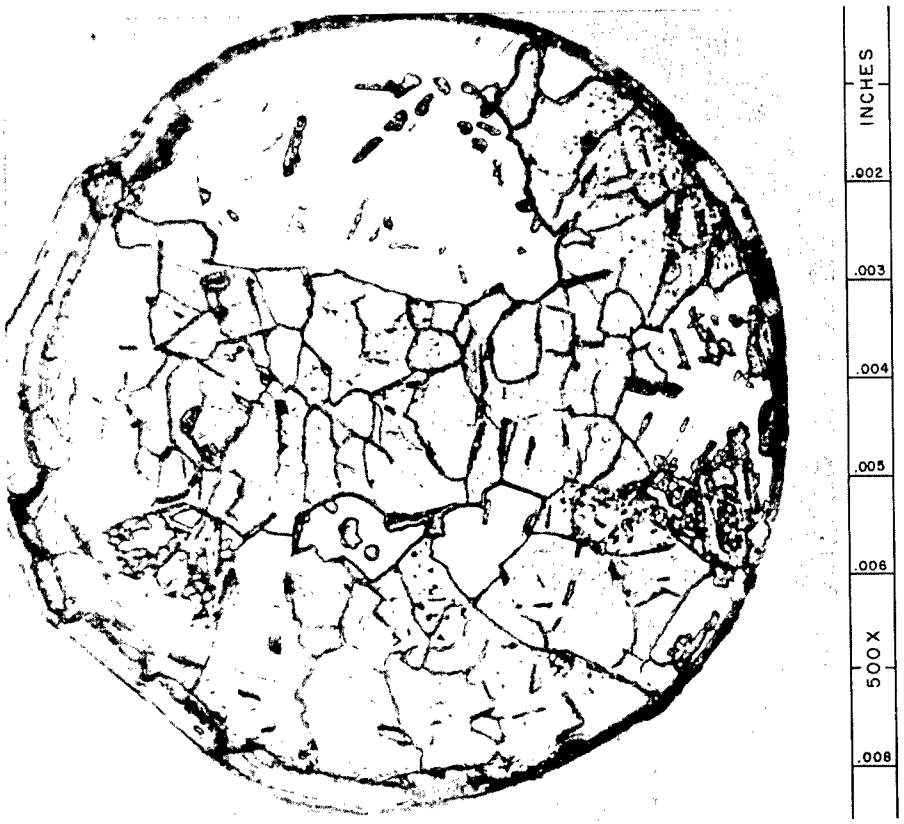

Y-52589 (b)

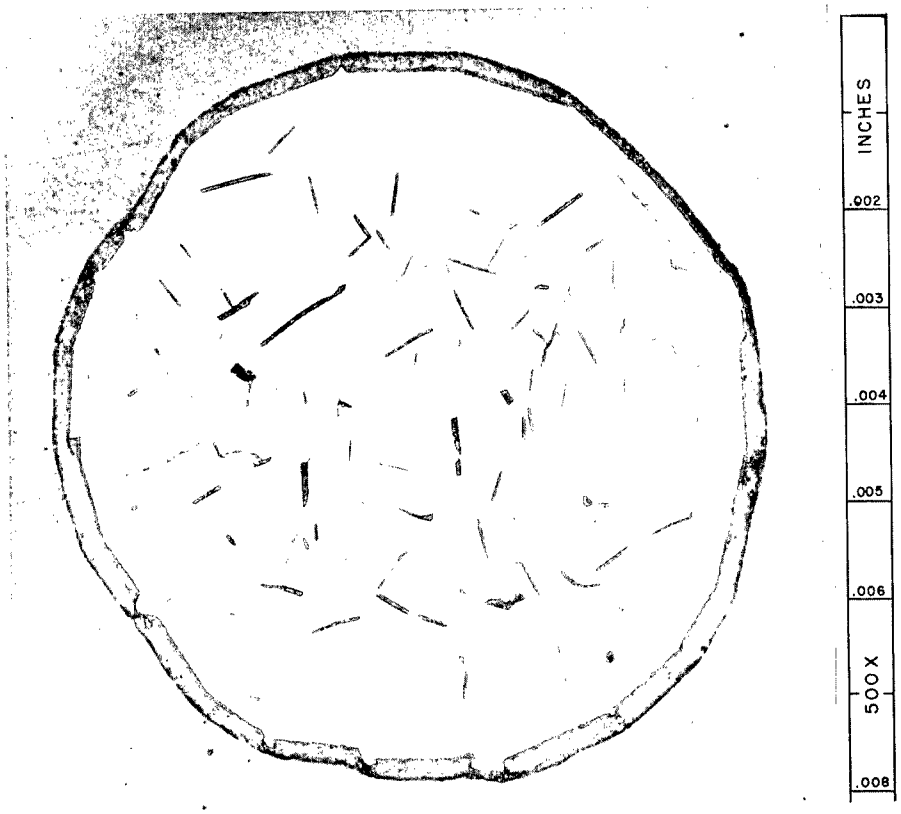

Fig. 1. Effect of Atmospheric Environment on Vibratory Polishing of $(Th,U)C_2$ Particles of 0.6 Th/U Ratio. (a) Particle with reaction, vibratorily polished in room atmosphere. (b) Particle without reaction, vibratorily polished in dry box. 500 X.

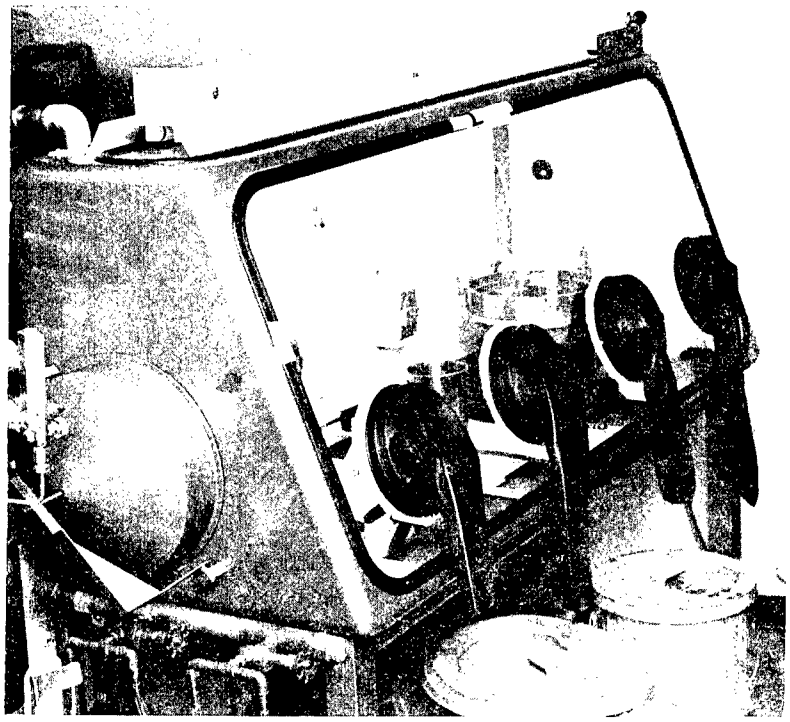

Y-54739

Fig. 2. Glove Box Used for Vibratory Polishing.

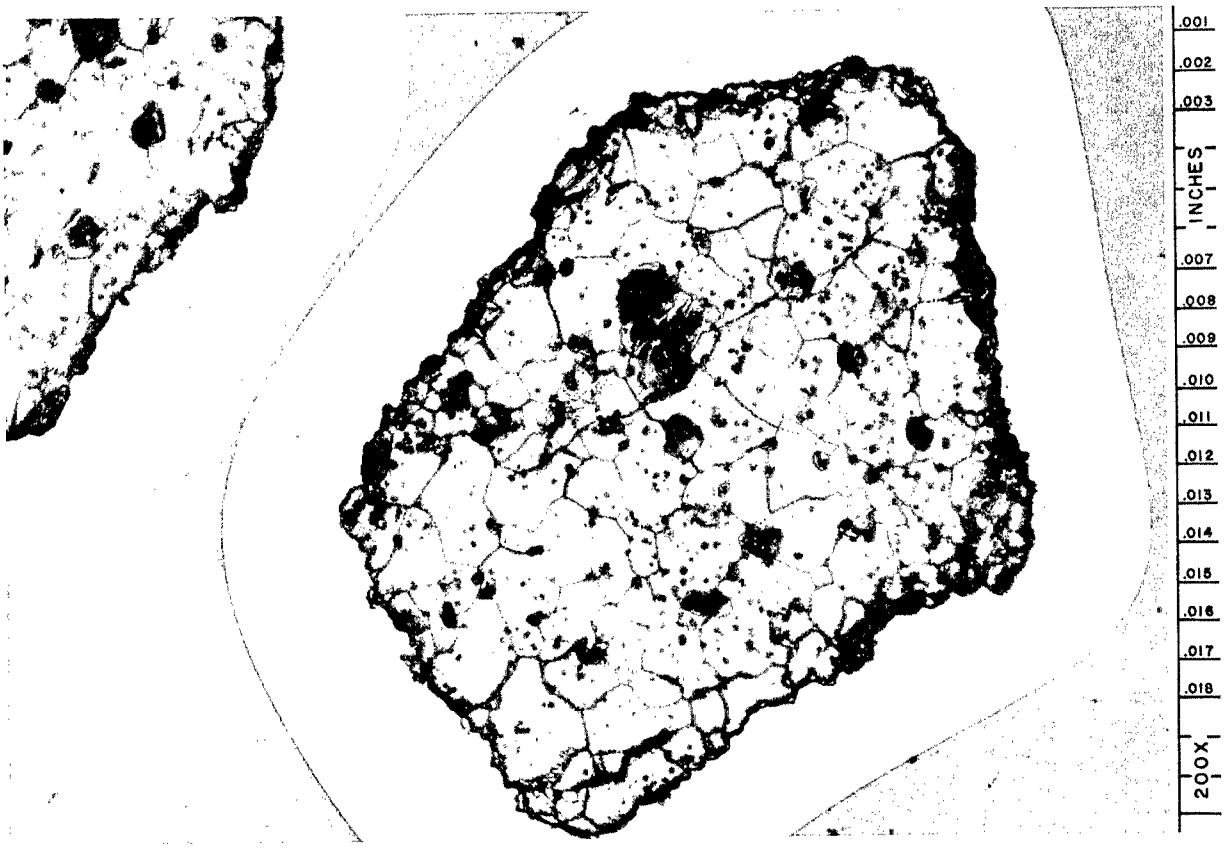

Y-44075

Fig. 3. Air Etched Pyrolytic Carbon-Coated (Th,U)C_2 Particle of 2.2 Th/U Ratio. 200 X.

Fig. 4. Pyrolytic Carbon-Coated $(Th,U)C_2$ Particle of 2.2 Th/U Ratio. (a) Passivated by immersing 30 sec in HNO_3-H_2O. (b) Air etched during vibratory polishing in room atmosphere. 200 X.

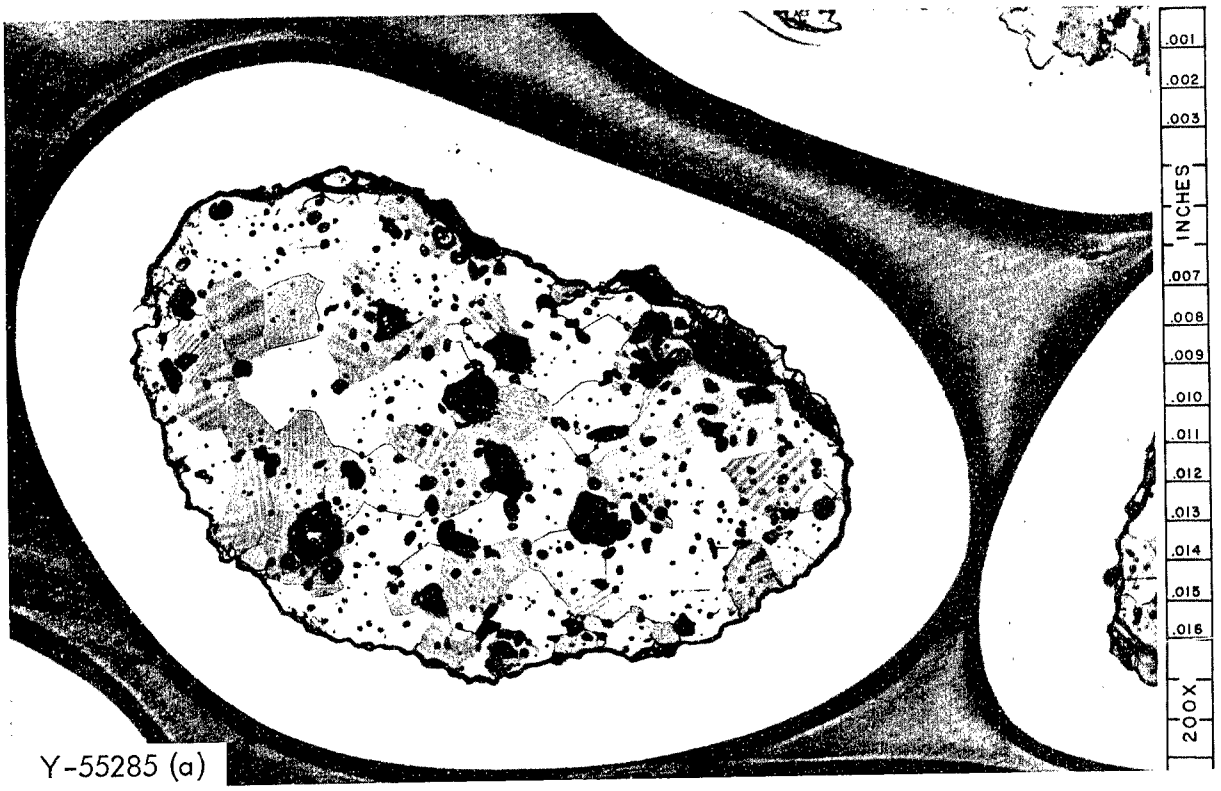

Fig. 5. Pyrolytic Carbon-Coated $(Th,U)C_2$ Particle of 2.2 Th/U Ratio. (a) Etched by immersing 5 min in HNO_3-H_2O, bright field. (b) Etched as in (a), polarized light. 200 X.

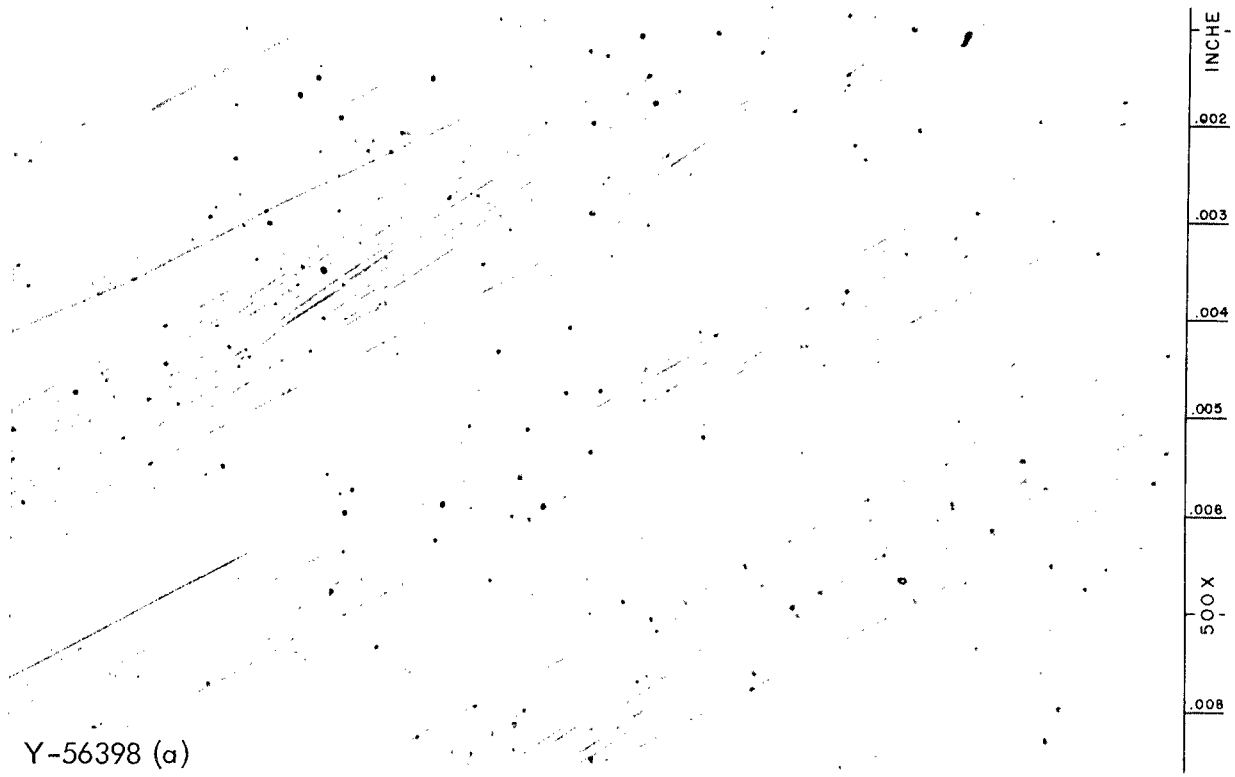

Fig. 6. Arc Cast ThC_2 Etched by Immersing 45 min in 1:1 HNO_3-H_2O. (a) Bright field. (b) Polarized light. 500 X.

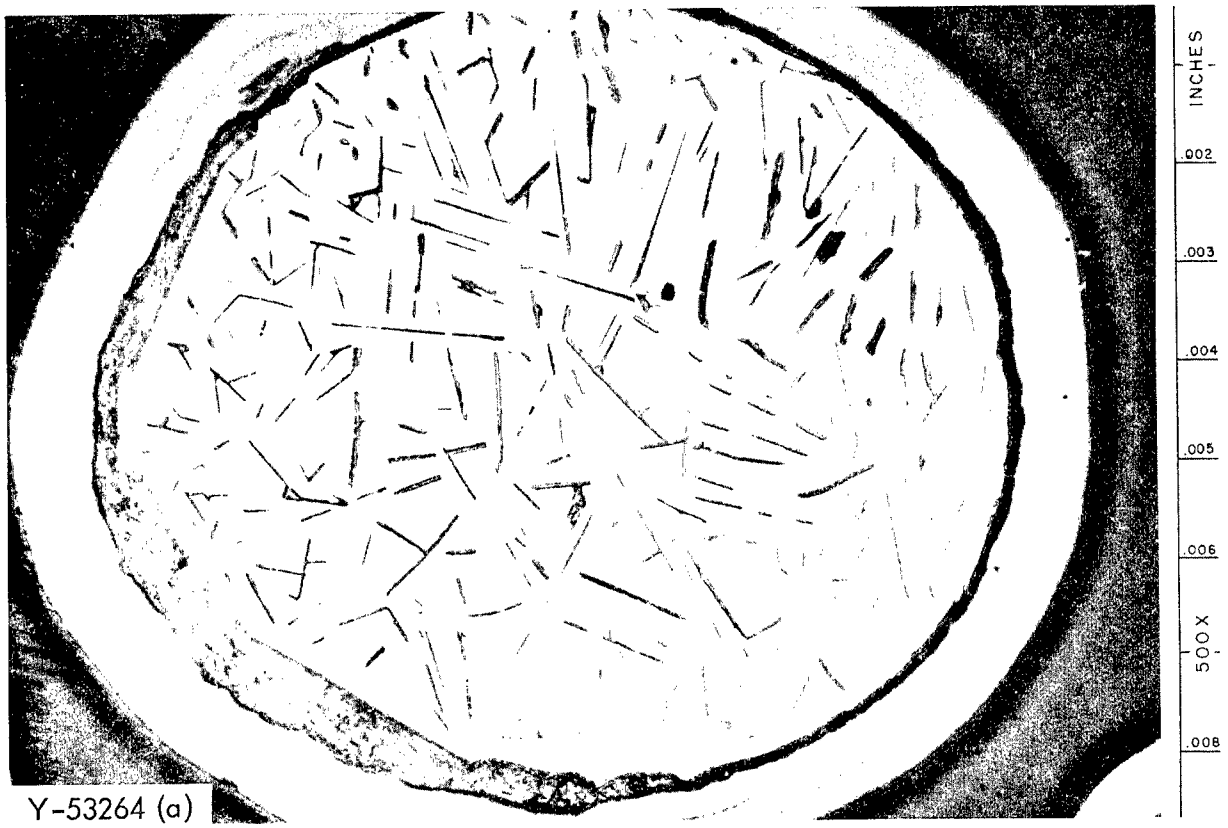

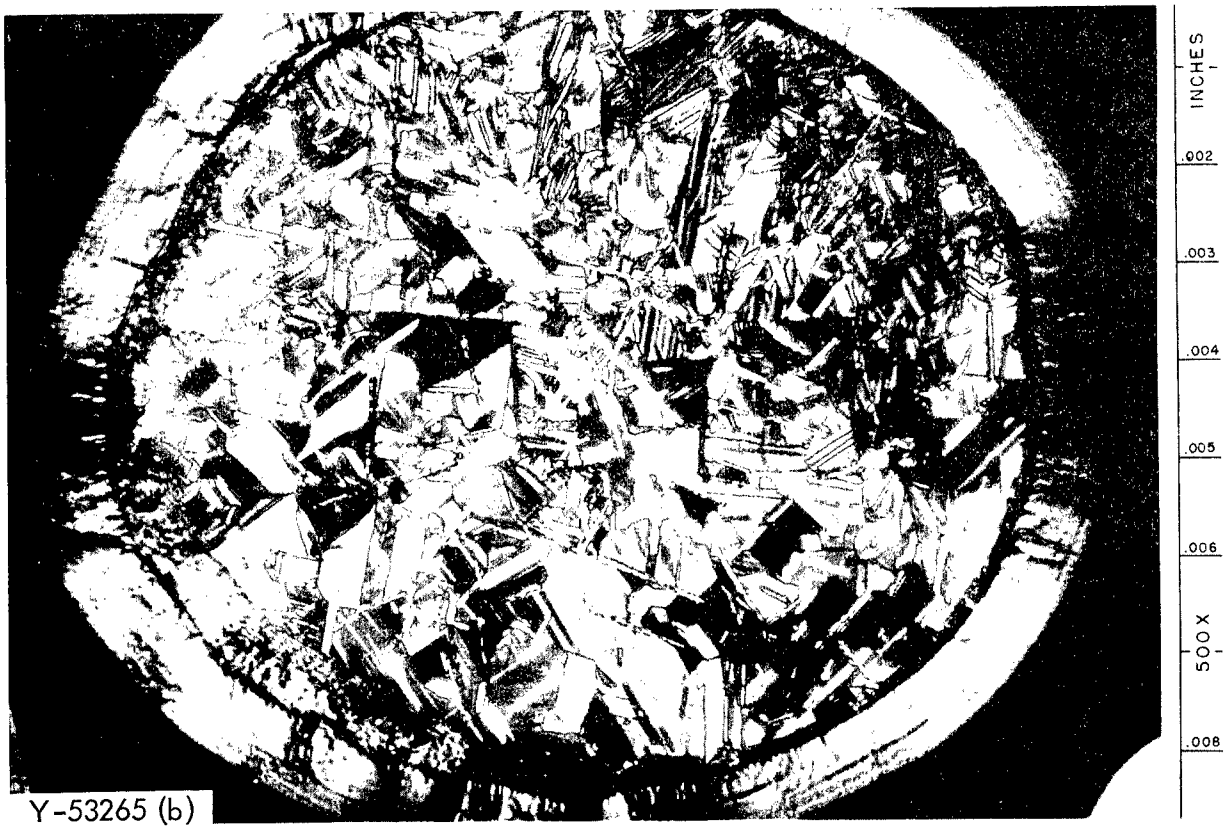

Fig. 7. Pyrolytic Carbon-Coated ThC_2 Particle Passivated by Immersing 1 min in 1:1 HNO_3-H_2O. (a) Bright field. (b) Polarized light. 500 X.

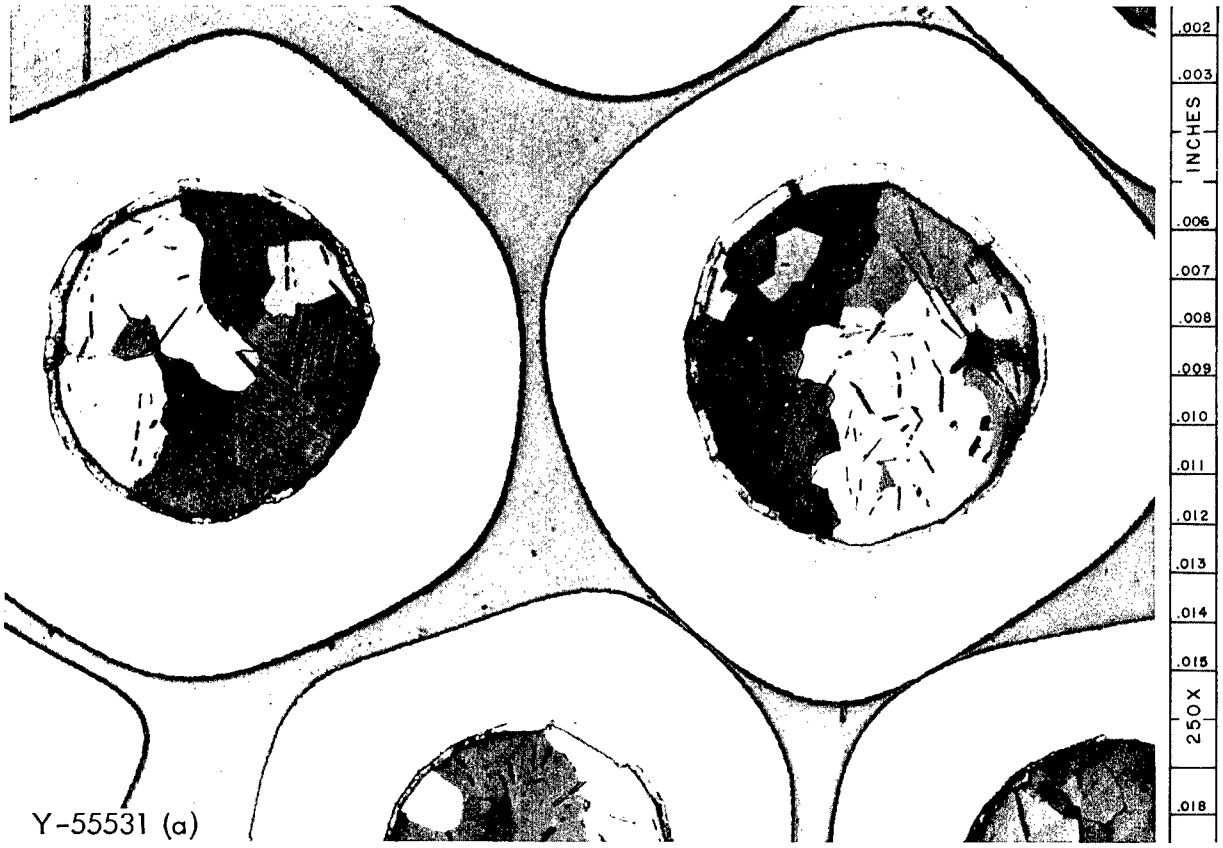

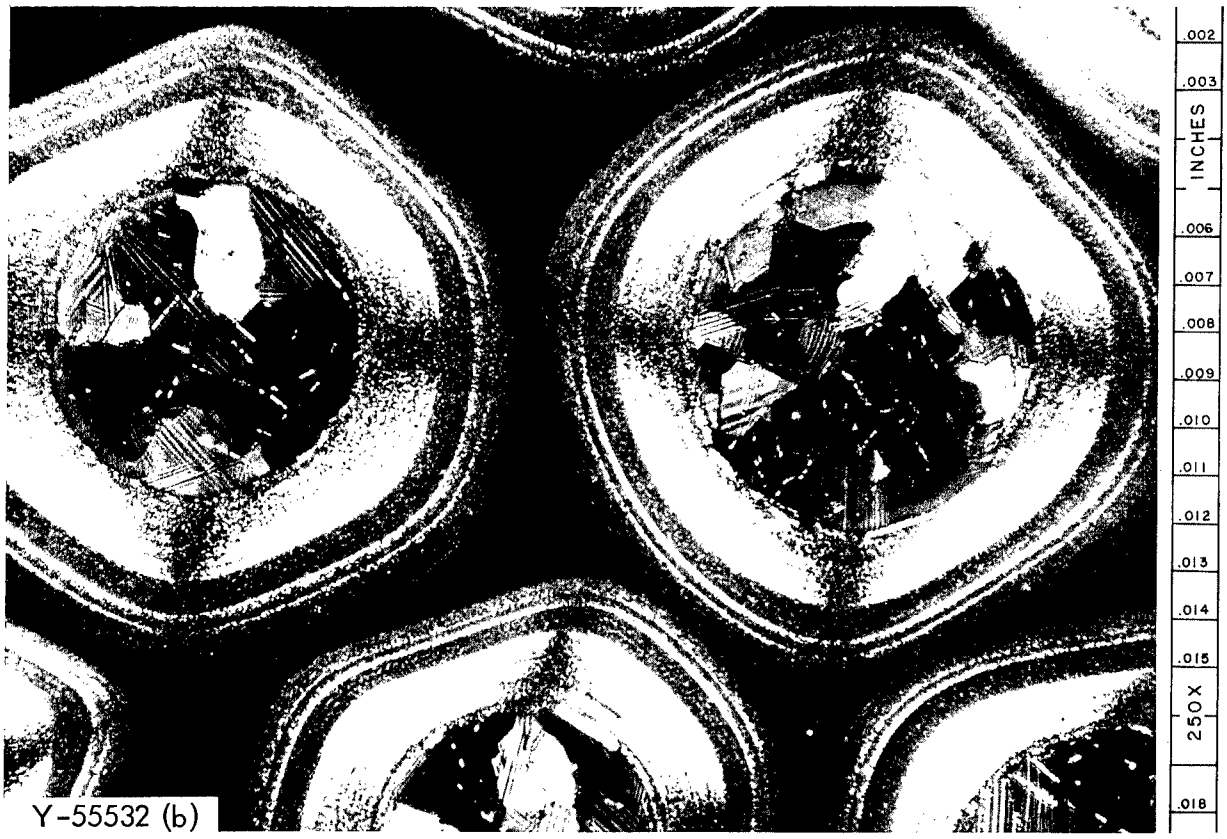

Fig. 8. Pyrolytic Carbon-Coated $(Th,U)C_2$ Particles of 1.0 Th/U Ratio, Etched by Immersing 5 min in 1:1 HNO_3-H_2O. (a) Bright field. (b) Polarized light. 250 X.

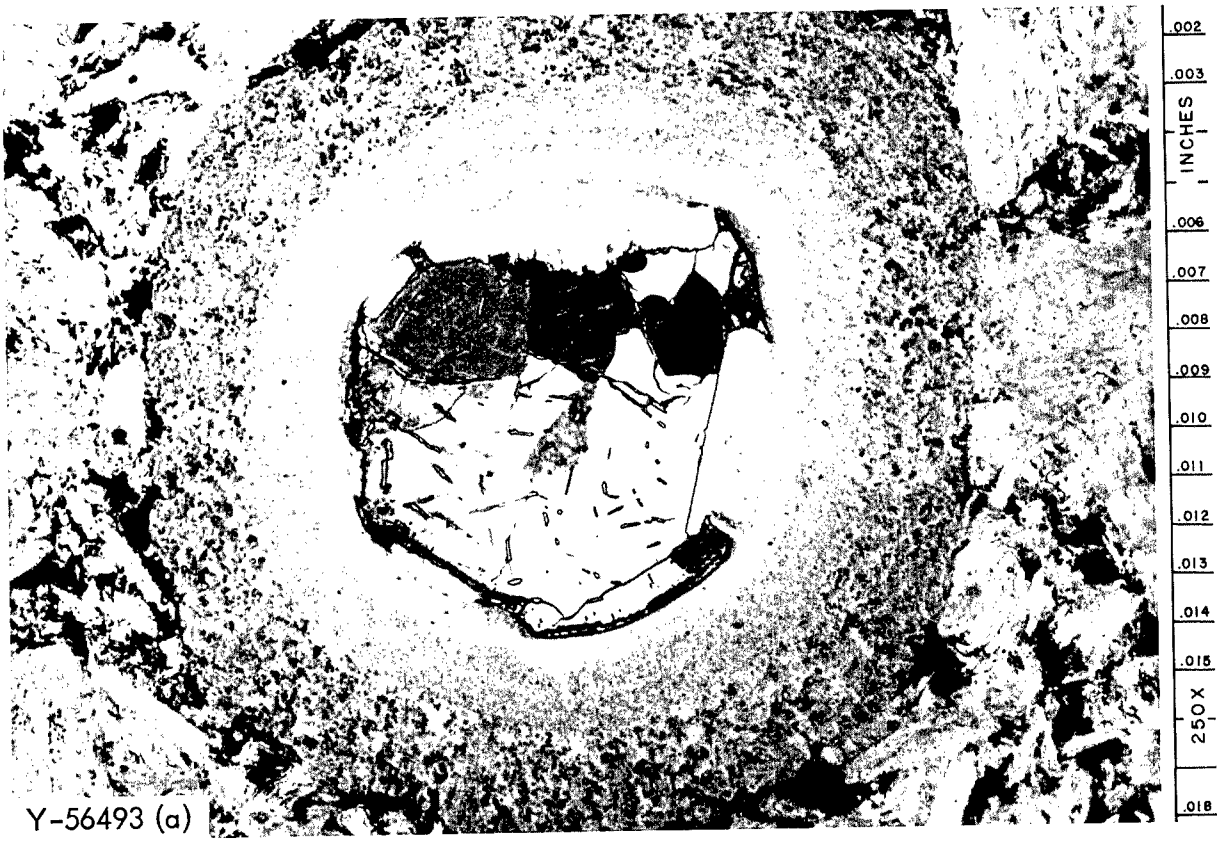

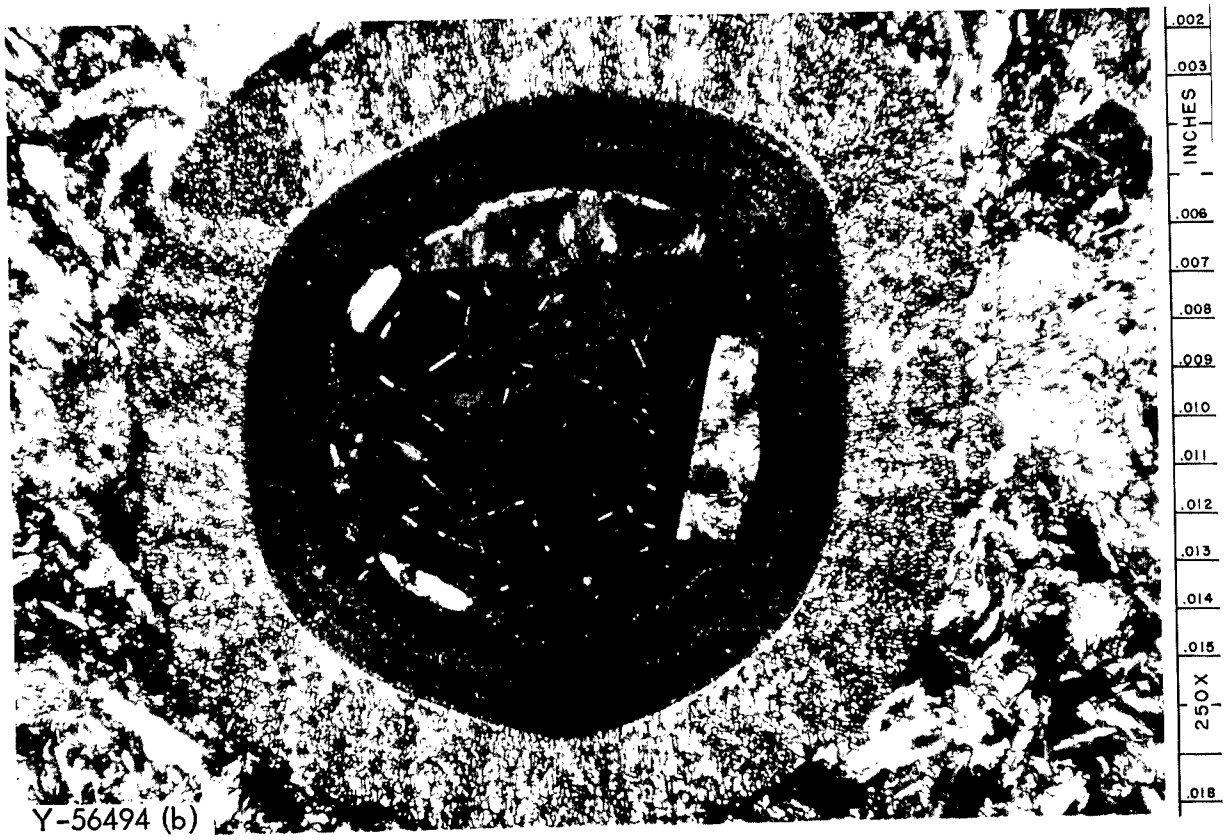

Fig. 9. Pyrolytic Carbon-Coated $(Th,U)C_2$ Particles of 0.6 Th/U Ratio Embedded in Fueled Graphite Body. Etched by immersing 5 min in 1:1 HNO_3-H_2O. (a) Bright field. (b) Polarized light. 250 X.

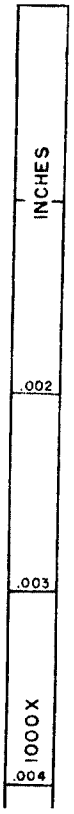

Y-53542 (a)

Y-53543 (b)

Fig. 10. Arc Cast ThC_2 Passivated by Immersing 1 min in 1:1 HNO_3-H_2O. (a) Bright field. (b) Polarized light. 1000 X.

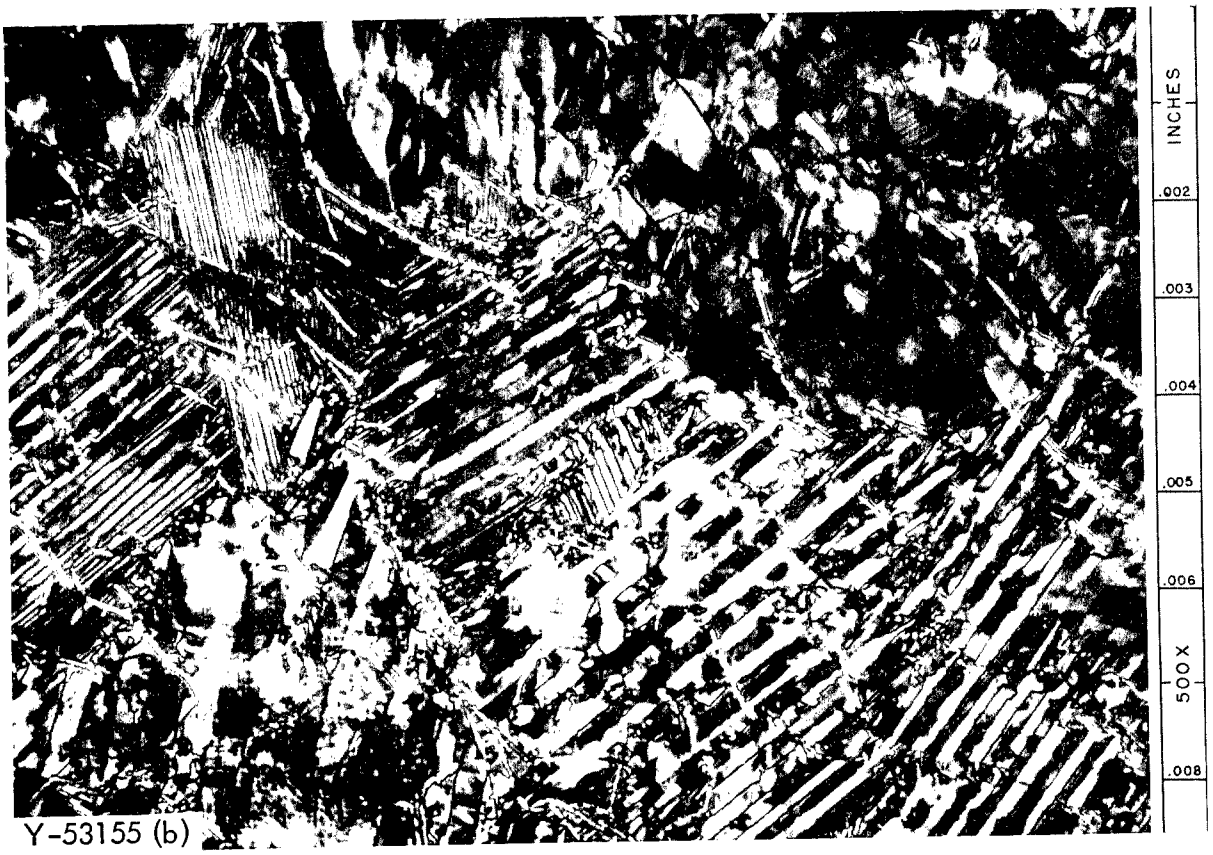

Fig. 11. Arc Cast $(Th,U)C_2$ of 7 Th/U Ratio with Excess Graphite, Passivated by Immersing 1 min in 1:1 HNO_3-H_2O. (a) Bright field. (b) Polarized light. 500 X.

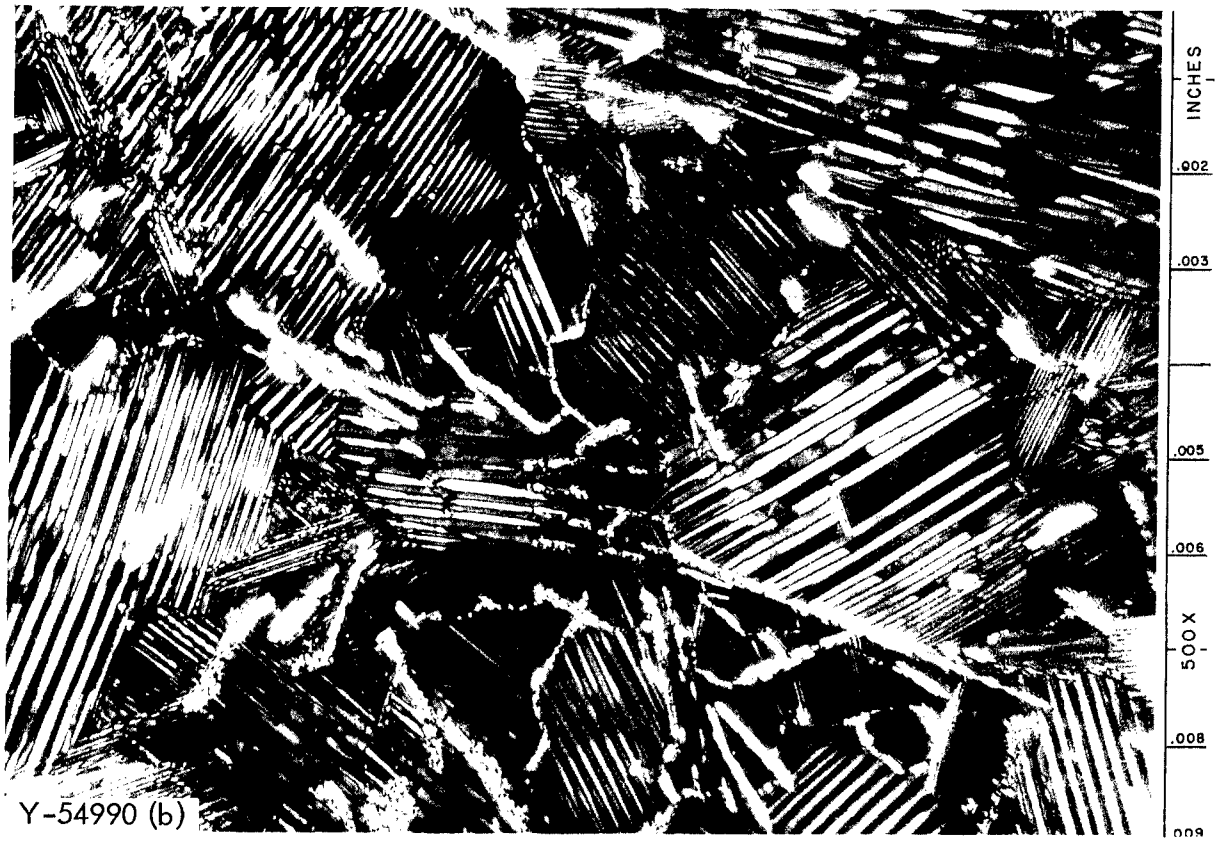

Fig. 12. Arc Cast $(Th,U)C_2$ of 3 Th/U Ratio with Excess Graphite, Etched by Immersing 5 min in 1:1 HNO_3-H_2O. (a) Bright field. (b) Polarized light. 500 X.

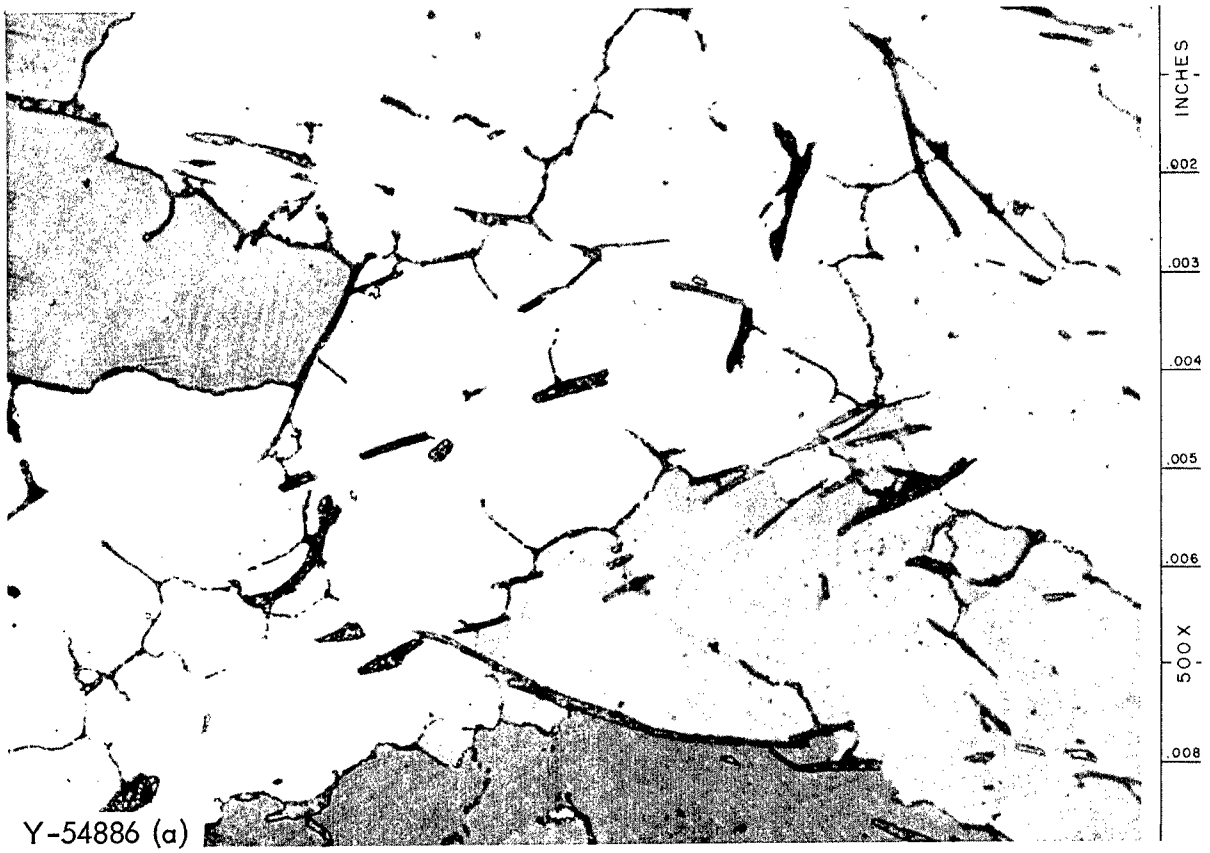

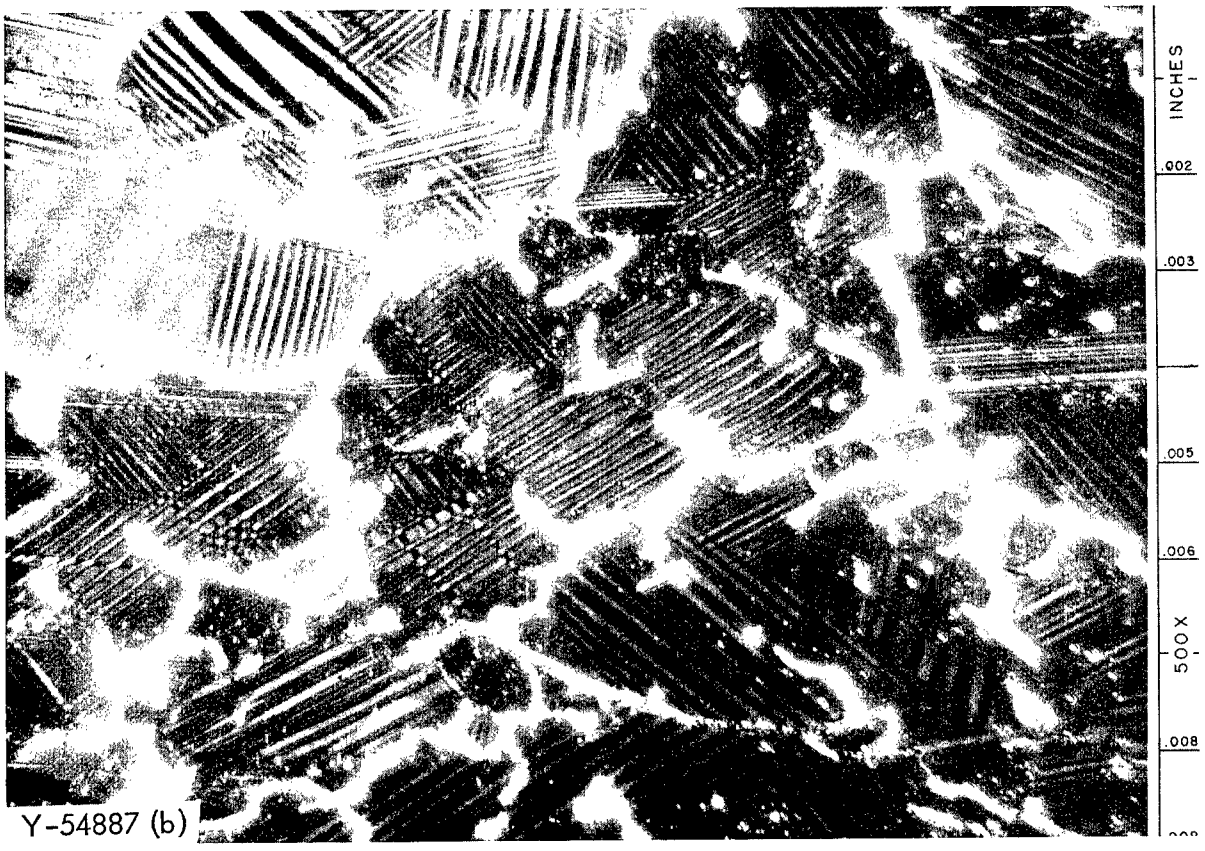

Fig. 13. Arc Cast $(Th,U)C_2$ of 1 Th/U Ratio with Excess Graphite, Etched by Immersing 5 min in 1:1 HNO_3-H_2O. (a) Bright field. (b) Polarized light. 500 X.

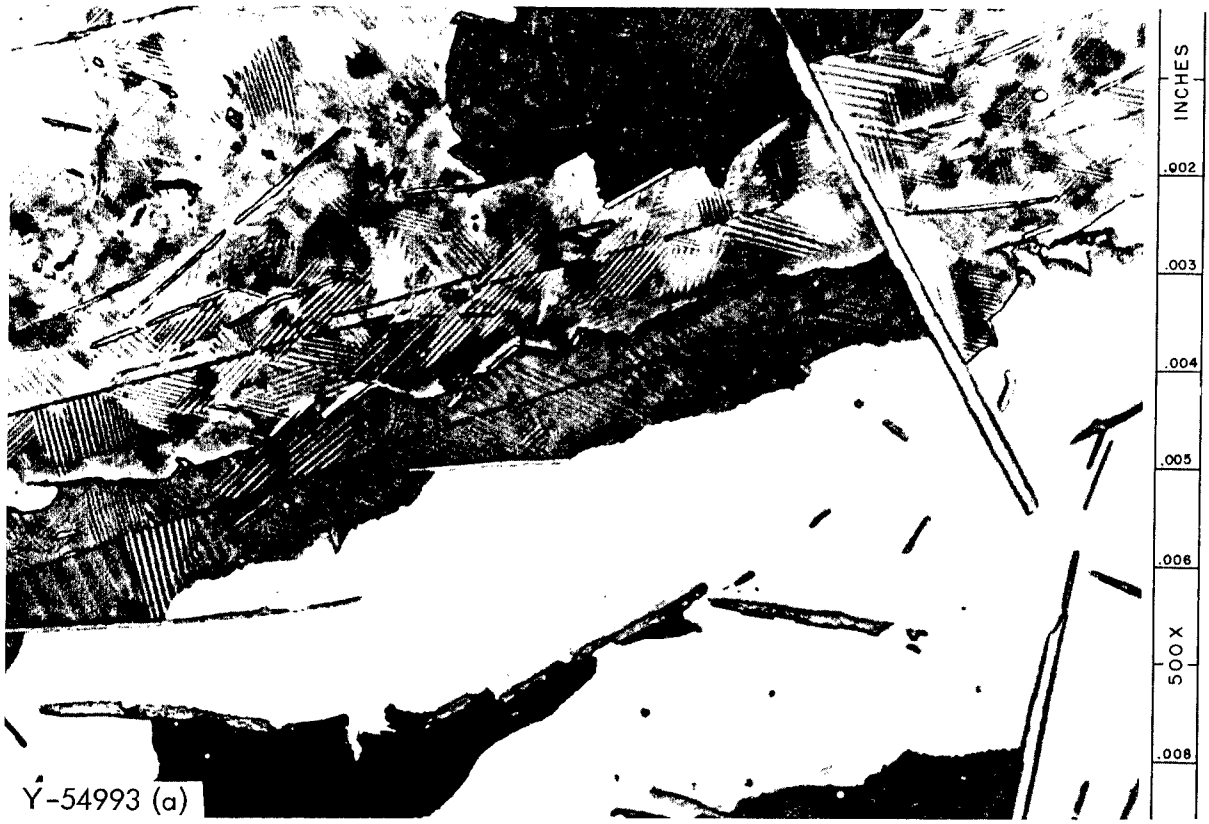

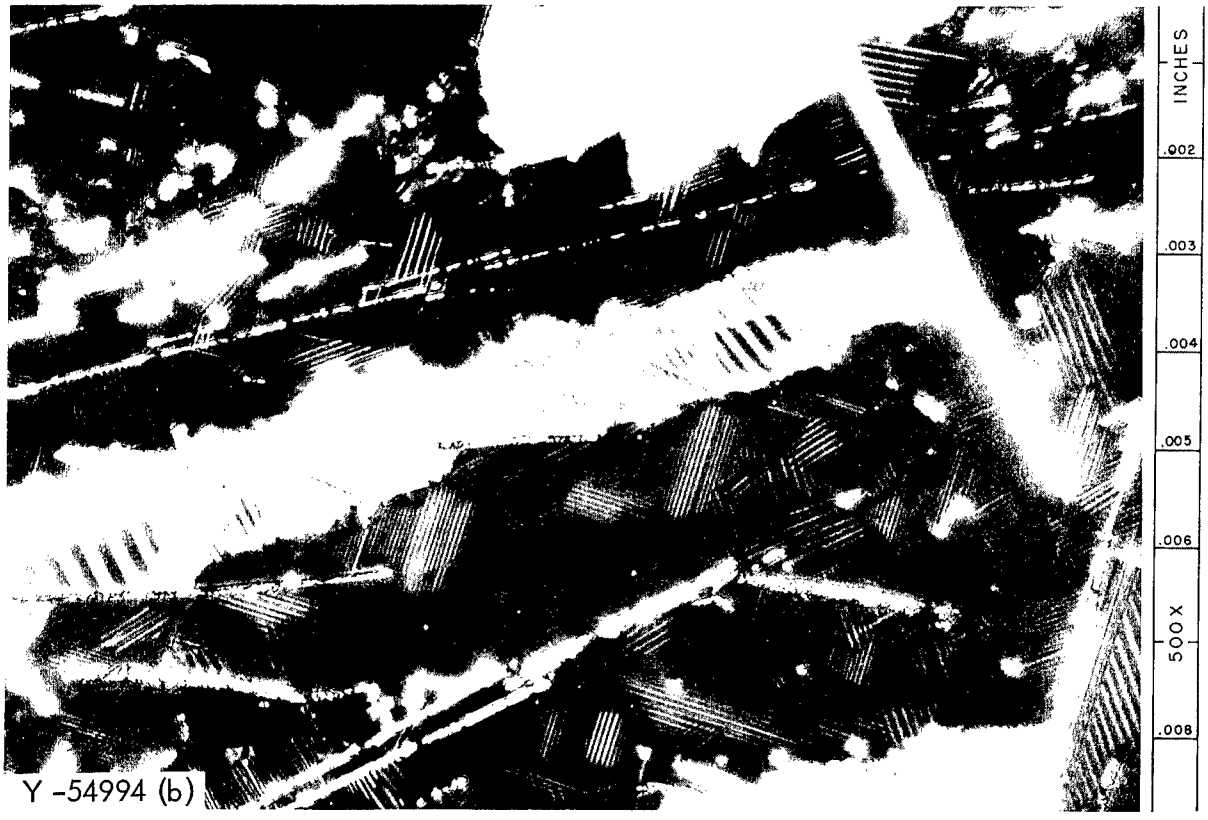

Fig. 14. Arc Cast $(Th,U)C_2$ of 3 U/Th Ratio with Excess Graphite, Etched by Immersing 5 min in 1:1 HNO_3-H_2O. (a) Bright field. (b) Polarized light. 500 X.

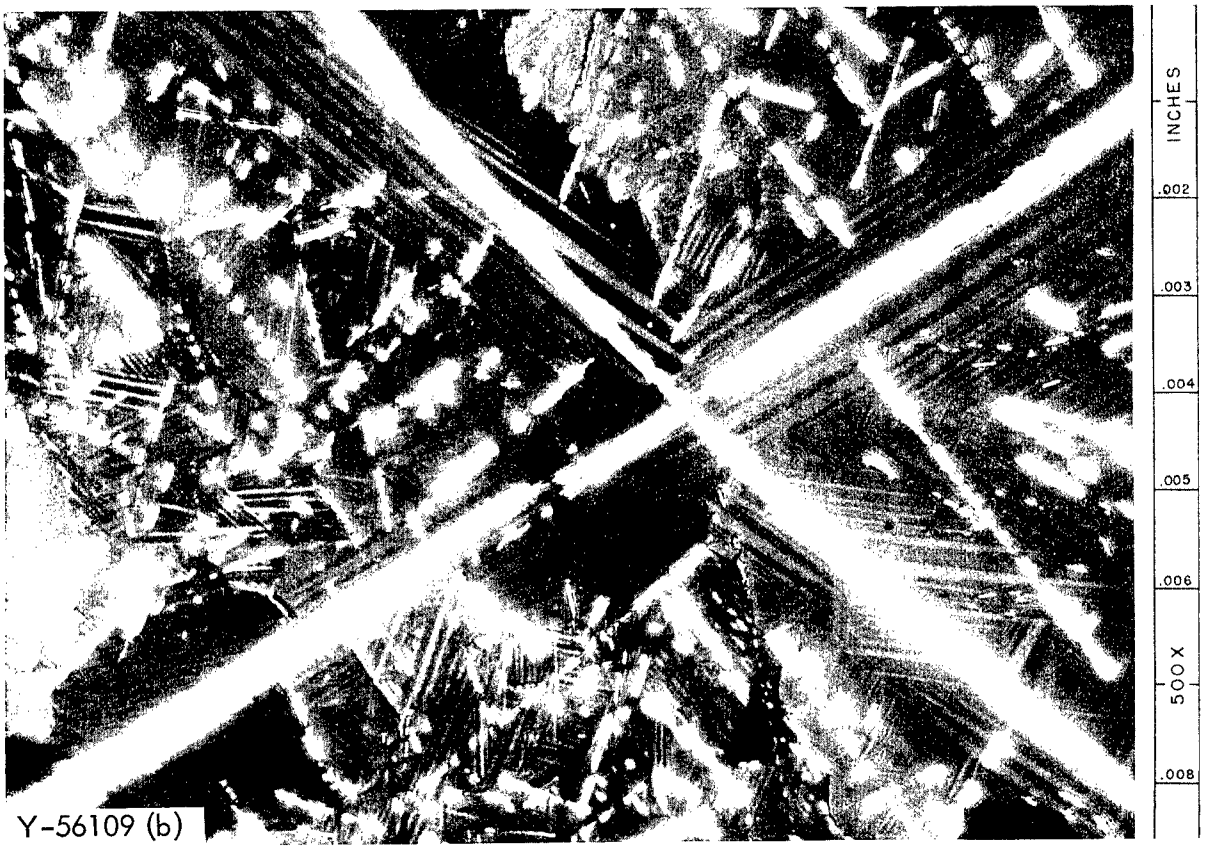

Fig. 15. Arc Cast $(Th,U)C_2$ of 9 U/Th Ratio with Excess Graphite, Etched by Immersing 5 min in 1:1 HNO_3-H_2O. (a) Bright field. (b) Polarized light. 500 X.

QUANTATIVE METALLOGRAPHY OF HYPOSTOICHIOMETRIC URANIUM MONOCARBIDE

E. E. Ritchie and J. L. Tibbetts

ATOMICS INTERNATIONAL
A Division of North American Aviation, Inc.

This report is a compilation of data obtained from three statistical test methods for determining the amount of excess alpha uranium present in hypostoichiometric uranium carbide. The three test methods were:

(1) Superimposing a grid on several areas of a photomicrograph and counting the number of grid intercepts falling on alpha uranium. The percent of intercepts on alpha uranium is converted to weight percent carbon.

(2) Comparison of metallographically prepared microstructure to photomicrographs of standards with known carbon contents.

(3) Chemical carbon analysis of the material.

The following conclusions were obtained from this evaluation:

(1) Precision of both the grid intercept and the metallographic comparison methods increase with increasing carbon content.

(2) Precision also increases with an increasing number of samples.

(3) No significant variation was observed between evaluations made by two metallographers.

(4) A curvilinear regression analysis of data obtained by the grid intercept method indicates that precision as a function of the number of samples satisfied the relationship

$$\text{Precision } (1\ 0\ ) = 0.0021 + 0.0591 \left(\frac{1}{\sqrt[1]{N}}\right)$$

(5) Precision obtained by more than one placement of the grid on a photomicrograph is not significantly better than a single placement.

I INTRODUCTION

Fuel for the Empire State Atomic Development Association (E.S.A.D.A.) pilot core is uranium carbide. The fuel has been limited to a carbon range between 4.5 weight percent and stoichiometric (4.8 weight percent) carbon in order to reduce radiation damage and compatability problems to a minimum. Therefore, the amount of excess alpha uranium present in the microstructure must be closely controlled and have a uniform distribution.

Several methods were considered for obtaining a volume-fraction of excess uranium in a uranium carbide material. They are:
(1) The systematic point count method in which a grid is superimposed on several areas of a photomicrograph of the fuel. The number of grid intercepts falling on alpha uranium is converted from volume percent alpha uranium to weight percent carbon.
(2) Comparison of the metallographically observed microstructures to photomicrographs of standards with carbon content determined by chemical analysis.
(3) Chemical carbon analysis of the material. The chemical analysis method was used as the unbiased standard.

Several factors which can effect the observed carbon content were not considered in this report but are discussed in Reference 1.

(1) Impurities: Nitrogen and oxygen replace carbon in uranium carbide and raise the apparent carbon content as determined metallographically.
(2) Kinetics: Rapid cooling rates attained in casting raise the apparent carbon content by quenching excess uranium in metastable solid solution or as unresolvable precipitates.
(3) Accuracy of Standards: Photomicrographs used as standards for comparison must truly represent the carbon contents for which they are designated.

II TEST PROCEDURE AND DISCUSSION OF RESULTS

A series of three evaluation procedures were investigated.
(1) General comparison of the grid intercept method, metallographic comparison technique and chemical carbon analysis.
(2) Determination of the optimum number of areas required to obtain a given precision using the grid intercept method. (3) Determination of the precision of a different sampling procedure.

A. Comparison of the Three Techniques

A fuel sample approximately ½ inch in diameter by ¼ inch long from six different E.S.A.D.A. fuel heats were analyzed by the grid intercept method, by metallographic comparison and by chemical carbon analysis. Photomicrographs at 100X magnification were randomly taken along a diameter across each end of the six samples.

A grid of 100 points with a ¼ inch spacing was superimposed on

each photomicrograph as shown by Figure 1. The number of line intersections falling upon alpha uranium was counted and converted directly to volume percent alpha uranium. The volume percent alpha uranium was converted to weight percent carbon, using the graph shown in Figure 2. Each specimen was analyzed by two metallographers. The grid was placed on five different photomicrographs; the procedure was then repeated, using ten photomicrographs.

The six fuel samples were analyzed by the metallographic comparison technique. Five photomicrographs at 100X magnification were repeated, using ten photomicrographs. Each analysis was made by two metallographers; therefore, the determinations could be compared directly to the grid intercept method.

The six samples above were then submitted to chemistry for chemical carbon analysis, which served as a base line for comparison of the various methods. The estimated precision of the chemical carbon analysis is 0.032 weight percent carbon.

The estimated bias of the metallographic comparison method and the estimated carbon content of the fuel varies linearly with carbon content and satisfied the relationship,

$$Y = 1.808 + 0.415X$$

where Y is the estimated bias, and X is the estimated carbon content. Figure 3 shows the accuracy and precision to be expected by the metallographic comparison method.

Precision of both the grid intercept and the metallographic comparison methods increases with increasing carbon content.

An evaluation of ten photomicrographs from a given specimen, as opposed to five, also increases the precision of the estimated carbon determination as shown by Figure 4. No significant variation in the carbon evaluation by the two technicians was observed.

B. Determining the Optimum Number of Areas for the Grid Intercept Method.

A second test was initiated to determine the optimum number of areas required to obtain a given precision using the grid intercept method. Four samples from a E.S.A.D.A. fuel slug were analyzed using the grid intercept method at 42 different locations per sample. The ¼ inch diameter end surface of the specimen was divided into 121 equal areas approximately 0.035 inch by 0.045 inch, the area with sufficient overlap of a 4 x 5 inch photomicrograph at 100X magnification. The 42 locations were selected from a table of random numbers.

Evaluation of the data obtained from the four samples at a 90% confidence level revealed no significant difference between the mean values or the variance. Based on these data, it was possible to assume that all 168 determinations from the four samples were from the same general population. An equivalent visible carbon content of 4.615 weight percent carbon was obtained from an average of the 168 determinations.

An estimate of the precision of the grid intercept method as a function of the number of samples was made from the average standard deviation of five determinations of the equivalent carbon content. Each determination was based on five sets of samples where the number of samples per set varied from five to twenty-five samples in increments of five samples. The samples were selected randomly, with replacement from the 168 determinations. The results of this evaluation are given in Table I.

A curvilinear regression analysis was performed on the five data points resulting in following regression equation:

Precision ($1\,\sigma$) = $0.0021 + 0.0591 \left(\frac{1}{\sqrt{N}} \right)$. The equation for the upper 95% confidence limit is:

$$UCL_{.95} = 0.0098 + 0.0591 \left(\frac{1}{\sqrt{N}} \right)$$

and the lower 95% confidence limit is:

$$LCL_{.95} = -0.0056 + 0.0591 \left(\frac{1}{\sqrt{N}} \right)$$

A plot of the data points and the 95% confidence limits is shown in Figure 5. The regression equation predicts a precision ($1\,\sigma$) of 0.011 weight percent carbon based on 42 samples. The estimated precision of the four determinations of 42 samples each was 0.012 weight percent carbon, providing an excellent confirmation of the regression analysis.

C. Precision of a New Sampling Procedure

A third evaluation was initiated to obtain the precision of a new sampling procedure. The grid was randomly placed using five orientations on each of six photomicrographs from each of four different uranium carbide specimens.

Data obtained by this procedure gave an estimated precision of 0.017 weight percent carbon based on four determinations of thirty samples each (six photos with five grids per photo). A significance test showed that the estimated precision for this test was not significantly different at the 90 percent confidence level than the predicted regression equation. Therefore, the precision obtained by five random placements of the grid on a photomicrograph is not significantly different than the precision obtained by a single placement of the grid on a photomicrograph.

III CONCLUSIONS

A. Precision of both the grid intercept and the metallographic comparison methods increase with increasing carbon content.

B. Precision also increases with an increasing number of samples.

C. No significant variation was observed between evaluations made by the two metallographers.

D. A curvilinear regression analysis of data obtained by the grid intercept method indicates that precision as a function of the number

of samples satisfies the relationship

$$\text{Precision } (1\ \sigma^-) = 0.0021 + 0.0591\ \left(\frac{1}{\sqrt{N}}\right)$$

E. Precision obtained by more than one placement of the grid on a photomicrograph is not significantly better than a single placement.

IV REFERENCES

1. Kerr, W. R., "Comparison of Microstructure and Chemical Carbon Content for Hypostoichiometric Uranium Monocarbide", NAA-SR-TDR-8943, September 9, 1963.
2. Hillard, J. E., Cann, J. W., "An Evaluation of Procedures in Quantitative Metallography for Volume Fraction Analysis", Trans. AIME Vol. 221 (1961) pp 344-352.
3. Marnoch, K., "Metallographic Analysis of Weight Percent Carbon in Uranium Carbide", NAA-SR-TDR-6819, October 20, 1963.
4. "Evaluation of the Grid Method of Qualitatively Determining the Volume Percent of Alpha Uranium in Uranium Carbide", IL, D. N. Glass, April 18, 1963.
5. "Statistical Evaluation of the Grid Method for Determining the Volume Percent of Alpha Uranium in UC Fuel Slugs", IL, D. N. Glass, May 21, 1963.
6. "Statistical Evaluation of a Proposed Sampling Procedure for, and the Precision of, the Grid Method of Determining the Equivalent Carbon Content in UC Fuel Slugs", IL, D. N. Glass, July 12, 1963.

TABLE I

Results of Randomly Selected "Grid" Determinations

	Sample Size									
	5		10		15		20			
	$\bar{X}$[1]	S^2	$\bar{X}$	S	$\bar{X}$	S	$\bar{X}$	S	$\bar{X}$	S
"Grid Determination (Wt % C	4.604	0.0268	4.620	0.0173	4.583	0.0179	4.612	0.0192	4.615	0.0114
	4.646	0.0175	4.617	0.0249	4.633	0.0199	4.616	0.0108	4.612	0.0084
	4.609	0.0351	4.616	0.0216	4.624	0.0241	4.604	0.0055	4.624	0.0148
	4.626	0.0303	4.618	0.0169	4.608	0.0220	4.609	0.0164	4.622	0.0091
	4.594	0.0286	4.626	0.0185	4.617	0;0220	4.615	0.0224	4.594	0.0082
Over-All Avg.	4.616		4.619		4.613		4.611		4.613	
Precision (1 σ)		0.0282		0.0201		0.0213		0.0160		0.0106

NOTES: 1. $\bar{X}$ equals the sample mean in Wt % C

2. S equals the sample standard deviation in Wt % C

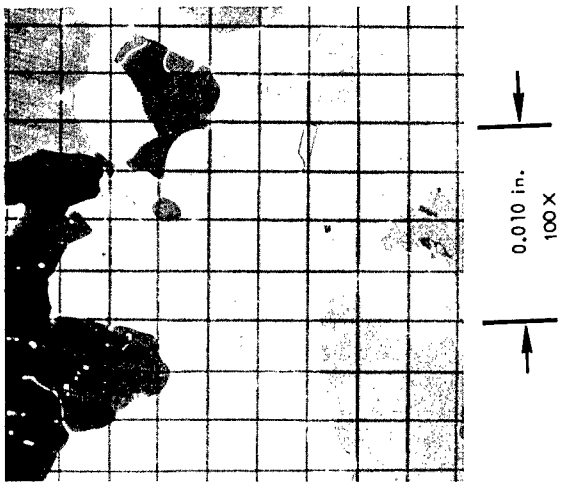

Figure 1
Uranium Carbide with 100 point grid superimposed
100 X Neg 5444-1-1

Figure 2
Transformation from Volume %
Alpha Uranium to Weight % Carbon for
Hypostoichiometric UC

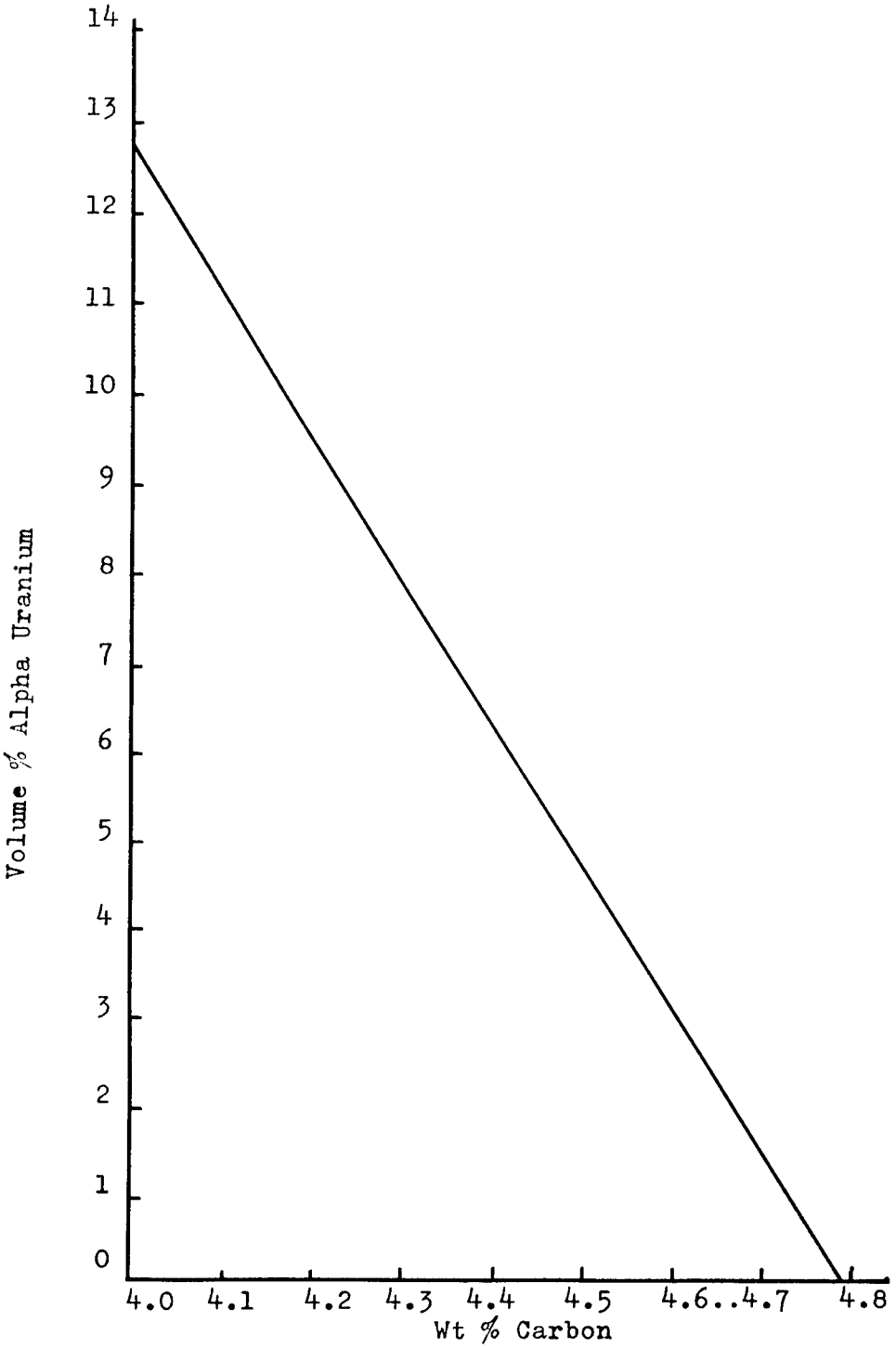

Figure 3
Regression Lines Showing Ralationships of
Accuracy and Precision to Carbon Content
for Carbon Determinations by Metallographic
Analyses Bases Upon Photographic Standards

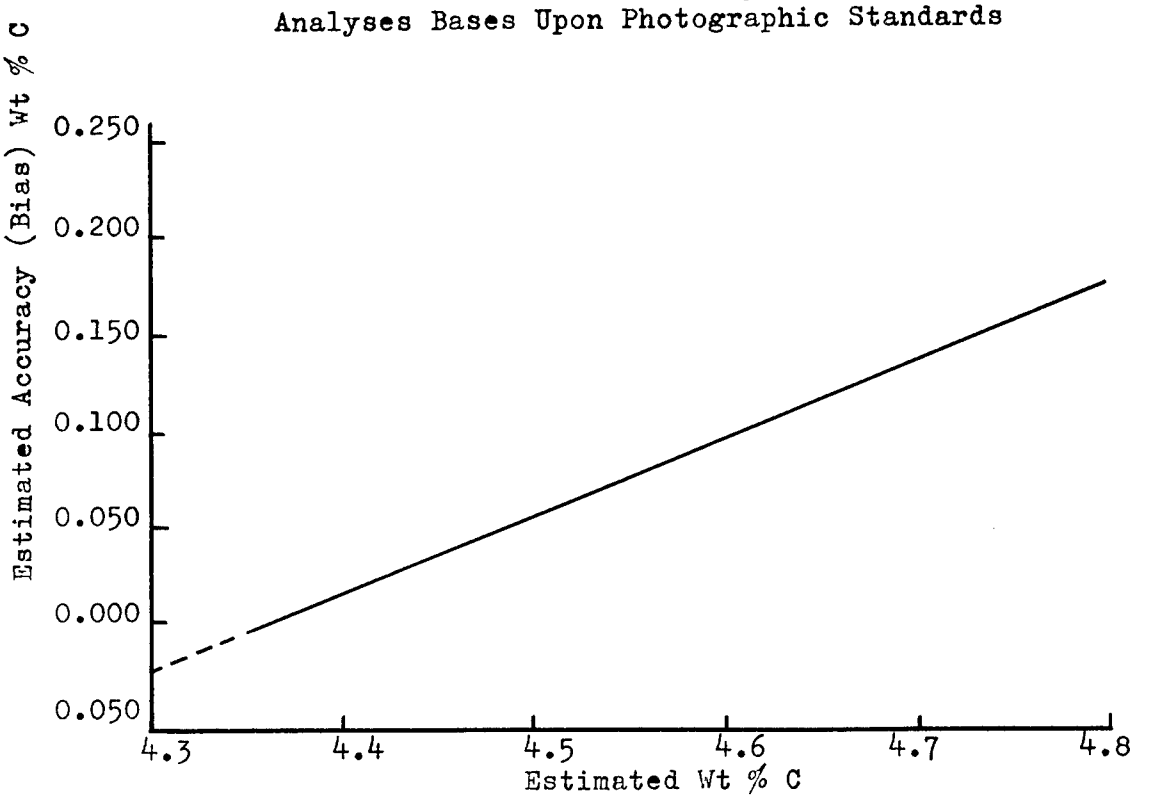

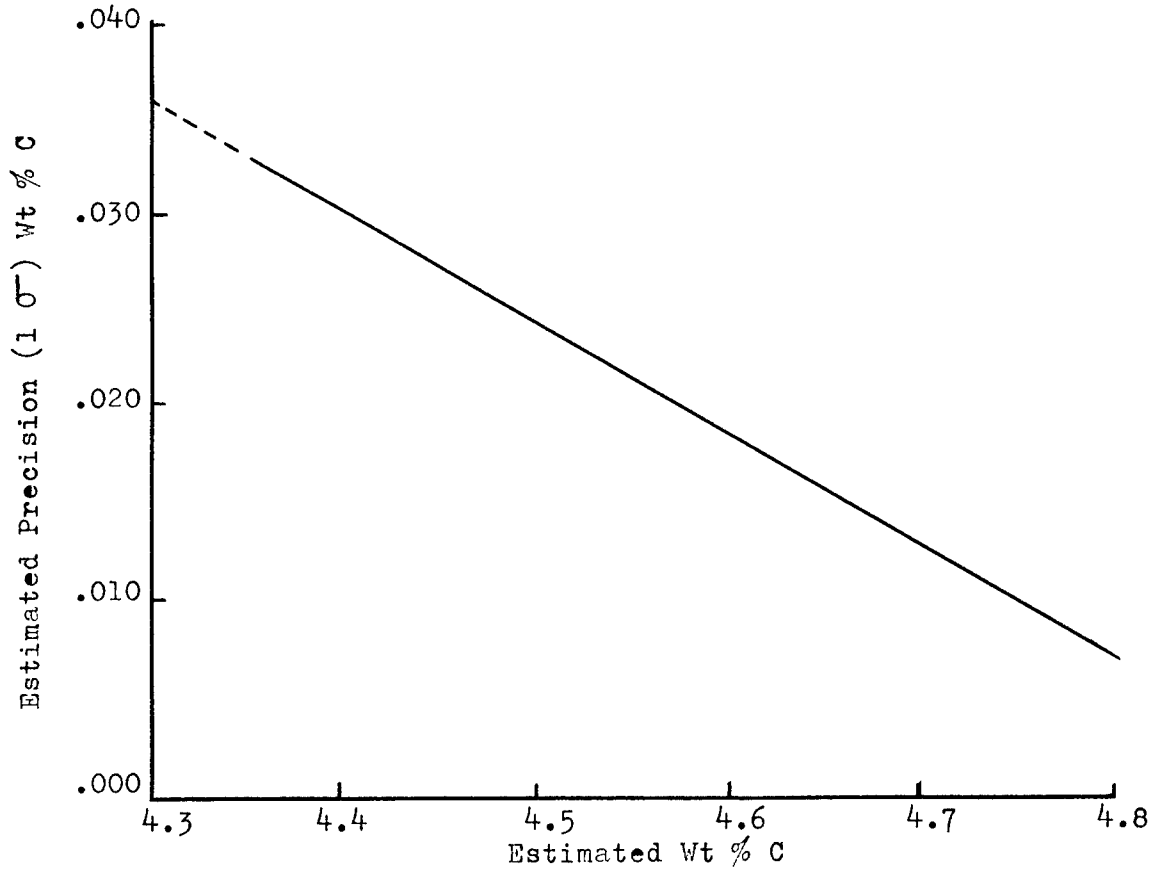

Figure 4
Regression Lines Showing Relationships of Precision to Carbon Content for Carbon Determinations Using the "Grid" Method Based Upon Five and Ten Grids

Figure 5
Regression Line Shoping Relationship
Between Sample Size per Determination
and Precision of the Determination for
UC Material with an Estimated Equivalent
Visible Carbon Content of 4.615 Wt % C

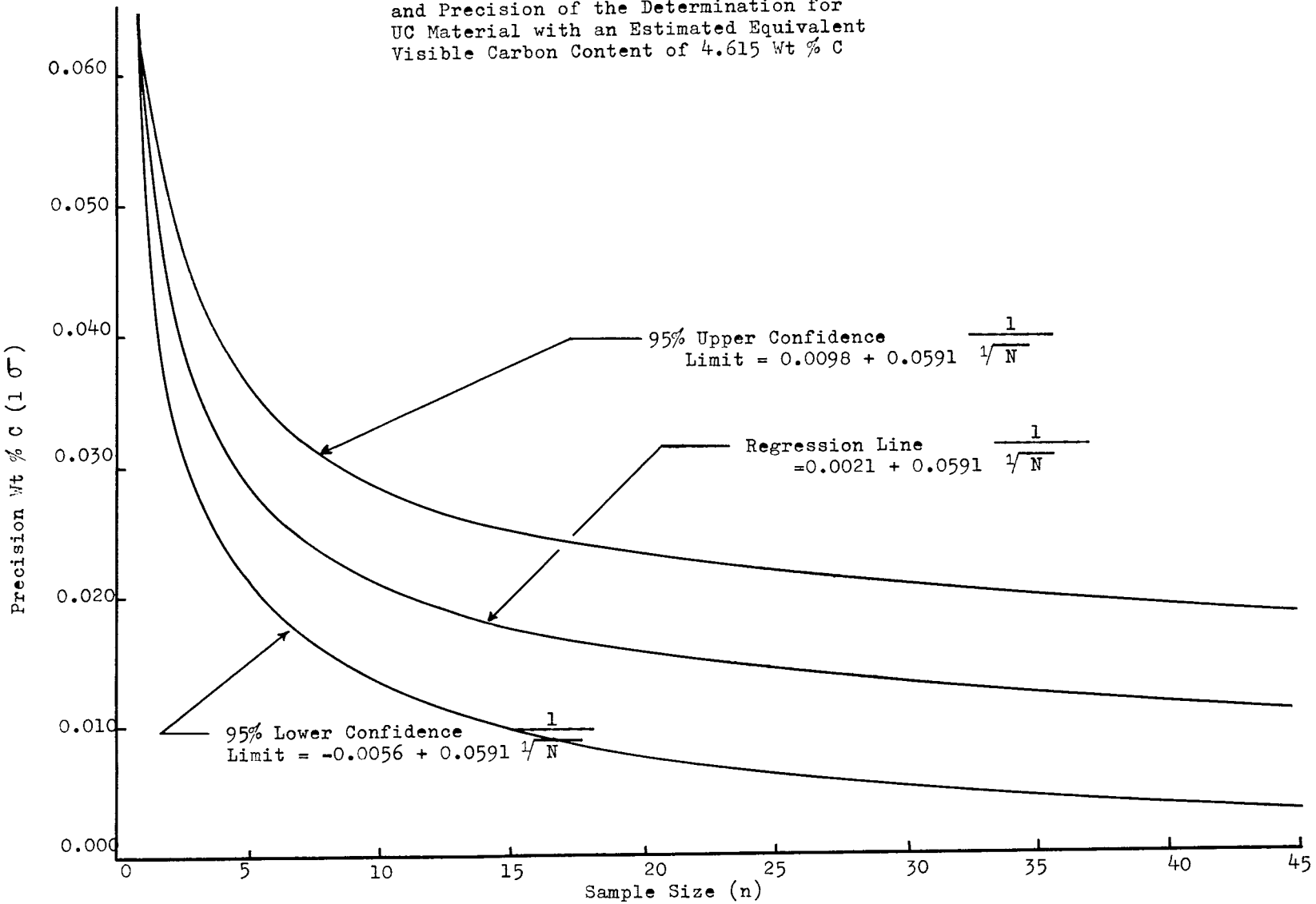

STANDARDS FOR METALLOGRAPHIC EVALUATIONS OF URANIUM METAL

By

M. H. Cornett

ABSTRACT

Visual standards are presented for rating the degree of recrystallization of formed uranium metal, the inclusion content of as-cast uranium metal, and the inclusion and stringer content of formed uranium metal.

INTRODUCTION

Fuel cores are fabricated from cast uranium metal by various forming processes. Those most commonly employed are rolling and extrusion. These forming processes change the grain structure from the as-cast condition to a partially or completely recrystallized condition.

Prior to the addition of alloying elements to uranium, very few problems were encountered in producing rolled or extruded uranium metal that was completely recrystallized. Now, however, with the routine use of small quantities of alloying additives in the uranium, it is sometimes difficult to achieve complete recrystallization in the formed uranium products. Because of this reduced recrystallization, it became necessary to develop accurate standards for evaluating the degree of recrystallization of formed uranium metal from zero to 100%.

Several methods have been used in the past to evaluate the inclusion and stringer content of uranium metal. These methods have been useful, but a need has developed for visual standards that could be adopted for use by all persons in the AEC complex concerned with the evaluation of inclusions and stringers. The development of such standards was the objective of this work.

SUMMARY OF RESULTS

The following three sets of standards were developed to serve as guides in the metallographic evaluation of uranium metal:

1. Standards to rate the degree of recrystallization at 100X of formed uranium metal (Figure 1).

2. Standards to evaluate the inclusion content at 100X of as-cast uranium metal (Figure 2).

3. Standards to evaluate the inclusion and stringer content at 100X of formed uranium metal (Figure 3).

PROCEDURES

The procedure used to obtain the 100X recrystallization standards (Figure 1) was as follows:

1. Cut the sample under coolant on a Campbell cutting machine using an Allison cut-off wheel No. C120PRAG6.

2. Rough-grind on a grinding wheel using 60-grit abrasive paper.

3. Fine-grind on a grinding wheel using 400-grit abrasive paper. Then wash with water, rinse in alcohol, and dry with air.

4. Attack-polish the sample using the following procedure:

   a. Prepare a mixture of the following composition:

      10% 118g CrO_3 in 100 ml H_2O

      10% Saturated solution of $Na_2Cr_2O_7 \cdot 2H_2O$ in water

      5% Linde A compound in water (paste consistency)

      75% Distilled water

   b. Use above solution on a lap covered with a Buehler Ltd. Microcloth No. 40-7208AB and polish the sample for 1 minute at approximately 500 rpm. Then wash with water, rinse in alcohol, and dry with air.

5. Photograph the sample at 100X under polarized light.

The procedure used to obtain the 100X inclusion and stringer standards (Figures 2 and 3) was identical to the one above for the first three steps. The remaining steps were as follows:

4. Polish the sample on a lap covered with a polishing cloth using 6-micron diamond compound as the abrasive. Then wash with water, rinse in alcohol, and dry with air.

5. Mechanically polish the sample on a lap covered with a polishing cloth using 1-micron diamond compound as the abrasive. Then wash with water, rinse in alcohol, and dry with air.

6. Prepare a bath consisting of one part of a solution of 118 grams CrO_3 in 100 ml water and 4 parts acetic acid. Electropolish the sample for 15 seconds at 20 volts using a stainless steel cathode and the sample as the anode. Then wash with water, rinse in alcohol, and dry with air.

7. Photograph the sample at 100X under bright field illumination on a metallograph.

In both this procedure and the one preceding, the photographs were taken on Kodak Royal Pan film, 5 inches by 7 inches, ASA 160. The film was developed in DK-50. The negatives were contact-printed on Illustrators Azo No. 5.

APPLICATION OF STANDARDS

The 100X standards developed to rate the degree of recrystallization of formed uranium (Figure 1) are designed for use as comparison standards. The field being viewed can be compared directly with the standards or a comparison can be made by utilizing 100X photomicrographs of the sample to be rated.

The 100X standards developed to evaluate the inclusion content of as-cast uranium metal and the inclusion and stringer content of formed uranium metal are also designed for use as comparison standards. It is necessary, however, that the metallograph have a magna-viewed marked off in 1/2-inch squares before these standards can be used.

The application of the 100X standards for evaluating the inclusion content as as-cast uranium (Figure 2) is described in the following paragraphs:

The standards contain photomicrographs of two types of inclusions, random and clustered. The random inclusions are evaluated as to size, type, and concentration. The size and type of random inclusions are evaluated by comparison with the 100X standards. The concentration of random inclusions is obtained by counting the average number of inclusions per 1/2-inch square at 100X from the grid on the magna-viewer of the metallograph. The concentration standards are used only as a guide when this type of evaluation is being made.

The clustered inclusions are evaluated as to type, size, and concentration. The type of inclusion is determined by comparison with the 100X standards. The size refers to the size of the inclusions that make up the clusters and can be evaluated by comparison with the 100 X standards. The concentration refers to the number of inclusions that make up a cluster and not to the number of clusters. This evaluation is made by counting the average number of inclusions that are contained in each cluster. The concentration standards are used only as guides when this evaluation is being made.

The application of the 100X standards for evaluating the inclusion and stringer content of formed uranium (Figure 3) is described in the following paragraphs:

The random inclusions are evaluated as to type, size, and concentration. The size and type of the inclusions are evaluated by comparison with the 100X standards. The concentration of random inclusions is evaluated, as before, by counting the average number of inclusions per 1/2-inch square at 100X on the magna-viewer of the metallograph. The concentration standards are used only as a guide when this evaluation is being made.

The stringers of inclusions are evaluated as to the number of stringers per field, the length of the stringers, and their width. The number of stringers per field can be obtained by counting the actual number of stringers that appear in any given field at 100X. The length of the stringers is based on 1 inch at 100X. The actual length of a stringer is obtaindd by counting the number of 1/2-inch squares on the magna-viewer covered by the stringer and converting this into inches (that is, multiply inches by 2). The width of the stringers is based on 1/2 inch at 100X. This evaluation can be obtained by determining what fractional part of a 1/2-inch square on the magna-viewer is covered by the width of any given stringer. The standards for stringer content are to be used only as a guide when this type of evaluation is being made.

RECRYSTALLIZATION CHART FOR FORMED URANIUM

MICRO EXAMINATION

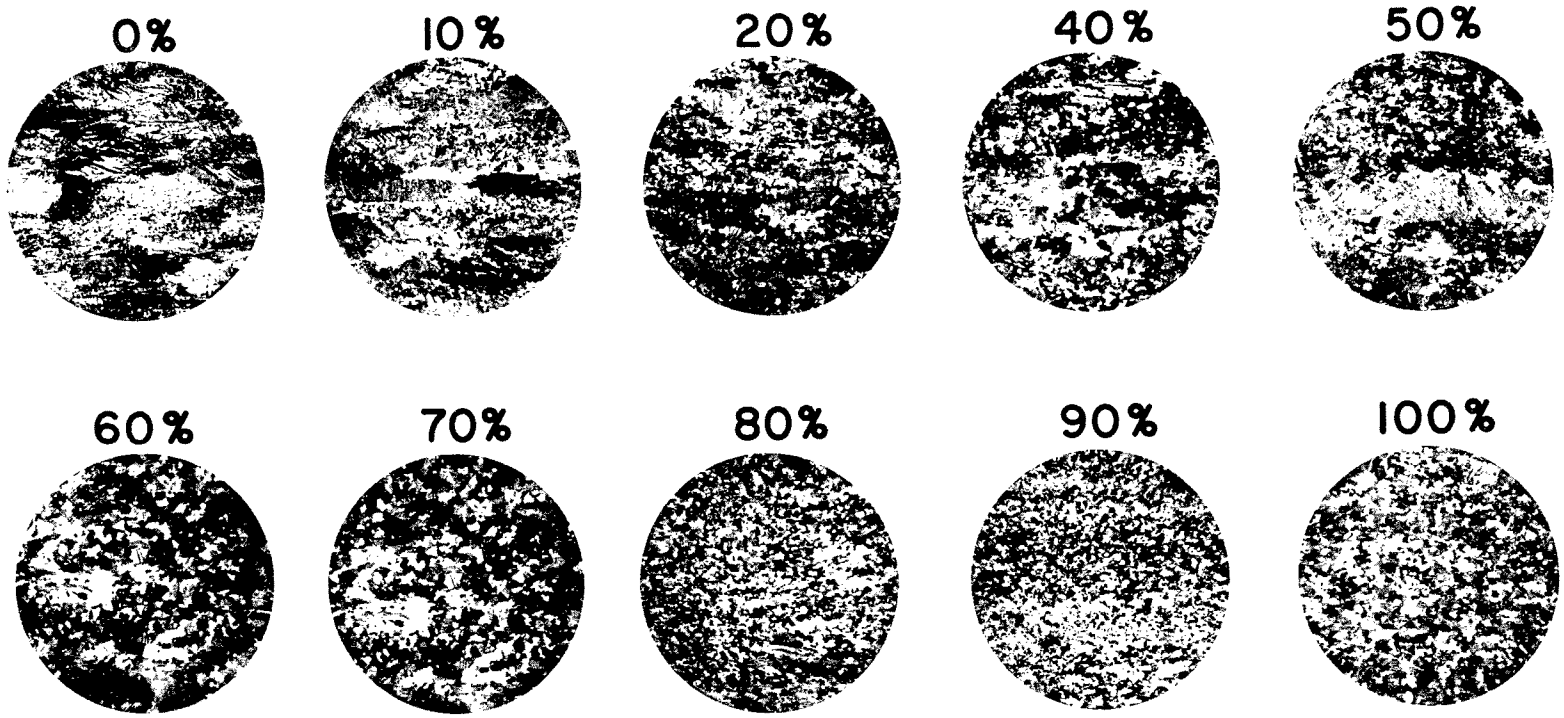

100X Reduced 62%

Figure 1

INCLUSIONS — CAST URANIUM

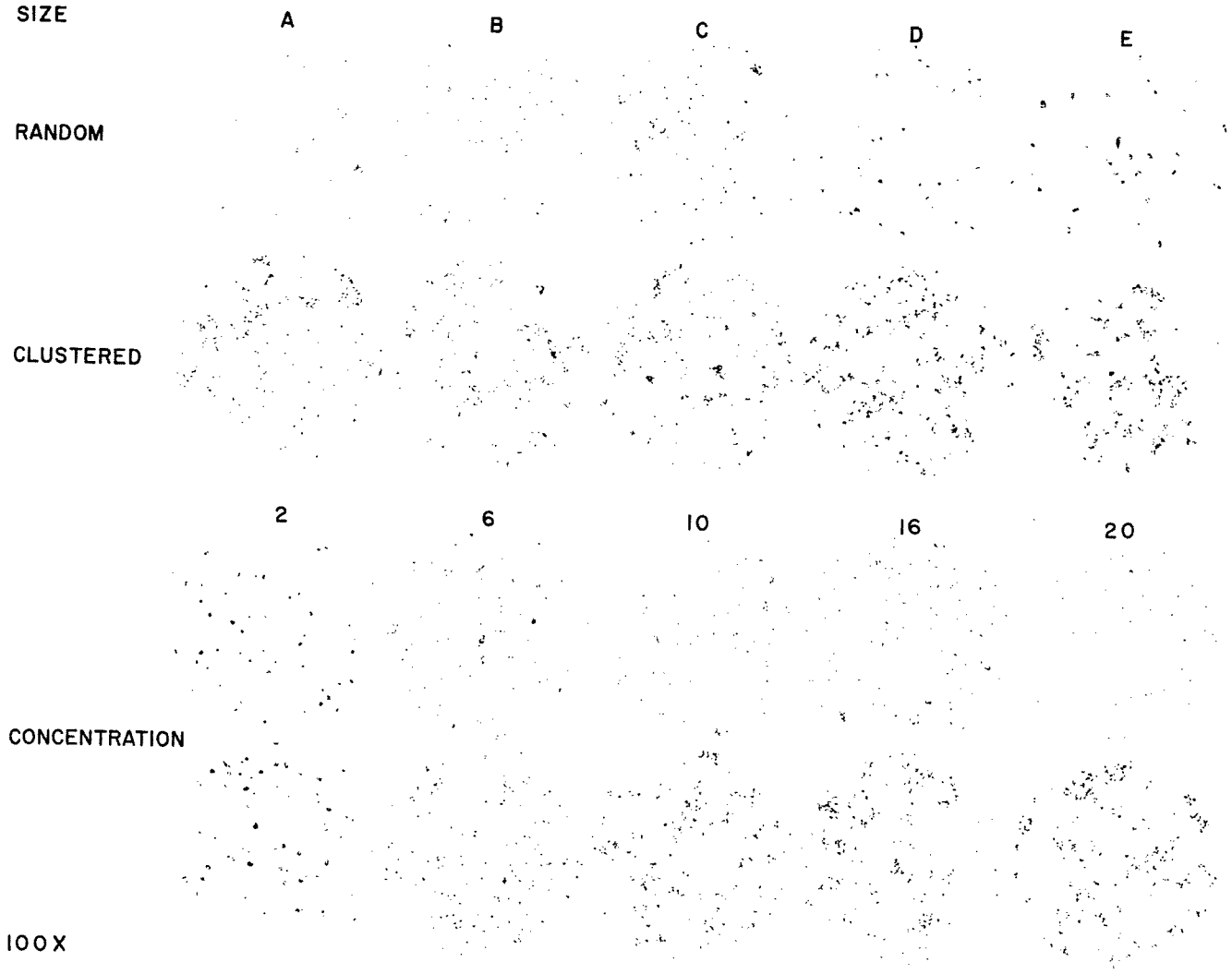

Reduced 65%

Figure 2

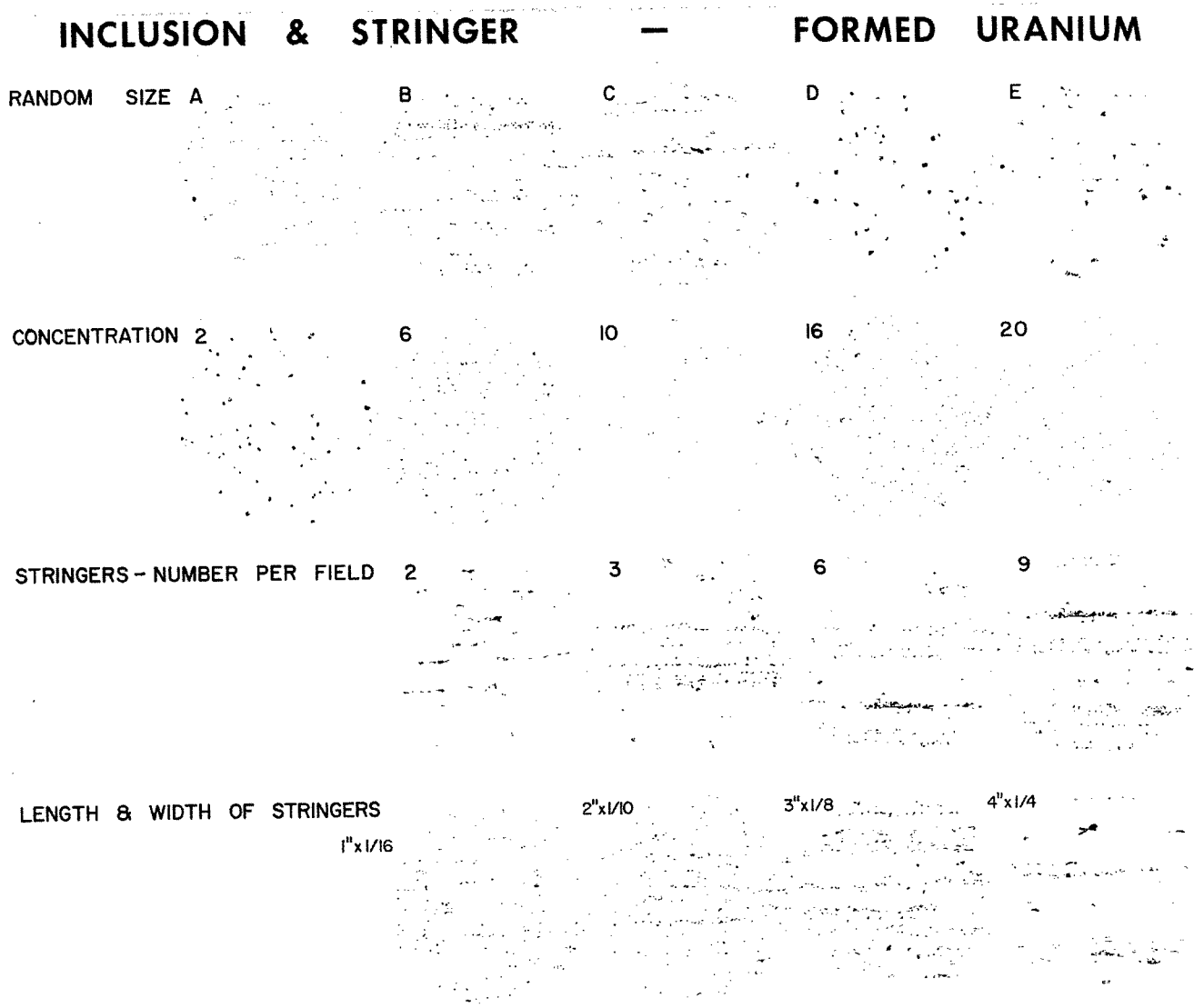
INCLUSION & STRINGER — FORMED URANIUM
RANDOM SIZE A
B
C
D
E
CONCENTRATION 2
6
10
16
20
STRINGERS - NUMBER PER FIELD 2
3
6
9
LENGTH & WIDTH OF STRINGERS
1"x1/16
2"x1/10
3"x1/8
4"x1/4
LENGTH OF STRINGERS BASED ON ONE INCH AT 100 X.
WIDTH OF STRINGERS BASED ON ONE HALF INCH AT 100 X.
100X Reduced 64%
NLO

Figure 3

GRAIN SIZE STANDARDS FOR BETA HEAT-TREATED URANIUM FUEL CORES

By

M. H. Cornett

ABSTRACT

Visual standards are presented for rating grain size at 3X of the following beta heat-treated uranium fuel cores: (1) oil-quenched, extruded tubular fuel cores, (2) oil-quenched, rolled I&E fuel cores, and (3) water-quenched, rolled I&E fuel cores.

INTRODUCTION

The introduction of additives to the uranium produced at the National Lead Company of Ohio refined the beta-quenched grain structure to such an extent that the existing 3X FEDC grain size standards were inadequate for rating the finer grains. New 3X standards were therefore developed with sufficient range to cover any grain size likely to occur in uranium containing alloying additives.

SUMMARY OF RESULTS

Standards were developed to rate the beta-quenched grain size at 3X of the following types of fuel cores (in this report the reproduction makes the magnification about 1-1/2X):

1. Oil-quenched, extruded tubular fuel cores (Figure 1).
2. Oil-quenched, rolled I&E fuel cores (Figure 2).
3. Water-quenched, rolled I&E fuel cores (Figure 3).

The grain size range is from 1 to 9 for each type of core examined. The letters preceding the grain size numbers indicate the type of fuel core or the type of heat treatment.

PROCEDURE

The heating medium for all fuel cores sampled and evaluated was molten salt. The samples were prepared and photographed according to the following procedure:

1. Cut the sample under coolant on a Campbell cutting machine using an Allison cut-off wheel No. C120PRAG6.

2. Rough-grind on a grinding wheel using 60-grit abrasive paper.

3. Macroetch in a bath of concentrated HCl acid and rinse in water for 3 to 5 seconds.

4. Rinse in concentrated HNO_3 acid for 3 to 5 seconds or until the desired contrast is obtained and wash in water.

5. Place the sample on the macro camera and photograph wet at 3X. The film used was Kodak Royal Pan, 5 inches by 7 inches, ASA 160; it was developed in DK-50. The negatives were contact-printed on Illustrators Azo No. 3.

APPLICATION OF STANDARDS

The 3X standards developed to rate beta-quenched grain size of the various types of fuel cores are designed for use as comparison standards. This can be a direct visual comparison at 3X on the macro camera or a comparison of 3X photomacrographs of the samples to be rated with the 3X standards.

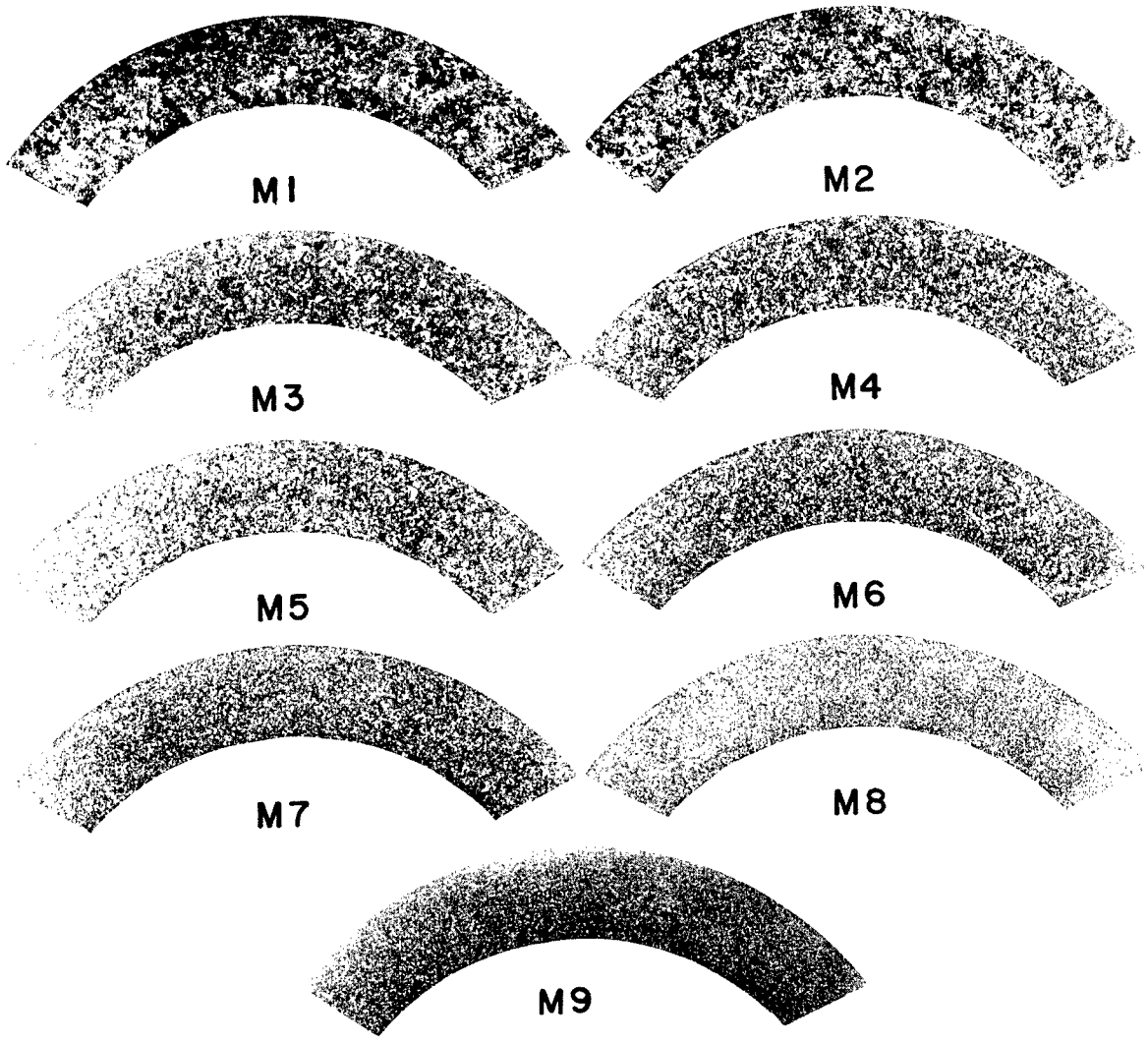
(3X) OIL QUENCHED EXTRUDED TUBULAR STANDARDS
M1
M2
M3
M4
M5
M6
M7
M8
M9

Figure 1

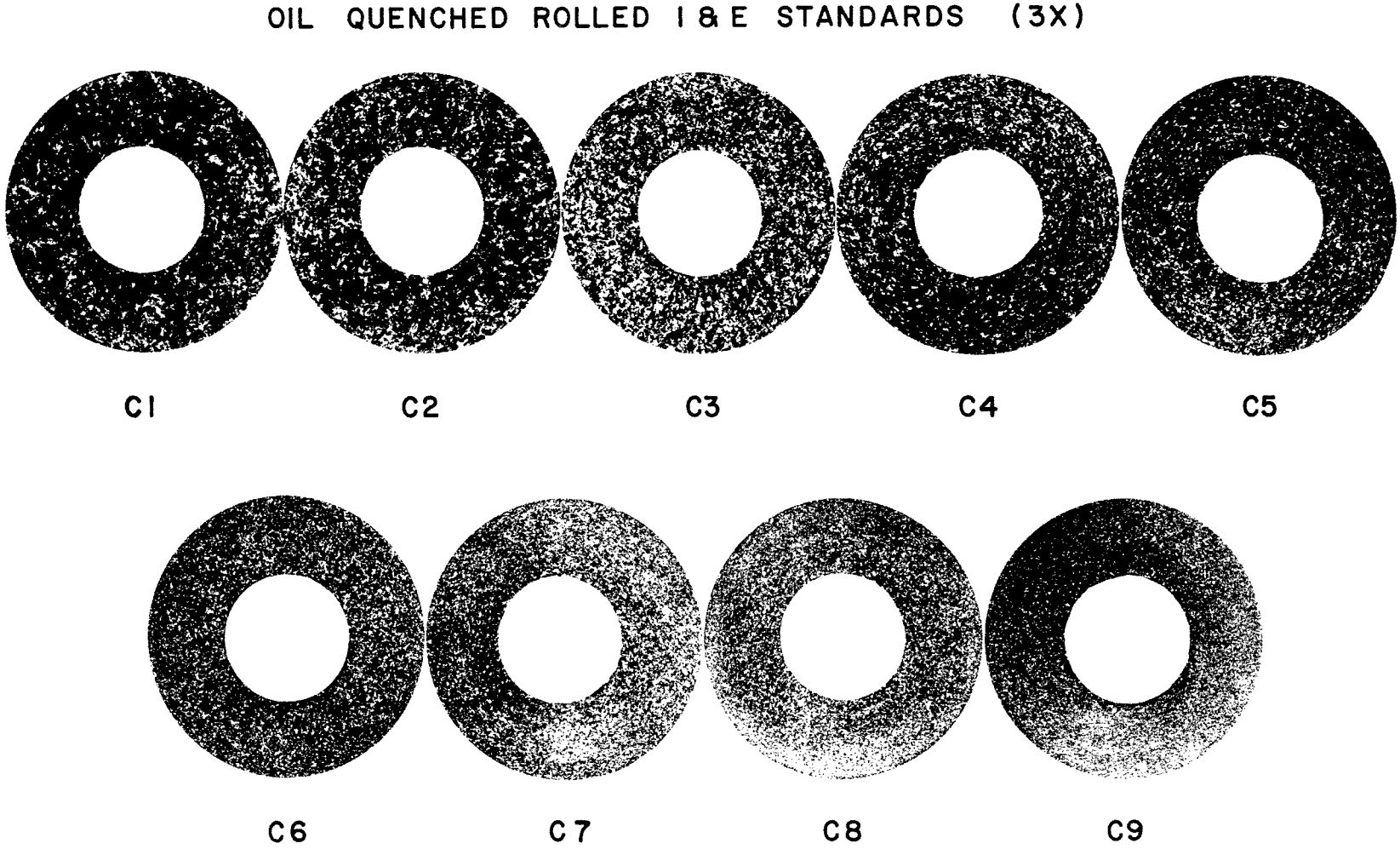

Figure 2

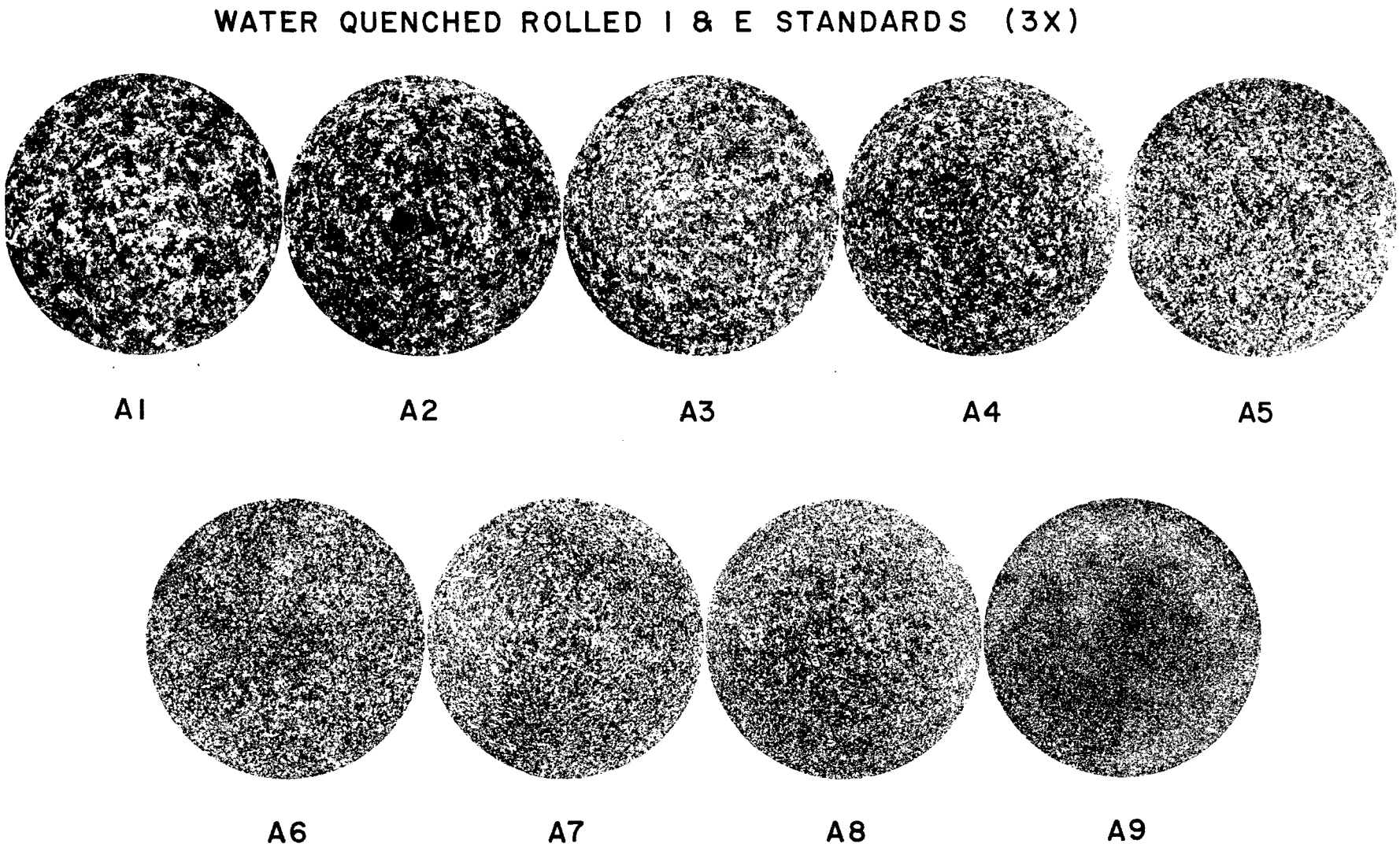
WATER QUENCHED ROLLED I & E STANDARDS (3X)
A1
A2
A3
A4
A5
A6
A7
A8
A9

Figure 3

ELECTRON MICROPROBE STUDIES OF DILUTE URANIUM-BASE ALLOYS

By

J. W. Colby and W. N. Wise

ABSTRACT

This paper describes some preliminary studies of uranium employing a recently acquired Applied Research Laboratories EMX microprobe analyzer. In particular, the results of studies on solid metal and shot containing phosphorus additions and on uranium shot containing zirconium additions are described. Results from a study of cladding failures of some Mark V-E fuel cores (Savannah River) are also discussed.

INTRODUCTION

Uranium shot has been produced at the National Lead Company of Ohio with additions of phosphorus, carbon, and zirconium. These latter two elements have been added separately and in various combinations. The shot was examined in the microprobe in an effort to identify the phases present.

Uranium fuel cores which had been nickel plated and canned in aluminum jackets exhibited poor bonds in some cases, and Savannah River personnel requested that these clad fuel cores be examined in the microprobe in an effort to learn the cause of bond failure.

EXPERIMENTAL PROCEDURES

The microprobe analyzer employed for the investigation was the Applied Research Laboratories model previously described.[1,2] The operating conditions for the analysis were: accelerating voltage, 20 kv; emission current, 105 μa; average sample current, 0.07 μa. The spectrometers employed were a 4-inch EDT crystal and FPC minitron with P-10 gas (90% argon and 10% methane) for U Mβ X rays, and a 4-inch ADP crystal and FPC minitron with P-10 gas for Zr Lα X rays and P Kα X rays. Both detectors are of the fully focusing type (Johannson geometry). For the quantitative analysis, the "Fixed-Time" method was em-

ployed. Pure uranium, zirconium, and a specimen of UP obtained from Argonne National Laboratory were used as standards, and the data were corrected for background, dead time, and absorption (Philibert Method[3]). No corrections were made for fluorescence by line or continuum, or for atomic number.

Cathodoluminescence

The identification of the pure oxides and hydrides was based on the known cathodoluminescence[4,5,6] of these materials. UO_2, SiO_2, ZrO_2, Al_2O_3, and MgO have been examined in the microprobe and all visibly fluoresce a bluish color under the impact of the electron beam (cathodoluminescence). This luminescence affords a qualitative identification of oxides. Similarly, it has been noted that MgF_2 exhibits a yellowish luminescence and UH_3 and ZrH_2 exhibit a pink or red luminescence under electron bombardment. CaF_2 on the other hand, exhibits a deep blue luminescence. As an example of the use of cathodoluminescence, Figures 1 and 2 are photomicrographs of a sample while under the impact of the electron beam taken through the optical system of the microprobe, but with the external light source turned off. The electron beam was expanded to cover the entire field. The sample current was approximately 12 μa (at 15 kv) and the exposure time was 5 minutes on Polaroid color film. The bright yellow regions are MgF_2, light blue regions are MgO, deep blue regions are CaF_2, and the brown or unexposed regions are uranium metal. In general, uranium oxide (UO_2) fluoresces a deeper blue than the MgO, but not as deep as the CaF_2. ZrO_2 appears similar to UO_2 in color.

Whereas identification based on cathodoluminescence is not positive, it does provide useful qualitative information. It also helps to distinguish uranium carbides and uranium nitrides from fluorides, oxides, and hydrides, because the carbides and nitrides are not cathodoluminescent. (Of course, if the microprobe does not permit observation of the sample during analysis, such information cannot be obtained.)

Analyses of 20 to 80 Mesh Uranium Shot

Figure 3a is a back-scattered electron (BSE) image of one of the pores which was rimmed with hydride; Figure 3b is a zirconium X-ray image showing the distribution of the (Zr,U) hydrides at the periphery of the pore. Figures 4a and 4b are BSE and zirconium X-ray images of (Zr,U) oxide inclusions in uranium shot. Figures 5a and 5b are BSE zirconium X-ray images of low carbon shot showing a few isolated (Zr,U)C inclusions.

Figure 6 is a photomicrograph of a typical field in uranium shot of higher carbon content. Figures 7a, b, c,

and d are BSE and zirconium X-ray images of shot from the same sample as that in Figure 6, showing the (Zr,U)C segregation and the relatively large carbide size.

Figure 8 is an optical micrograph of uranium shot containing no zirconium and 633 ppm carbon, showing the type of second phase distribution that is preferred. Figure 9 is a BSE image of shot from the same sample as that in Figure 8, showing primary UC dendrites and a finely dispersed secondary phase.

A large (Zr, U)C inclusion and several smaller ones were step-scanned. In step-scanning, the electron beam is held stationary and the sample is stepped in increments of one to ten microns. After each step, a "fixed-time" analysis is performed. As many as three elements may be analyzed simultaneously. In the present case, the sample was stepped in 1-micron increments, and the zirconium content was determined at 1-micron intervals across the large inclusion. The resulting counts were corrected for background, dead time, and absorption, converted to weight per cent, and plotted in Figure 10. The solid black line shows the weight per cent of zirconium in pure ZrC. It can be seen that the inclusion was a mixture of ZrC and UC, and approached pure ZrC in only one spot in the inclusion. Other inclusions showed the same tendency.

Several individual inclusions were analyzed, and it was found that in general the small inclusions had a higher zirconium content than did the large ones.

Uranium shot, selected at random from a sample with a reported composition of 1.8 w/o zirconium, was analyzed in the microprobe. The zirconium contents of the individual shots ranged from 0.8 w/o to 3.7 w/o, with an average value of 1.6 w/o. The difference in the two average values could be attributable to the small number of samples (eight) examined in the microprobe. One of these shot was then scanned; the zirconium content varied from 1.7 w/o at the edge to 0.7 w/o at the center.

From the preceeding results, we conclude the following:

1. Shot produced from uranium with zirconium additions shows a solid solution of zirconium in uranium when the carbon content is low (less than 150 ppm).

2. Shot produced from uranium with 600 ppm carbon as the only additive shows a finely dispersed carbide phase.

3. The combination of zirconium and carbon (greater than 150 ppm) in uranium shot produces large, mixed carbides which are heterogeneously dispersed throughout the shot.

We have previously examined derby, cast, and fabricated uranium which contained phosphorus, and the results are given elsewhere[1,2,7] In general, the phosphorus is present as UP in the form of large angular inclusions, much like carbides or nitrides, or as a eutectic.

Figure 11 is a sample current image showing the angular type UP precipitate in derby uranium containing approximately 350 ppm phosphorus. Figures 12a and 12b are a back-scattered electron image and a phosphorus X-ray image, respectively, of the eutectic. The electron beam was enlarged to cover the region shown in the circle and the phosphorus content determined. This was repeated for several areas. The phosphorus content so determined should give the composition of the eutectic. We found this to be 2200 ppm. Earlier estimates by R. Kemper of Hanford Laboratories based on metallography indicated that the eutectic occurs at approximately 1200 to 1500 ppm phosphorus.

Figures 13a and 13b are a back-scattered electron image and phosphorus X-ray image of a large phosphide inclusion occurring in uranium shot (containing 350 ppm phosphorus). This was an isolated case and not typical of the shot in general. Figure 14 is a sample current image of the phosphorus network structure that is typical of the shot. The composition of the network phase is approximately that of the eutectic.

Based on these and earlier results, we conclude that phosphorus is a potentially good additive to uranium. UP is quite stable and its presence as a finely dispersed precipitate should increase the creep strength over unalloyed uranium.

Study of Cladding Failure

Recently, Savannah River encountered clad uranium fuel cores having poor bond strength. The cores were of the Mark V-E type that had been nickel plated and aluminum clad. In general, the bond strengths were lower than for Mark V-B cores similarly treated. Samples were brought to our laboratory and to Mallinckrodt for examination by microprobe in an effort to learn the cause of the poor bonding characteristics of these V-E cores as compared with the V-B cores. SRL had already concluded that the failure was occurring in the "delta" phase (phase between the nickel and uranium), and they noticed that there was a finely dispersed phase present in or near the delta phase in cores exhibiting failures (Figure 15).

On analyzing the various layers present, we found them to be Al, Al_3Ni (beta), Al_3Ni_2 (Gamma), Ni, delta phase,

and uranium. The delta phase was found to consist of two phases; one was UNi_5 and the other was probably U_6Ni. This latter phase was too thin to identify in the probe. We concluded, after examining typically good cores and typically bad cores, that we could detect no difference between them. We could find no elements present in the delta phase other than Ni and U, and the delta phase was present in both types of cores.

Mallinckrodt reported[8] that UNi_5 was present in the good cores only. However, we find it present in both types of cores and this is substantiated by SRL electron micrograph replicas[9] (Figure 15). Cathodoluminescence, however, does not show the presence of any oxide particles in either type of core. Further, we find from sample current traces that this delta phase contains small cracks, and in some instances, the delta phase is separated from the Ni (Figures 16a and 16b).

It has been reported[10] that the interface between UNi_5 and Ni is extremely brittle and that despite precautions these two are easily separated by mechanical shocks and are not rejoined during cladding. From the above apparent discrepancies in reported results, it is evident that additional analyses must be performed to determine the true cause of bond failures.

CONCLUSIONS

In conclusion, it may be noted that the microprobe analyzer may provide very positive, quantitative, information on a micron scale. In some cases, when the region to be analyzed is on a submicron scale, the microprobe may only provide qualitative information or sometimes information of a "negative" type. However, even these latter two types of information are often adequate to prove or reject certain hypothesis and, so, are useful to the metallurgist.

REFERENCES

1. J. W. Colby. "Electron Microprobe Examination of Phosphides in Uranium," Summary Tech. Rpt. for the Period January 1, 1963 to March 31, 1963, USAEC Report NLCO-870, pp. 83-91. May 10, 1963.

2. J. W. Colby. Electron Microprobe Examination of Uranium, Paper Presented at the 13th Annual National Lead Company Analytical and Physical Testing Symposium, Hightstown, New Jersey, October 10-11, 1963, USAEC Report NLCO-892. September 16, 1963.

3. J. Philibert. "A Method for Calculating the Absorption Corrections in Electron Probe Microanalysis," International Symposium on X-Ray Optics and X-Ray Microanalysis, 3rd Stanford, 1962, pp. 379-392. New York: Academic Press, 1963.

4. J. V. P. Long. "Recent Advances in Electron Probe Analysis," Advances in X-Ray Analysis, Vol. 6, pp. 276-290. New York:Plenum Press, 1963.

5. K. F. J. Heinrich. "Oscilloscope Readout of Electron Microprobe Data," Advances in X-Ray Analysis, Vol. 6, pp. 291-300. New York:Plenum Press, 1963.

6. J. V. P. Long. "The Application of the Electron Probe Microanalyzer to Metallurgy and Minerology," International Symposium on X-Ray Optics and X-Ray Microanalysis, 3rd Stanford, 1962, pp. 279-295. New York: Academic Press, 1963.

7. W. N. Wise and J. W. Colby. "Gamma-Phase Annealing of Uranium Containing Phosphorus," Summary Tech. Rpt. for the Period April 1, 1963 to June 30, 1963, USAEC Report NLCO-885, pp. 21-26. July 18, 1963.

8. duPont de Nemours (E. I.) and Company, Savannah River Laboratory. "Report from Mallinckrodt Chemical Works, Uranium Division," Report of Working Committee of the Fuel Element Development Committee, January 14-16, 1964, USAEC Report DPST-64-129, pp. 29-34. January, 1964 (Classified).

9. duPont de Nemours (E. I.) and Company, Savannah River Laboratory. "Report from E. I. duPont de Nemours and Company (SRP)," Report of the Working Committee of the Fuel Element Development Committee, January 14-16, 1964, USAEC Report DPST-64-129, pp. 109-112. January, 1964 (Classified).

10. F. Brossa, R. Theisen, J. J. Huet, and D. Tytgat. Study of Nickel as a Diffusion Barrier Between Uranium and Aluminum, Translated from Report EUR-171, USAEC Report HW-TR-49. 1962.

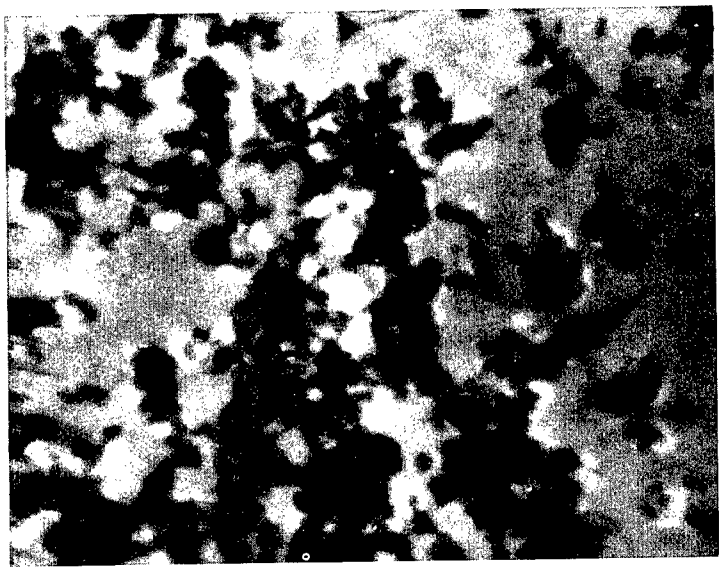

Figure 1 - Cathodoluminescent image of sample. Yellow area is MgF_2; light blue areas are MgO; dark blue areas are CaF_2; and brown areas are uranium metal. (~300X).
(these colors appeared on the original photograph.)

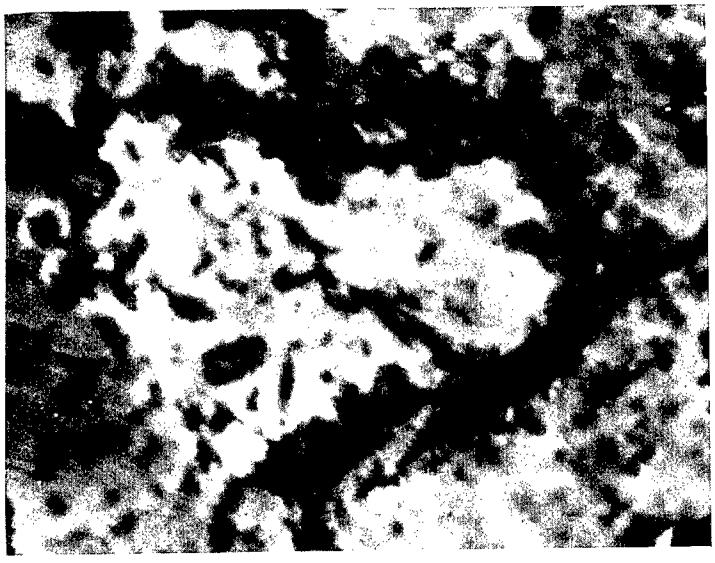

Figure 2 - Cathodoluminescent image of same sample, different field. Yellow area is MgF_2; light blue areas are MgO; dark blue areas are CaF_2; and brown areas are uranium metal. (~300X)
(these colors appeared on the original photograph.)

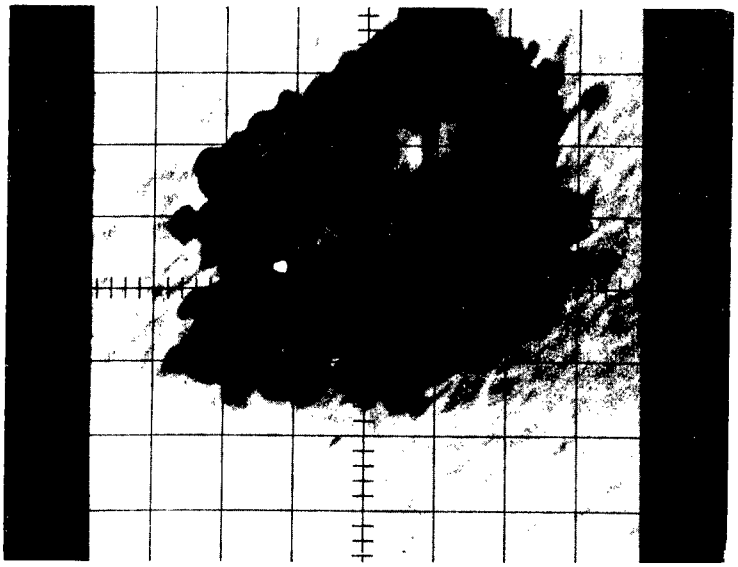

Figure 3a - Back-scattered electron image of pore in uranium shot containing 1.74 w/o zirconium and 152 ppm carbon. (1770X).

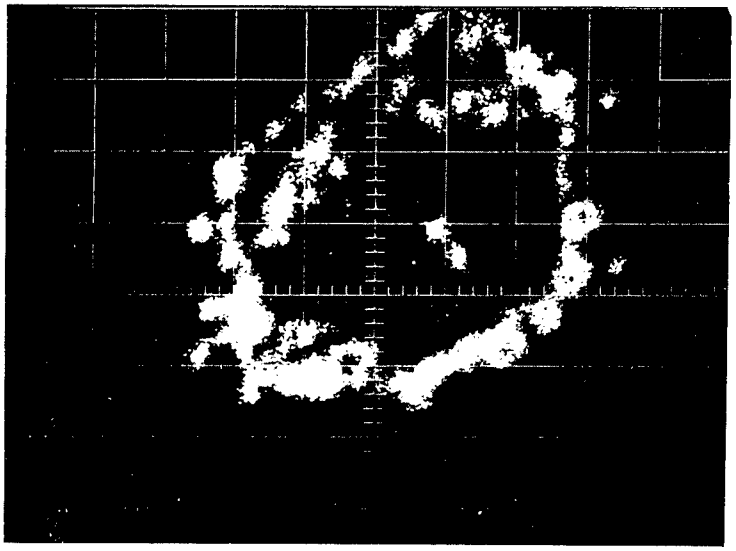

Figure 3b - Zirconium Lα X-ray image showing distribution of (Zr,U) hydrides at the periphery of the pore. (1770X)

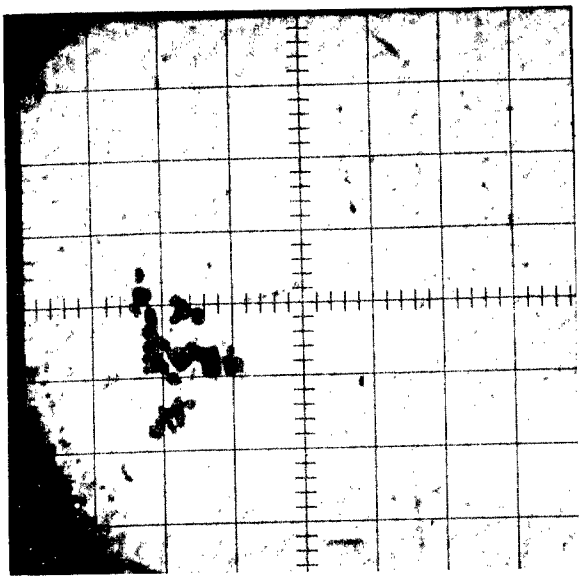

96A-3

Fig. 4a- Back-scattered electron image of uranium shot containing 2 w/o zirconium and 27 ppm carbon. (44OX)

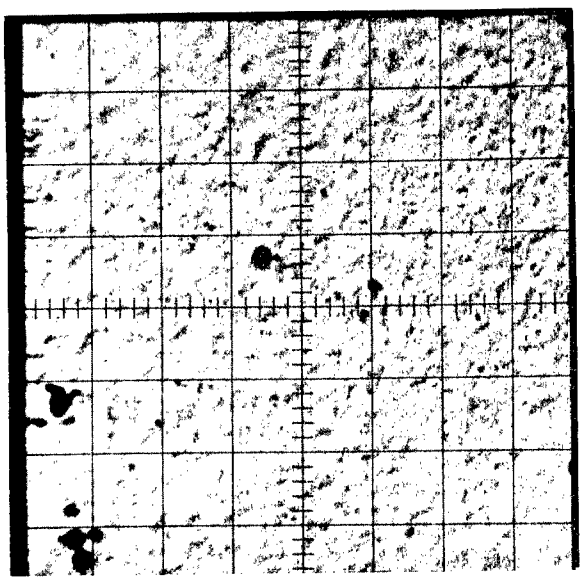

96A-8

Fig. 5a- Back-scattered electron image of uranium shot containing 1.74 w/o zirconium and 152ppm carbon. (44OX).

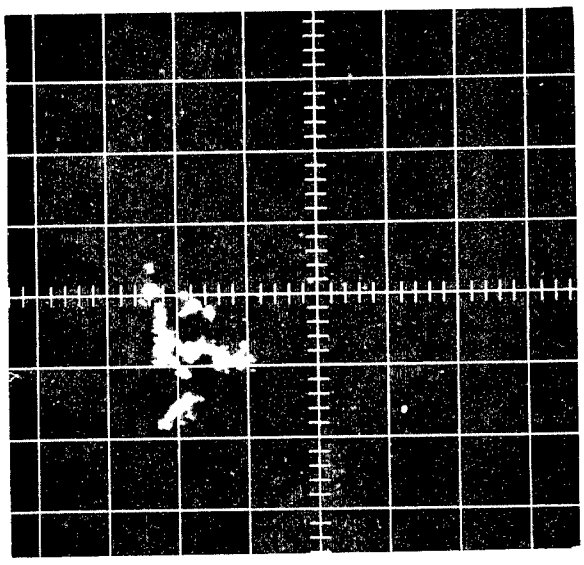

96A-4

Fig. 4b- Zirconium L_α X-ray image showing distribution of zirconium in (Zr,U) oxide inclusions. (44OX)

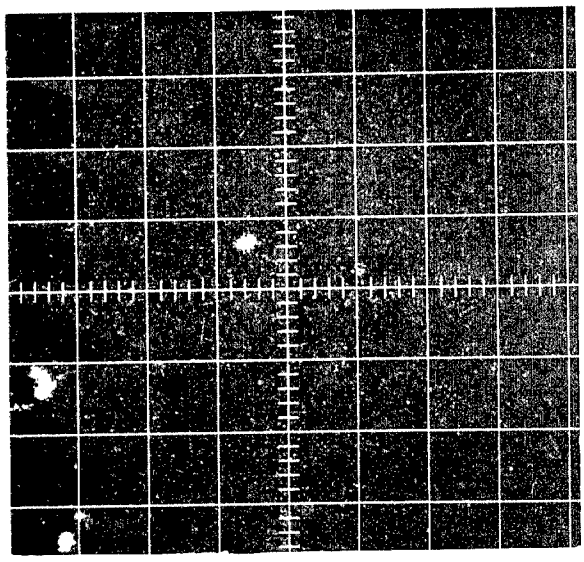

96A-9

Fig. 5b- Zirconium L_α X-ray image showing distribution of zirconium. Inclusions are (Zr,U)C. (44OX)

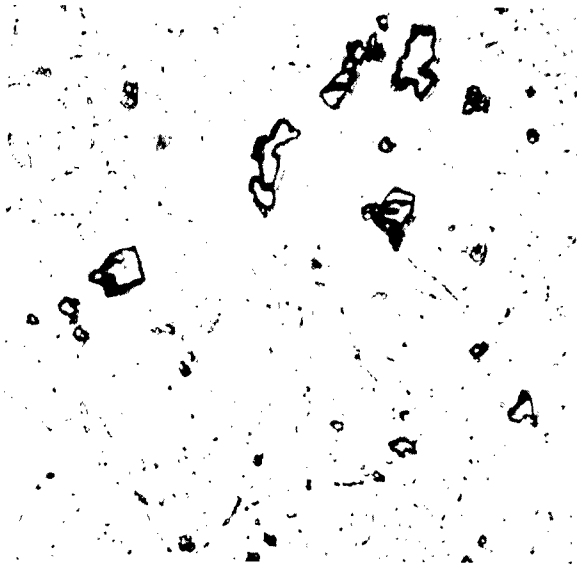

96A-7

Fig. 6- Optical micrograph of uranium shot (typical field) containing 1.8 w/o zirconium and 350 ppm carbon. Large gray inclusions are (Zr,U)C. (560X)

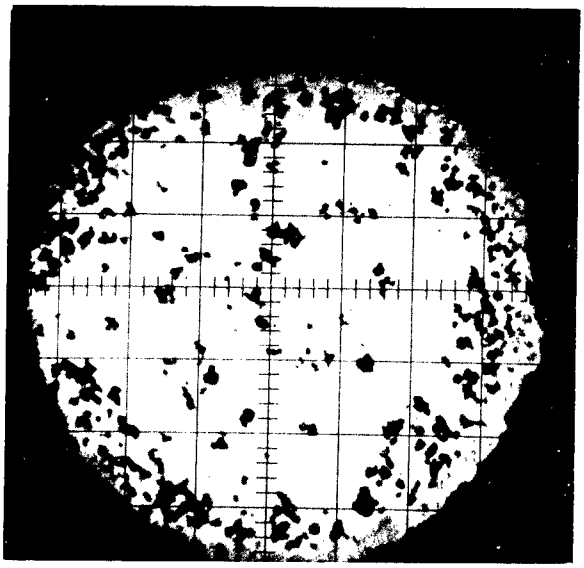

96A-12

Fig. 7a- Back-scattered electron image of uranium shot containing 1.8 w/o zirconium and 350 ppm carbon (same as figure 6). (220X)

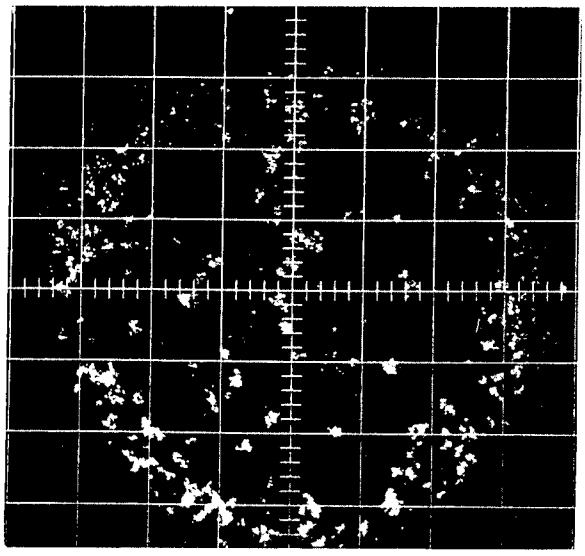

96A-13

Fig. 7b- Zirconium L_α X-ray image showing distribution of zirconium (same field as Fig. 7a) (220X)

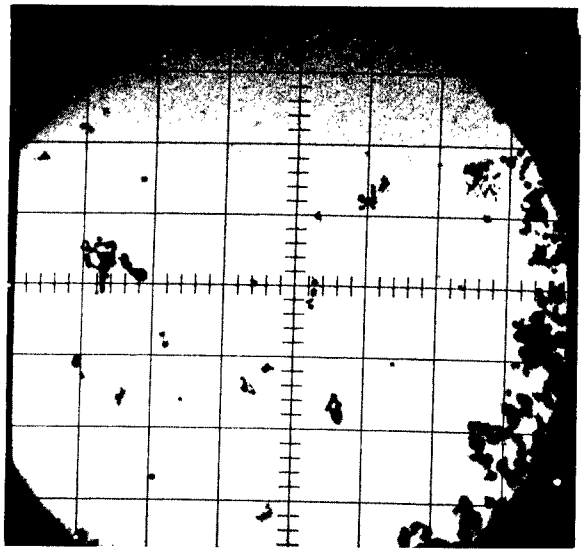

96A-14

Fig. 7c- Back-scattered electron image of uranium shot (same sample as Fig. 6). (220X)

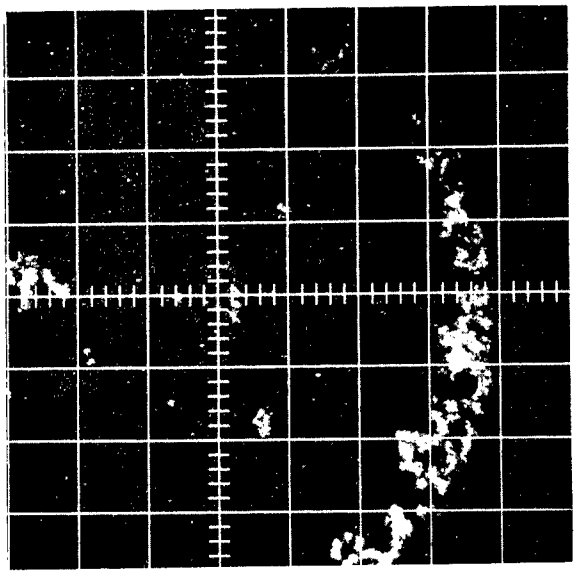

96A-15

Fig. 7d- Zirconium L_α X-ray image showing zirconium distribution (same field as Fig. 7c) (220X)

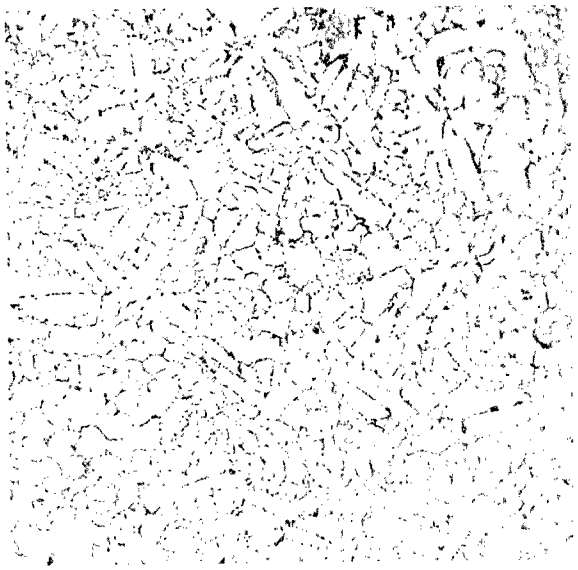

96A-16

Fig. 8- Optical micrograph of uranium shot containing 633 ppm carbon. (280X)

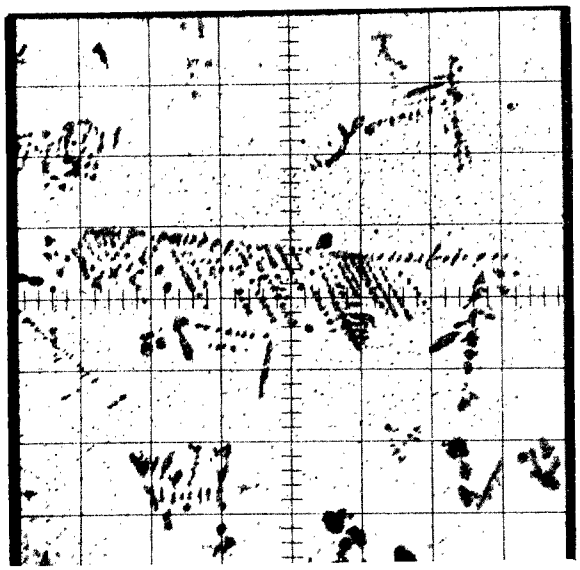

96A-17

Fig. 9- Back-scattered electron image of uranium shot showing primary carbide dendrites and finely dispersed background phase (same sample as Fig. 8) (1700X)

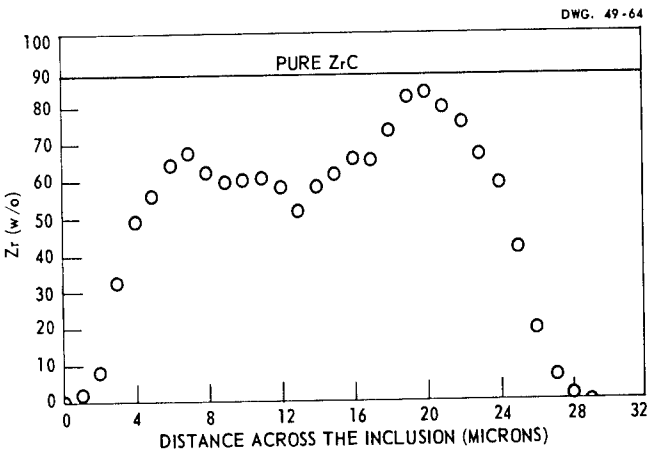

Fig. 10- Zirconium content vs position in large carbon inclusion.

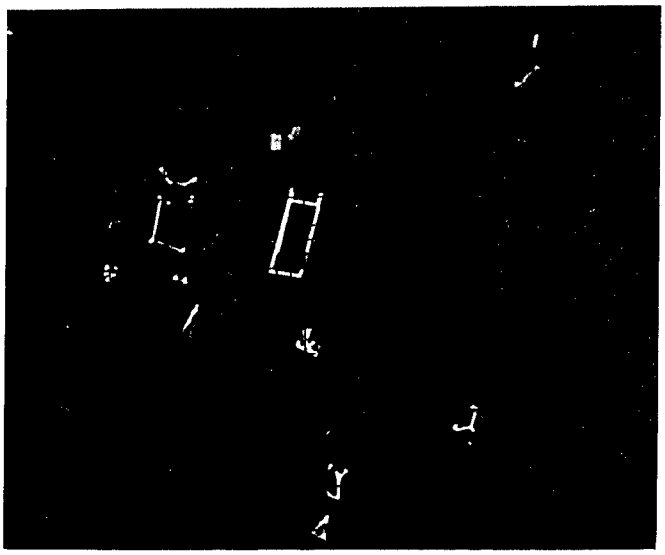

107A-20

Figure 11 - Sample current image of derby uranium showing angular type UP precipitate. (320X)

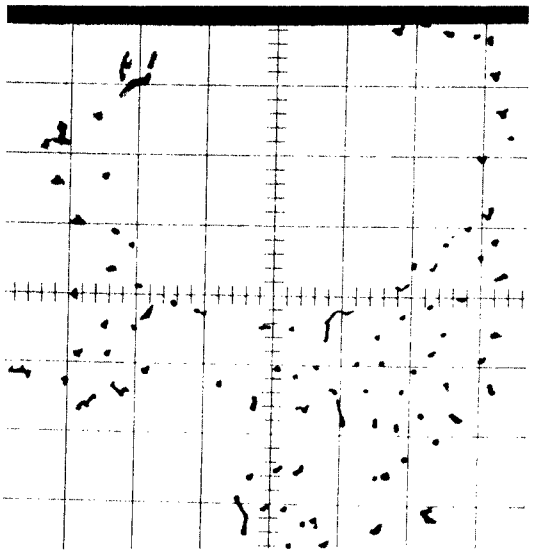

107A-21

Fig. 12a- Back-scattered electron image of derby uranium showing phosphorus eutectic. (320X)

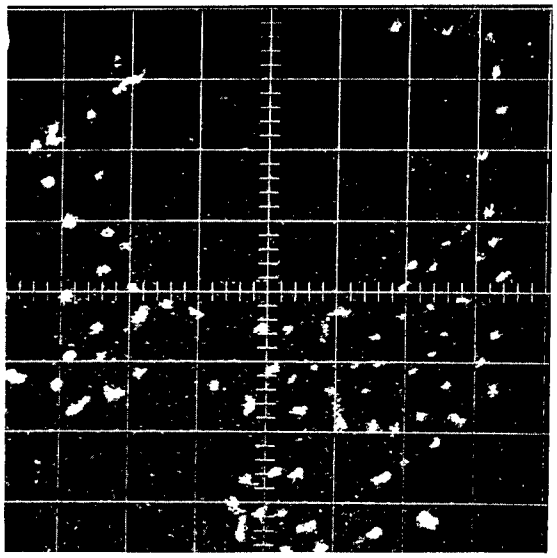

107A-22

Fig. 12b- Phosphorus X-ray image of same field as Fig. 12a. (320X)

107A-17

Fig. 13a- Back-scattered electron image of UP inclusion in uranium shot. (1280X)

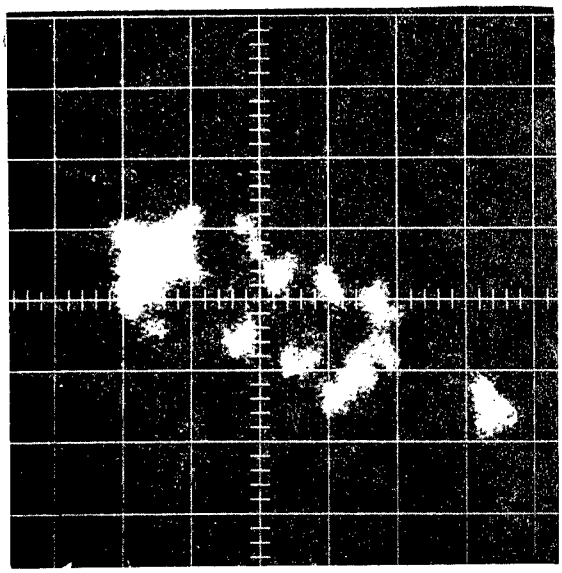

107A-18

Fig. 13b- Phosphorus X-ray image of same field as Figure 13a. (1280X)

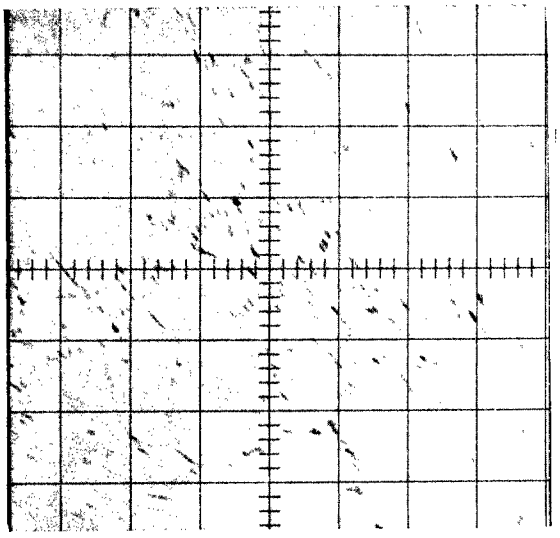

107A-19

Figure 14 - Sample current image of phosphorus Network in uranium shot. (640X)

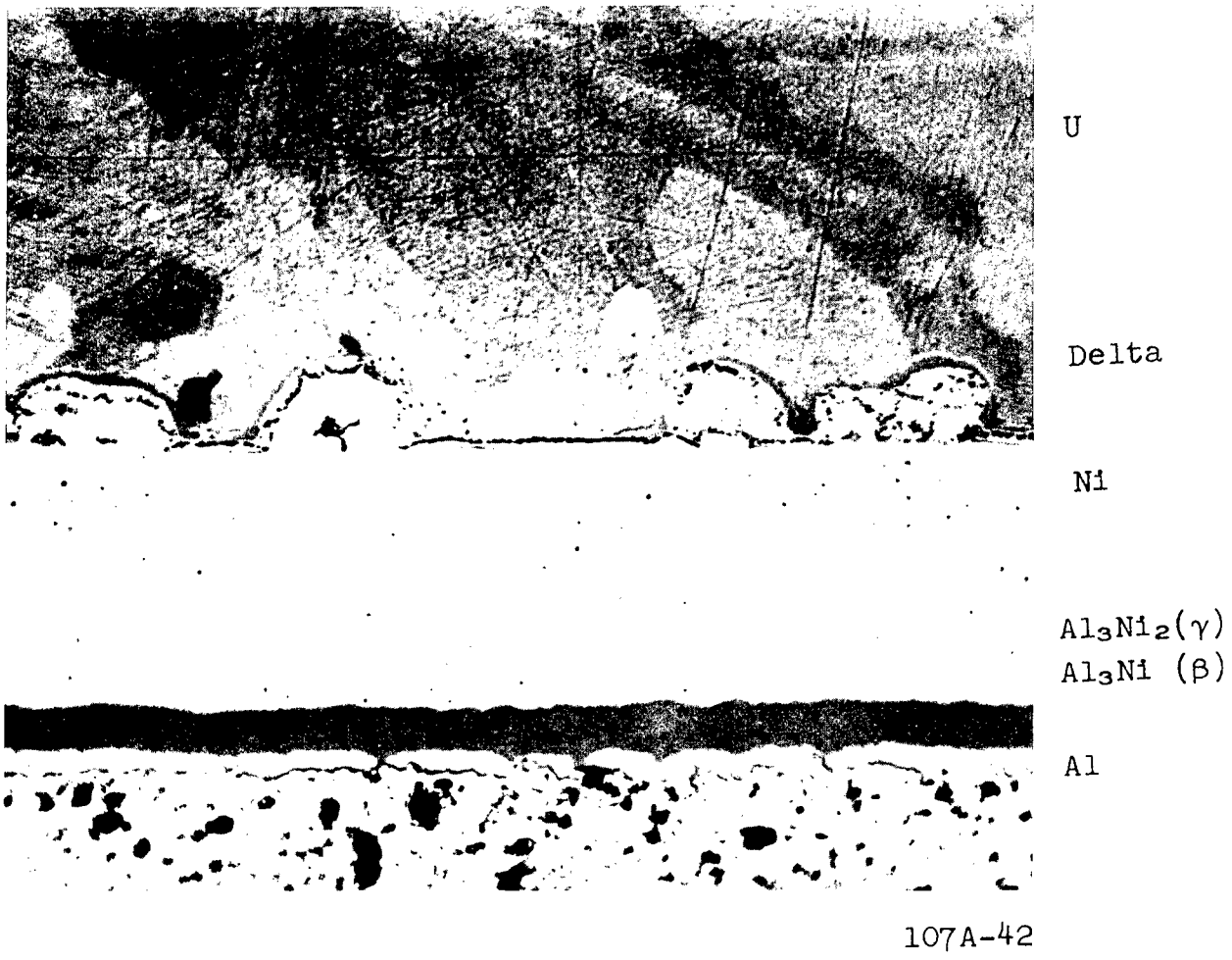

Figure 15 - Optical micrograph of clad uranium fuel core. (1000X)

107A-40

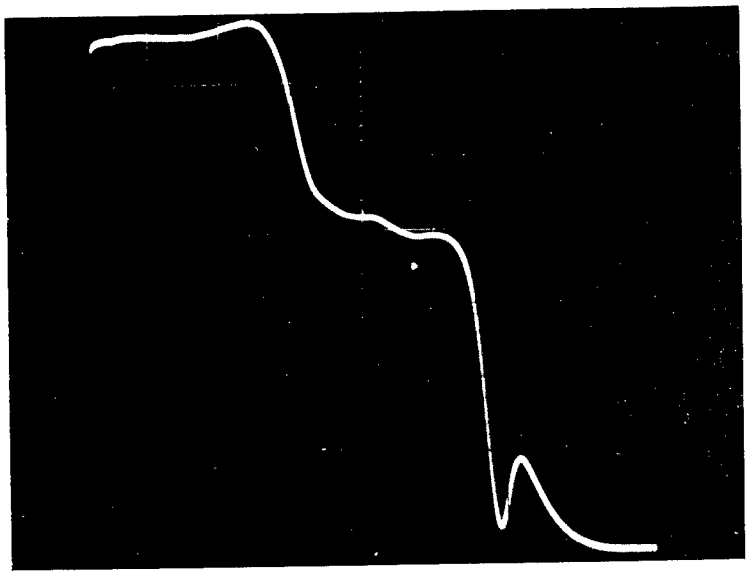

Figure 16a - Sample current trace across diffusion zone in typically good Mark V-B fuel core.

107A-41

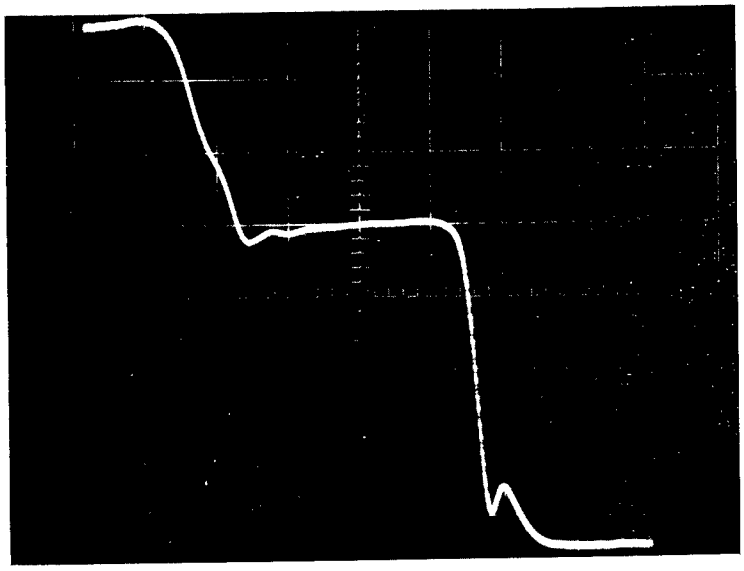

Figure 16b - Sample current trace across diffusion zone in typically weak Mark V-E fuel core.

MICROSTRUCTURAL STUDIES OF CAST URANIUM

by

A. A. Bauer, C. R. Thompson, and M. S. Farkas*

Battelle Memorial Institute
Columbus, Ohio.

INTRODUCTION

The microstructure of uranium has been studied extensively over the years and the general structural features observed in uranium are well characterized. This is especially true of wrought uranium which has been studied in much greater detail than cast material.

Studies to identify and characterize the inclusions in uranium have also been extensive. However, much of this effort has been concentrated, quite logically, on the large inclusions observed in uranium. These are readily observable metallographically and are subject to identification by fairly conventional techniques.

In this report the results of a brief program which was undertaken to evaluate the use of metallographic and electron microscopic techniques in detecting microstructural differences in cast uranium of varied chemistry and casting history are described. Of particular interest was evidence of differences in substructure and in fine-particle distribution and form between the various materials. Since this program was a very short term, the major accomplishment was the development of suitable techniques. The effectiveness of these techniques is illustrated by a series of micrographs from which some preliminary conclusions concerning the effects of chemistry and casting history on microstructure have been drawn.

EXPERIMENTAL PROCEDURES

Materials and Specimen Selection

Specimens were taken from seven cast ingots for examination. The ingots were cast at NLO. Two of these were 8-inch-diameter production ingots, designated B-85559, and B-85560. The remaining five were experimental ingots. Three ingots, B-49, B-50 and B-57 were 6-3/16 inches in diameter and were slow cooled in the melting crucible. Two experimental ingots, B-51 and B-52, were chill cast in a 2-1/2-inch-diameter cast-iron mold.

Slices were cut from the top of each ingot immediately below the crop. Specimens for examination were cut from the center of the slice and 1/4 inch from the edge of each slice. Samples for chemical analysis were taken from these same slices.

The results of chemical analyses for selected elements are shown in Table 1. The major variations in chemistry occurred in carbon content.

TABLE 1. CHEMICAL ANALYSES FROM URANIUM INGOTS CAST AT NLO

	Chemical Analysis, ppm						
	Production Ingots		Experimental Ingots				
Element	B-85559	B-85560	B-49	B-50	B-51	B-52	B-57
C	495	441	281-458[a]	675	340	68	138
Al	8	11	21	13	17	26	22
Fe	141	137	147	133	130	144	154
Si	97	95	127	127	135	116	95

(a) Range in analysis is indicative of inhomogeneity in ingot.

Techniques of Specimen Preparation

Approximately 1/8 inch was removed from the surface of each specimen by grinding and electropolishing to eliminate surface working which may have been introduced by the cutting operation in obtaining the specimens.

Three primary techniques of specimen preparation (Methods 1 through 3) were investigated after which specimens were examined both metallographically and in the electron microscope. A fourth preparation (Method 4) was used to prepare the specimens specifically for electron microscopic examination. The techniques of preparation are outlined below.

All specimens were ground through 600-grit silicon carbide paper. This was followed in the first three methods of preparation by a polish with 1-μ diamond paste on Forstmann cloth and then by the following procedures.

Method 1:

(1) Polished with 5 per cent gamma alumina in 95 per cent H_2O_2 on Gamal cloth

(2) Electropolished with 8 parts ethyl alcohol, 5 parts ethylene glycol, and 5 parts phosphoric acid at 40 v dc for 1 to 3 seconds

(3) Electroetched in 18:1 acetic:chromic acid solution in Disa Electropol at 20 v dc for up to 2 minutes

Method 2:

(1) Polished with 5 per cent gamma alumina in 95 per cent H_2O_2 on Gamal cloth

(2) Electropolished with 200 ml acetic acid, 50 ml phosphoric acid, and 5 g CrO_3 at 40 v dc for up to 10 seconds

(3) Electroetched in same solution at 20 v dc for up to 5 minutes.

Method 3:

(1) Polished with 5 per cent gamma alumina in 95 per cent H_2O_2 on Gamal cloth

(2) Electropolished in 8:5:5 solution of ethyl alcohol, ethylene glycol, and phosphoric acid at 40 v dc for 2 to 5 seconds

(3) Vacuum-cathodically etched in argon at 25 to 30 μ and 3500 v for times up to 1 hour.

The specimen preparation designed specifically for electron microscopic examination consisted of the following steps after grinding:

Method 4:

(1) Polished with 6-μ diamond paste on cheesecloth

(2) Polished with 1-μ diamond paste on cheesecloth

(3) Polished with 0.5-μ diamond paste on cheesecloth

(4) Electropolished on glass-cloth-covered wheel with 22 ml ethyl alcohol, 45 ml phosphoric acid, 38 ml ethylene glycol at 30 v dc for 105 seconds

(5) Electroetched in 1:1 acetic:chromic acid solution at 10 v dc for 6 seconds.

Plastic negative replicas and carbon-platinum replicas were obtained of the prepared specimens surfaces for electron microscopic examination.

Plastic negative replicas were prepared by flowing an 0.5 per cent solution of cellulose nitrate in amyl acetate over the surface of the specimen. After drying the replica was stripped off and shadowed with a vacuum deposit of platinum at a 45-degree angle.

The carbon-platinum replica was prepared by first replicating the surface with a 5-mil-thick sheet of cellulose acetate softened in acetone. This replica was platinum shadowed and then was covered with a vapor-deposited coating of carbon. The plastic was then dissolved away to obtain the final replica.

In developing these techniques initial efforts were concentrated on the production-ingot material with occasional preparations of specimens from the other ingots. When suitable techniques were developed they were

further evaluated by preparation of specimens from the remaining ingots. Within the limits of time available, a thorough examination of all ingots was impossible and significant information was derived mainly from the production ingots and from Ingots B-50, B-52 and B-57. Use of the latter ingots permitted comparisons of structure between low-carbon ingots which were either chill cast or slow cooled (Ingots B-52 versus B-57) and between slow-cooled ingots of high and low carbon content (Ingots B-50 versus B-57).

EXPERIMENTAL RESULTS

Metallographic Results

All photomicrographs shown in this section were taken from surfaces in a direction transverse to the axis of the cast ingots.

Typical photomicrographs of as-polished uranium showing the massive carbides in the as-cast structure appear in Figures 1 through 3. This structure is produced after the electropolishing step in Method 1. Large dendritic carbides as shown in Figure 1 were observed in the edge specimen from Ingot B-50 which was slow cooled and high in carbon. These were not observed in the center specimen from this same ingot although numerous elongated carbides which apparently are the beginning of dendrites were seen.

More typical, cubic-form carbides are shown in the production ingot, B-85559. A typical etched structure of this latter ingot is shown in Figure 4. This structure is obtained after the etching step in Method 1.

Figures 5 and 6 show the structures obtained by Method 2 after electroetching for 1 and 5 minutes, respectively. After 1 minute of etching, in addition to the large carbides, a cellular distribution of fine particles is visible. These particles are masked to a considerable extent when the etching time is increased and grain boundaries are delineated.

Method 3, in which the specimens are vacuum cathodically etched, produced the microstructures shown in Figures 7 through 13. This technique delineates all of the structural details developed by the previous methods and at the same time reveals considerably more substructural detail. The cellular pattern of fine particles is emphasized particularly in Figure 7 and in the darker etching areas of Figure 8. These particles exhibit no resolvable form in the higher magnification photomicrograph of Figure 9. It should be noted that the particular ingot from which these structures were obtained, B-52, was low in carbon (138 ppm) and was chill cast.

The structure of the low-carbon (68 ppm) slow-cooled ingot, B-57, is shown in Figure 10. Both grains and subgrains are larger in this ingot than in the chill-cast ingot. In addition, the fine particles are considerably larger and, rather than forming randomly, have apparently grown on preferred crystallographic planes of the uranium matrix. One other feature that appears different in the chill-cast and slow-cooled uranium structures is the width of the twins; the twins appear to have significantly greater breadth in the slow-cooled material.

The structure of the high-carbon slow-cooled ingot, Figure 11, is similar to that of the previous ingot except that the grain size appears slightly smaller and there are a greater number of large carbides. However, the greater carbon content does not significantly change the amount or distribution of the finer particles.

All of the previous specimens were taken from the center of the ingot. Figure 12 shows the structure in a slow-cooled ingot, B-49, at the edge. The grain size is considerably smaller than in the previous slow-cooled ingots. A number of very small grains can also be seen which suggests that at least partial alpha-phase recrystallization has been initiated; this is probably due to higher cooling rates and higher stresses near the edge of the ingot. The fine particles are considerably smaller and are also contained in more widely separated regions than observed in specimens from the center of the ingot.

The structure at the edge of one of the production ingots, B-85559, is shown in Figure 13. The structure is very similar to that at the center of the slow-cooled experimental ingots, indicating considerably lower cooling rates in the production material.

Electron-Microscope Results

Specimens were prepared for electron microscopic examination by all four methods outlined previously. Methods 1, 2, and 4 produced replicas which showed the same structural features although replicas from specimens prepared by Method 4 showed cleaner and more detailed structures than the other two methods of preparation. Specimens prepared by Method 3, the vacuum-cathodic etch, showed additional different features. Consequently, while electron micrographs were taken of specimens prepared by all four methods, only those prepared by Methods 3 and 4 are shown in this report. It was found that greater resolution is obtained with the carbon-platinum replicas, and, for this reason, only a few plastic negative replicas were prepared during the course of this study.

Figure 14 shows a large carbide surrounded by a number of small particles, parts of which were transferred to the replica. Areas where transfer occurred appear black in the micrograph. A number of

these small particles were removed by etching through a plastic negative and were identified by X-ray diffraction as uranium carbide. Figure 15 shows a large carbide containing a typical void in its center.

Figure 16 shows a small carbide particle of unusual form in Ingot B-85560. A number of small particles are also visible in this figure, some appearing within the larger carbide. These may be carbides but of different composition. One or the other may be combined with either oxygen or nitrogen, rendering the etching characteristics slightly different.

Figures 17 and 18 show fine carbide distribution in Ingot B-57. Characteristically, in all the experimental ingots, these particles tended to be coarser in the center of the ingots as illustrated by Figure 19. The carbides showed a greater tendency for alignment at the center of the ingot, presumably growing on crystallographic planes of the uranium matrix.

The carbides in Ingot B-52 tended to be somewhat smaller in size but also more random in size and distribution than in the other experimental ingots. This may be related to the higher cooling rate. The carbides in Figure 20 appear at either a grain or subgrain boundary.

All of the previous electron micrographs were obtained from replicas of surfaces prepared by Method 4. The remaining micrographs were obtained from specimens prepared by vacuum-cathodic etching as described in Method 3.

Figure 21 shows the structure of a cell boundary such as appears in Figure 7. It is seen to consist of a large number of carbide particles. A great deal of substructure was also visible in this same specimen. This is well developed in Figure 22. The morphology is reminiscent of subgrain structures which are normally bounded by dislocation tangles or networks. The structural features outlining the substructure in this figure are of unknown origin, and while they may simply be etching artifacts they could be related either to dislocations or subtle compositional variations which are revealed by cathodic etching.

DISCUSSION AND CONCLUSIONS

Of the techniques investigated, Method 4 is regarded as most useful for electron microscopy studies of small inclusions in uranium. Replicas from specimens prepared by this method showed clean and clear structural detail.

Vacuum-cathodic etching appears to be a powerful tool for revealing structure in uranium primarily for metallographic observation. Besides revealing all of the structural details developed by chemical etching, considerable substructure is revealed. Additional substructure

is revealed by electron microscopic examination, although the nature of the structures is unknown; and additional study to evaluate the use of this technique for electron microscopy is needed. It would be desirable to perform thin-film transmission studies of uranium to see if any correlation exists between the structures observed by the two techniques. Additional study to optimize the vacuum-cathodic etching procedures is also desirable. The micrographs shown in this report represent the results of a single successful preparation by this technique; and the effects of variable etching time, pressure, and voltage were not studied.

The results of this study of cast uranium microstructures revealed a number of interesting microstructural features and some significant structural differences between slow-cooled and fast-cooled ingots and between the structures at the edge and center of the slow-cooled ingots. Most of these observations are related to fine particles, identified as uranium carbide, which are present in the cast ingots. However, it must be pointed out that this study was extremely limited in scope; and, consequently, any conclusions reached must be considered as tentative in nature until confirmed by more detailed studies.

As a general observation, no particles other than carbide were observed or identified. Thus it appears that in cast uranium the aluminum, iron, and silicon, when present as impurities in the amounts contained in these ingots, remain in solution. Working or annealing at alpha-phase temperatures may be required for their precipitation.

A single experiment was performed to determine the mode of formation of the fine carbide particles. For this purpose, a specimen was taken from a rod which had been produced by hot rolling a production ingot. This specimen was annealed at 1100 C and furnace cooled. The resulting structure is shown in Figure 23 and indicates that the fine carbide is not a eutectic product but rather is a product of decreased carbon solubility accompanying a uranium solid-state eutectoid transformation. This conclusion is further supported by the observation that the formation and amount of fine carbide particles in cast uranium are independent of carbon concentration, within the limits of carbon concentrations investigated.

It is difficult to correlate the observed structures with a eutectic uranium-carbon diagram in view of the absence of an identifiable eutectic structure, and only a partial analysis of the structures is possible on the basis of the limited observations made in this study. However, it appears that carbide dendrites form in the melt when the carbon content is in excess of about 500 ppm. It also appears likely that the large cubic carbides result from decreasing solubility of carbon in the gamma phase of uranium.

The tentative conclusions reached as a result of this study are listed below.

(1) The amount or mode of formation of fine carbide particles is not related to carbon concentration; the principal effect of carbon concentration is on the number of large carbide particles present. Carbide dendrites tend to form and grow at the edge of high-carbon ingots.

(2) Carbon content has a slight effect on final grain size, the grain size being smaller when the carbon content is high.

(3) Grain and subgrain size is smaller in fast-cooled than in slow-cooled ingots.

(4) In slow-cooled ingots, the fine carbides tend to be aligned, apparently growing along crystallographic planes of the uranium. In fast-cooled material the fine carbide particles are more irregular and random.

(5) The fine carbides in a fast-cooled ingot also tend to be smaller and of more varying size than the carbides in slow-cooled ingots.

(6) The twins formed in a fast-cooled ingot tend to be narrower than the twins formed in a slow-cooled ingot.

(7) The fine carbides are smaller at the edge than at the center of the ingots.

(8) At the edge of the ingot, the fine carbides show a tendency for elongation in a direction perpendicular to the axis of the ingot, or in the direction of cooling.

(9) The grain size is smaller and the fine carbide particles tend to be smaller and clustered in more widely separated regions at the ingot edge than in the center of the ingot. Partial alpha recrystallization may be initiated at the ingot edge as a result of cooling stresses.

In examinations of the two production ingots, no significant structural differences between the ingots were observed.

The results of this study are quite preliminary in nature. It is recommended that the techniques developed be applied to more detailed studies of cast uranium structures. While such studies should include effects of ingot cooling rate and variable carbon content, the

effect of variable levels of aluminum, iron, and silicon additions on cast structure also requires investigation. These studies should then be extended to worked and annealed material to trace structural changes produced by various production processes.

The vacuum-cathodic etching techniques also warrants additional development to determine its applicability to specimen preparation for electron microscopy studies. At the present its usefulness is limited primarily to metallographic studies. Studies of etching variables and studies to identify the structures observed in the electron microscope are recommended.

REFERENCES

This paper is taken from work reported in BMI-1664, "A Study of the Tensile Fracture and Microstructure of Uranium".

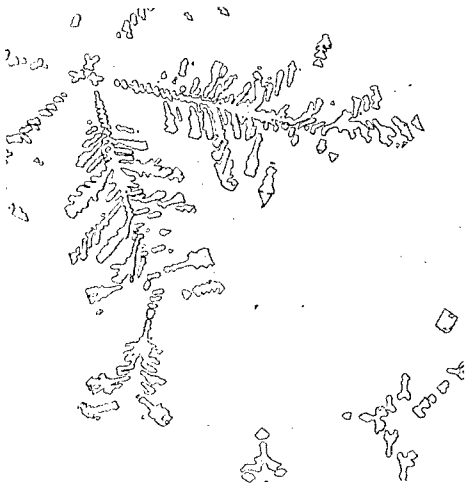

250X RM-25365

FIGURE 1. CARBIDE DENDRITES AT EDGE OF INGOT B-50
Preparation technique: Method 1, electropolished state.

100X RM-25367

FIGURE 2. ELONGATED CARBIDES AT CENTER OF INGOT B-50
Preparation technique: Method 1, electropolished state.

100X RM-25350

FIGURE 3. CUBIC-FORM CARBIDES IN CENTER OF INGOT B-85559
Preparation technique: Method 1, electropolished state.

100X RM-25354

FIGURE 4. GRAIN STRUCTURE IN CENTER OF INGOT B-85559
Preparation technique: Method 1, electroetched state.

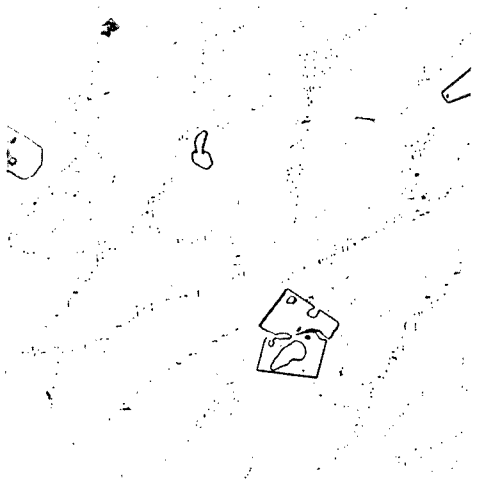

250X RM-25352

FIGURE 5. CELLULARLY DISTRIBUTED PARTICLES IN CENTER OF INGOT B-85559
Preparation technique: Method 3, electroetched 1 minute.

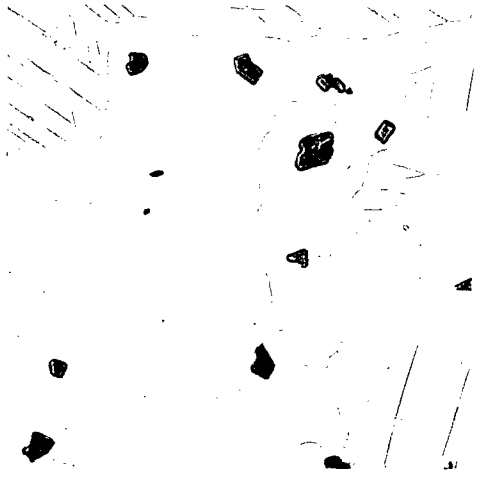

100X RM-25356

FIGURE 6. GRAIN STRUCTURE IN CENTER OF INGOT B-85559
Preparation technique: Method 2, electroetched 5 minutes.

100X RM-25429

FIGURE 7. CELLULAR OUTLINE OF FINE PRECIPITATE IN CENTER OF INGOT B-52
Preparation technique: Method 3, etched 1 hour.

100X RM-25432

FIGURE 8. FINE PRECIPITATE IN CENTER OF INGOT B-52
Preparation technique: Method 3, etched 1 hour.

250X RM-25434

FIGURE 9. UNRESOLVABLE PRECIPITATE IN CENTER OF INGOT B-52
Preparation technique: Method 3, etched 1 hour.

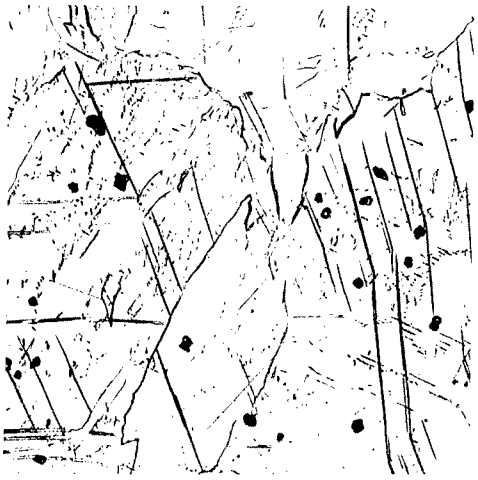

100X RM-25441

250X RM-25444

FIGURE 10. LARGE GRAINS, SUBGRAINS, BROAD TWINS, AND ORIENTED FINE PRECIPITATE IN CENTER OF INGOT B-57.
Preparation technique: Method 3, etched 40 minutes.

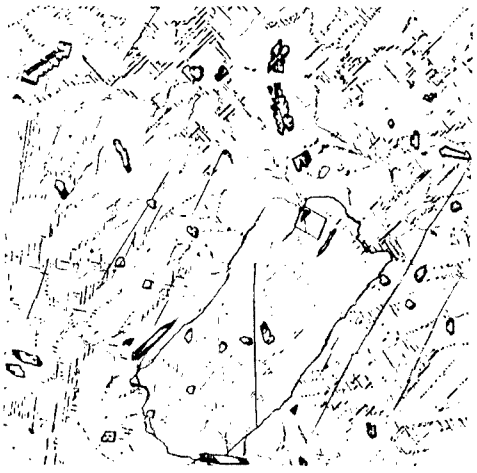

100X RM-25420

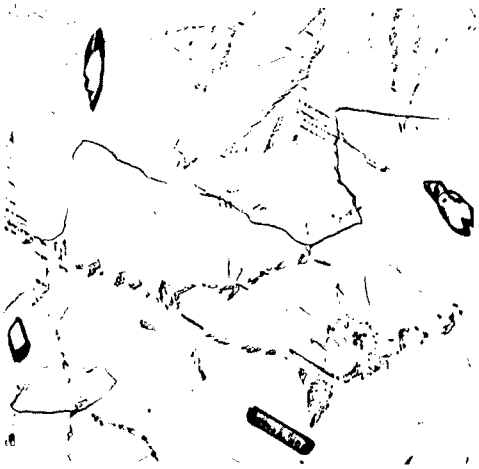

250X RM-25424

FIGURE 11. STRUCTURE AT CENTER OF INGOT B-50.
An increased number of large carbides and a smaller grain size as compared with the structures shown in Figure 10 are evident.
Preparation technique: Method 3, etched 40 minutes.

100X RM-25412

250X RM-25410

FIGURE 12. EDGE OF INGOT B-49 SHOWING SMALLER GRAIN SIZE AND REFINEMENT OF FINE PARTICLE SIZE TYPICAL AT EDGE LOCATIONS.
Preparation technique: Method 3, etched 1 hour.

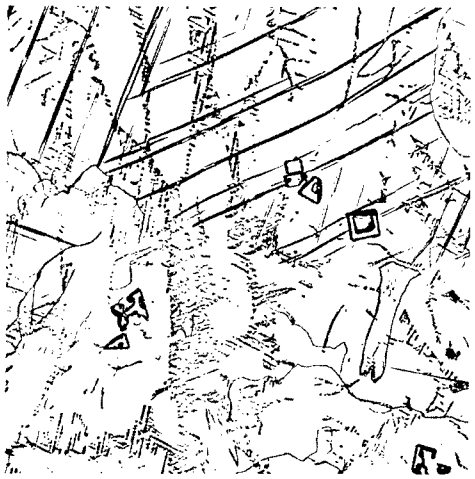

100X RM-25394

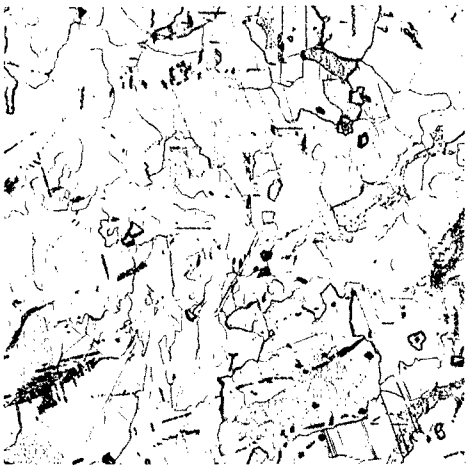

500X RM-25403

FIGURE 13. EDGE OF PRODUCTION INGOT B-85559 EXHIBITING STRUCTURE SIMILAR TO THAT OBSERVED IN THE CENTERS OF SLOW-COOLED EXPERIMENTAL INGOTS.
Preparation technique: Method 3, etched 1 hour.

17,500X J7277

FIGURE 14. LARGE CARBIDE AND SMALL PARTICLES IDENTIFIED AS URANIUM CARBIDE AT EDGE OF INGOT B-85559.

Preparation technique: Method 4, plastic negative replica, longitudinal section.

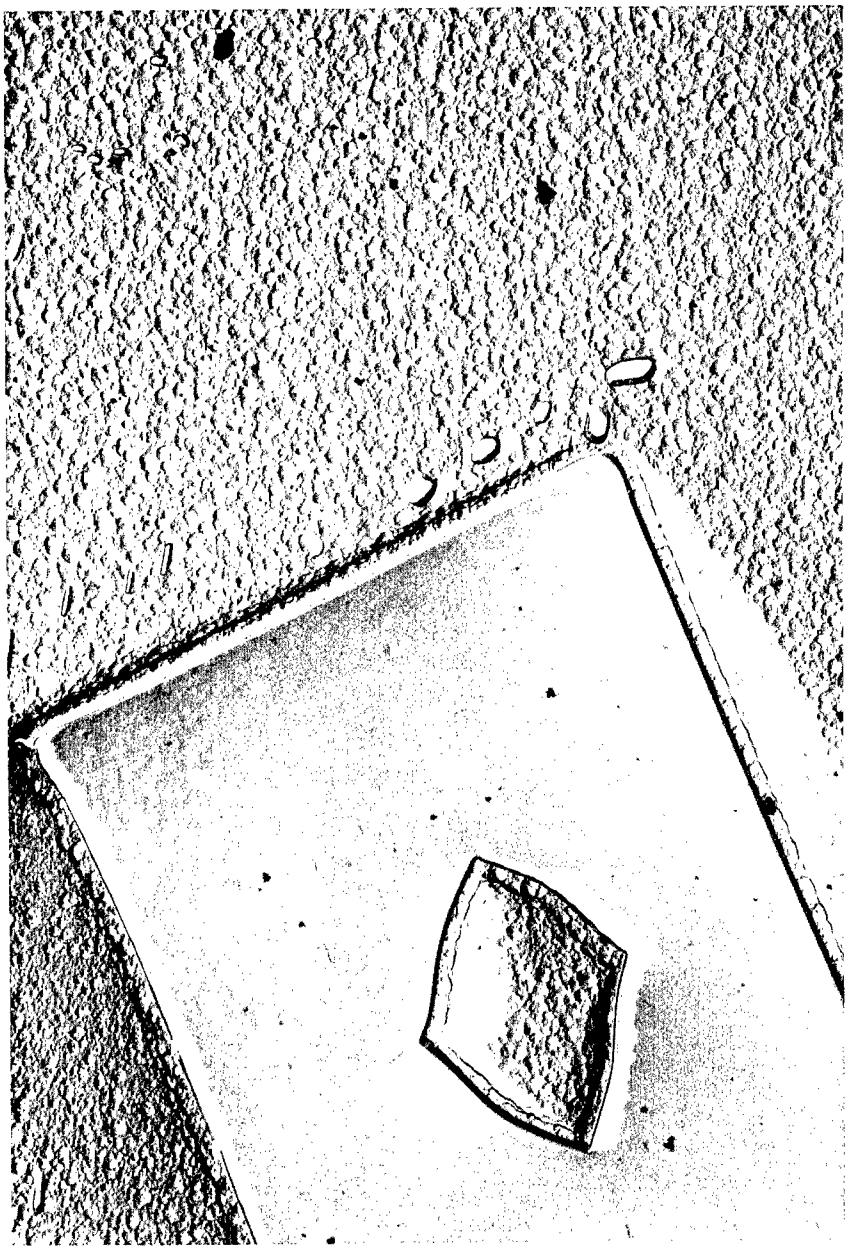

17,500X J7355

FIGURE 15. LARGE CARBIDE WITH VOID IN CENTER AS SEEN IN INGOT B-85559.

Preparation technique: Method 4, carbon-platinum replica, transverse section.

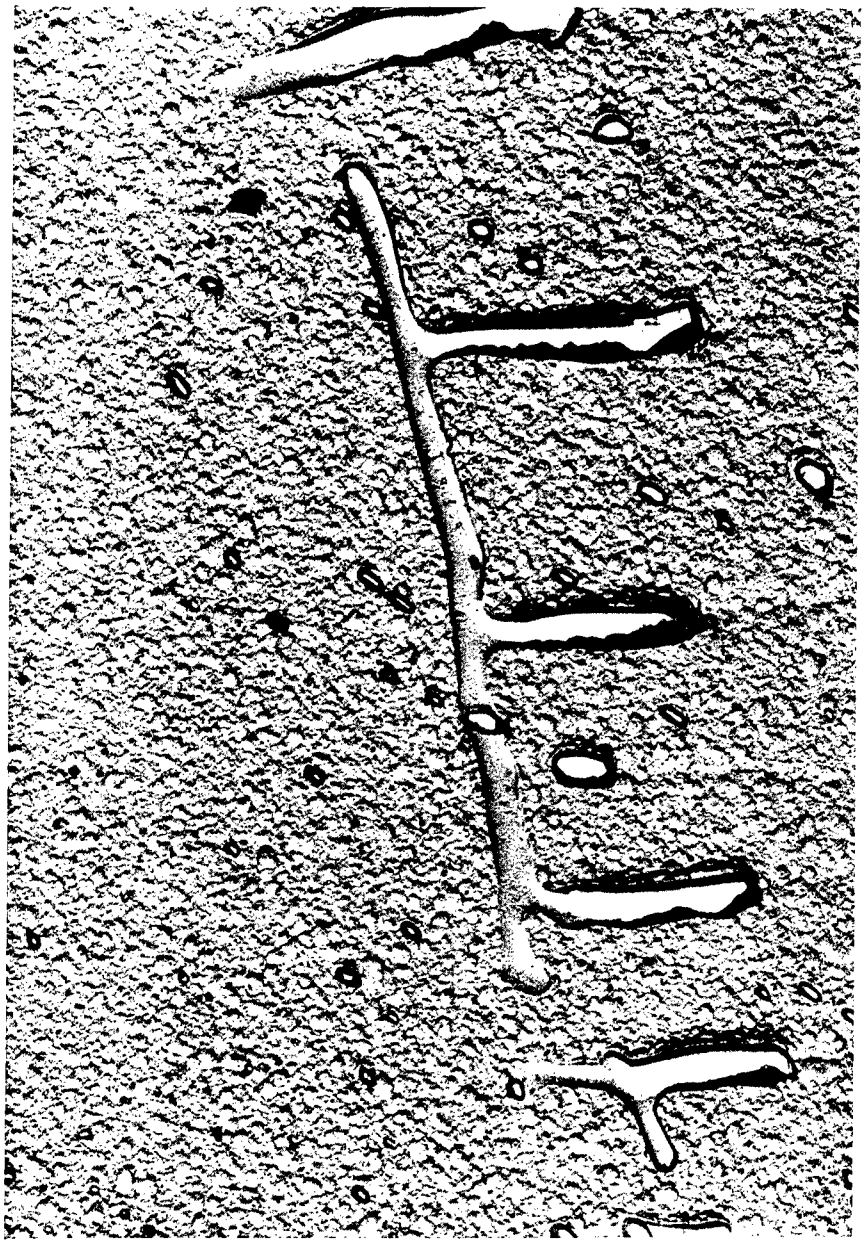

17,500X J8027

FIGURE 16. SMALL DENDRITIC CARBIDE WITH OTHER SMALL INCLUSIONS IN INGOT B-85560.

Preparation technique: Method 4, carbon-platinum replica, transverse section.

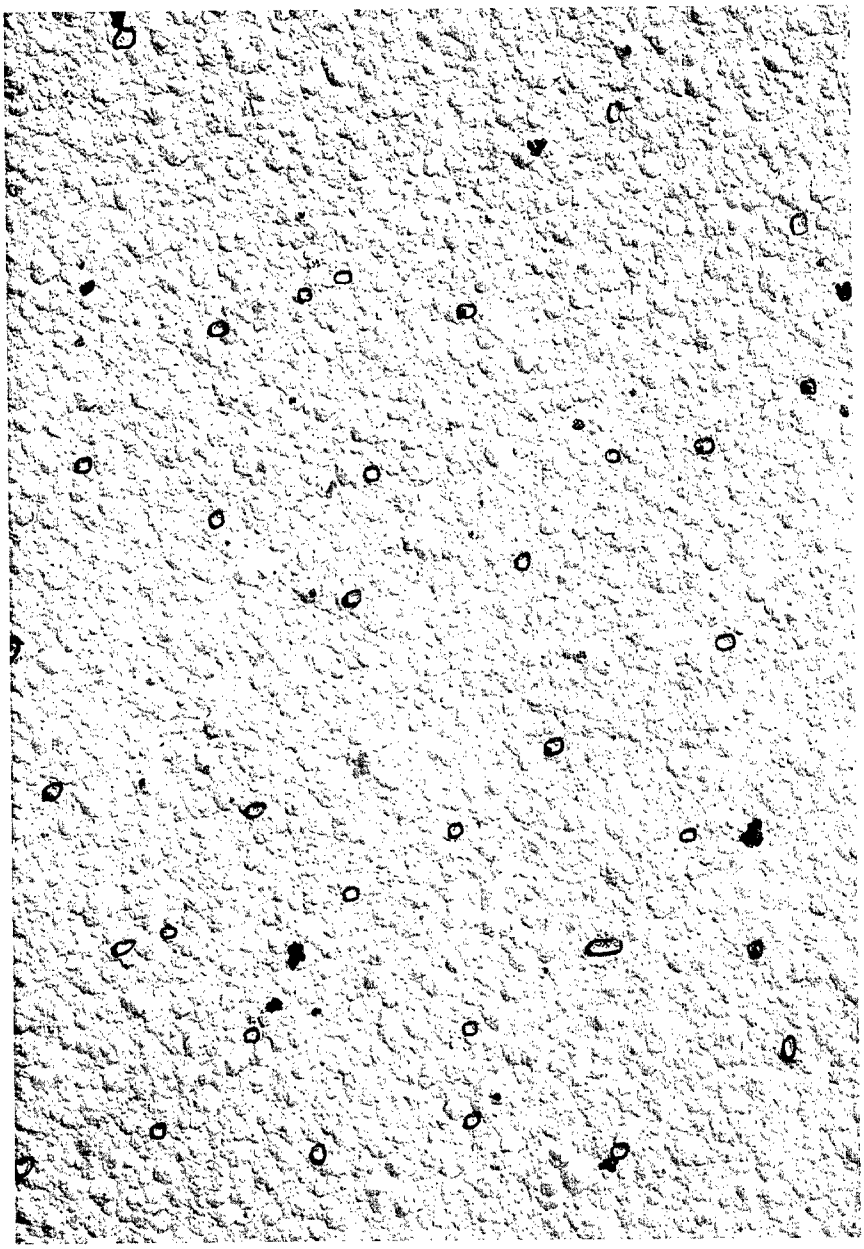

17,500X J8087

FIGURE 17. FINE RANDOMLY DISTRIBUTED CARBIDES IN EDGE OF INGOT B-57.

Preparation technique: Method 4, carbon-platinum replica, transverse section.

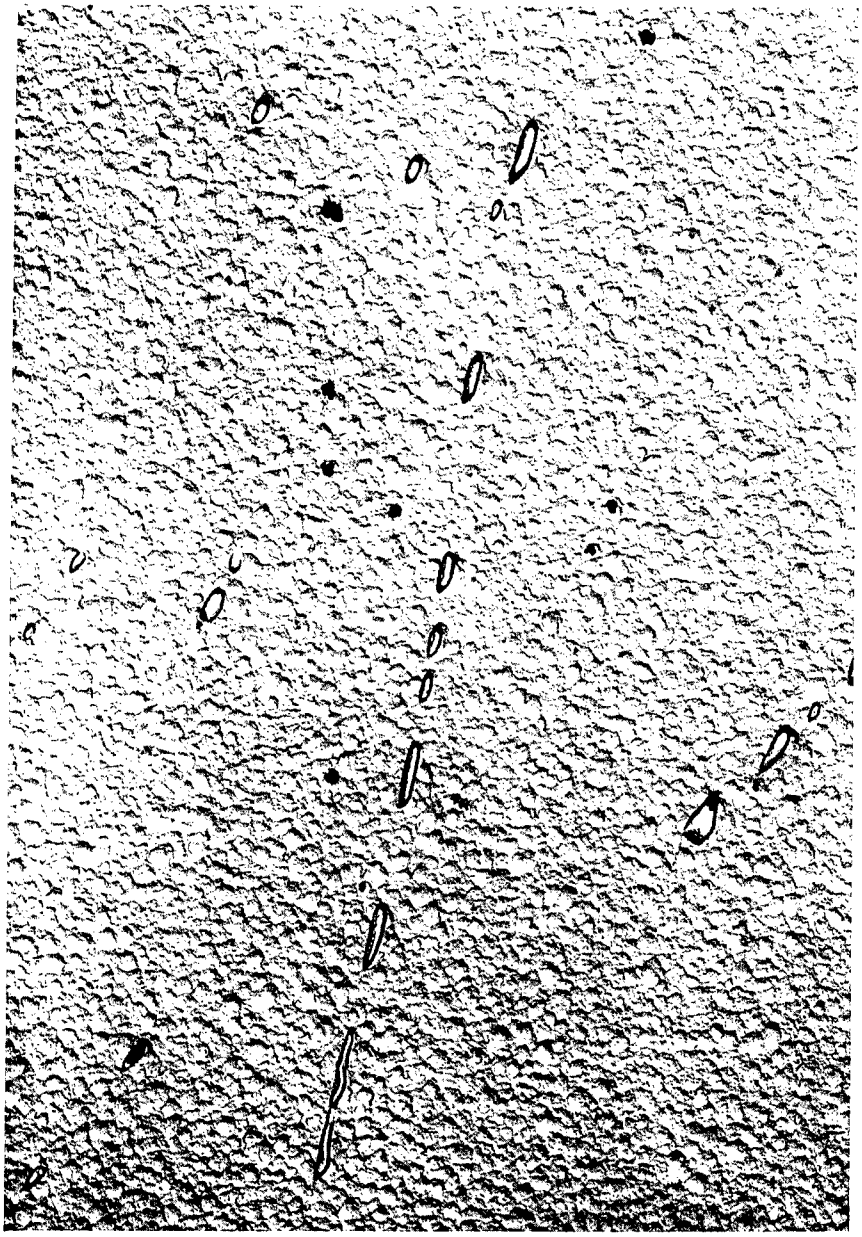

17,500X J8097

FIGURE 18. STRINGER OF ELONGATED CARBIDE PARTICLES IN INGOT B-57.

Preparation technique: Method 4, carbon-platinum replica, transverse section.

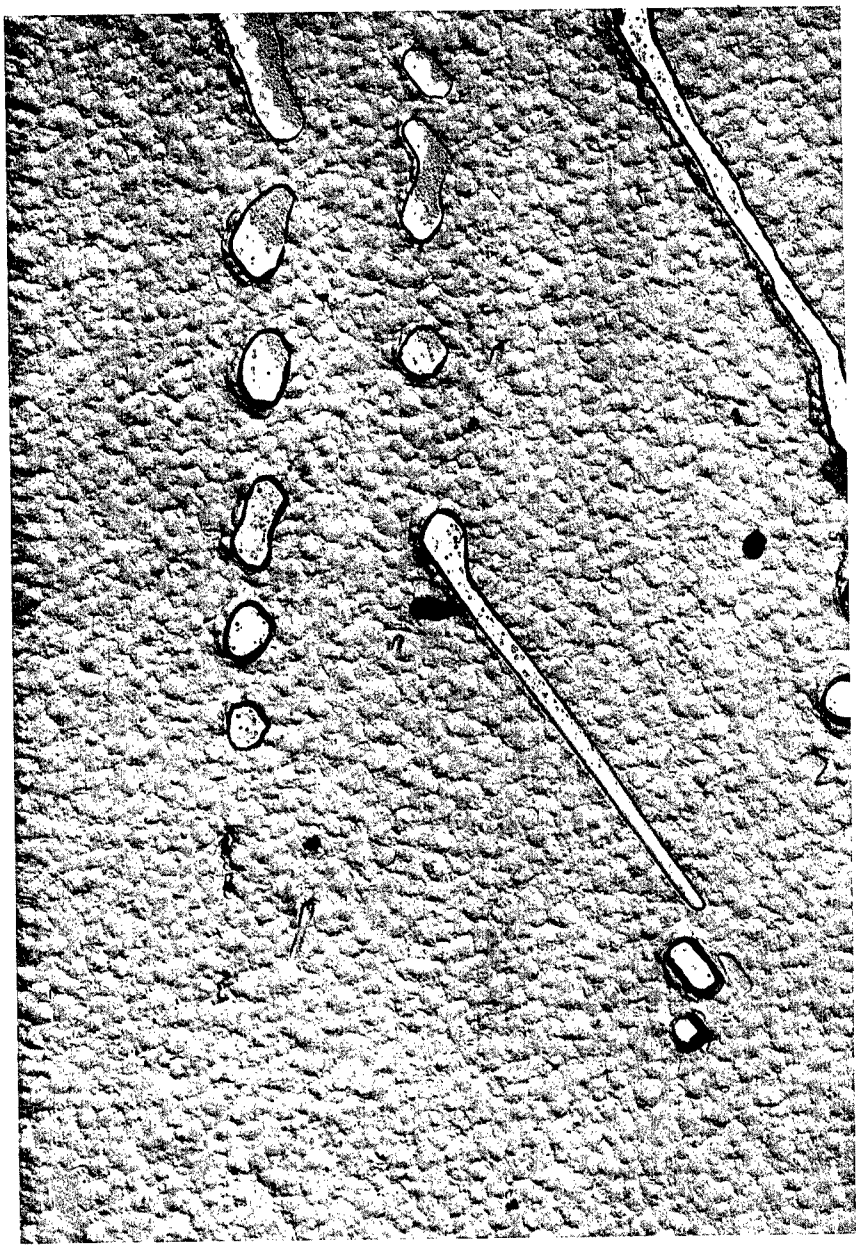

17,500X J8095

FIGURE 19. LARGE ELONGATED PARTICLES IN CENTER OF INGOT B-57.

Preparation technique: Method 4, carbon-platinum replica, transverse section.

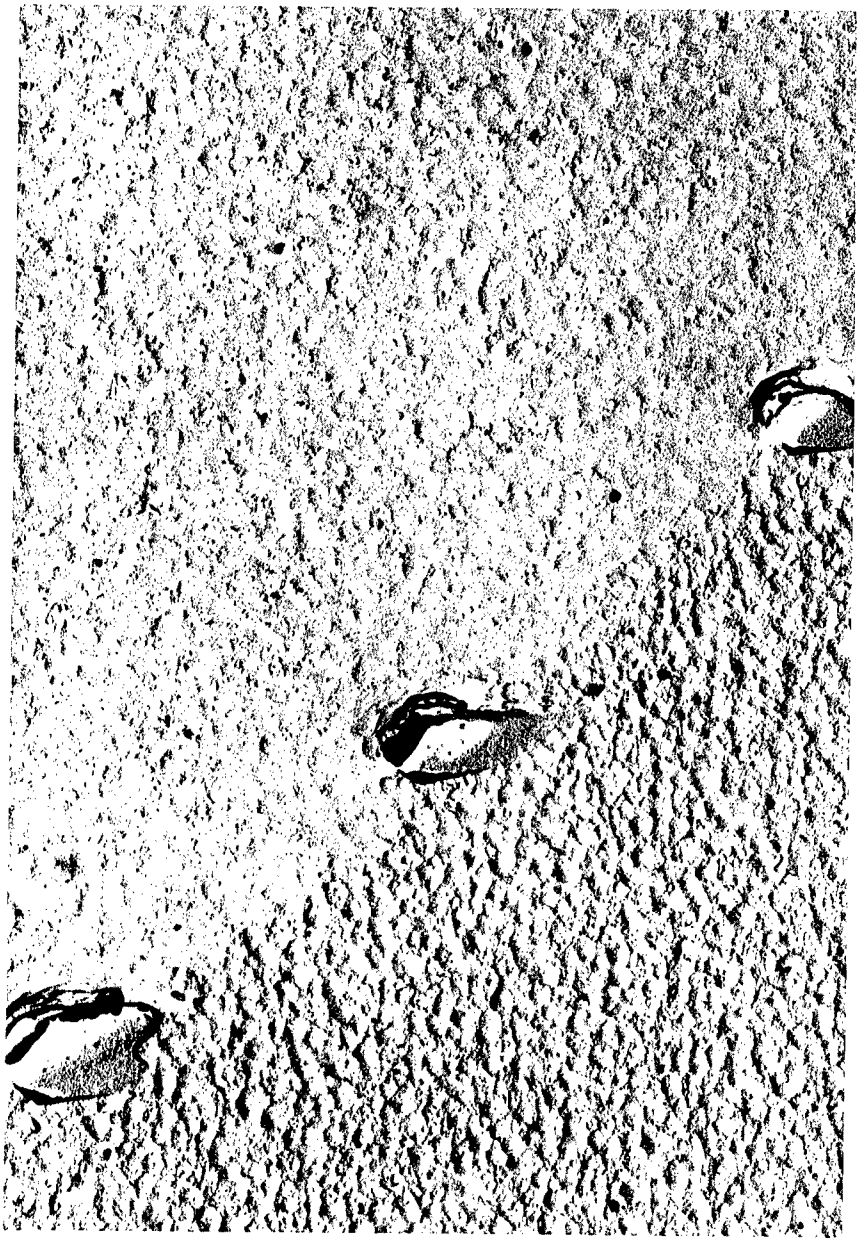

17,500X J8037

FIGURE 20. CARBIDES AT GRAIN OR SUBGRAIN BOUNDARY IN CENTER OF INGOT B-52.

Preparation technique: Method 4, carbon-platinum replica, transverse section.

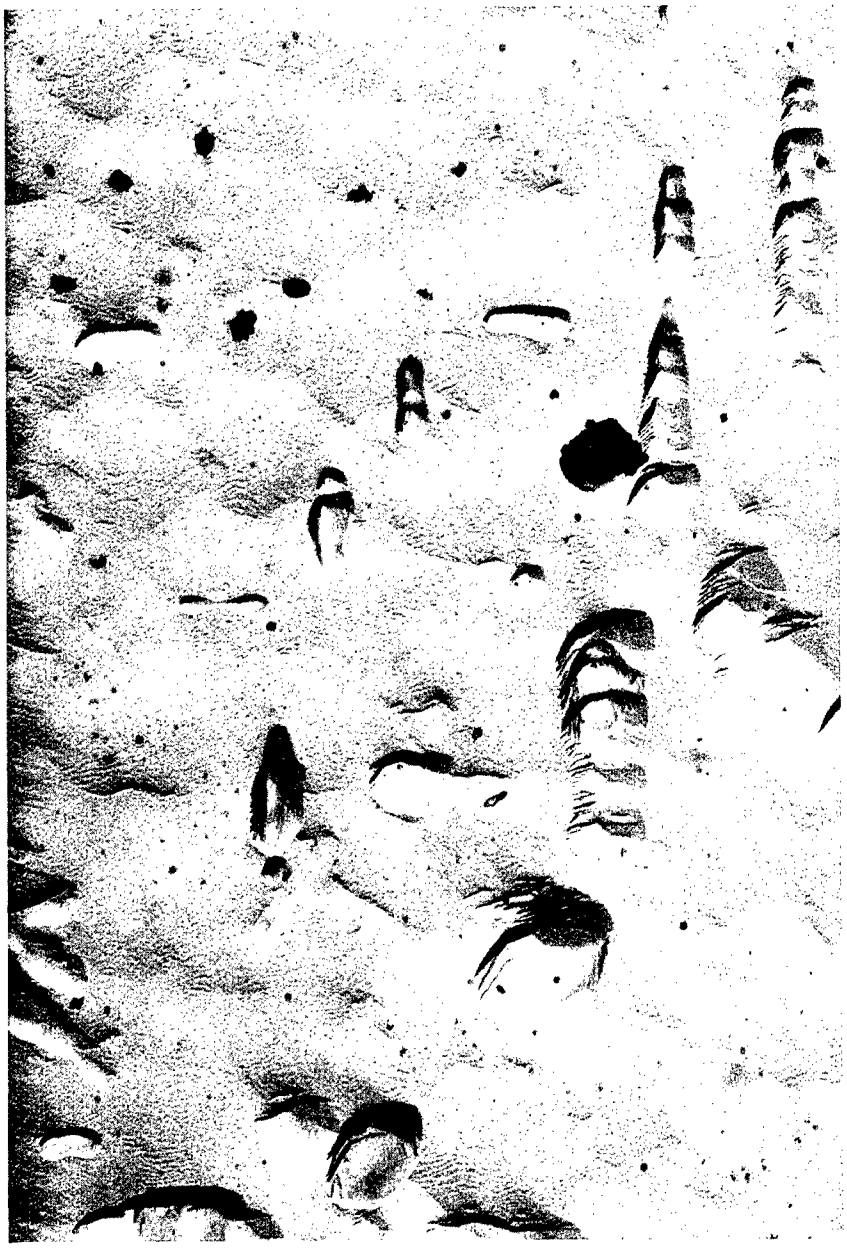

17,500X J7966

FIGURE 21. CARBIDES IN CELL BOUNDARY AT CENTER OF INGOT B-52.

The cell boundary structure is shown in Figure 7. Preparation technique: Method 3, carbon-platinum replica, transverse section.

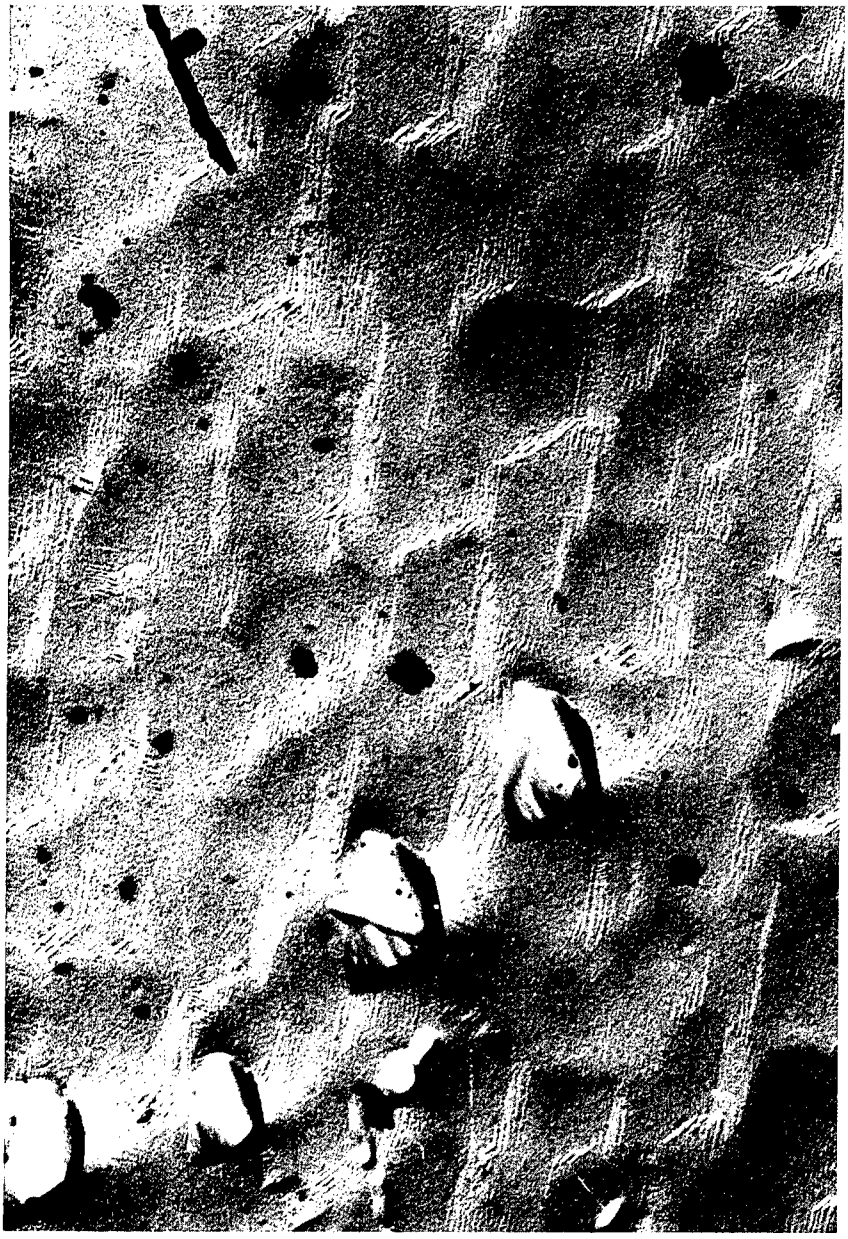

17,500X J7959

FIGURE 22. SUBGRAIN-TYPE STRUCTURE AND CARBIDES IN CENTER OF INGOT B-52.

Preparation technique: Method 3, carbon-platinum replica transverse section.

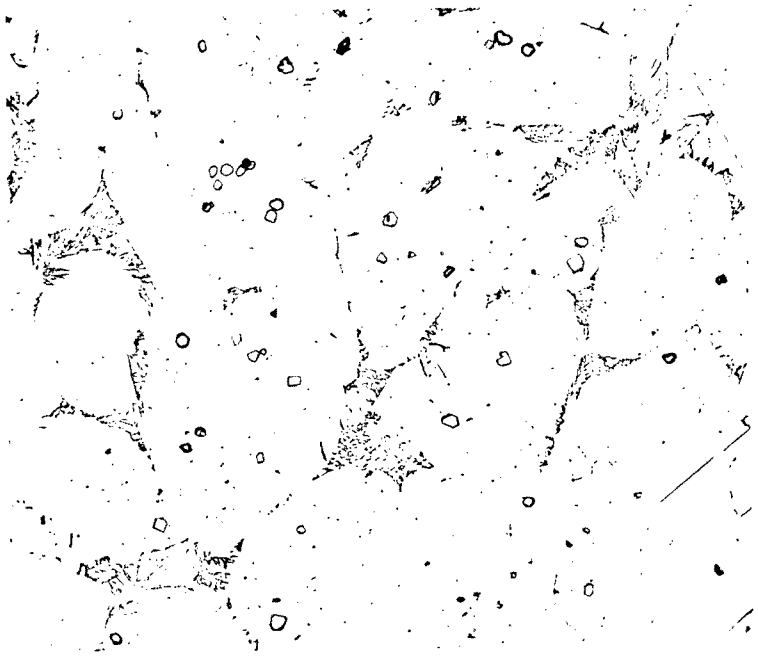

250X RM-27502

FIGURE 23. STRUCTURE OF HOT-ROLLED PRODUCTION INGOT MATERIAL AFTER ANNEALING AT 1100 C AND FURNACE COOLING.

Note fine carbide precipitate.

A BRIGHT FIELD ETCH FOR ALPHA-PLUTONIUM

by

V. W. Storhok, R. H. Snider, and M. S. Farkas*

Metallographic examination of alpha-plutonium is generally limited to polarized light studies, because of the lack of a suitable etchant. Recently, however, an etchant which produces a fine, delineated microstructure under bright field illumination, has been developed. The etchant, which is used electrolytically, consists of the following:

75 cc ethyl alcohol
20 cc nitric
5 cc water

After the specimen is polished through 1/2 micron diamond on a Gamal covered wheel, it is etched using the following sequence:

3 sec. at 25 volts, D.C.
5 sec. at 16 volts, D.C.
10 sec. at 6 volts, D.C.

An example of the resulting microstructure is shown in Figure 1.

It should be noted that this etching technique has not been consistently successful and the variables which may effect results have not yet been determined.

* All authors are affiliated with Battelle Memorial Institute, 505 King Avenue, Columbus, Ohio.

200X PL-664

FIGURE 1. ALPHA-PLUTONIUM AS SEEN UNDER BRIGHT FIELD ILLUMINATION.

MODIFICATION OF AN ATTACK-POLISH PROCEDURE

By

M. H. Cornett and E. L. Schaich

ABSTRACT

This paper describes the modification of an attack-polish procedure which reduced sample preparation time and provides a scratch-free surface on uranium metal.

INTRODUCTION

The production metallographer is always concerned with the problem of finding a procedure for sample preparation that will require the least amount of time and yet produce a surface good enough for accurate evaluation and scratch-free photomicrographs. Many procedures now in use require much time for sample preparation. They may also require that the production metallographer spend a large amount of time searching for fields to photograph that are scratch-free and that exhibit the desired structures.

The objective of this work was to modify an attack-polish procedure so that an acceptable surface could be produced for metallography without requiring the use of diamond compound or electropolishing.

SUMMARY OF RESULTS

The modified attack-polish procedure permits the evaluating or photographing of grain structures or inclusion content of uranium metal without the use of diamond polishing or electropolishing. Only about one-third as much time is required for sample preparation as is required when samples are mechanically polished with diamond compound. The modified procedure, when properly followed, retains all inclusions and provides a scratch-free surface for photographing grain structures or inclusions in uranium.

PROCEDURE

The procedure employing the modified attack-polishing step is as follows:

1. Grind the sample with 60 and 400-grit abrasive papers.
2. Polish the sample by the modified attack-polish procedure described below.
3. Evaluate or photomicrograph the grain structure under polarized light.
4. Rinse the sample in 1.1 HNO_3 acid for 5 to 15 seconds.
5. Evaluate or photograph the inclusion content under bright field illumination.

Electropolishing can be used to replace Step 4 if desired.

The following mixture is required to perform the modified attack polishing:

10%	118g CrO_3 in 100 ml H_2O
10%	Saturated solution of $Na_2Cr_2O_7 \cdot 2H_2O$ in water
5%	Linde A compound in water (paste consistency)
75%	Distilled water

The above solution is used on a lap covered with Beuhler Ltd. No.40-7208AB Microcloth. The time required for polishing depends on the type of grinding preparation that has been given the sample. A well-ground surface can be given an excellent polish in 30 to 60 seconds.

CONCLUSION

The polishing procedure described is very versatile and has many applications in the preparation of uranium metal samples for accurate evaluations and excellent photomicrographs. The photomicrographs (Figures 1 and 2) illustrate the results that can be obtained with this procedure without the use of diamond compound or electropolishing.

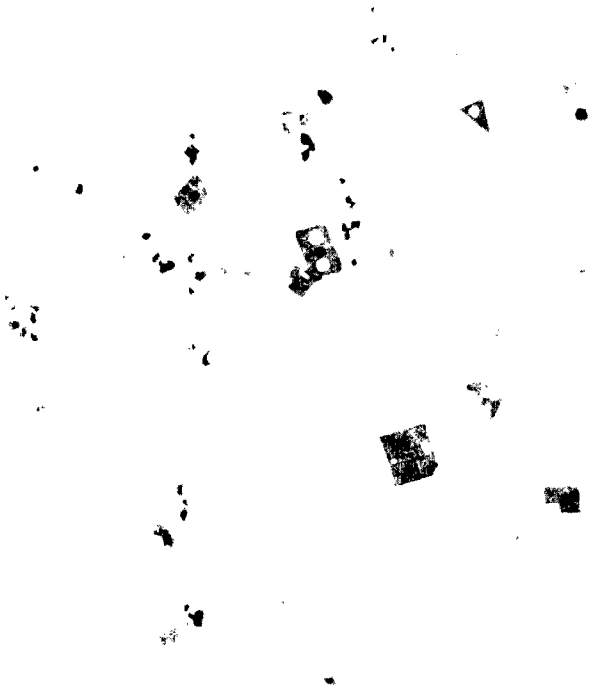

Figure 1 Inclusions in Uranium Metal, Bright Field (100X)

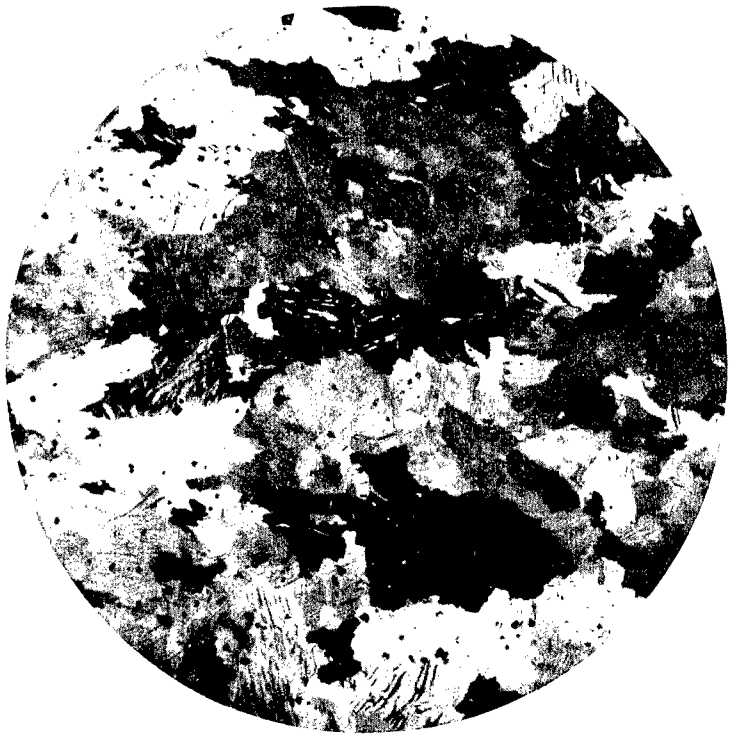

Figure 2 Grain Structure of Uranium Metal, Polarized Light (100X)

ELECTRON METALLOGRAPHY OF PYROLYTIC CARBON COATINGS ON FUEL PARTICLES*

C.K.H. DuBose and J. O.Stiegler

Oak Ridge National Laboratory
Oak Ridge, Tennessee

ABSTRACT

A replica electron microscope study of as-polished and cathodically etched surfaces of pyrolytic carbon coatings on fuel particles has been made in an attempt to characterize coatings that showed as much as 30 % difference in bulk density. High and low density coatings could be characterized by their polished surface textures; however, these features were not indicative of the true structure as seen by direct electron transmission. Microvoids detected by the transmission study of cleavage flakes exist on too fine a scale to be observed either optically or by electron microscope examination of replicas of the polished surfaces. Other features such as the effect of cathodic and chemical etching, coating delamination, and duplex coating interfaces have also been examined.

---

*Research sponsored by the U.S. Atomic Energy Commission under contract with the Union Carbide Corporation.

I. INTRODUCTION

Pyrolytic carbon deposits produced by the decomposition of gaseous hydrocarbons on heated substrates currently are being considered as coatings for fuel particles for nuclear reactors. By varying the deposition conditions, it is possible to alter the physical and mechanical properties of the carbon over very wide ranges. For example, deposits ranging in density between about 1.4 and 2.2 gm/cm^3 can be formed by changing the deposition temperature or rate. Furthermore, by altering the deposition conditions during formation of a batch of coatings, it is possible to prepare multilayer coatings having a combination of desirable properties (e.g., a low density, spongy inner layer to absorb fission recoils and a high density outer layer to provide strength and fission product retention).

It was the purpose of this study to characterize on a microscale deposit formed under varied conditions in order to correlate physical and mechanical properties with structure. Transmission electron microscopy and electron diffraction were used to determine the true nature of the various pyrolytic carbons studied. Replica studies of polished and etched surfaces of the same materials were also carried out to determine distinguishing features of the different deposits.

II. NATURE OF THE TRUE STRUCTURE

Pyrolytic carbon exists in the unique class of crystalline solids having two dimensional crystal lattices. X-ray[1] and electron[2] diffraction studies have shown that the deposits consist of monolayer crystallites on the order of 100 Å in diameter having the hexagonal Bernal graphite structure that are twisted and rotated randomly with respect to one another. The C axis parameter of 3.43 Å and greater indicates that the stacking is not totally random, but nearly so.[3]

The optical microstructures of the deposits fall into two broad classes depending on the deposition conditions: 1) a laminar structure typified by the coating shown in Fig. 1(a), and 2) a columnar structure characterized in Fig. 1(b). Although deposits belonging to either class appear quite similar to one another in bright field illumination, their physical and mechanical properties may vary over a wide range. It is felt that the microstructural differences occur on too fine a scale to be detected by optical microscopy.

Transmission electron micrographs of cleavage flakes extracted from both high and low-density laminar and columnar deposits are shown in Figs. 2 and 3. Contrast variations in these micrographs arise from differences in thickness. That is, the degree of darkening is proportional to the mass of material traversed by the electron beam. The small white areas, therefore, correspond to thinner regions in

the sample or, in this case, microvoids. It is readily apparent that as the bulk density decreases, the pore density increases. The lowest-density materials appear quite spongy; they evidently consist of blocks of carbon and voids, both on the order of 100 Å in diameter.

III. RELATED SURFACE MICROSTRUCTURES

Obtaining suitably thin cleavage flakes from particle coatings is a difficult and time consuming procedure. An electron microscope study was made of replicas taken from polished and etched surfaces in order to determine whether or not details of the structure could be inferred from such observations, which are considerably easier to make than transmission observations.

A. Polished Surfaces

The resulting microstructures of the high and low densities of the laminar and columnar material after standard metallographic polishing are shown in Fig. 4. It is obvious that the replica studies of the as-polished surfaces do not suggest the same structure of the pyrolytic carbon as seen in transmission; they do, however, reveal that the polishing characteristics of these materials vary with the density. The voids that exist in these coatings apparently are too small to be distinguished above the general surface roughness caused by their characteristic polishing behavior. There are, however, significant differences in the structure between the high density and low density material observed by the replication technique. The low density material always exhibits a smoother surface than does the high density material, see Fig. 4(a) and (c), and shows polishing scratches. This leads one to the assumption that the low density material is less brittle and smears more easily during polishing than does the high density material. The high density material is more brittle and possible fractures on a microscale during the polishing operation, and thus exhibits the coarser texture as seen in Fig. 4 (b) and (d).

The microstructures of the various degrees of density are reproducible for a particular range of density, (i.e., a low density coating always gives a rather smooth texture upon replication for electron microscopy). The high density material, on the other hand, gives a much coaser texture. The intermediate ranges of densities lead to intermediate ranges of polished surface textures.

Slight differences exist in the as-polished surface textures between the laminar and columnar materials, as may be seen in Fig. 4. In the low density material the difference in texture is rather subtle, whereas, in the high density materials considerably greater differences are evident. The exact nature of the

swirled texture of the high density columnar material is not known; it is, however, typical of high density columnar pyrolytic carbon.

In many cases surface texture differences were noted within the same coating, indicating varying densities within the same coating. The specimen shown in Fig. 5(a) and (b), for example, has a much coarser texture near the outer edge than near the core, [see also Fig. 6(a) and (b)] . This may arise from changes in the deposition variables or from the increase in surface area of the coating as deposition progresses. Cleavage flakes for transmission examination of selected areas such as this would be impossible to obtain.

With this background information, one can infer a great deal about a coating from looking at a replica of its polished surface in the electron microscope. It is possible, for example, to observe quickly and easily how the density of a coating varies with thickness or if densities on different particles are appreciably different. In addition, rough estimates of the actual coating density can be made.

B. Cathodic Etching

Particles representative of high density (2.01 gm/cm^3) and a low density (1.71 gm/cm^3) laminar coatings were mounted in an electrical conductive mount for cathodic etching. To ensure identical etching conditions, they were located side by side in the same mount. Prior to etching, a replica was made of the polished surfaces for examination in the electron microscope. In the as-polished state, the high density material exhibited a coarser texture than did the low density material. Near the outer edge of the high density particles, a much coarser texture was noted than was found near the core, see Fig. 5(a) and (b). The reverse of this was found in the low density particles, see Fig. 6 (a) and (b). These variations in texture could be related to density changes during deposition of the coatings. After cathodic etching for 15 min at 3500 v with a current of 35 ma, numerous pits were found in the area of the less coarse texture. The high density coatings showed many more pits than did the low density material. The pits were located near the core area in the high density material [Fig. 5(c) and (d)] , whereas they were near the outer surface of the low density coatings [Fig. 6(c) and (d)] .

Based on the transmission work of the coatings, the pits appear to bear no relationship to true structure. They may be sites of "micro-inclusions" that have been greatly enlarged by the nature of cathodic etching.

C. Chemical Etching

In an attempt to reveal the pore structure obscured by flowed material due to polishing, a chemical etchant also was employed on high and low density laminar

pyrolytic carbon coatings. A standard graphite etchant of hot potassium dichromate-phosphoric acid was used. The structure, however, was virtually unchanged from the as-polished condition. Considerable experimentation would be necessary to develop a meaningful chemical etchant for pyrolytic carbon.

D. Macrostructures

1. Delaminations

Delaminations in the laminar coatings were very common, and appeared to be related to some possible changes in the system during the coating process. The size of the cracks varied considerably in width and depth. Large cracks, as shown in Fig. 7(a) are clearly visible optically, however, small fissures, as shown in Fig. 7(b) at 12,500 X, may not be seen in the optical microscope.

2. Duplex Interfaces

The interface between the laminar and columnar structures of duplex coatings was very smooth, for the most part, in the particles that were examined. However, for some applications, small voids at the interface of the duplex coatings is beneficial. Such is the case in trying to reduce crack propogation due to irradiation effects.

A duplex coating consisting of a columnar coating on top of a laminar coating is shown in Fig. 8(a). Only slight differences in densities between coatings comprise the duplex coating represented in Fig. 8(b). Good interface bonding is represented in these micrographs; however, many particles examined did exhibit cracks at the duplex interface.

REFERENCES

1. O. J. Guentert, J. Chem. Phys., 37, 884 (1962).

2. J. O. Stiegler, C.K.H. DuBose and J. L. Cook, ORNL-TM-863 (in press).

3. J. Biscoe and B. E. Warren, J. Appl. Phys., 13, 364 (1942).

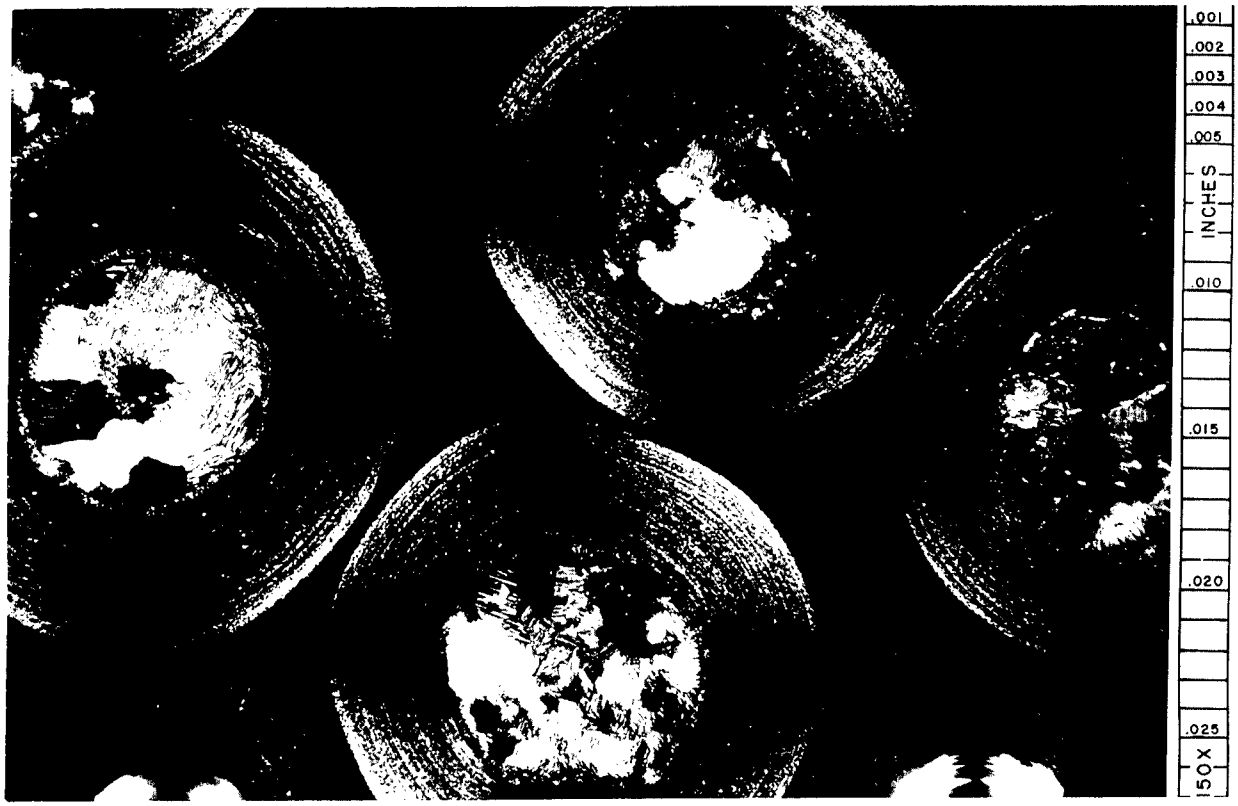

(a)

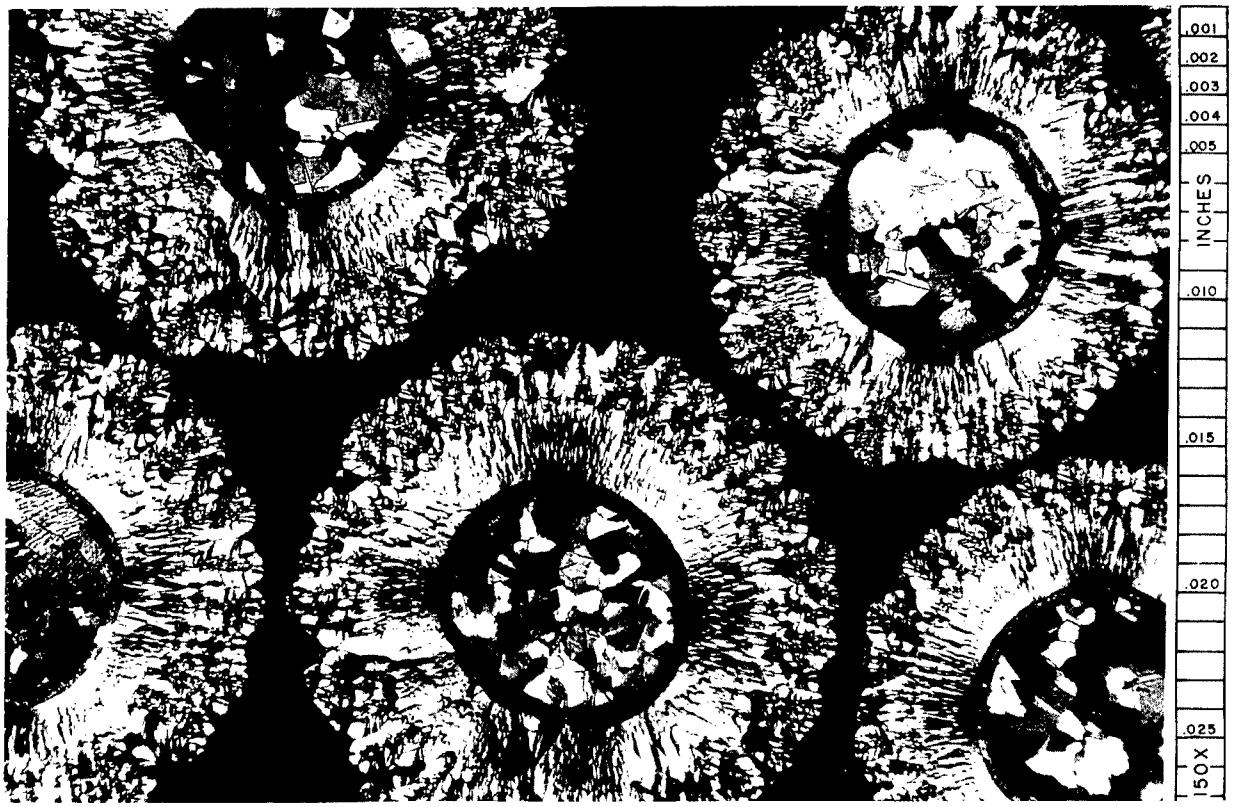

(b)

Fig. 1. Polarized Light Microstructures of Pyrolytic Carbon Coatings. (a) Laminar structure. (b) Columnar structure.

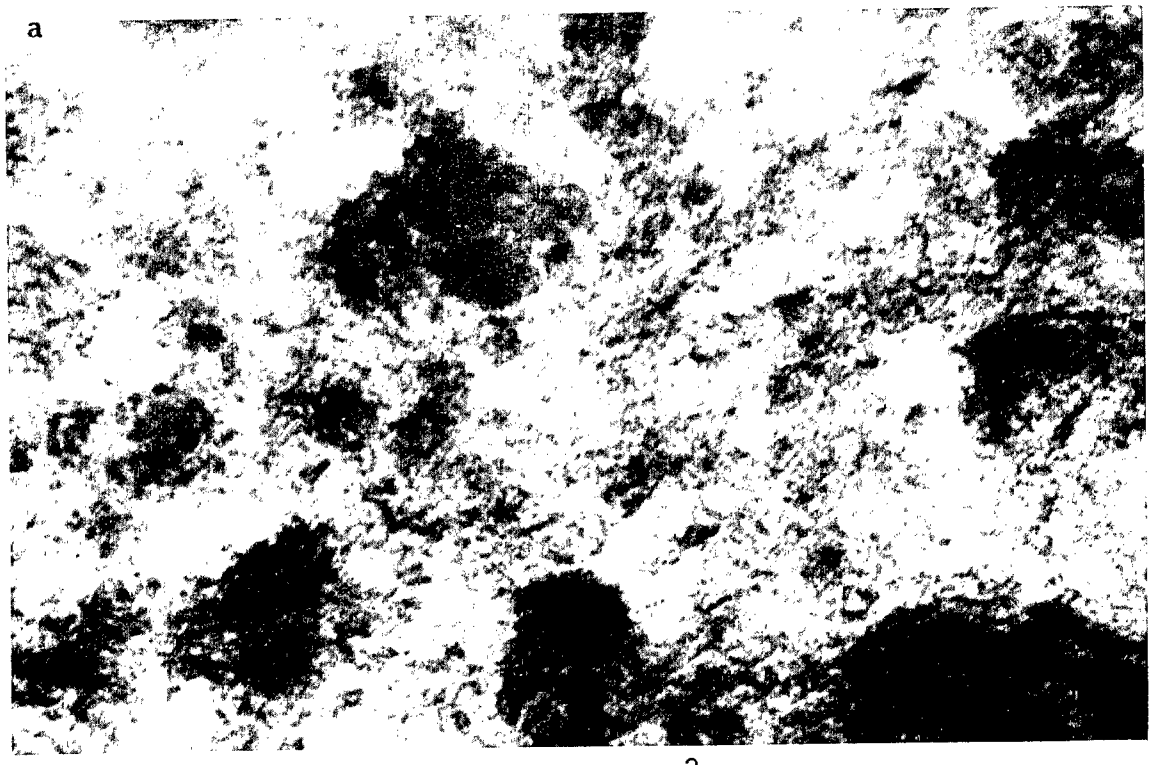

(a) $\rho = 1.41$ gm/cm^3 90,000 X

(b) $\rho = 2.08$ gm/cm^3 105,000 X

Fig. 2. Transmission Electron Micrographs of High and Low Density Laminar Pyrolytic Carbon Coatings.

(a) $\rho = 1.39\ gm/cm^3$ 102,000 X

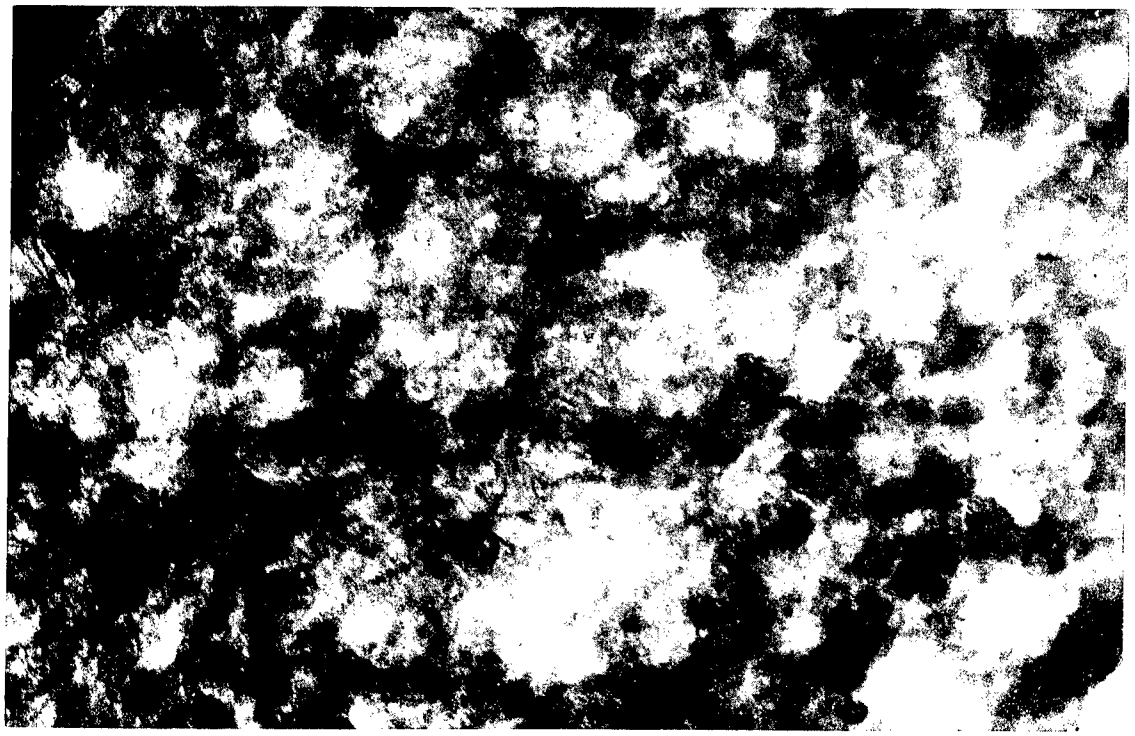

(b) $\rho = 2.08\ gm/cm^3$ 75,000 X

Fig. 3. Transmission Electron Micrographs of High and Low Density Columnar Pyrolytic Carbon Coatings.

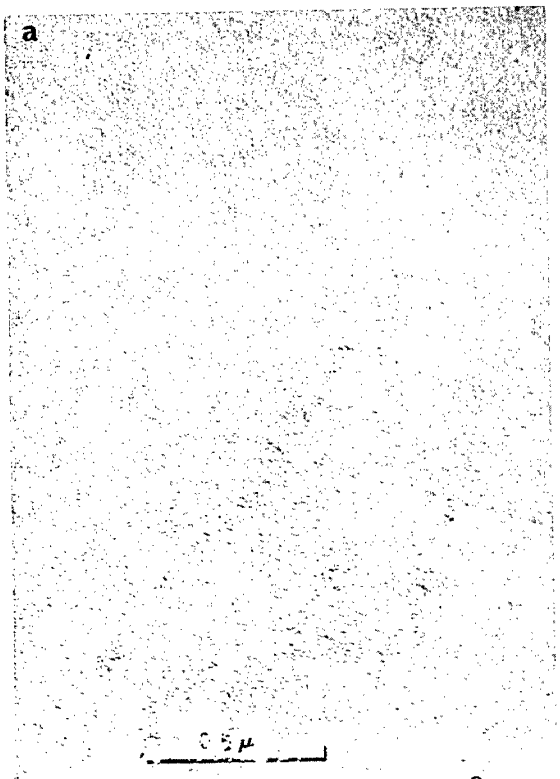

(a) Laminar, $\rho = 1.41$ gm/cm^3

(b) Laminar, $\rho = 2.08$ gm/cm^3

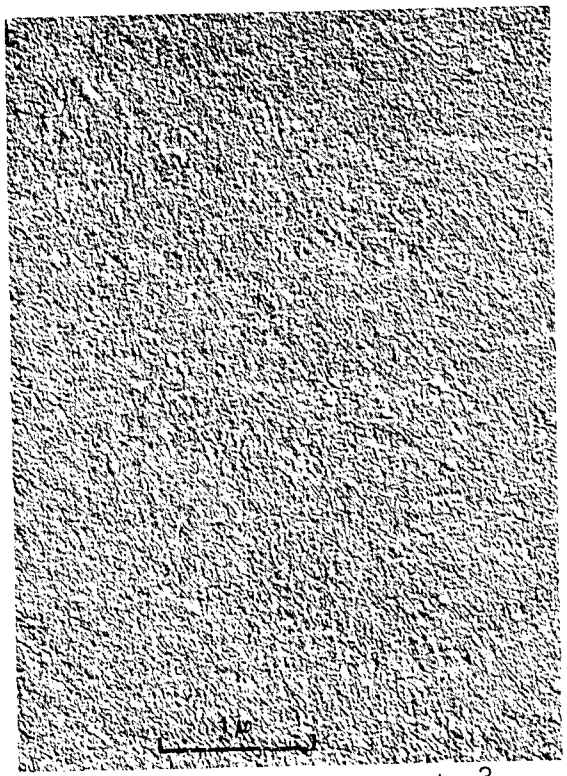

(c) Columnar, $\rho = 1.39$ gm/cm^3

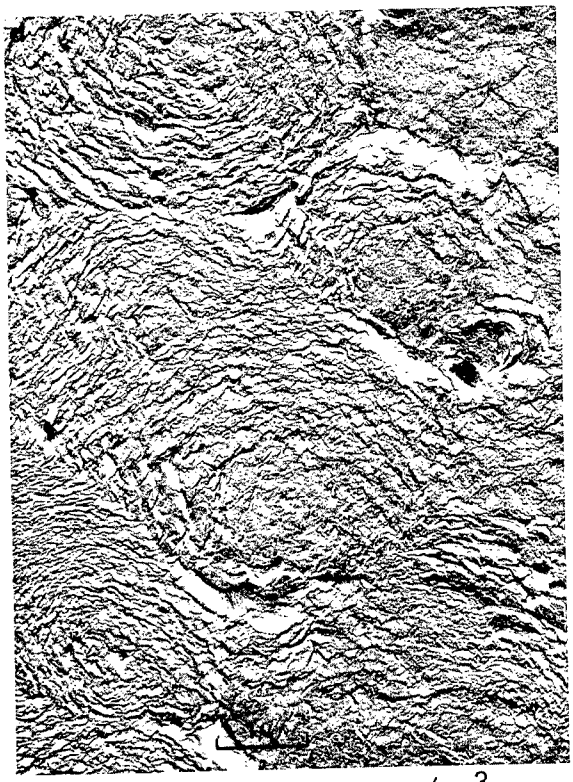

(d) Columnar, $\rho = 2.08$ gm/cm^3

Fig. 4. Replica Study of As-Polished Surfaces of Various Pyrolytic Carbon Coatings.

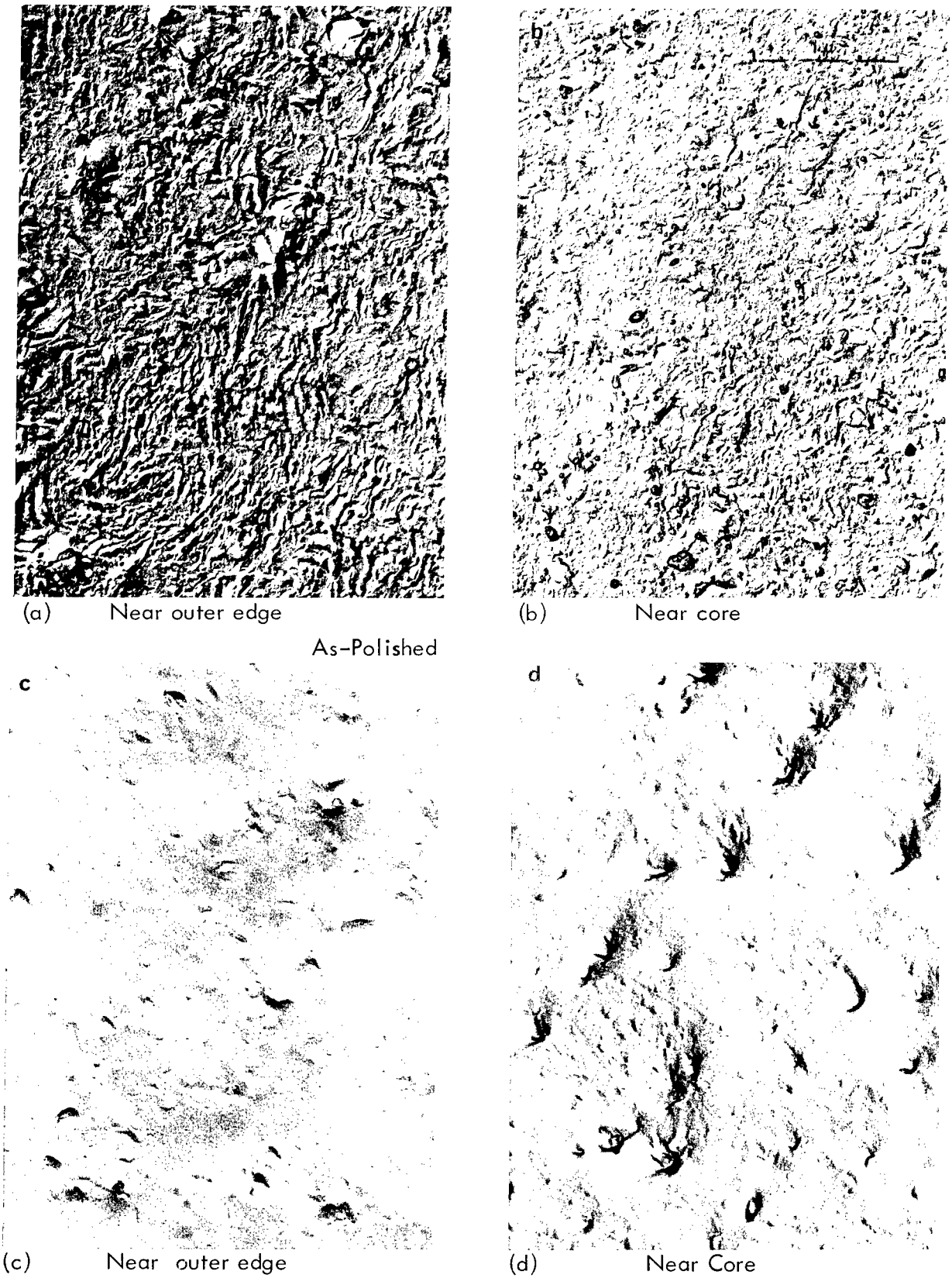

(a) Near outer edge (b) Near core

As-Polished

(c) Near outer edge (d) Near Core

Cathodically etched

Fig. 5. Replicas of High Density (2.01 gm/cm^3) Laminar Coatings Before and After Cathodic Etching.

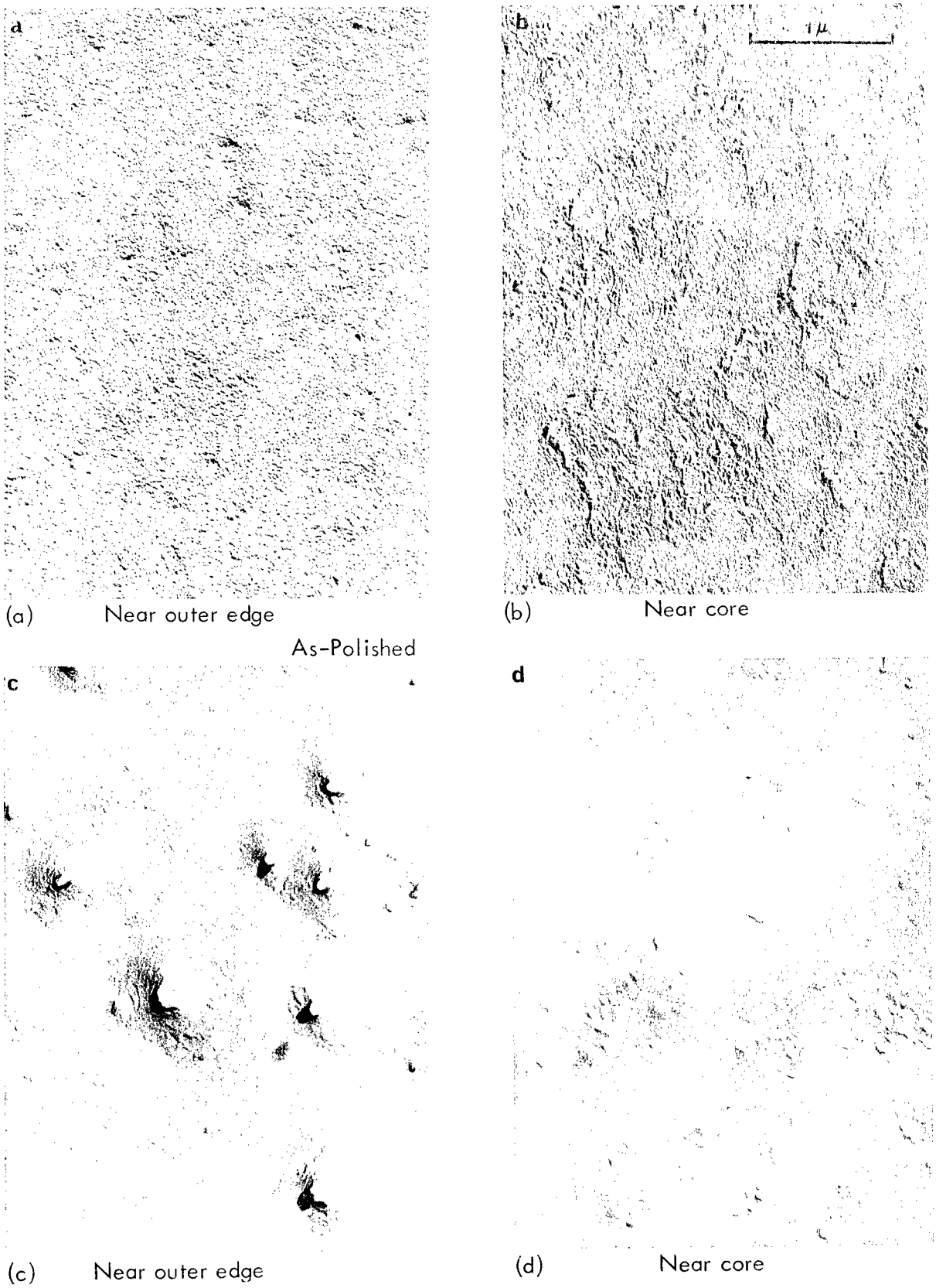

(a) Near outer edge

(b) Near core

As-Polished

(c) Near outer edge

(d) Near core

Cathodically etched

Fig. 6. Replicas of Low Density (1.7 gm/cm^3) Laminar Coatings Before and After Cathodic Etching.

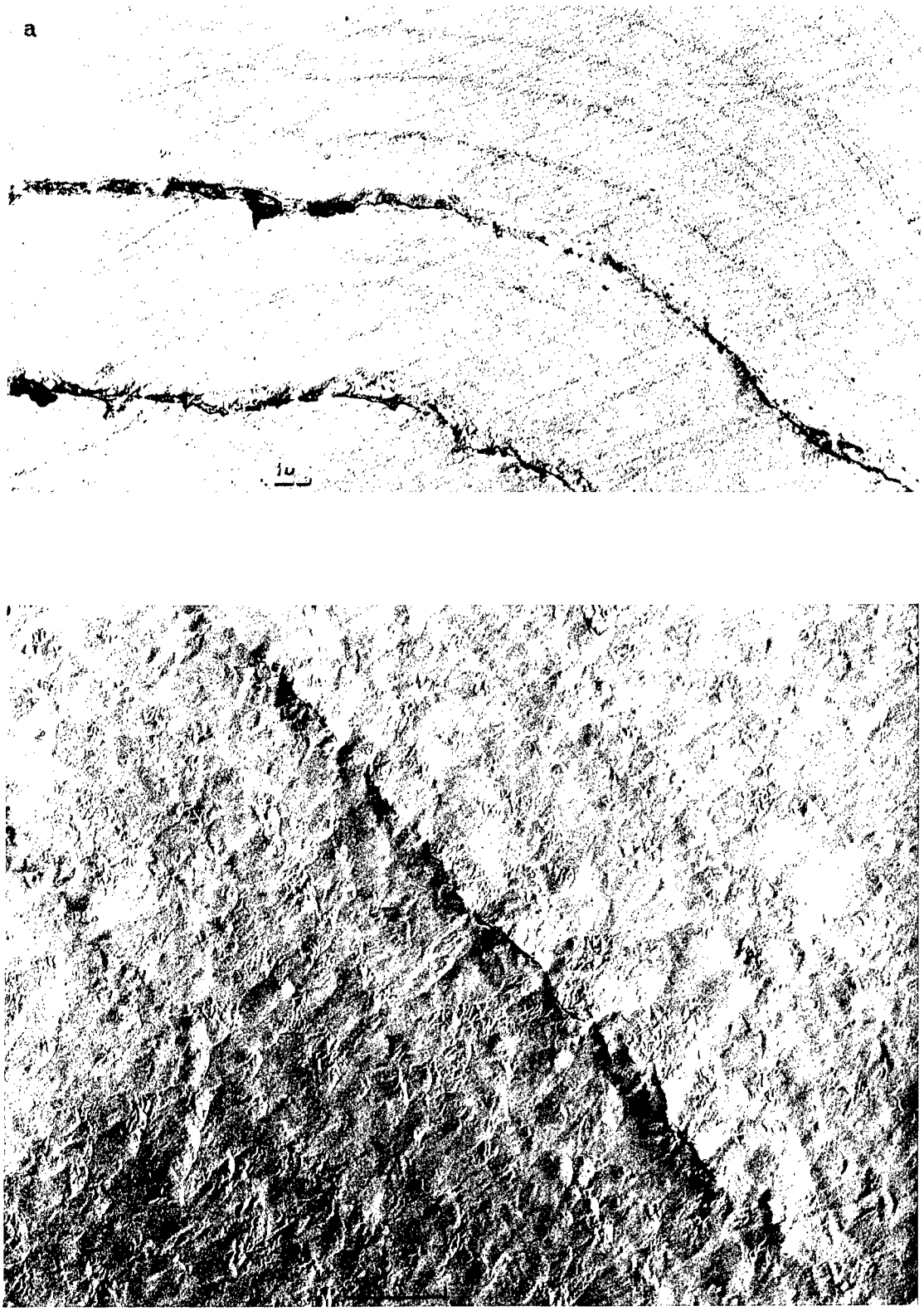

Fig. 7. Electron Micrographs of Replicas Taken of Delaminations in Laminar Coatings. (a) Large cracks, as polished. 6,250 X. (b) Micro cracks, cathodic etch. 12,500 X.

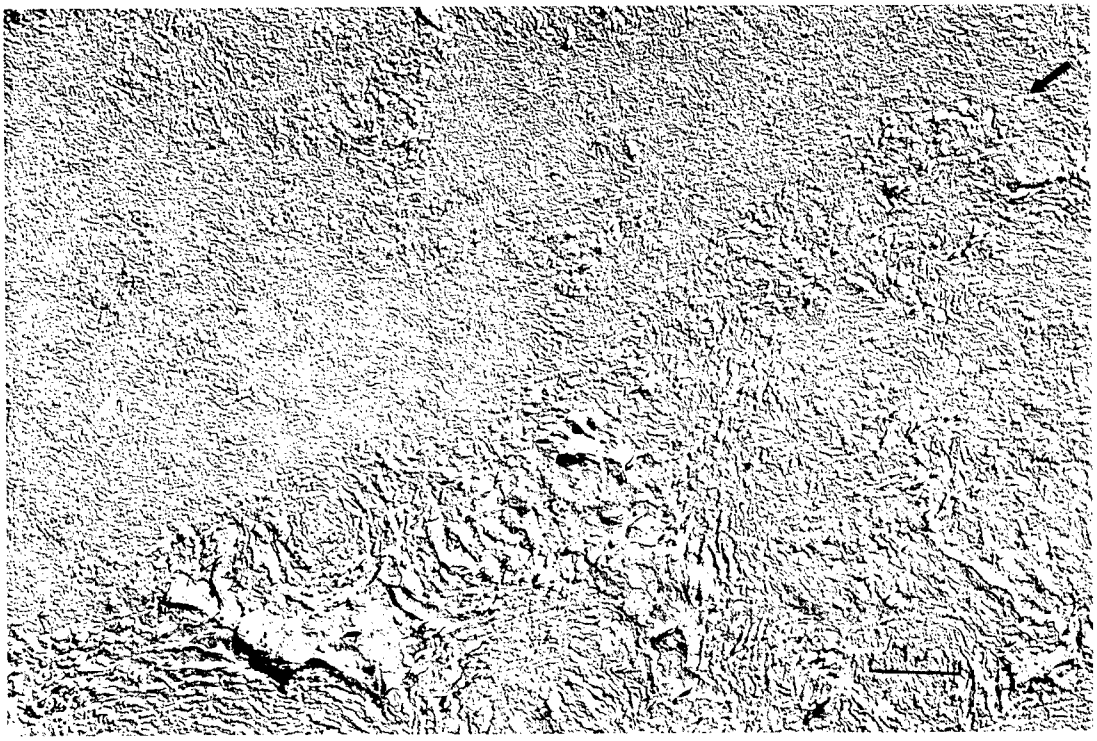

(a)

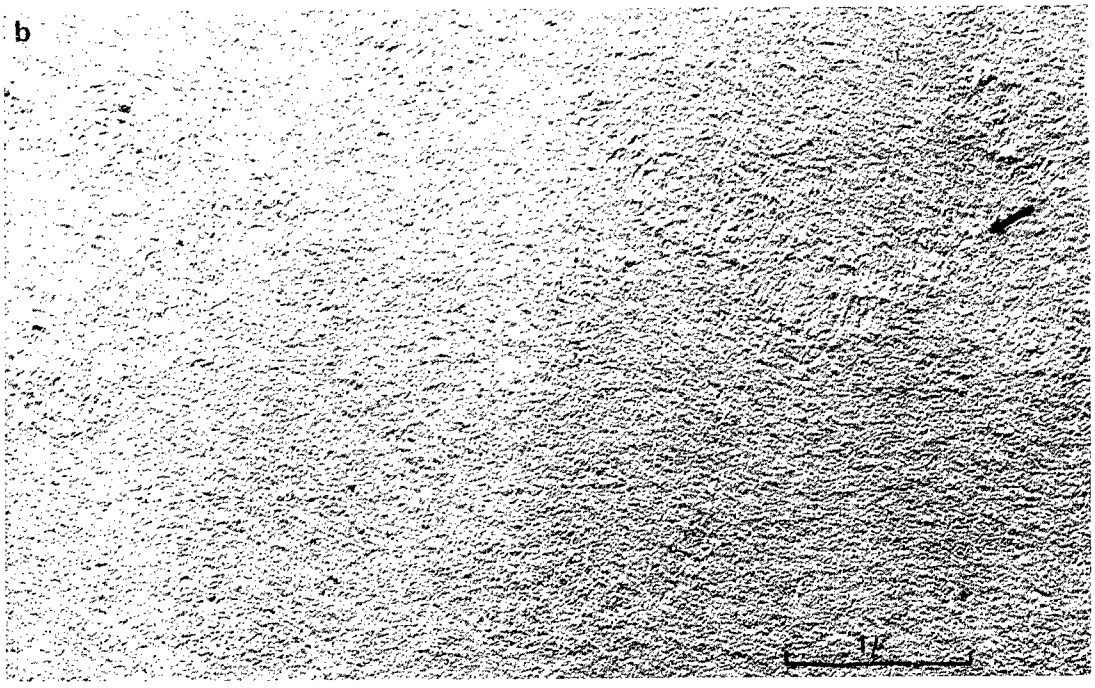

(b)

Fig. 8. Electron Micrographs of Replicas Taken of As-Polished Surfaces of Duplex Coatings, Showing Interface. (a) Columnar-laminar duplex. (b) Laminar Coating of Varying Densities. Arrows indicate interface.

IN-CELL VACUUM IMPREGNATION OF METALLOGRAPHY SPECIMENS

F. L. Cochran
H. E. Shoemaker

General Atomic Division of General Dynamics Corporation
John Jay Hopkins Laboratory for Pure and Applied Science
San Diego, California

ABSTRACT

The problem of preparing porous, damaged, or badly cracked irradiated specimens for metallographic analysis was solved by vacuum impregnation of the specimens prior to preparation. It was found that the most desirable impregnating material was a mixture of Epon 815, Epon 812, and allyl glycidyl ether, using Dmp-10 as the hardening catalyst. The extremely low viscosity and long curing time of the epoxy compound resulted in complete impregnation at vacuum levels of from 1 to 30 μ. The impregnation apparatus was designed to accommodate a modified vacuum desiccator, which permitted impregnation and simultaneous mounting of from one to ten specimens during a single impregnation cycle. Direct radiation fields of from 5, 000 to 10, 000 r/hr did not embrittle the epoxy compound.

INTRODUCTION

The preparation of radioactive specimens for metallographic analysis has become one of the most sophisticated and elaborate phases of hot-cell technology. This paper describes a significant phase of remote metallographic preparation--the vacuum impregnation of specimens. The technique described is applicable to nearly any type of material, but graphite and graphitic materials are used to illustrate the technique.

In many cases, materials exposed to long-term thermal and irradiation cycles exhibit such a degree of disintegration that, without impregnation, metallographic preparation would be quite impossible. Another reason for impregnation is to isolate any damage to the specimen that might occur as a direct result of grinding and polishing, i. e., cracks, pores, and defects that are filled with the epoxy compound cannot be interpreted as defects originating as a result of metallographic preparation. The impregnation of voids, pores, and defects not only strengthens and preserves the true condition (structure) of the specimen but also provides a material of uniform grinding hardness across the mounted surface.

The technique to be described was designed and modified primarily for in-cell impregnation, but the device is mobile and may also be used out-of-cell for the impregnation of nonradioactive materials.

DESCRIPTION OF APPARATUS

The basic concept of the in-cell apparatus designed at General Atomic for vacuum impregnation was based on one used by Clark at Hanford (1). At first glance, the General Atomic apparatus may appear objectionable because it is fabricated almost entirely from glass (see Figs. 1a and 1b), but despite the construction material no component has ever been broken by manipulator operation. The major reason for using glass was to permit visual observation of all phases of the impregnation process. The modified vacuum desiccator (Fig. 2), which

(1) T. J. Clark, "Metallographic Studies of Reactor Graphite Materials, Part 1," General Electric Company Report HW-68182, February, 1961.

is a detachable section of the apparatus, was the only area adversely affected by radiation; i. e., after a 12-hr evacuation of nine specimens reading approximately 500 r each, the desiccator glass became brown enough to obstruct visual observation; it was disposed of and replaced by a new one before starting the next impregnation series.

The apparatus is divided into three distinct sections: a modified vacuum desiccator, an epoxy reservoir, and a supporting frame of aluminum (Fig. 3).

The desiccator is fitted with a rotating plate which is grooved on the top surface to provide automatic alignment of the specimen molds. The bottom of the plate is fitted with three or four magnets which correspond to magnets mounted on the exterior ring around the desiccator. Thus, the internal plate can be rotated by turning the outside ring with the manipulator. The interior specimen plate lifts out for cleaning; however, the inner track of the external ring assembly is cemented to the desiccator, and if its removal is desired (to replace the desiccator) a solvent (MEK) must be used to dissolve the cement (a hysol-epoxy adhesive).

The desiccator lid is cemented permanently to the framework, and the desiccator is raised or lowered by a laboratory jack attached to the base of the frame. A guide ring is provided at the rear of the desiccator lid to automatically align the desiccator as the two ground-glass joints come together. A lever is provided to shift the desiccator and "break" the vacuum seal after impregnation is completed.

The reservoir (top portion of the impregnation assembly) is attached to the desiccator lid by a ground-glass joint. Pressure-type stopcocks are inserted in the glass vacuum "T" line leading to the desiccator and the reservoir. A stopcock is also used to vent the desiccator. The stopcock at the bottom of the reservoir is used to control the flow of the epoxy compound during impregnation. The entire assembly is light and can be moved in and out of the cell with ease.

IMPREGNATING COMPOUND

After a careful evaluation of commercial epoxy materials, the Schneiderhohn mixture, and other plastic-base materials, empirical experimentation revealed that the best impregnating material for in-cell

use was one containing a mixture of 20 cc Epon 815, 3 cc Epon 812, 3 cc allyl glycidyl ether, and 2 cc Dmp-10 (hardener). The addition of the allyl glycidyl ether gives the compound a much lower viscosity and increases its wetting ability; the hardener is added just prior to use. This mixture gives the qualities needed for in-cell impregnation, is easily prepared, and requires no heat for curing; it has a very low viscosity and a long pot-life, and is not adversely affected by radiation. When mixed and allowed to cure out-of-cell at room temperature, the compound does not begin to thicken until about 19 hr after the catalyst (hardener) has been added. When used in a radiation environment of approximately 10, 000 r/hr at room (cell) temperature, the compound has a working life of about 10 hr, indicating that the pot-life is reduced almost 50% by this radiation level. When the epoxy starts to solidify, about 8 hr are required for complete curing.

Although the epoxy compound has a slight amber color, it allows excellent visual examination of the mounted specimen; however, after prolonged exposure (3 weeks) the material will become opaque. The compound produces a mount with a hard finish, without embrittlement, grinds and polishes extremely well, and can be easily cut and milled.

The 812 and 815 resin and the allyl glycidyl ether are manufactured by Shell Chemical; the Dmp-10 hardener is manufactured by Rohm and Haas. The mount, or any geometry of the resin, can be decomposed by soaking it in ethylene dichloride or methylene dichloride.

IMPREGNATING PROCEDURE

The specimens to be impregnated and mounted can be precut, or the desired metallographic sections can be cut after impregnation and solidification of the resin. If the molded specimens are sectioned after impregnation, the cut sections should be remounted in another molding ring using the same impregnating epoxy. The standard-size mount used in-cell is 1-1/4 in. long with a diameter of 1-1/4 in., which means that metallographic specimens or sections cannot exceed the size of the plastic mounting ring. (Aluminum and stainless steel mounting rings may be substituted for the plastic molds, if desired.) Regardless of the type of mounting ring used, it becomes a part of the specimen mount after the epoxy solidifies. The inside walls of the

plastic rings are slightly grooved to prevent separation of the ring after solidification of the resin.

The molding rings are numbered and one end (bottom) is closed by taping with a piece of double-sided masking tape before placing the rings in the desiccator.

The specimens illustrated in Fig. 4 were evacuated for about 4 hr, which produced a vacuum slightly less than 10 μ. The epoxy compound (200 cc) was poured into the reservoir and the reservoir cap replaced; this was done without disturbing the desiccator vacuum. The vacuum was then shifted to the reservoir by closing stopcock C (see Fig. 1a) and opening stopcock B; stopcocks A and D are, of course, closed. The epoxy was evacuated for 1 hr. During the first few minutes of evacuation, the vapor pressure of the epoxy causes violent degasing and turbulence, but this can be reduced by opening stopcock B by degrees: within 5 min the stopcock may be half opened; after about 30 min the stopcock may be fully opened. After approximaterly 30 min, stopcock C may be reopened and the desiccator and epoxy are then evacuated simultaneously.

Impregnation is accomplished by opening stopcock D until the mount locked under the reservoir tube is filled with resin; each specimen is rotated under the tube and filled. After all the mounts are filled, the desiccator is held under vacuum for 1 hr before bringing it to atmospheric pressure. The mounts are then removed from the desiccator and stored until the epoxy is cured. Various impregnating times and techniques were tried, such as alternately evacuating and pressurizing the impregnated specimens, but the method described provided the best results.

When impregnation has been completed, the impregnating apparatus should be flushed with acetone, thoroughly cleaned, and (if desired) removed from the cell.

METALLOGRAPHIC PROCEDURE

The impregnated specimens were ground on silicon carbide papers (320, 400, and 600 grit) using Metadi as the lubricant-coolant; fine grinding was done on a single 4/0 aluminum oxide paper. They were then rough polished on a nylon-covered wheel using 1-μ aluminum

oxide particles suspended in Metadi. Final polishing was done on a vibratory polisher (syntron) using a micro cloth with a 0.05-μ aluminum oxide–Metadi solution as the abrasive. The specimens were prepared one at a time because of the nature of the carbon-coated fuel particles; i.e., (Th, U)C_2 hydrolyzes very rapidly in air and the particle must be photographed immediately. Moisture-free materials were used during all stages of preparation to retard the conversion to the oxide. The specimens were examined and photographed on a modified Bausch and Lomb research metallograph.

ACKNOWLEDGMENTS

The authors would like to thank John C. Bellville, Bernard Siefner, O. H. Kilgore, and Ruth Bartolacci for their specialized contributions to the project.

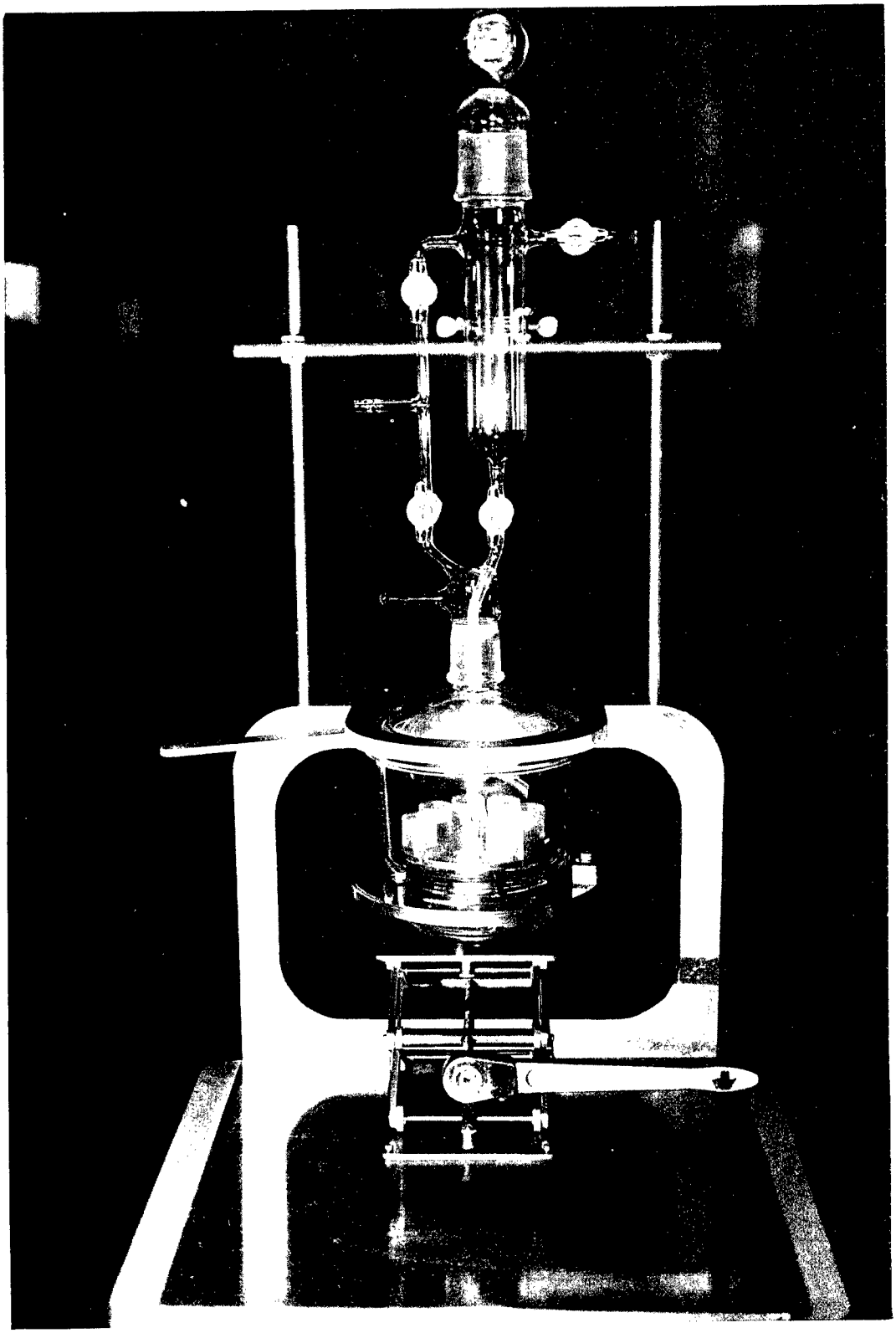

1a--Front view of impregnating apparatus

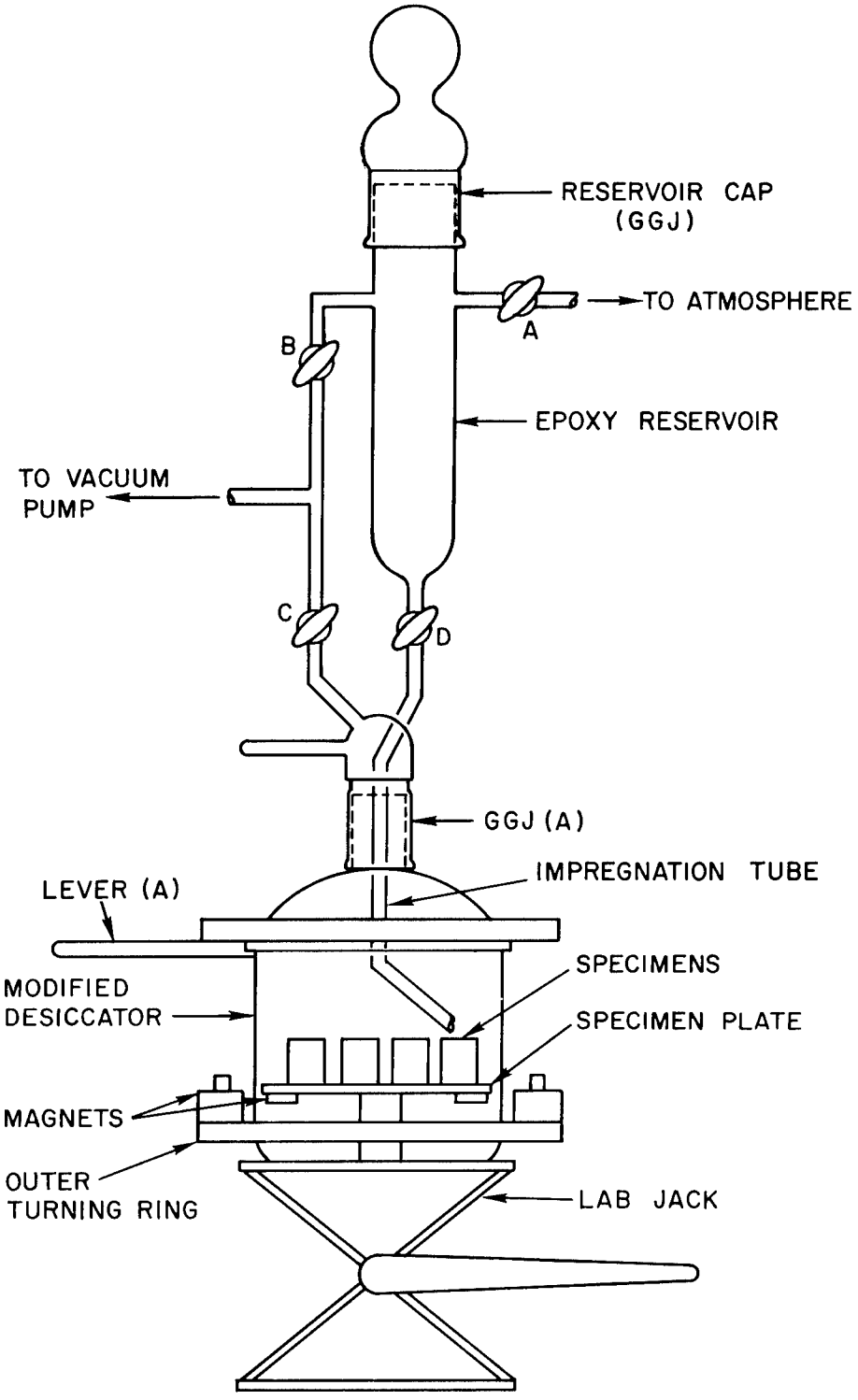

1b--Schematic diagram of impregnating apparatus

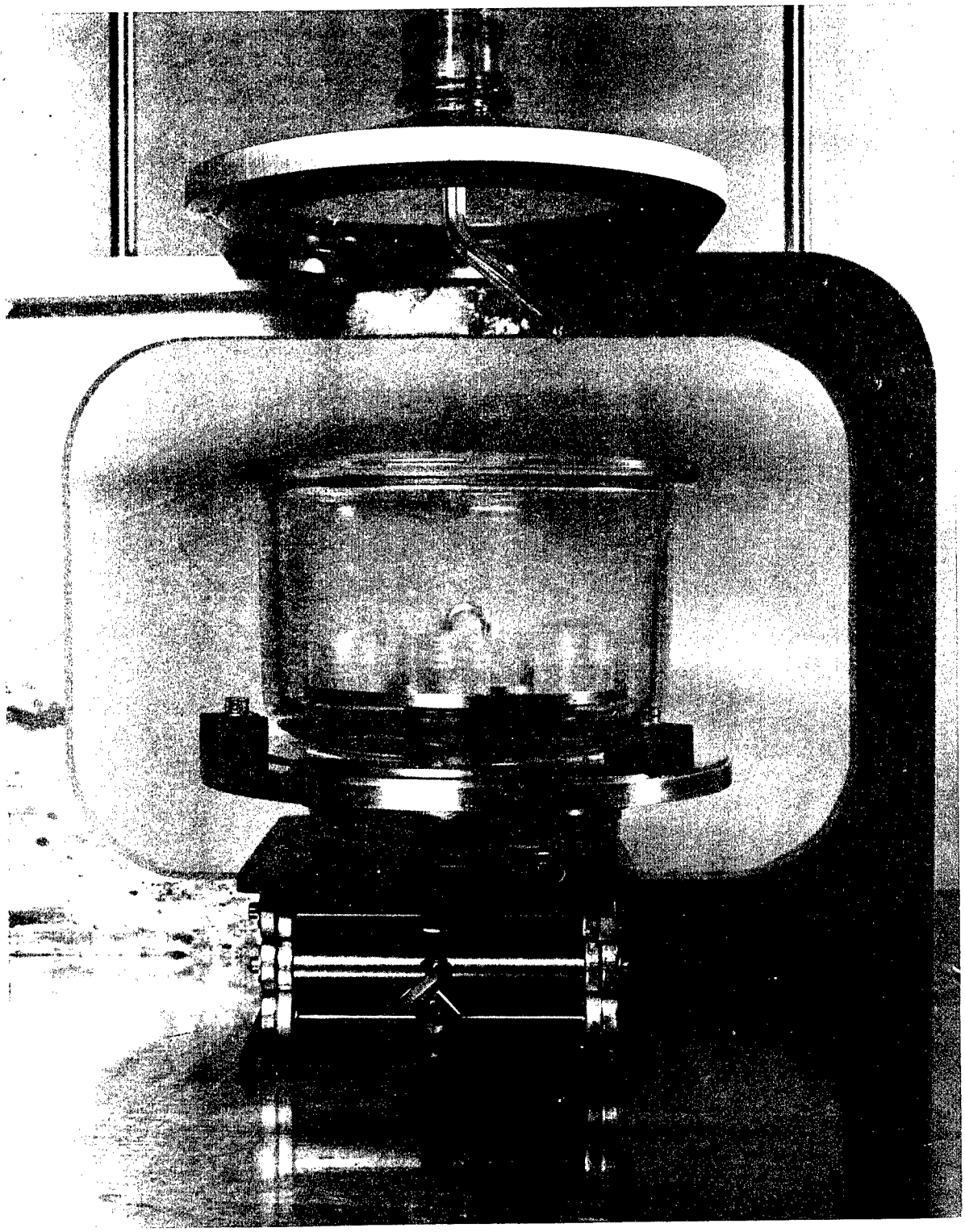

2--Front view of unit showing desiccator and lid

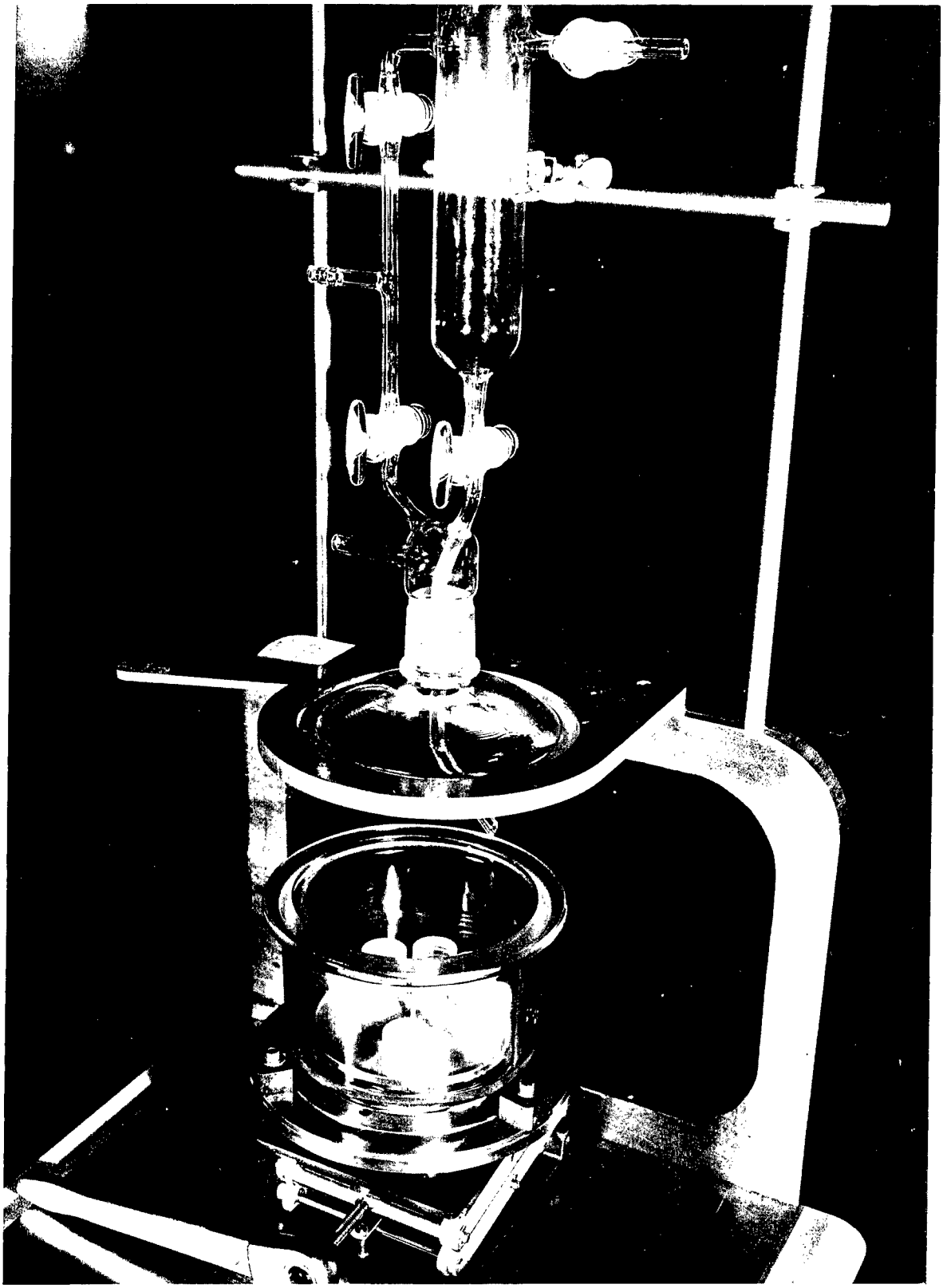

3--View of unit showing desiccator in down position

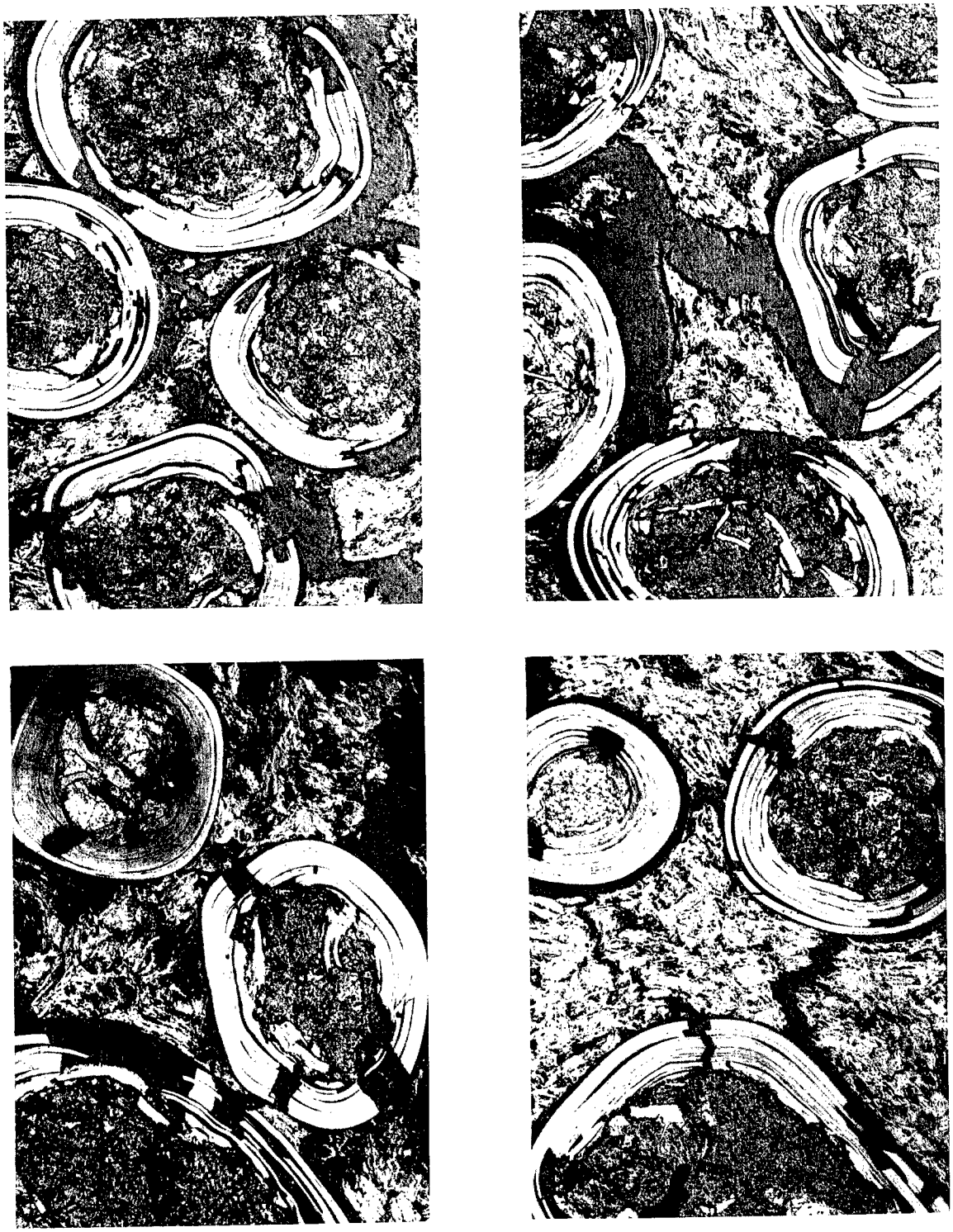

4--Typical microstructures of irradiated fuel compacts: (Th, U)C_2 carbon-coated particles dispersed in a graphite matrix; impregnating resin is smooth, gray material (200×)

VIBRATORY GRINDING AND POLISHING OF METALLOGRAPHIC SPECIMENS*

S. Matras

Argonne National Laboratory
Argonne, Illinois

ABSTRACT

The range of metallographic specimen preparation by vibratory polishing has been extended to include the grinding operation. A controlled method has been developed that reduces the metallographic grinding operation to essentially one step. This was achieved by: (1) controlling the horizontal and vertical components of vibration by changing the springs and the weight of the base of the apparatus to conform to the specific requirements of grinding, (2) providing a special fixture that guides the specimen in a controlled and predetermined manner.

The grinding fixture consists of a Lucite bowl that holds an 8 in. diameter silicon carbide paper disc and a rotating turret in which the specimens are spaced and loaded with appropriate weights. The grinding produces specimens with surfaces which possess a minimum of disturbed metal with virtually no embedded abrasive. The specimens have flat surfaces and their edges are well preserved. Inclusions and second phases, not normally

*Work performed under the auspices of the U. S. Atomic Energy Commission.

in evidence at this stage of specimen preparation, are clearly delineated in the matrix. Retention of hard inclusions in a soft matrix is excellent.

The commercial vibratory polishers do not always produce a scratch-free final polish, especially with high-purity materials that are soft and ductile. To achieve satisfactory surfaces a final polishing fixture utilizing a center mounted rotating carrier was devised. This fixture replaces the standard stainless steel polishing bowl and retaining ring. The fixture is mounted on a standard vibratory polishing unit. In contrast to standard vibratory polishing units that require specimen loadings of 300 to 600 gm, the new device may be operated without any load on the specimen and will produce a superior polish.

Preparing metallographic specimens now involves only three steps: specimen grinding on 400 or 600 grit paper, intermediate polishing, and final polishing. No more hand operations are necessary. The method has broad applicability; for example, it is routinely used for the specimen preparation of cermets; and high-purity thorium and thorium-plutonium alloys have also been successfully prepared. The technique is presently adapted to glovebox work for plutonium and its alloys, diffusion couples and alloys and cermets that are difficult to prepare.

INTRODUCTION

The introduction of the vibratory metallographic specimen preparation by Krill[1] in 1956 was a significant departure from the conventional metallographic technique. The method is a form of automation. Most previous approaches to the automating of the conventional method imitated the manual procedure and, therefore, did not change the basic difficulties inherent in manual preparation. Indeed many metallographers still prefer manual grinding and polishing of critical and difficult materials to avoid surface deformation and the creation of defects caused by mechanical methods. With the need for examination of radioactive materials the development of automatic methods became imperative and vibratory specimen preparation looked highly attractive. The vibratory process was developed by Long and Gray[2-4] with the help of Meador[5] and was further developed by Rothstein and Turner[6] who presented a detailed analysis of the principles of vibratory polishing. The process was adopted by many U. S. laboratories, but was essentially limited to the polishing steps. Grinding before polishing still was done by the conventional manual or mechanical methods. See for instance the report by Nicholson and Williamson[7]. Hopkins and Peterson[8] in their study of vibratory polishing variables found that the method gives surfaces of excellent quality, but they also discussed some undesirable factors such as the large variation of metal removal with changes in vibrational amplitude. They expected an improvement from an increase in horizontal and decrease in vertical motion.

In Germany, Petzow, Gessner and Hölscher[9] were able to grind specimens on a vibratory polishing apparatus. By carefully cementing abrasive paper to a glass plate and grinding either wet or dry, and by adjusting the amplitude of the vibration and the weight attached to the specimen, they succeeded in grinding simultaneously materials of different hardnesses. Their polishing method did not significantly differ from the American procedure.

This laboratory is investigating a great variety of so-called exotic materials. They may consist of a hard and extremely brittle phase imbedded in a soft or refractory metal matrix, they may be diffusion couples wherein hard and soft diffusion bands neighbor each other and where internal boundaries must be clearly outlined, they may be high-purity metals containing trace amounts of residual second phases, they may be alpha-active materials that must be handled in gloveboxes, or they may be materials wherein microcracks must be distinguished from other faults, or they may be single crystals. In all of these cases vibratory metallographic specimen preparation appears to be a highly promising method provided one really controls all of the important variables. This is achieved by: (1) doing away with the uncontrolled movement of the specimens in the apparatus and by providing a series of fixtures that guide the specimen in a predetermined manner, (2) controlling the horizontal and vertical components of vibration and changing the springs and the weight of the base of the apparatus to conform to the specific requirements of grinding or polishing, (3) by controlling the pressure on the sample and providing a suitable carefully centered load.

The result is an automatic specimen preparation process that, after machining[a] of the specimen and vibratory grinding of the backside of the mount to render the flat faces parallel, consists of:

1. vibratory grinding of the specimen itself in a single operation

2. intermediate polishing

3. final polishing

This report describes the fixtures that were devised for the three steps of vibratory grinding, intermediate polishing, and final polishing and gives the reasoning that led to each particular device. The method has been successfully applied to a variety of materials. Some significant results are shown at the end of this report. The method is now used on gamma-active materials in our hot cells and on alpha-active materials in our plutonium laboratory.

A Syntron Model LP-01 Type C Vibratory Polishing Apparatus was used in all of our experiments.[10]

STEP I. VIBRATORY GRINDING

The initial exploratory work with slurries of 400- and 600-grit silicon carbide abrasives with a variety of cloths proved ineffective if metal was to be removed at a practical rate. Coarse abrasive grit, because of its larger size, rolls under the weight of the specimen. Grinding action with such grit is slight. When a loose slurry was used, much of the abrasive was imbedded in the specimen surface. The grinding marks were non-uniform and the metal was worked. After the use of slurries was abandoned, attention was then turned to fixed abrasives such as the abrasive paper discs commonly used for wet-grinding on rotating wheels. The selection of a paper disc with fixed abrasive resulted in a greater rate of metal removal. The grinding medium, however, aggravated two characteristic properties of the vibratory method:

1. Single-specimen mounts tend to overtake one another and to clatter when tracking at the periphery of the bowl.

2. A "bouncing" motion is imparted to the specimen by an interaction with the vibrating bowl.

The overtaking tendency by itself normally only decreases the rate of polishing. Also, parallelism of the mount faces was not maintained particularly when a relatively coarse abrasive was used. When a coarser abrasive medium was used, this tendency also resulted in embedding abrasive

[a] Machining is generally unnecessary except in glovebox work with plutonium materials.

particles into the specimen. The embedding of abrasive particles did not occur when a fine abrasive such as alumina was used. These effects were remedied by devising a light-weight fixture to confine and to separate the mounts. The overtaking tendency was thereby prevented, and furthermore, the fixture assured positive flat contact of the specimen with the abrasive disc by holding the mount face parallel to the grinding surface.

The "bouncing" motion of the specimen was attributed to a "grabbing" tendency of the fixed abrasive and to an excessive vertical component of motion of the polishing bowl. By reducing the weight of the top of the unit as much as design would permit, and compensating for this weight reduction with a softer vibrational spring system, the vertical component of the vibratory motion was reduced. The reduction of vertical amplitude and the practical elimination of the attendant "bouncing" solved the basic problem of grinding of metallographic specimens.

DESCRIPTION OF EQUIPMENT

The grinding fixture, Figure 1, is of all Lucite construction and was designed to use an 8 in. diameter abrasive paper disc. This fixture, shown schematically in Figure 2, consists of a turret in which specimens and their weights are confined, and a bowl in which grinding is performed. The bowl serves as a support and a guide for the rotating turret. The rotating turret is essentially an annular ring with 12 bored holes in which 3.2 cm (1.25 in.) diameter mounted specimens are constrained when they move over the abrasive disc. The turret is positioned over the abrasive disc - but not in contact with it - by a peripheral low-friction track that is lubricated with ethylene glycol. Ethylene glycol is used because of its non-evaporating property and its miscibility with water and with alcohol. A SiC abrasive disc with a 2.5 cm (1 in.) diameter punched hole is placed in the center of the bowl, Figure 3, and is secured by means of a Lucite retainer nut. The Lucite nut has recently been replaced by a stainless steel nut. The abrasive disc is not cemented to the bowl. It is merely held down at its center. A recess is machined into the bowl at the periphery of the abrasive disc. This recess traps abraded material and any dislodged abrasive.

The grinding fixture, with six of the specimen wells loaded, is shown in Figure 4, mounted on a Syntron vibratory base. Weights, each weighing 500 gms, are shown in position on top of the mounts. The fixture is fastened to an aluminum adapter plate that also functions as a bowl to contain possible spatter. When one is grinding or polishing radioactive materials, this precaution is necessary. Smooth and effective grinding in this bowl and rotating turret device necessitated the modification of the standard vibratory unit. A decrease in the vertical component of motion of the system without too great a loss in horizontal displacement was desired. The vertical component of motion was decreased by reducing the mass of the top fixture and by using softer springs. Weight reduction was accomplished

by constructing the bowl and turret from Lucite and the adapter-bowl plate from 6061-T6 aluminum alloy. The total weight of the grinding fixture and adapter plate was reduced from the original 10.6 kg (23 lbs. 7 ozs.) of the commercial unit to 4.3 kg (9 lbs. 8 ozs.).

The commercial Syntron vibratory unit employs flat springs, 0.3 cm (1/8 in.) thick and 15.2 cm (6 in.) long. These are arranged in 4 gangs of 4 springs each and are inclined 75 degrees from the base of the machine. A trial and error approach was adopted in determining the balanced, softer spring system required. This was accomplished by varying the size and number of springs in each gang of springs. There are two rules which must be adhered to when modifying the spring system:

1. The spacers between springs should be placed symmetrically.

2. Opposite spring gangs should have the same spring arrangement.

The spring system which was adopted for the grinding device of 4.3 kg weight consists of four flat springs, 1.6 mm (0.063 in.) thick and 15.2 cm (6 in.) long, in each of the four gangs. Each 4-spring gang is arranged symmetrically; the outer two spaces are fixed at 1.6 mm (0.063 in.) and the inner space at 3.2 mm (0.125 in.). A nominal air-gap setting of the electromagnet of 0.4 mm (0.016 in.) proved adequate. This balanced arrangement of softer spring system and lighter top resulted in a maximum vertical displacement of 0.64 mm (0.025 in.). Table I compares displacement amplitudes as a function of rheostat settings for the modified unit and the standard Syntron unit. Maximum vertical displacement occurred at a rheostat setting of 50 and a horizontal displacement of 1.65 mm (0.065 in.) for the modified unit. Increased rheostat settings increased the horizontal displacement with little increase in vertical displacement.

PROCEDURE

The vibratory grinding step is standardized to No. 600-grit silicon carbide abrasive discs. A 200 cc mixture of 40% ethylene glycol with methanol, ethyl alcohol, or water is used as the lubricant. Sectioning of the specimen and initial mount preparation are important to the vibratory grinding step in that the surfaces of the mount must be flat and parallel to within 0.05 mm (0.002 in.). True parallelism of the flat surface is easily achieved by the vibratory grinding of the backside of the mount. This is done in the grinding fixture, as described below. The abrasive disc is discarded after this step. The mounted specimens are then dropped, face down, into the specimen wells of the rotating turret. Approximately 4 cc of ethylene glycol are placed on top of each mount. A 500 gm weight is inserted into the well on top of the specimen displacing the ethylene glycol into the clearance between the mount and the well. The displaced glycol provides a cushion between the weight and Lucite well and also provides a thin liquid film between weight and mount. The liquid film couples mount and weight and enables them to move vertically in unison. The film also facilitates removal

of the specimen after the grinding operation; and since no clamping or screwed on weights are used the film makes for rapid sample removal and replacement. With this arrangement, the mount height is not important, although a 1.9 cm (3/4 in.) high bakelite mount appears to be convenient.

A horizontal displacement amplitude of approximately 1.52 mm (0.060 in.) measured at the 24.1 cm (9.5 in.) outside diameter of the Lucite support bowl, results in turret rotation of about 5 to 7 revolutions per minute. While this displacement is not the maximum that is attainable on vibratory units, it does promote uniform and smooth grinding action in this adaptation. A grinding time of one hour is the maximum allowable. Grinding is practically complete after the first 30 minutes. Additional grinding time has a smoothening effect; but grinding longer than one hour can be detrimental because of abrasive paper wear and work hardening of the specimen surface. Although grinding striations produced by this method are directional, the results are excellent, particularly with respect to the retention of inclusions. The presence of directional grinding striations aids readily in determining when the subsequent step is completed.

RESULTS AND CONCLUSIONS

Examples of some of the as-ground surfaces obtainable with the rotating turret grinding fixture are shown in Figures 5, 6, and 7. All specimens were ground for one hour, each under a 500-gram load.

Figure 5 at 100X compares the as-ground surfaces produced on No. 400-grit SiC papers by (a) hand-grinding on a rotating wet wheel and (b) by vibratory grinding. Note the smoothness and evenness of grinding striations and the absence of smeared metal in the vibratory ground sample.

Figures 6 through 8 show the vibratory-ground surfaces produced by No. 600-grit abrasive discs. Figure 6(a) indicates that a comparable surface can be produced with No. 600-grit silicon carbide abrasive and that no real advantage is gained by first grinding on a No. 400 paper. Metal removal appears to be the same for both grades of abrasive. Figure 6(b) shows good edge-preservation. Cracks at and near the edge are clearly revealed in the as-ground surface. Figures 7(a) and 7(b) show the excellent retention in the as-ground condition of friable materials at the surface and the grain boundaries. Figures 8(a) through 8(d) of thorium and thorium-uranium alloys are included to show the retention of inclusions and the absence of disturbed metal attained in specimens having a range of hardnesses. In particular, Figure 8(d) shows the presence of phases not normally in evidence in this stage of sample preparation.

No attempt was made to determine the rate of metal removal to a high degree of accuracy. All measurements were done with a hand micrometer. Table II is a partial record of specimens that were vibratory ground, and correlates metal removed with the hardness of the specimens.

A diamond-impregnated aluminum disc (3M Company, grade-fine) was also tried. This resulted in a coarse-ground surface with insignificant metal removal. Vibratory grinding was also done using a Pellon disc (grade PAW) impregnated with 15-micron diamond abrasive. Lubricant in this trial was Hyprez oil. In this case a grinding time of one hour resulted in a satisfactory surface with 2.5 to 6.3 microns (0.1 to 0.5 mils) removed from tungsten-UO_2 cermet specimens.

STEP II. INTERMEDIATE POLISHING

DESCRIPTION

The commercial vibratory unit is used without modification in the second, intermediate, step of polishing. To facilitate its use and to allow for long-time or overnight polishing of specimens a three-hole holder, Figure 9, is used. Three spacing lugs on the underside minimize contact between holder and polishing cloth. Single-specimen holders track only along the periphery of the bowl resulting in a wearing out of the cloth at this location. Also, single specimens with clamped-on or screwed-on weights have the tendency to overtake each other with resultant clattering and a slowdown in polishing action. The three-hole holder eliminates the danger of specimens overturning and tearing of the cloth. Since the holder rotates as it travels around the bowl, a large portion of the area of the polishing cloth is utilized and directional polishing is minimized.

PROCEDURE AND RESULTS

The bakelite mounted specimens after having been vibratorily ground and thoroughly cleaned to remove loose No. 600-grit contamination are placed into the wells of the three-hole holders used with the commercial vibratory unit. The vibratory unit can accommodate four such holders. This permits all 12 specimens after grinding to be transferred to the intermediate polishing step. In most cases, 500 gm weights are being used to load the specimens, but 1000 gram weights have been used to polish cermets with a tungsten matrix.

The abrasive slurry consists of 15 to 20 gms of Linde B alumina suspended in a mixture of 20 v/o ethylene glycol with either water or methanol. A quantity of 400 cc is maintained in the bowl. This mixture of a carrier liquid and ethylene glycol appears to be the optimum and has the advantage that when the carrier liquid evaporates, the ethylene glycol remains behind. The presence of the ethylene glycol permits intermittent operation of the vibratory units without caking of the polishing slurry. To make the unit operational again it is only necessary to replenish with water or alcohol to the required level. This results in a savings of expensive polishing cloths. A nylon cloth underlayed with a less expensive Met-cloth is the lap material.

To determine the proper amplitude for polishing, the unit is allowed to operate initially with the rheostat set at its maximum. Then the rheostat is turned back slowly to decrease the amplitude. When the holders begin to rotate counterclockwise while orbiting at the periphery of the bowl, the amplitude is correct and polishing will take place. Frequently the weighed specimens will rotate within the holder. Polishing time and displacement amplitude will vary with the type of specimens being polished and the weights used. Some of the polishing times and weights used are summarized in Table III.

Generally, the use of the unmodified unit in the intermediate step should be restricted to materials with polishing characteristics similar to steel or with equal or greater hardness values. Very soft materials - because of their resistance to abrasion - proved exceptionally difficult to polish by this method. Intermediate polishing with an abrasive of larger average particle size (0.3 micron - Linde A) was attempted. Metal removal from specimens of pure thorium was insignificant. The rate of metal removal was determined by measuring the diagonals of DPH impressions before and after polishing. From the known geometry of the indenter the amount of metal removed was calculated. Four microns/hr were removed under a 500 gm load on a nylon cloth. Polishing on microcloth under the same conditions of weight and abrasive removed only three microns/hr. The surfaces produced were not satisfactory. In contrast, more than seven microns of material were removed from a specimen of a 50 w/o Th-U alloy by polishing for one hour on nylon cloth. The exact amount removed is not known since the seven micron depth of the hardness indentation was exceeded. The rates of metal removal of the other materials polished in the intermediate step were not determined. Figure 10 shows the scratch size and distribution developed in a specimen of pure thorium under a 250 gm weight. Similar results were obtained using a 500 gm or a 1000 gm weight. These observations suggest that specimens which are allowed to track freely at the periphery of the bowl, do not make positive contact with the polishing cloth and momentarily tend to ride the edge of the mount. Effective cutting action would then be decreased. Perhaps this type of action is inherent in vibratory polishing machines. The effect of this action is more noticeable in the soft materials. Harder specimens do not seem to be seriously affected and the slight polishing scratches or directional striations resulting can readily be removed in the final-polishing device.

STEP III. FINAL POLISHING

The final-polishing fixture, Figure 11, also constructed of Lucite, is standardized for 30 cm (12 in.) diameter polishing cloths. This fixture is an adaptation of the three-hole holder used in the intermediate polishing step and features a rotating carrier with a center-mounted frictioning device. Figure 12 is a schematic cut-away section of the rotating carrier and friction loading device and shows the placement of specimens within 3-hole holders. The three-hole holder fits closely into the rotating carrier but rotates independently. A commercial vibratory unit[1] is used, but the stainless bowl and

and retaining ring were replaced with the final-polishing fixture, a Lucite bowl, and an adapter plate of the same total weight. Successful polishing with this fixture depends on the restraining effect of the center mounted snubbing device, which, when properly loaded by tightening the loading nut and locking it, slows the carrier down, and thereby introduces counterclockwise rotation of the specimen holders. Figure 13 is a disassembled view and shows the rotating carrier and a clamping ring positioned over the bowl. The ring holds a cloth by means of an O-ring and groove, and stretches and clamps the cloth securely into a recess at the periphery of the bowl.

PROCEDURE AND RESULTS

Since the bored specimen wells (1.250 in. in diameter) have the same size as those used in the two prior steps, the specimens may be quickly and easily transferred for final-polishing. As in steps I and II, ethylene glycol is used as the liquid interface between specimen and weight. The abrasive slurry consists of 15 to 20 g of Linde B alumina in 200 cc of a mixture of 20 v/o ethylene glycol with water or methanol. Microcloth, because of its short and stiff nap, is used as the polishing cloth. Polishing can be done without any load on the specimen.

When specimens are polished without a load, one of the holders must be loaded with dummy weights of at least 250 gms in each hole to promote rotation of the carrier. In this application the bowl is operated at maximum amplitude. If a new cloth has been installed, the carrier is allowed to rotate at maximum for a short time to aid in conditioning the cloth. For proper and non-directional polishing the snubbing nut is gradually tightened until the three-hole holders begin to rotate. Rotation is counterclockwise. The specimens will tend either to oscillate or to rotate within their holes. Polishing time for most specimens will vary between one to two hours. The use of excessive weights will result in relief polishing. Figures 14 through 19 are photomicrographs of a variety of materials successfully polished to a striation- and scratch-free surface. Table III summarizes the steps required to prepare these materials metallographically by the three-step vibratory method. Pure thorium specimens - whether arc-melted or as-received crystal-bar stock-proved difficult to final-polish. As noted earlier in Figure 10, this may be due to improper surface preparation in the intermediate step. Figure 14 is a specimen of commercial grade thorium. The presence of a high-impurity phase probably contributed to successful vibratory preparation of this material. The harder thorium alloys, examples of which are shown in Figure 15, did not pose any particular problem. Highly polished surfaces were easily attained. Figure 16 shows a sensitized Type 304 stainless steel specimen at a magnification of 500X. Figure 17 at a magnification of 200X shows tungsten electroformed onto a copper rod, and is shown as an example of polish attained on materials of dissimilar hardness and properties. The copper was etched with a 10% ammonium persulfate solution. The black area between the copper and tungsten is not a step due to relief polishing, but is a void or separation existing between the two materials. Cermets of

tungsten and UO_2 are routinely prepared by this method with the intermediate step done overnight. Figure 18 shows UO_2 particles in a sintered tungsten matrix. The cobalt-5.5 w/o boron alloy, shown in Figure 19, is an interesting specimen because of its high hardness. The surface shown is as-polished for three hours, unweighted. Because of its high hardness, prolonged polishing did not produce a visibly disturbed surface. This is confirmed in the polarized light photo of the same as-polished surface. Vibratory grinding of this specimen took four hours under a 500-gram weight and required four changes of abrasive paper.

Figure 20 shows the vibratory metallography installation in use at ANL. The vibratory grinder is on the left; intermediate polishing is done in the middle unit, final polishing is accomplished in the unit on the right. The three-step procedure used is outlined in the following summary:

SUMMARY OF VIBRATORY GRINDING AND POLISHING PROCEDURES

Step 1 - Vibratory Grinding:

Abrasive:	400 or 600 grit silicon carbide paper.
Lubricant:	200 cc of a mixture of 60 v/o methanol or ethyl alcohol (low in water content) 40 v/o ethylene glycol.
Track Lubricant:	Ethylene glycol.
Load:	500 grams, 1000 grams for very hard specimens. After placing of the specimen into the hole of the guide ring 4 cc of ethylene glycol are put into the hole with an eye dropper. Then the weight is inserted. It displaces the ethylene glycol which forms a lubricating film around specimen and weight and also between specimen and weight. The film between the specimen and the weight makes the two adhere to each other and facilitates their removal.
Time:	Maximum 1 hour. Most grinding completed in 1/2 hour.
Precautions:	To prevent trapping of hard particles, do not remove specimens for inspection during grinding. Use new silicon carbide paper each time.
Preparation:	Grind mount first on back side to obtain parallel end faces. Discard silicon carbide paper disc.

Step 2 - Intermediate Polishing:

Abrasive:	Linde B alumina on nylon cloth (napless) cushioned by Metcloth.
Lubricant:	80 v/o methanol or, ethyl alcohol 20 v/o ethylene glycol (400 cc).
Load:	500 gram applied with 4 cc ethylene glycol as above.
Time:	Three to six hours, or overnight for hard specimens.
Precaution:	Maintain liquid level by adding alcohol to replace loss by evaporation. The presence of ethylene glycol permits intermittent use of polisher by preventing caking of the abrasive slurry. Different from grinding, specimen may be removed for inspection and replaced.

Step 3 - Final Polishing:

Abrasive:	Linde B alumina on microcloth (short nap).
Lubricant:	80 v/o methanol or, ethyl alcohol. 20 v/o ethylene glycol (200 cc).
Load:	None or up to 250 grams. Dummy weights of 250 grams in another three-hole holder to promote rotation of carrier.
Time:	One to two hours.
Precaution:	Same as with intermediate polishing.

DISCUSSION

The new mechanical fixtures incorporated into the vibratory apparatus make the metallographic specimen preparation easier and produce surfaces of excellent quality with materials that heretofore were extremely difficult to handle. These improvements make it possible to introduce a large degree of automation into remote handling and glovebox work. The fixtures developed may not represent the most economic design but they establish the principle that controlled guidance of the specimens over the vibratory grinding and polishing surfaces are mandatory in the preparation of good specimen surfaces. Under such conditions only a limited amount of work hardening of the surface of the metal takes place as evidenced by the appearance of inclusions and some of structural features already visible after the grinding operation. Vibratorily

polished specimens frequently require less severe etching to develop the structure than do manually prepared specimens, and the vibratory polishing minimizes the need for repeated polishing and etching.

The materials used in the construction were selected because of their light weight and not necessarily because of durability.

Much work needs to be done with regard to the selection of polishing cloths, abrasives, and carrier liquids for the abrasive. Ethylene glycol as a non-evaporating vehicle for the abrasive was given preference over other solvents because of the utilization of the vibratory method in gloveboxes with a dry inert atmosphere. Because of its lubricity, the presence of ethylene glycol may have compromised the cutting action of the abrasive.

In general the vibratory grinding approach proved successful on a wide variety of materials and also on the few composites that were available. A disadvantage of the method lies in the recurring track that the specimen takes over the abrasive disc. A hard material will actually groove the disc slightly. The greater wear imparted to the abrasive disc in a localized track leaves a visible raised section on the surface of softer materials. This does not allow the simultaneous grinding of materials with a great dissimilarity in hardness for long periods of time when the harder material is smaller in size than the companion specimens. In some instances this effect can be removed in the intermediate step of polishing.

The use of the grinding fixture in an intermediate step of polishing with an intermediate grade of abrasive should be investigated. Although the surface produced would then be characterized by fine directional striations, this would not be objectionable at this stage of specimen preparation. It has been observed that soft specimens coming off the intermediate step with a surface of fine directional polishing striations - due to non-rotation of the holder - possessed a much cleaner looking surface than soft specimens that had rotated. In such a fixture the lap material is fastened around a center post and is allowed to expand radially outward. Since the lap material is not restrained at its periphery, it would have to be stiff enough to resist wrinkling under the gripping action of the weighted mounts. Also, it would have to be flexible enough to dampen out resonant vibrations. The abrasive used could either be fixed into the lap material, or else it could be a loose slurry since it would be of relatively fine size.

Because metal removal occurs in minute increments, the preservation of inclusions and phases is good. Any method that confines the mounts and prevents their rotation as does the grinding fixture insures positive flat contact with the lap material. Uniform cutting action is thereby increased.

Although the intermediate and final polishing steps were carried out on unmodified commercial vibratory units, a further improvement in polishing action might have been achieved by reducing the vertical component of displacement. This can be done - as indicated earlier - by reducing the weight of the

top-fixtures and by compensating for the weight difference with a softer spring system. In addition, a departure could be made from the center mounted rotating carrier in the final-polishing fixture to a similar device which would be supported at its periphery as in the grinding device. Snubbing to restrain rotation and to introduce polishing action could then be done at the peripheral track. This type of arrangement would leave the center of the bowl free for a cloth holding-and-stretching device.

CONCLUSIONS

The application of the principle of controlled guidance of the specimens in vibratory polishing has brought significant advantages to the preparation of metallographic specimens by this method in addition to the advantages already noted by earlier investigators. The method is applicable to remote handling and glovebox work and produces specimens of high quality from a great variety of materials which otherwise are difficult to prepare.

ACKNOWLEDGEMENTS

The work was done under the supervision of Robert A. Noland and I wish to express my appreciation to him for the opportunity to undertake this work.

Special thanks go to Dr. B. Blumenthal for his able assistance in the preparation of the manuscript. His interest in the project from the very start was a source of encouragement.

The schematic line drawings were done by T. N. Czaplicki to whom I also owe my gratitude.

REFERENCES

1. F. M. Krill, Vibratory Polishing of Metallographic Specimens, Metal Progress, 70, No. 1, 81-82, (1956).

2. E. L. Long, Jr. and R. J. Gray, Preparation of Metallographic Specimens by Vibratory Polishing, ORNL-2492, (1958).

3. E. L. Long, Jr. and R. J. Gray, Better Metallographic Techniques - Polishing by Vibration, Metal Progress, 74, No. 4, 145-148 (1958).

4. E. L. Long, Jr. and R. J. Gray, Vibratory Polishing of Metallographic Specimens for Optical and Electron Microscopy, Am. Soc. Testing Materials, Symposium on Advances in Electron Metallography, 24 (1958).

5. E. L. Long, Jr., J. T. Meador, and R. J. Gray, Experience with Vibratory Polishers and Design for Hot Cell Application, Symposium on Methods of Metallographic Specimen Preparation ASTM Spec. Techn. Publ. No. 285, 79-89 (1960).

6. P. Rothstein and F. R. Turner, Metallographic Specimen Preparation by Vibratory Grinding and Polishing, Symposium on Methods of Metallographic Specimen Preparation, ASTM Spec. Techn. Publ. No. 285, 90-102 (1960).

7. C. K. Nicholson and C. L. Williamson, A Vibratory Polisher for Remote Metallography, DP-764 (August 1962).

8. E. N. Hopkins and D. T. Peterson, Investigation of Vibratory Polishing Variables, IS-662 (June 1962).

9. G. Petzow, L. Gessner and D. Holscher, Über die Schliffherstellung nach dem Vibrationsverfahren, Zeitschr. Metallkunde 53, 535-540 (1962).

10. Syntron Company, Horner City, Pa.

TABLE I

A COMPARISON OF DISPLACEMENT AMPLITUDES AS A FUNCTION OF RHEOSTAT SETTINGS

Rheostat Setting	Modified Unit					Standard Vibratory Unit				
	Horizontal Displacement		Vertical Displacement		Vert. Displ. / Horiz. Displ.	Horizontal Displacement		Vertical Displacement		Vert. Displ. / Horiz. Displ.
	(mm)	(in.)	(mm)	(in.)		(mm)	(in.)	(mm)	(in.)	
10	0.64	0.025	0.13	0.005	0.20	1.50	0.060	0.75	0.030	0.50
20	1.1	0.045	0.25	0.010	0.22	1.90	0.075	0.8	0.032	0.43
30	1.4	0.055	0.38	0.015	0.27	2.08	0.082	0.9	0.035	0.43
40	1.52	0.060	0.58	0.023	0.38	2.24	0.088	0.95	0.037	0.42
50	1.65	0.065	0.64	0.025	0.38	2.29	0.090	0.95	0.038	0.42
60	1.90	0.075	0.64	0.025	0.33	2.34	0.092	0.95	0.038	0.41
70	2.16	0.085	0.64	0.025	0.29	2.46	0.097	1.0	0.040	0.41
80	2.29	0.090	0.64	0.025	0.28	2.67	0.105	1.0	0.040	0.38
85	2.29	0.090	0.64	0.025	0.28	2.67	0.105	1.0	0.040	0.38

TABLE II

METAL REMOVAL AS A FUNCTION OF SAMPLE HARDNESS

Load: 500 gms.

Lubricant: 200 cc of a methanol - 40% ethylene glycol mixture.

Abrasive: No. 600-grit SiC paper disc (8 in. diameter).

Time: 1 hour.

Specimen	Hardness	Metal Removed	
		(mm)	(in.)
Commercial Th	--	0.127	0.005
Crystal bar Th	DPH 46	0.076	0.003
Th-2w/oU	--	0.076	0.003
Th-10w/oU	R_b 30	0.076	0.003
Th-40w/oU	R_b 64	0.051	0.002
Th-50w/oU	R_b 78	0.051	0.002
304 Stainless Steel	R_b 87	0.051	0.002
Tungsten	R_c 40	0.048	0.0015
Cobalt-Boron alloy	$> R_c$ 70	0.030	0.0012

TABLE III

SUMMARY OF FINAL-POLISHED SPECIMENS LISTING TIME AND WEIGHT FOR EACH STEP

Specimen		Vibratory Ground		Intermediate Polish		Final Polish	
Figure No.	Identification	Time (hr.)*	Load (gm.)	Time (hr.)	Load (gm.)	Time (hr.)	Load (gm.)
14	Commercial Th	1	500	4	500	2	0
15	Th-50w/oU	1	500	3	1000	1	250
16	304 stainless steel, sensitized	1	500	2	500	2	125
17	W on Cu rod	1	500	6	1000	2	0
18	UO_2 in tungsten	1	500	16	1000	2	0
19	Co-5.5w/oB	4	500	over-night	500	3	0

*Changing the abrasive disc every 1/2 hr. - while time consuming - minimizes work-hardening effects.

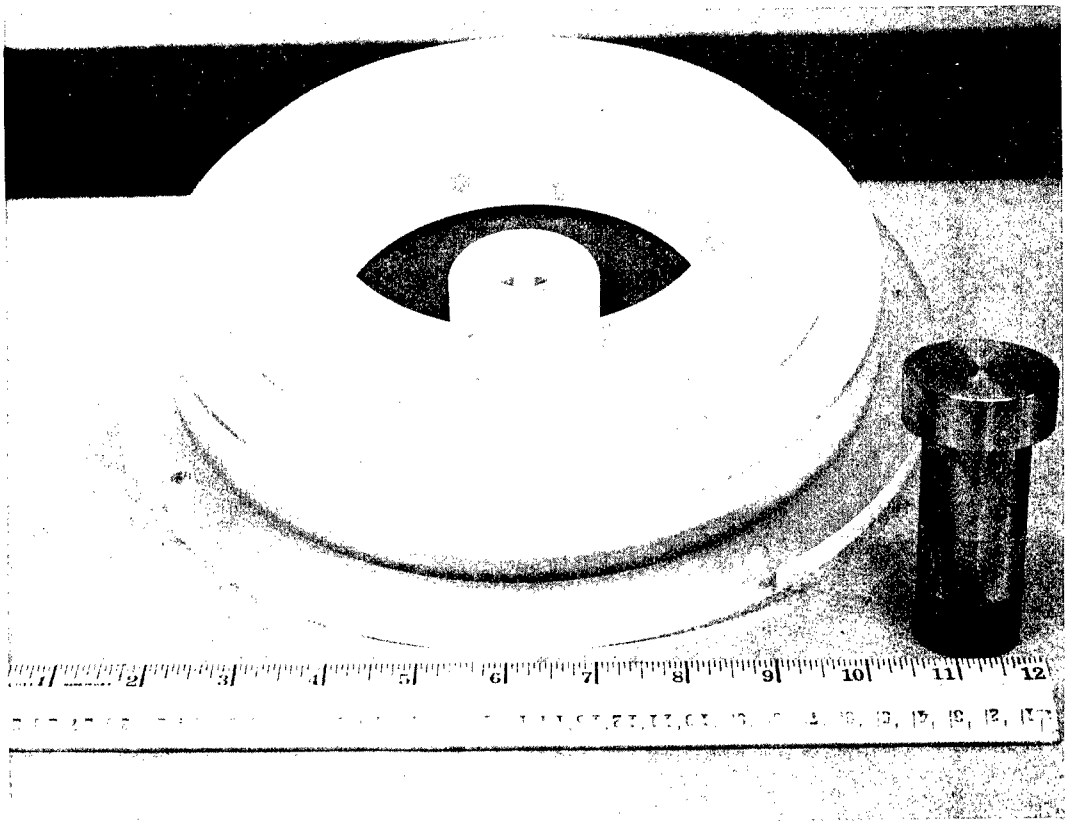

36184

Figure 1. Grinding Fixture and 500-gram Weight.

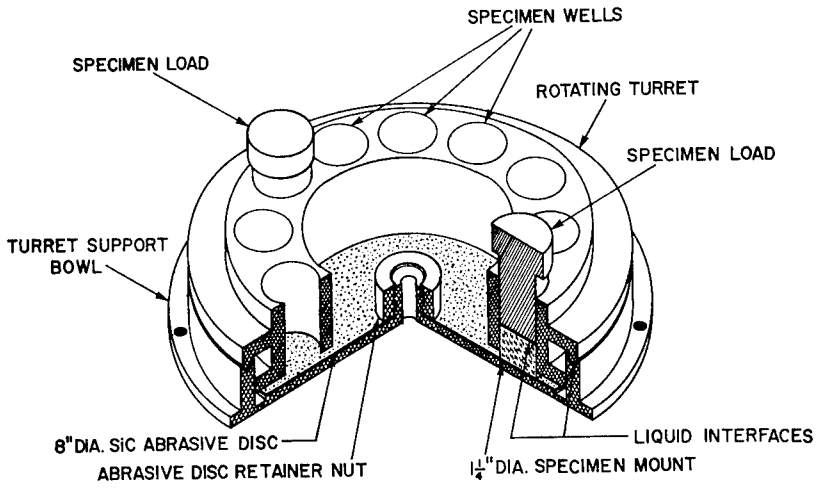

Figure 2. Schematic Cut-away.

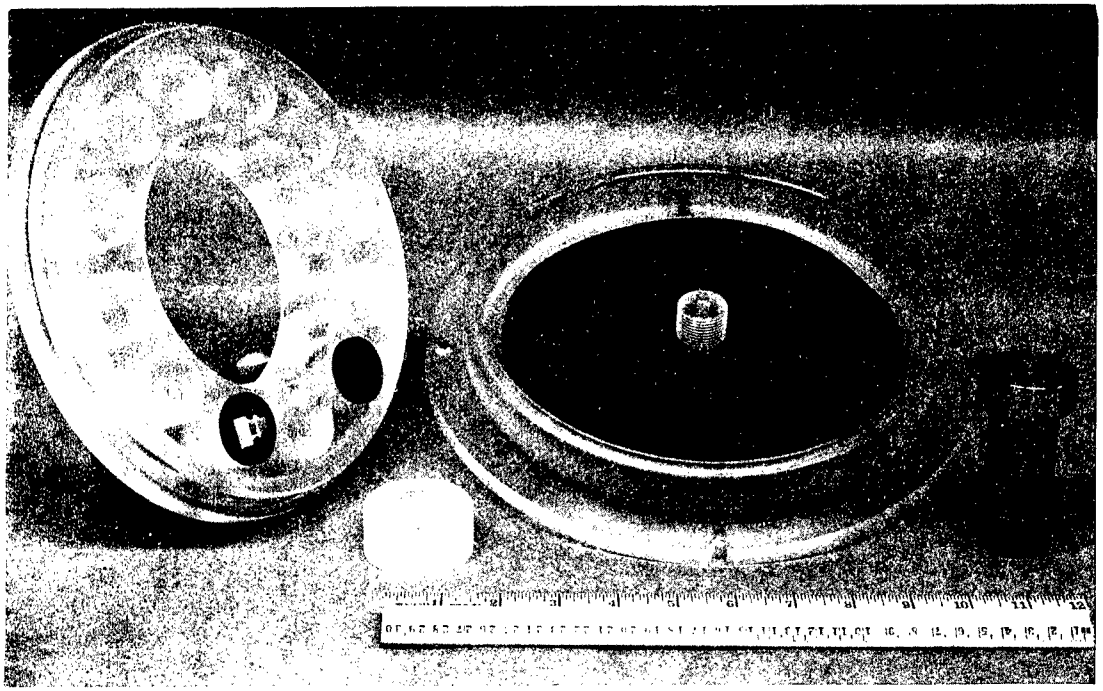

36183

Figure 3. Components of Vibratory Grinding Fixture.

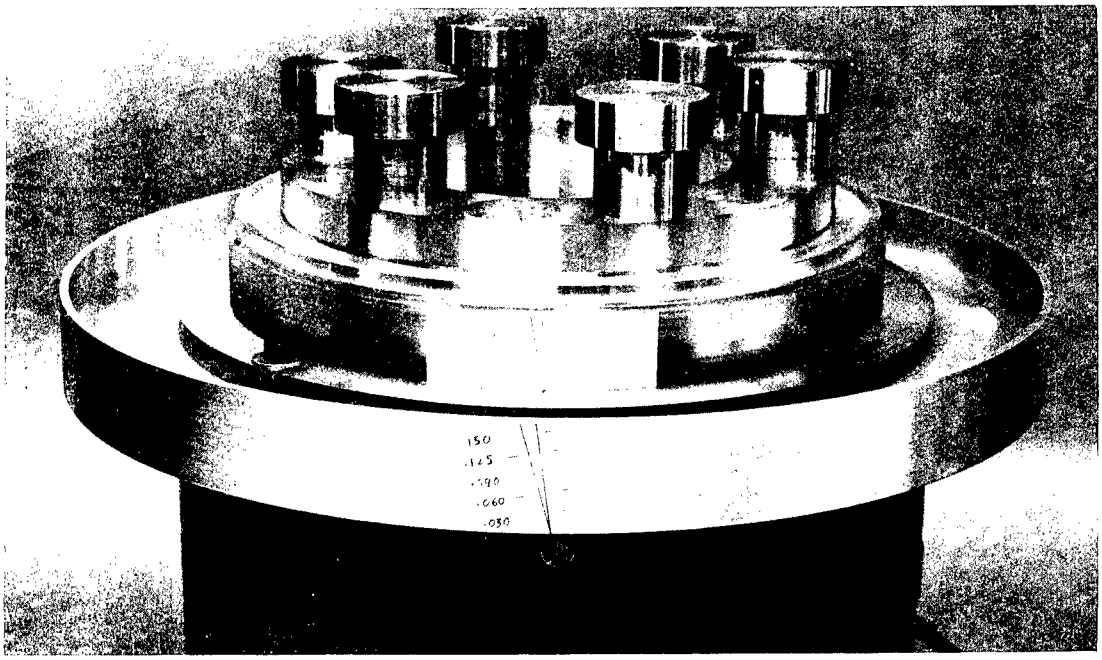

36187

Figure 4. Partially Loaded Grinding Fixture Fastened to an Aluminum Bowl-Plate.

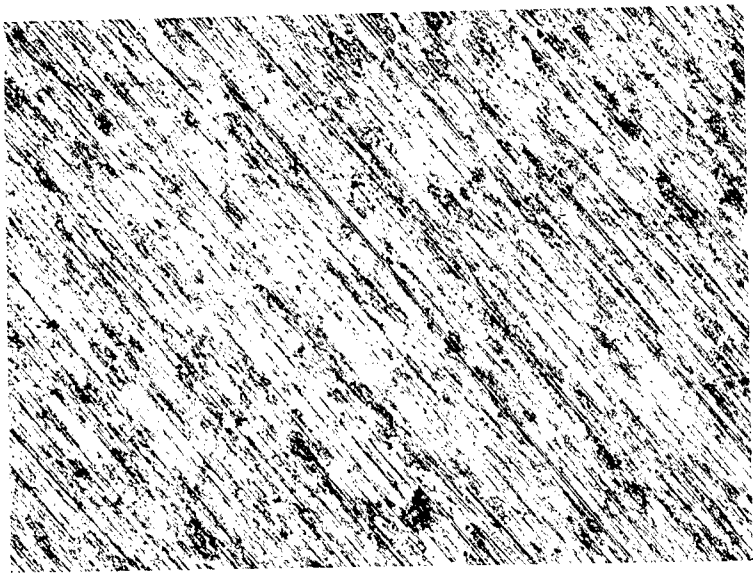

36194 100X

(a) Titanium hand ground on a rotating wet wheel. No. 400 SiC abrasive disc; shows the coarseness of the abraded surface and areas of smeared metal.

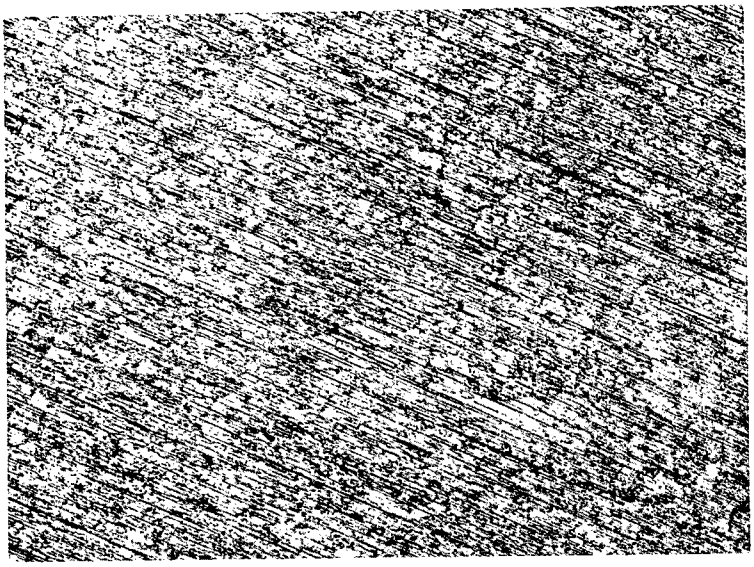

36196 100X

(b) Titanium vibratory ground on a No. 400 SiC abrasive disc, 1 hour under a 500-gram load; shows the smoothness and evenness of striations and the absence of smeared metal.

Figure 5. Comparison of Hand Grinding on a Rotating Wet Wheel (a) and Vibratory Grinding (b).

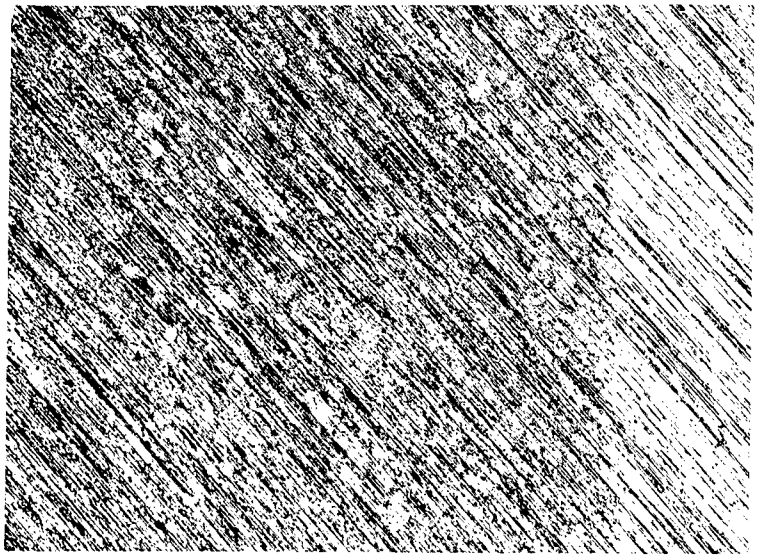

36198 100X

(a) Titanium dip coated with aluminum, vibratorily ground on a No. 600-grit abrasive paper disc. The surface produced indicates that no real advantage is gained by first grinding on a No. 400 silicon carbide paper. (Compare with Figure 5b).

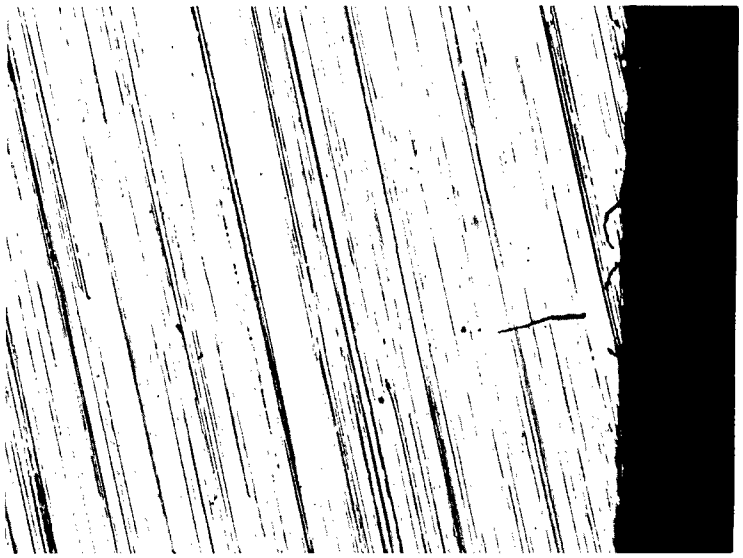

36200 250X

(b) Type 304 stainless steel shows good edge preservation; cracks at and near the surface are clearly revealed.

Figure 6. Examples of Surfaces Produced by Vibratory Grinding on No. 600-Grit SiC Paper for 1 Hour Under 500-Gram Weights.

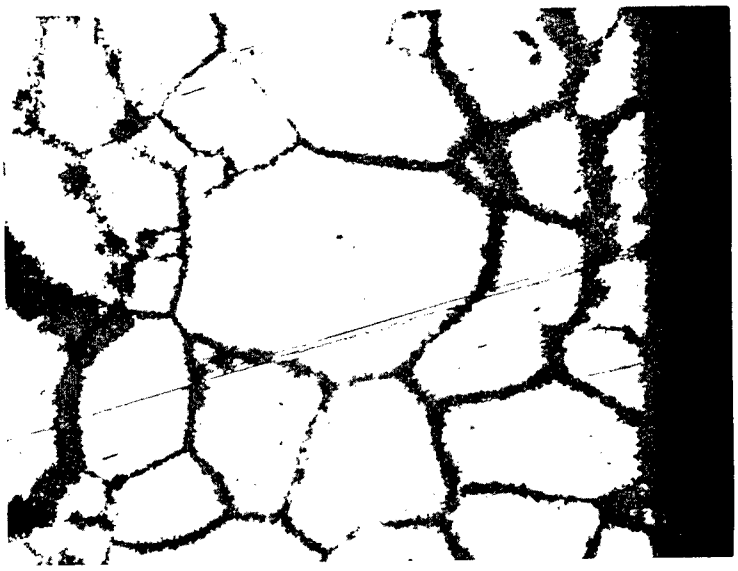

36478 250X

(a) "A" nickel, corrosion tested, shows retention of friable material at the surface and at the grain boundaries

36476 250X

(b) Aluminum alloy (X8001), corrosion tested, the corrosion layer is protected by a strip of aluminum foil placed onto the surface before mounting.

Figure 7. Examples of Surfaces Produced by Vibratory Grinding on No. 600-Grit Silicon Carbide Paper for One Hour Under 500-gram Load.

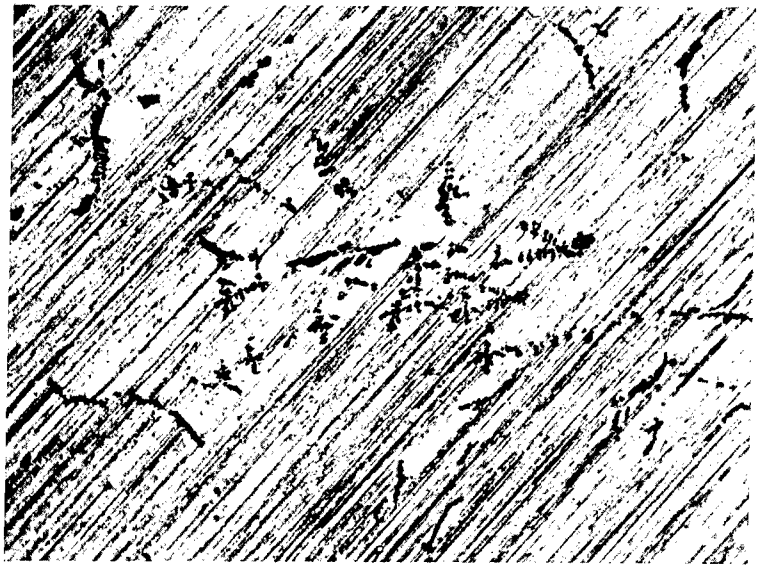

36201 250X

(a) Commercial-grade thorium with a high-impurity content; shows good retention of hard inclusions in a soft matrix.

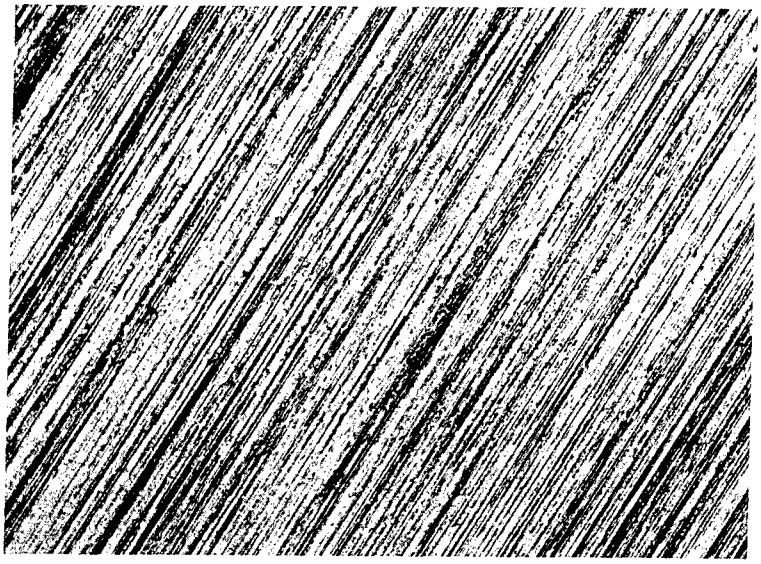

36202 250X

(b) High-purity thorium, shows the clean as-ground surface obtained with a very soft material.

Figure 8(a-d). Examples of Vibratorily Ground Thorium Samples. All Specimens are As Arc-Melted. Grinding Was Done on No. 600-Grit Silicon Carbide Paper for 1 Hour with 500-Gram Weights.

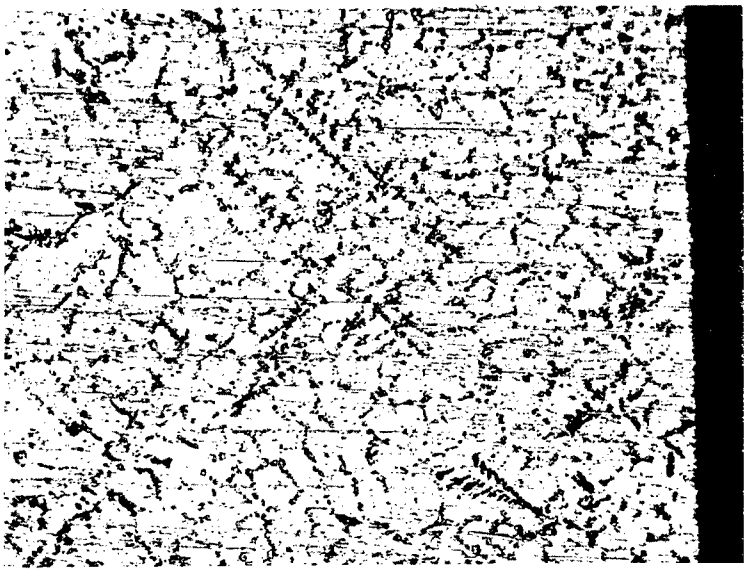

36203 250X

(c) Th-10w/oU.

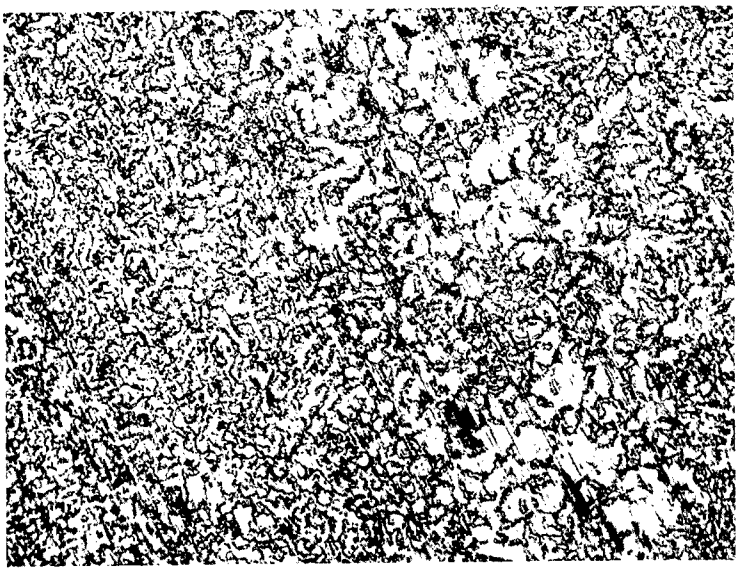

36204 250X

(d) Th-40w/oU alloy; shows presence of phases not normally seen at this stage of sample preparation.

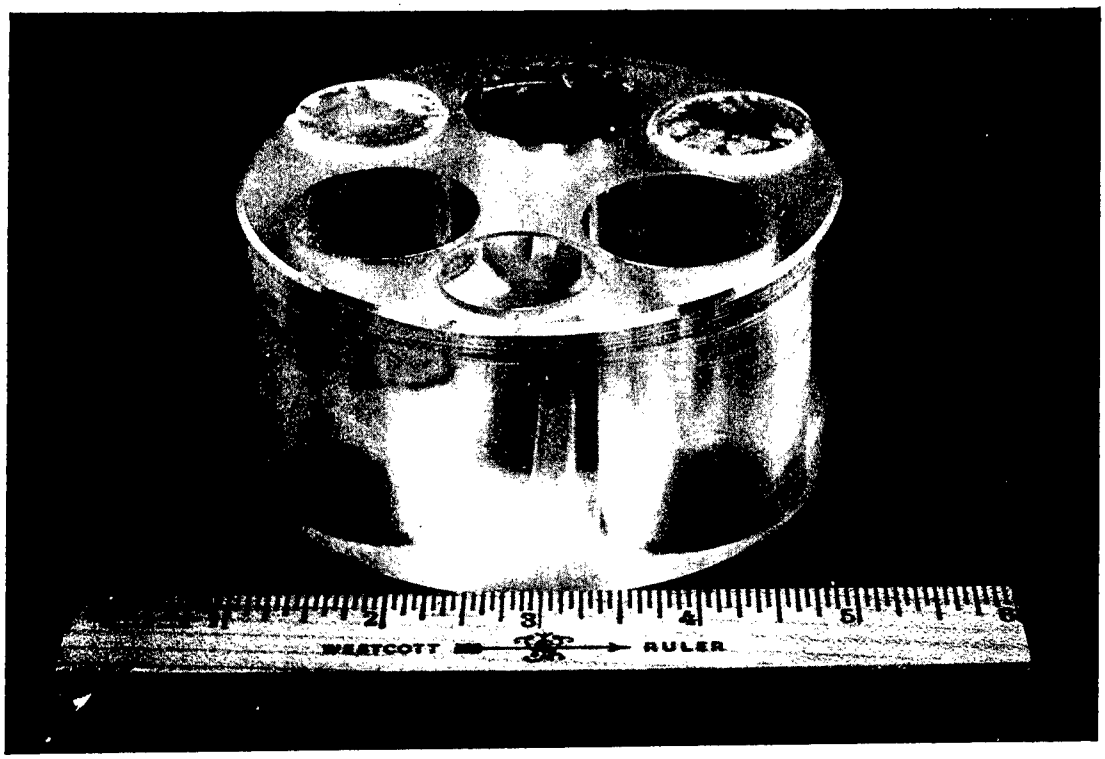

38661

Figure 9. Holder Used in the Intermediate Polishing Step.

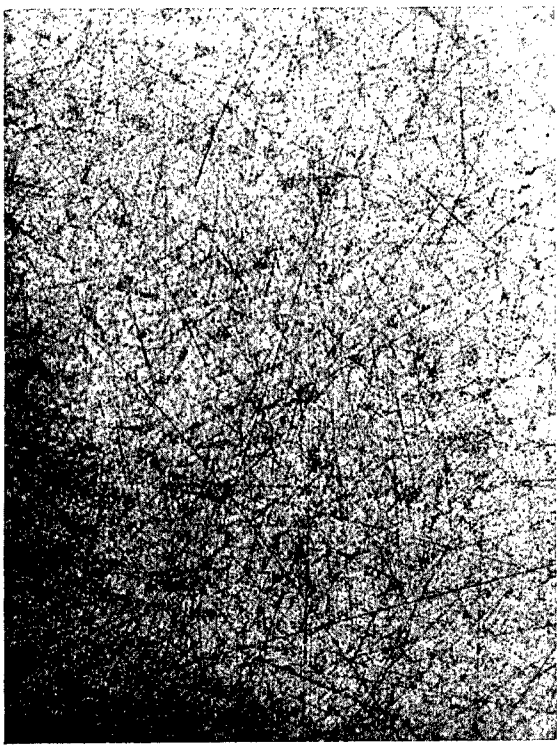

36785 250X

Figure 10. Pure Thorium; Scratch Size and Distribution Resulting from the Intermediate Step of Polishing of a Very Soft Material.

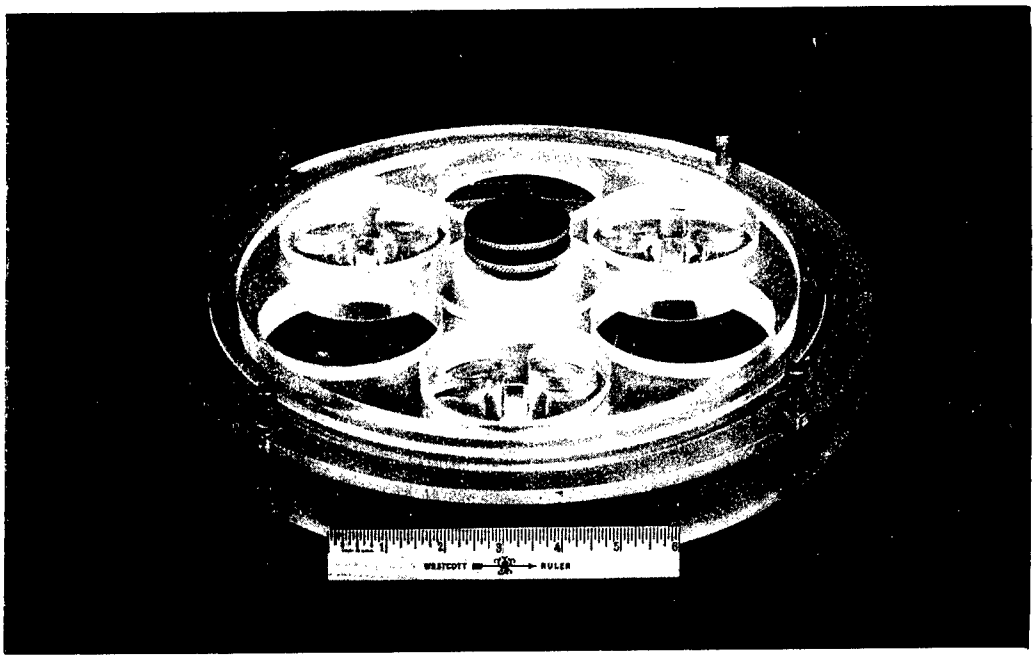

38658

Figure 11. Final-Polishing Fixture and Bowl.

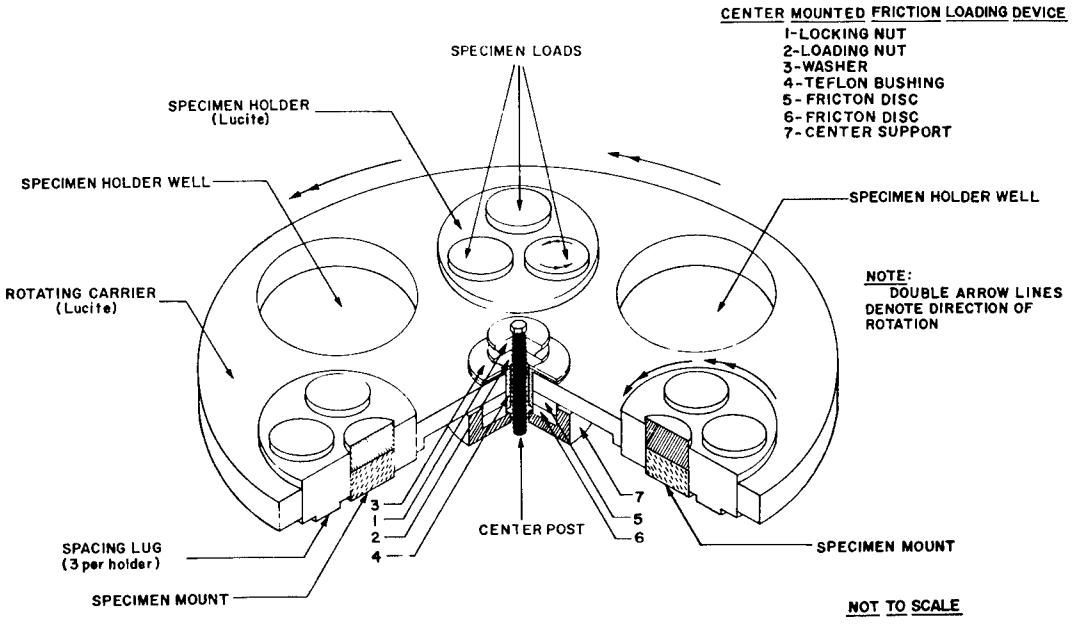

Figure 12. Schematic Cut-away.

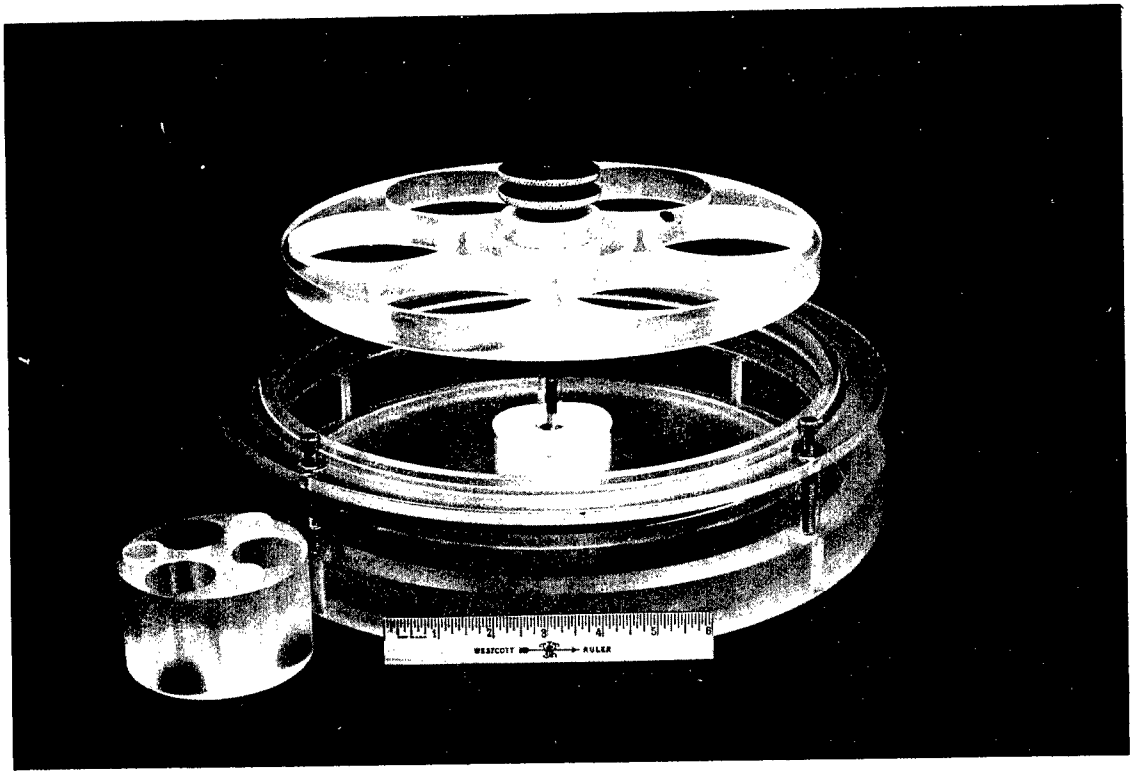

38659

Figure 13. Components of Vibratory Final-Polishing Fixture - Unassembled.

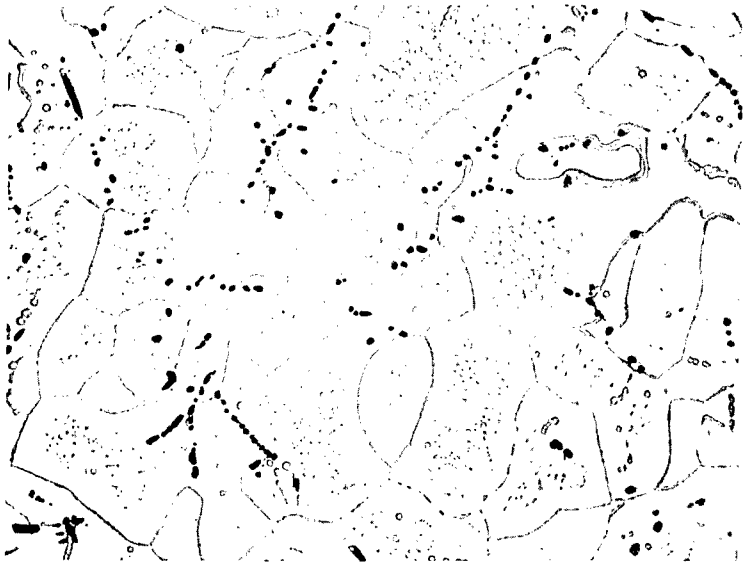

36480 250X

Figure 14. Commercial Thorium - with High-Impurity Content, As-Polished Surface, Time 2 Hours, Unweighted.

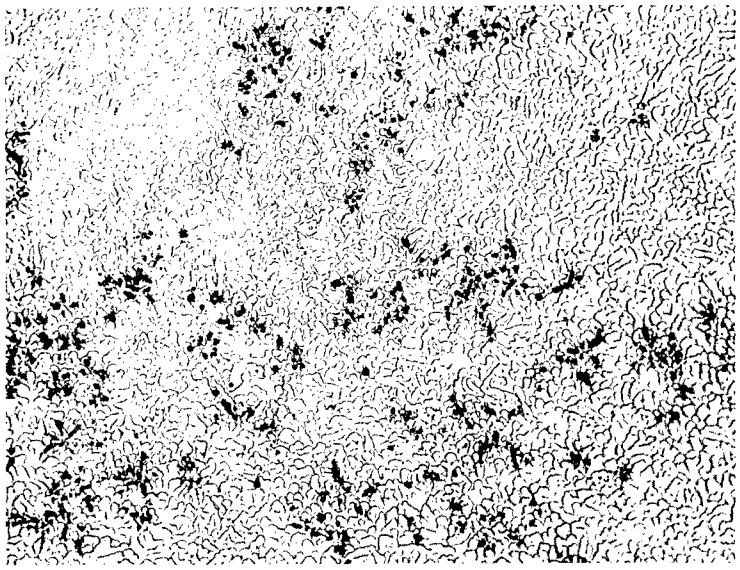

39054 250X

(a) As-polished surface.

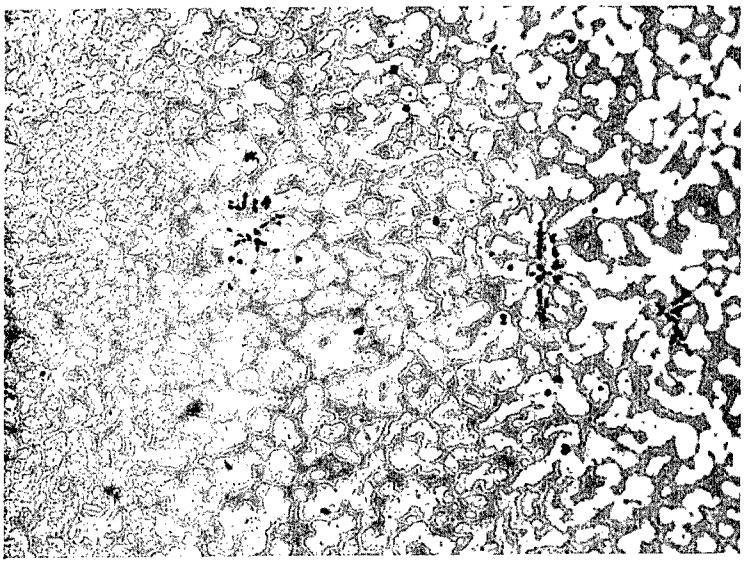

39057 250X

(b) As-polished surface with a light air-etch.

Figure 15. Two Examples of An Arc Melted Th-50w/oU Alloy. Polished 1 Hour Under a 250 gm. Weight. Photomicrographs Were Taken of Different Areas of the Same Specimen.

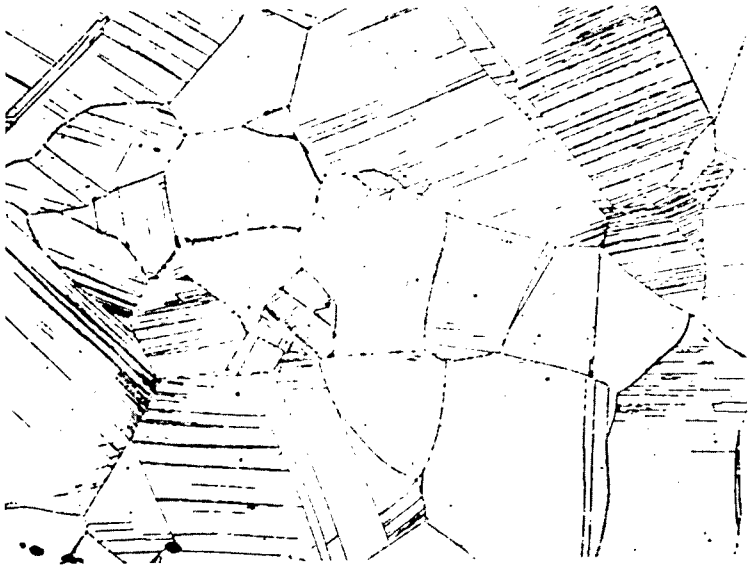

39004 500X

Figure 16. Type 304 Stainless Steel, Sensitized, Polished 2 Hours under a 125-Gram Load. Etched Electrolytically in 10% Oxalic Acid.

38874 200X

Figure 17. Electroformed Tungsten on a Copper Rod, Polished 2 Hours, Unweighted, Etched in 10% Ammonium Persulfate.

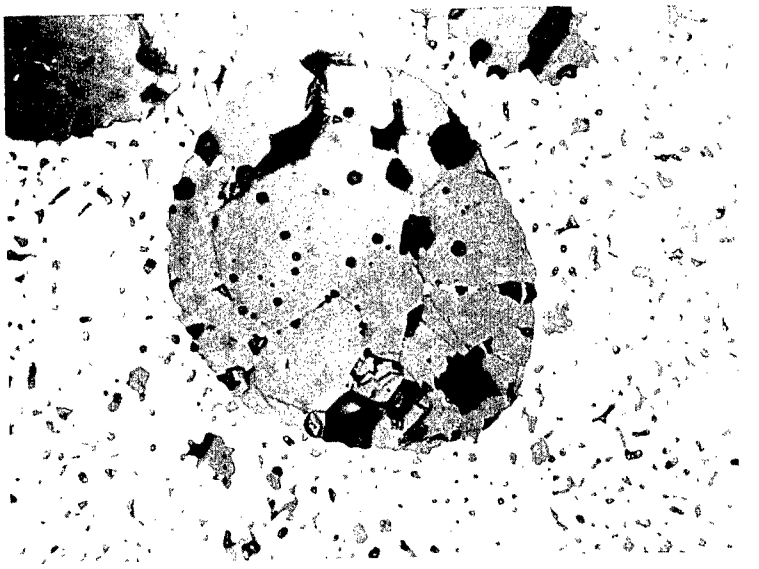

38716 500X

Figure 18. UO_2 Particle in a Sintered Tungsten Matrix. As-Polished, Unweighted, Polishing Time 2 Hours.

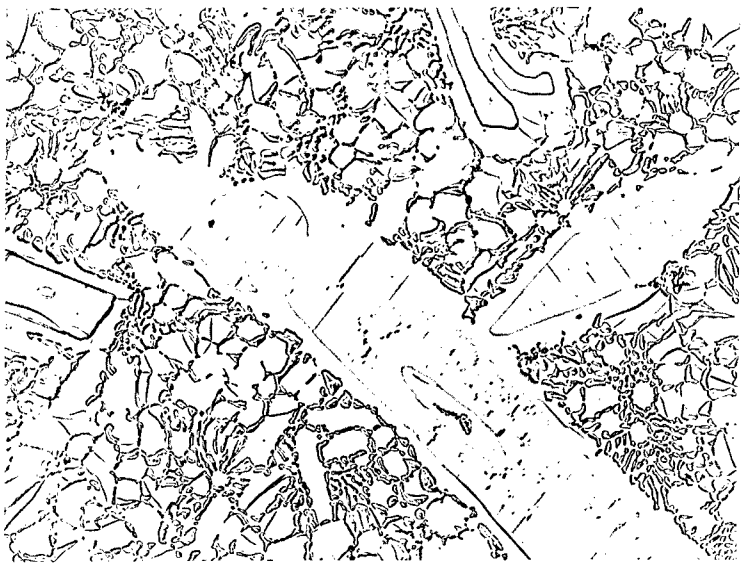

EI-1231 100X

(a) As-polished surface.

EI-1232 100X

(b) As-polished - polarized light photograph.

Figure 19. Co-5.5w/o Boron. Melted at 1250°C, Annealed for 18 Hours at 1000°C. Overall Hardness, 1250-1375 DPH, RC >70. Final-Polishing Time, 3 Hours. Unweighted.

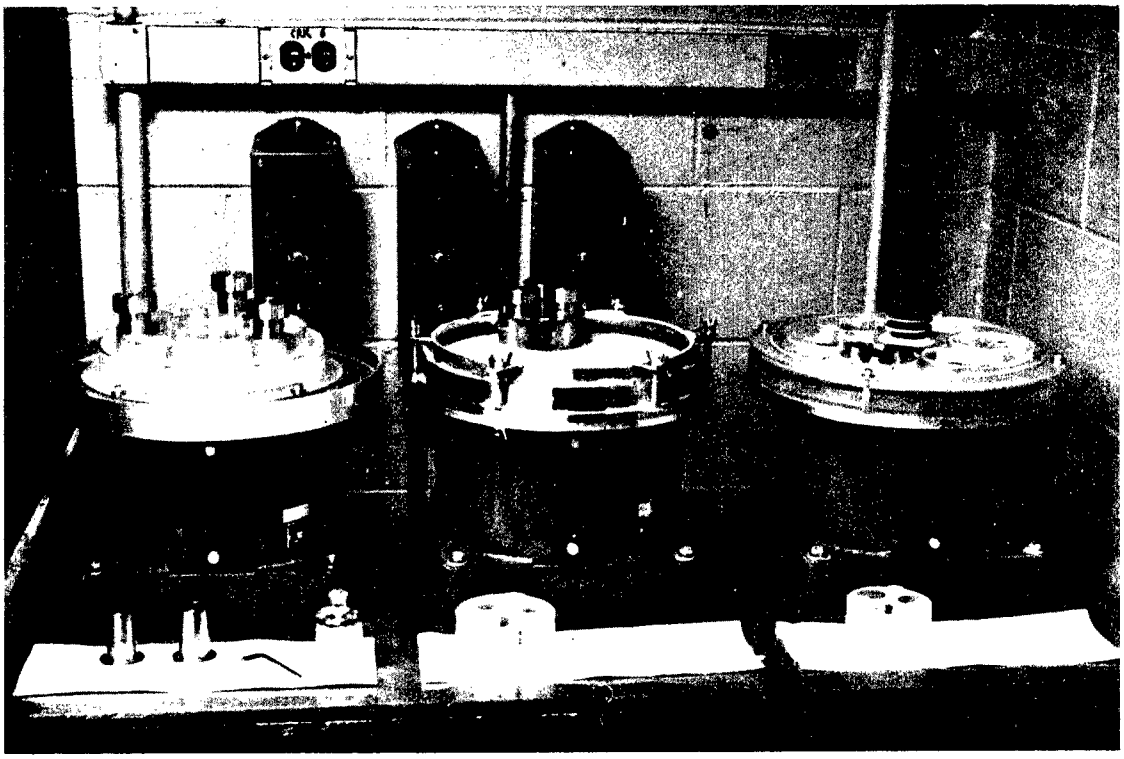

38657

Figure 20. Vibratory Metallography Installation in Use at ANL.